ADVERTIMENT. La consulta d'aquesta tesi queda condicionada a l'acceptació de les següents condicions d'ús: La difusió d'aquesta tesi per mitjà del servei TDX (www.tesisenxarxa.net) ha estat autoritzada pels titulars dels drets de propietat intel·lectual únicament per a usos privats emmarcats en activitats d'investigació i docència. No s'autoritza la seva reproducció amb finalitats de lucre ni la seva difusió i posada a disposició des d'un lloc aliè al servei TDX. No s'autoritza la presentació del seu contingut en una finestra o marc aliè a TDX (framing). Aquesta reserva de drets afecta tant al resum de presentació de la tesi com als seus continguts. En la utilització o cita de parts de la tesi és obligat indicar el nom de la persona autora.

ADVERTENCIA. La consulta de esta tesis queda condicionada a la aceptación de las siguientes condiciones de uso: La difusión de esta tesis por medio del servicio TDR (www.tesisenred.net) ha sido autorizada por los titulares de los derechos de propiedad intelectual únicamente para usos privados enmarcados en actividades de investigación y docencia. No se autoriza su reproducción con finalidades de lucro ni su difusión y puesta a disposición desde un sitio ajeno al servicio TDR. No se autoriza la presentación de su contenido en una ventana o marco ajeno a TDR (framing). Esta reserva de derechos afecta tanto al resumen de presentación de la tesis como a sus contenidos. En la utilización o cita de partes de la tesis es obligado indicar el nombre de la persona autora.

WARNING. On having consulted this thesis you're accepting the following use conditions: Spreading this thesis by the TDX (www.tesisenxarxa.net) service has been authorized by the titular of the intellectual property rights only for private uses placed in investigation and teaching activities. Reproduction with lucrative aims is not authorized neither its spreading and availability from a site foreign to the TDX service. Introducing its content in a window or frame foreign to the TDX service is not authorized (framing). This rights affect to the presentation summary of the thesis as well as to its contents. In the using or citation of parts of the thesis it's obliged to indicate the name of the author

Doctoral Thesis

Solar disinfection of secondary effluent and the subsequent bacterial regrowth: considerations, limitations and environmental perspectives

Stefanos Giannakis

Universitat Politècnica de Catalunya, Spain & Aristotle University of Thessaloniki, Greece

Thesis presented to obtain the qualification of Doctor from the Universitat Politècnica de Catalunya and the Aristotle University of Thessaloniki

Supervisors:

Prof. Dr. Antoni Escalas-Cañellas, UPC, Catalonia, Spain

Prof. Dr. Efthymios Darakas, AUTh, Greece

Doctoral Programs:

Environmental Engineering, Institute of Textile Research and Industrial Cooperation of Terrassa (INTEXTER) and Department of Chemical Engineering, Universitat Politècnica de Catalunya, Catalonia, Spain

Environmental Engineering, School of Engineering, Department of Civil Engineering, Aristotle University of Thessaloniki, Greece

Terrassa, 10/09/2014

(This page intentionally left blank)

Acta de calificación de tesis doctoral

Curso académico:

Nombre y apellidos

Programa de doctorado

Unidad estructural responsable del programa

Resolución del Tribunal

Reunido el Tribunal designado a tal efecto, el doctorando / la doctoranda expone el tema de la su tesis doctoral titulada _____

_____.

Acabada la lectura y después de dar respuesta a las cuestiones formuladas por los miembros titulares del tribunal, éste otorga la calificación:

☐ NO APTO ☐ APROBADO ☐ NOTABLE ☐ SOBRESALIENTE

(Nombre, apellidos y firma) Presidente/a		(Nombre, apellidos y firma) Secretario/a
(Nombre, apellidos y firma) Vocal	(Nombre, apellidos y firma) Vocal	(Nombre, apellidos y firma) Vocal

_____, _____ de _____ de _____

El resultado del escrutinio de los votos emitidos por los miembros titulares del tribunal, efectuado por la Escuela de Doctorado, a instancia de la Comisión de Doctorado de la UPC, otorga la MENCIÓN CUM LAUDE:

☐ SÍ ☐ NO

(Nombre, apellidos y firma) Presidente de la Comisión Permanente de la Escuela de Doctorado	(Nombre, apellidos y firma) Secretaria de la Comisión Permanente de la Escuela de Doctorado

Barcelona a _____ de _____ de _____

(This page intentionally left blank)

Abstract

The present Thesis deals with the solar disinfection of synthetic secondary effluent under laboratory controlled conditions, focusing on the post-irradiation bacterial regrowth. The influence of various internal and external factors and their effect on solar disinfection, as well as bacterial regrowth kinetics are the subject under question. With the aid of a common fecal indicator microorganism, the effects of light intensity, temperature, initial bacterial concentration, light energy (wavelength), manner of delivery (continuous-intermittent) were investigated. Also, the post-treatment events, such as dark repair, photoreactivation and the survival in natural water matrices were assessed, along with the use of technical means (flow photoreactors with recirculation) and advanced oxidation processes (photo-Fenton and sonication) for regrowth risk minimization. The findings provided valuable output, conclusions on the suitability of solar irradiation as a secondary wastewater disinfection technique, indicating the limitations of its applicability, the considerations on the treatment specifications and its environmental perspectives.

Περίληψη

Η παρούσα Διδακτορική Διατριβή πραγματεύεται την απολύμανση δευτεροβάθμια επεξεργασμένων τεχνητών λυμάτων υπό ελεγχόμενες συνθήκες, μελετώντας το φαινόμενο της επανανάπτυξης / επανεμφάνισης των μικροοργανισμών μετά την ακτινοβολία των λυμάτων. Αντικείμενό της είναι η μελέτη της επίδρασης μιας ευρείας γκάμας ενδογενών και εξωγενών παραγόντων τόσο κατά την διαδικασία της απολύμανσης, όσο και στην κινητική του βακτηριακού πληθυσμού. Με τη χρήση κοινών οργανισμών δεικτών κοπρανώδους μόλυνσης, μελετήθηκε η επίδραση του αρχικού βακτηριακού πληθυσμού, η ένταση και το μήκος κύματος της ακτινοβολίας, η θερμοκρασία απολύμανσης και ο τρόπος παροχής του φωτός (συνεχής-ασυνεχής) κατά την διαδικασία. Μελετήθηκαν ακόμα τα φαινόμενα που λαμβάνουν χώρα μετά την ακτινοβολία, όπως το φαινόμενο της επανανάπτυξης του βακτηριακού πληθυσμού στο σκοτάδι, η φωτο-επιδιόρθωση και η επιβίωση των μικροοργανισμών σε φυσικά νερά μετά την ακτινοβολία. Διερευνήθηκε τέλος η δυνατότητα χρήσης αντιδραστήρων συνεχούς ροής με επανακυκλοφορία και ο συνδυασμός εφαρμογής προχωρημένων μεθόδων οξείδωσης (αντιδραστήριο photo-Fenton) με υπερήχους, στοχεύοντας στην ελαχιστοποίηση της πιθανότητας επανανάπτυξης των μικροοργανισμών. Τα αποτελέσματα κατέδειξαν ενδεδειγμένες πρακτικές εφαρμογής, συμπεράσματα για την καταλληλότητα της ηλιακής ακτινοβολίας ως μεθόδου απολύμανσης δευτεροβάθμια επεξεργασμένων λυμάτων, προβληματισμούς όσον αφορά τις τεχνικές λεπτομέρειες και περιβαλλοντικές ανησυχίες.

Resum

Aquesta tesi tracta de la desinfecció d'un efluent secundari sintètic mitjançant llum solar en condicions controlades de laboratori, centrant-se en el recreixement dels bacteris després de la irradiació. La influencia de diversos factors interns i externs i el seu efecte en la desinfecció solar, així com la cinètica del recreixement bacterià són els temes estudiats. Amb l'ajuda d'un microorganisme indicador comú de contaminació fecal, es van investigar els efectes de la intensitat de la llum, de la temperatura, de la concentració inicial de bacteris, de l'energia lluminosa (longitud d'ona) i de la seva forma d'aplicació (contínua o intermitent). També es van estudiar els esdeveniments del posttractament, com son la reparació en foscor, la fotoreactivació i la supervivència en matrius naturals, així com l'ús de recursos tècnics (fotoreactors amb recirculació) i processos avançats d'oxidació (photo-Fenton i sonicació) per minimitzar el risc de recreixement. Els resultats obtinguts han permès formular conclusions valuoses sobre la idoneïtat d'utilitzar la radiació solar com a tècnica secundaria de desinfecció d'aigües residuals, indicant les limitacions de la seva aplicació, les consideracions sobre les especificacions del tractament i les seves perspectives ambientals.

Resumen

En la presente Tesis doctoral se estudia la desinfección solar de un efluente secundario sintético en condiciones controladas de laboratorio, centrándose en el recrecimiento bacteriano después del tratamiento de irradiación. La influencia de diversos factores tanto internos como externos y sus efectos sobre la desinfección solar, así como el recrecimiento bacteriano son el tema principal de esta investigación. Empleando un microorganismo indicador fecal común, se investigaron los efectos de la intensidad de la luz, la temperatura, la concentración bacteriana inicial, la energía de la luz (longitud de onda) y la forma de suministro (continua-intermitente). Asimismo, se evaluaron los eventos posteriores al tratamiento, tales como la reparación oscura, la fotorreactivación y la supervivencia en matrices acuosas naturales, así como el uso de medios técnicos (fotorreactores de flujo con recirculación) y procesos de oxidación avanzada (foto-Fenton y sonicación) para mitigar el riesgo de recrecimiento. Los hallazgos proporcionaron valiosos resultados, conclusiones referentes a las aplicaciones prácticas, conclusiones sobre la adecuación de la irradiación solar como técnica de desinfección de aguas residuales secundarias, con indicaciones a las limitaciones de su aplicabilidad, consideraciones sobre las especificaciones del tratamiento y sus perspectivas ambientales.

“It may be just “crap” to you, but it’s my bread and butter.”

Stanley Falkow, Father of Molecular Bacterial Epidemiology

(This page intentionally left blank)

Preface

The present work is developed in the framework of the qualification of Doctor, in a joint Doctorate, through a specific agreement between Aristotle University of Thessaloniki and Universitat Politècnica de Catalunya. This program was an initiative under the aegis of the Mediterranean Office for Youth Programme (MOY, call 2011-2014) resulting in joint supervision and separate PhD title from the two universities.

Its specific interest lies in the application of cheap, and environmentally friendly techniques of wastewater disinfection. The utilization of solar light provides a promising candidate for application, especially in sunny areas, or developing countries. Specifically, the disinfection of secondary effluent by solar irradiation is investigated, aiming to eliminate the potential risk of bacterial regrowth. The main effects of the involved parameters, as well as the possible mechanisms of regrowth appearance are in question, and the conclusions can influence the design and parameterization of relevant disinfection applications.

For the fulfillment of the targeted work, this thesis took place in three different countries, Greece, Spain and Switzerland. From each country, there is a significant number of people that aided towards the completion of this work and whose contribution should be acknowledged.

Greece

First of all, I would like to thank Prof. Efthymios Darakas for a thousand reasons, and the list would still not be exhaustive. Beginning in 2008, when he welcomed me in the Laboratory of Environmental Engineering and Planning to realize my Diploma work; in 2010, when he supervised my Master Thesis and the offer for a place as a Doctoral student, thus facilitating a dream of many years; in 2011, when he went through piles of documents to make the joint Doctorate possible; the restless support through all the rough patches all these years. The difficulties he has been through of keeping me guided, by supervising the experimental work, giving me invaluable input on the results, it all made me feel that I could really rely on his experience to get me through this task. But most importantly, for doing everything possible and impossible, to help achieve my every academic ambition. Special thanks should also be attributed to Prof. Margaritis Vafeiadis and the LEEP staff, Mrs. Domniki Ioannidou and Mrs. Anastasia Bellou, for their support during the first years of my studies.

Catalonia, Spain

The Mediterranean office for Youth initiative was warm welcomed by UPC, and Prof. Santiago Gassó Domingo. The orientation and support, especially during the first months in Terrassa, the arrangements for

the joint supervision were much appreciated. Special thanks are given to all the staff of the Laboratory of Control of Environmental Contamination in INTEXTER. Prof. Martí Crespi, Prof. Mercè Vilaseca Vallvé, Montserat Raspall Noguera and Prof. Carmen Gutiérrez Bouzán, who overcame too many difficulties, only to accommodate my work.

However, this work in at UPC (and the next years…) would never be successfully achieved without my second, only in order of appearance, Thesis supervisor, Prof. Antoni Escalas-Cañellas. Personally, I do not believe I can ever appreciate enough the contribution, as my free academic character and investigative perspectives were carefully shaped in a researcher with goals under his guidance. Always honest, with decisive contribution, his role was critical in the final outcome, and I cannot thank him enough for that. Finally, I would like to thank my Thesis Proposal Examination Panel (Prof. Martí Crespi Rosell, Prof. Jordi Mas Gordi and Prof. Kevin McGuigan) for accepting the invitation and providing me with useful comments for the evolution of the work.

Switzerland

The exchange in École Polytechnique Fédérale de Lausanne was one of the most fortunate academic and professional instances of my career. Under the guidance of Prof. César Pulgarin, I succeeded in completing most of my experimental part of the work, and his contribution is greatly acknowledged. In all aspects, the support was far from typical; academic guidance, personal support, thus boosting the evolution of the Thesis. His invaluable experience was selflessly provided, always giving me a new perspective, influencing the final outcome in many levels. Hence, special thanks to the Swiss Government for providing the Excellence Scholarships and along with them, real opportunities. I would also like to thank Prof. Christian Pétrier, for his guidance through the experimentation and publication period.

Finally…

In a Doctoral work, a truly demanding task, one should never forget the individuals who accompanied the way, for we are human beings, and our weak nature needs all the support it can get. Truly blessed are the ones who were lucky to find it in others. Three years, in three different countries, can really indicate the significant people in our lives, and their contribution cannot be measured by words. My parents, my brothers, my friends, the people who were there along the way. I hope they take the same pride in me, as I did, for having them into my life.

Lambros Alexandrou, Kostantinos Karalazos, Christoforos Zolotas, Giorgos Zarogiannis, in the limited days of face-to-face interaction but constant presence in Skype, were there for all merry and difficult moments, and my gratitude is really difficult to describe in words. Many years have passed, we have been all over Europe, but we are all still supporting each other.

I have to thank all the people who became my friends during my Master degree, who never stopped supporting me, especially Alexandra Demertzi, Anastasia Founta, Alexandra Papanastasiou, Panagiota Moysidou and Olga Aslanidou, for always caring and supporting me.

My colleagues in Spain, Raquel Urioz Rodriguez, Valentina Buscio Olivera and Mireia Sala, the friends I made there, Konstantinos Kampouropoulos, Theoni Paschou, Christina Giannakou, Konstantina Stavgianoudaki, Carolina Sanfona and Etienne Knipping, as well as tele-support from Anja Hočevar (Slovenia) and Zuzana Kralovicova (Slovakia), are the people who got me through a difficult year in Terrassa.

All the people I have worked with in Switzerland, spending infinite hours in the laboratory, deserve my deepest gratitude; Sami Rtimi, Stefanos Papoutsakis, Francesca Petronella, Jelena Nesic, Ana Isabel Merino Gamo, Alba Camarasa. My friends Ignasi Canales, Pedro Mansos, Thomas Götz, Vanessa Loudianou, Thomas Geelen and Kyriaki Ioannidou, with whom we jointly supported our days in Lausanne.

And last but not least, to my true Significant Other, the person who was there in this critical time in my life, the support that one must experience in order to appreciate the real meaning of "being there" for someone, the only person who can convert the "clichés" of a relationship in the brightest moments of the everyday life, my Sofia Samoili, sincerely, thank you for everything.

(This page intentionally left blank)

Table of Contents

List of Figures

and time. (d) Main effects plot (control variable: Regrowth after 1 day). (e) Main effects plot (control variable: Regrowth after 2 days).

Page 94 - Figure 3.3.2: Main results of non-irradiation experiments for synthetic secondary effluent at among 50-60˚C and all initial *E. coli* populations. (a) Post-treatment regrowth curves. (b) Contour plot of regrowth after 1 day vs. temperature and time. (c) Contour plot of regrowth after 2 days vs. temperature and time. (d) Main effects plot (control variable: Regrowth after 1 day). (e) Main effects plot (control variable: Regrowth after 2 days).

Page 97 - Figure 3.3.3: Main results of 800 W/m^2-irradiated experiments for synthetic secondary effluent at among 20-40˚C and all initial *E. coli* populations. (a) Post-treatment regrowth curves. (b) Contour plot of regrowth after 1 day vs. temperature and time. (c) Contour plot of regrowth after 2 days vs. temperature and time. (d) Main effects plot (control variable: Regrowth after 1 day). (e) Main effects plot (control variable: Regrowth after 2 days).

Page 98 - Figure 3.3.4: Main results of 800 W/m^2-irradiated experiments for synthetic secondary effluent at among 50-60˚C and all initial *E. coli* populations. (a) Post-treatment regrowth curves. (b) Contour plot of regrowth after 1 day vs. temperature and time. (c) Contour plot of regrowth after 2 days vs. temperature and time. (d) Main effects plot (control variable: Regrowth after 1 day). (e) Main effects plot (control variable: Regrowth after 2 days).

Page 99 - Figure 3.3.5: Overview of disinfection experiments. Process efficiency vs. treatment time and temperature is plotted. (a) 0 W/m^2. b) 800 W/m^2. c) 1200 W/m^2

Page 101 - Figure 3.3.6: Overview of the 1200 W/m^2-irradiation experiments, among 20-40˚C and all initial *E. coli* populations. (a) Contour plot of regrowth after 1 day vs. temperature and time. (b) Contour plot of regrowth after 2 days vs. temperature and time. (c) Main effects plot (control variable: Regrowth after 1 day). (d) Main effects plot (control variable: Regrowth after 2 days).

Page 103 - Figure 3.3.7: Overview of the 1200 W/m^2-irradiation experiments, among 50-60˚C and all initial *E. coli* populations. (a) Contour plot of regrowth after 1 day vs. temperature and time. (b) Contour plot of regrowth after 2 days vs. temperature and time. (c) Main effects plot (control variable: Regrowth after 1 day). (d) Main effects plot (control variable: Regrowth after 2 days).

Page 105 - Figure 3.3.8: Statistical interpretation of regrowth vs. disinfection efficiency. (a) Efficiency vs. Regrowth after 1 day. (b) Efficiency vs. Regrowth after 2 days. (c) Cultivable bacteria at the end of the treatment period (1-4 h) vs. Regrowth after 1 day. (d) Cultivable bacteria at the end of the treatment period (1-4 h) vs. Regrowth after 2 days.

Page 107 - Figure 3.3.9: Transferability of live bacteria through the post-irradiation treatment period. Regrowth after 24 h out of the live fraction subjected to i hours of treatment (i=1-4 h) vs. Regrowth after 48 h.

List of Tables

Nomenclature

List of abbreviations

Adj SS: Adjusted sum of squares

ANOVA: Analysis of variance

AOP: Advanced oxidation process

ATP: Adenosine triphosphate

BC: Before Christ

BL: Blacklight

CFU: Colony forming units

COD: Chemical oxygen demand

CPC: Compound parabolic collector

CPD: Cyclobutane pyrimidine dimer

DBPs: Disinfection by-products

DF: Degrees of freedom

DNA: Deoxyribonucleic acid

DOC: Dissolved organic carbon

DOE: Design of experiments

DR: Dark repair

EBD: Effective bacteriostatic dose

F: F-test value

FC: Fecal coliforms

hv: Light

IR: Infrared

LP: Low pressure

Max: Maximum

Min: Minimum

MP: Medium pressure

MSE: Mean square error

NTU: Nephelometric turbidity units

P: P-value

PAA: Peracetic acid

PCD: Programmed cell death

PET: Polyethylene terephthalate

pF: Photo-Fenton

PHR: Photoreactivation

PRE: Photoreactivation enzyme

PRESS: Prediction sum of squares

RSE: Relative standard error

RNA: Ribonucleic acid

RootMSE: Square root of MSE

ROS: Reactive oxygen species

R^2: Coefficient of determination

R^2-(adj): Adjusted R^2

R^2-(pred): Predicted R^2

Seq SS: Sequential sum of squares

SODIS: Solar disinfection

TC : Total coliforms

TCA cycle: Tricarboxylic acid cycle

US: Ultrasound

UV: Ultraviolet

UVA: Ultraviolet A

UVB: Ultraviolet B

UVC: Ultraviolet C

VNC hypothesis: Viable but non-cultivable hypothesis

WHO: World Health Organization

WW: Wastewater

WWTP: Wastewater treatment plant

List of equation symbols

C_c: Physiological cell state constant

C_i: Bacterial concentration (at time=i) (CFU/mL)

I: Light intensity (W/m^2)

k_1: First-order reactivation rate constant

k_2: Second-order reactivation growth rate constant

k_{max}: Inactivation rate (1/time unit)

k_s: Growth rate constant of solar reactivation (min^{-1})

M: Mortality (zero-order decay rate constant)

M_s: Solar decay rate constant (min^{-1})

N_0: *E. coli* concentration immediately after UV disinfection (logCFU/mL)

$N_{initial}$: *E. coli* initial concentration before UV disinfection (logCFU/mL)

N_m: Maximum bacterial population and

N_{res}: Residual density of the bacterial population (CFU/mL)

N_t: *E. coli* concentration at time of exposure for time t in the repair conditions

p: Shape parameter of the Weibull model

S: Repair rate after UV disinfection (%)

Sl (shoulder length): Shoulder-log linear model-specific constraint (time units)

S_m: Maximum survival ratio (N_m/N_o) x 100 (%)

S_o: Initial survival after ultraviolet disinfection (%)

T: Temperature (°C)

t: Time (s)

Greek letters

δ: Scale parameter of the Weibull model

Chapter 1. Introduction

Municipal wastewater contains a variety of microorganisms, able to pollute the receiving water bodies if not properly treated. From the health point of view, municipal wastewater contains bacteria, viruses and other microorganisms (Drinan, 2001), with many of them being pathogenic to the human species. Even the secondary treated effluent from municipal wastewater treatment plants contains from thousands to tens of thousands of fecal coliforms per 100 mL. This makes secondary effluent potentially harmful, often unsuitable for discharge or for some reuse applications, according to the regulations in several countries. Many microorganisms are harmless when they are inserted in the environment (Avery et al., 2008), but the limits set by the World Health Organization (WHO, 2006) for water discharge impose further inactivation prior to release. So, further treatment to remove or inactivate the pathogens is often needed in order to reach the limit values set in national or international regulations.

One of the most common methods of microorganism removal is chemical disinfection, usually through chlorine or other disinfectants, such as ozone, peracetic acid (PAA), or other chemicals or their combinations. Although these methods are highly efficient, their use is linked to safety operational issues or to the formation of harmful disinfection by-products (DBPs) (White, 2010). Furthermore, although this practice prevents a significant number of water-related diseases in around the world, the affordability of chemical disinfection has to be put under question for many areas in developing countries. Hence, research was turned to cheaper, while environmentally acceptable solutions.

In this framework UV disinfection was studied extensively over the years, as an environmentally friendly sterilization technique. The utilization of monochromatic low-pressure UVC lamps and polychromatic medium pressure ones causes alterations in the genome structure of microorganisms and yield significant results (Hijnen et al., 2006). Solar light, on the other hand, has demonstrated disinfecting capabilities, due to the action mode of UVB and UVA wavelengths. For drinking water, it has been greatly used as a practice in developing countries (McGuigan et al., 2012) and the application in form of ponds for wastewater treatment has also been investigated in tropical latitude (von Sperling, 2005). The aforementioned regions coincide with the higher number of sunny days per year and therefore are ideal candidates for such practices.

However, both UVC and solar UV disinfection share a shortcoming; unlike the chemical methods for disinfecting wastewater, they lack residual activity, and when the exposure is over, there is no disinfecting action (White, 2010). Many microorganisms (e.g. bacteria, viruses) have demonstrated a capability to mend the damages in their cell through several mechanisms, after the end of the exposure to UV (Cleaver, 2003). This process is called reactivation and results in regrowth of the population. The main two mechanisms are the light mediated one and the dark process, namely photoreactivation and dark repair. The difference underlies in the manner of activation of the enzyme capable of repairing the lesions.

Wastewater is a rich in nutrients matrix which could support microbial growth, and given the time treated water could spend in the dark, due to the storage times potentially required to further use, regrowth is rendered as a primary problem. Regrowth of bacteria in the natural environment could possibly mean a re-contamination of downstream water supplies or coastal areas. According to the type of receiving water body and conditions during discharge, there is different response expected.

While several studies have been made concerning SODIS of drinking water and the optimal conditions have been set long ago, the parameterization of solar disinfection of wastewater has been only partially studied. There is a significant gap of a systematic study focusing on the conditions of solar disinfection and the manner they affect the disinfection of water. Even more, contrary to UVC disinfection of water and wastewater, the problem of bacterial regrowth after solar disinfection of wastewater has been sparsely studied, and specifically, how the disinfection conditions are affecting the subsequent regrowth.

This Thesis focuses on some of the aspects concerning solar disinfection of (synthetic) secondary effluent, and the subsequent bacterial regrowth, through the most common pathways of photoreactivation and dark repair. Commonly involved parameters like solar light intensity or water temperature are systematically assessed, and the post-irradiation events are considered, focusing on bacterial regrowth in a variety of following conditions. A review on the scientific subjects relevant to the context of this research prior to the results' presentation is elaborated.

1.1. Solar disinfection

The utilization of sun's rays is one of the oldest recorded methods of water purification, dating back to at least 2000 BC in the Sanscrit text ''Oriscruta Sanhita'' (Patwardhan, 1990). However, it is only in more recent times that the underlying scientific basis of this approach has been established (Acra et al., 1984, Acra et al., 1989). For example, photocatalysis was first shown to be an effective sterilization process by Matsunaga et al. (1985), who reported on the killing of *L. acidophilus*, *S. cerevisiae* and *E. coli* (Dalrymple et al., 2010). Solar water disinfection (SODIS) is a simple, environmentally sustainable and low cost point of use treatment for drinking water in developing countries with consistently sunny climates under circumstances in which people had no access to alternative water treatment systems (Gelover et al., 2006). The simplest practice of SODIS is performed by filling transparent plastic PET bottles with contaminated water followed by exposure to sunlight for some hours, in order to inactivate the microbes (Reed, 2004).

Sunlight is able to inactivate microorganisms due to the synergistic effect of the UV and heating of water by infrared radiation. UV wavelengths which reach the earth's surface are classified as UVA (320–400nm) and UVB (290– 320nm) (Rincon and Pulgarin, 2004a). Solar disinfection is based on the bacteriostatic effect of the UVA solar radiation (wavelength 320–400nm) as well as in the presence of dissolved oxygen, as it plays an important role in killing the pathogens: sunlight produces highly reactive forms of oxygen (oxygen free radicals and hydrogen peroxides) in the water. These have a significant effect on water sterilization by this process (Gelover et al., 2006). In contrast, UV-B radiation can cause direct DNA damage by inducing the formation of DNA photoproducts, of which the cyclobutane pyrimidine dimer (CPD) and the pyrimidine (6–4) pyrimidinone (6–4PP) are the most common. The accumulation of DNA photoproducts can be lethal to cells through the blockage of DNA replication and RNA transcription (Harm, 1980; Britt, 1996; Rincon and Pulgarin, 2004a).

The mechanism is described briefly as by a partial decomposition of the outer membrane, followed by disordering of the cytoplasmic membrane, resulting in cell death (Sunada et al., 2003). Vital cellular functions like the transcription and translation apparatus, transport systems, amino acid synthesis and degradation, respiration, ATP synthesis, glycolysis, the TCA cycle, chaperone functions and catalase are targeted by UVA irradiation (Bosshard et al., 2010a).

1.1.1. General considerations

Previous research by the SODIS foundation has expressed their concern about some parameters affecting the SODIS procedure for drinking water in plastic bottles, including (Sodis Fundación, 1998):

1. The minimum irradiation time under clear sky required to eliminate 10^5 *E. coli*/100 mL (5 h or a 555 Wh/m^2 dose),

2. Container types and materials recommended for the disinfection (transparent PET bottles),
3. The influence of the bottle aging (their loss of light transmittance with extended use),
4. The possible presence of photoproduct precursors, that could affect the quality of water during disinfection,
5. The most favorable geographic area for the use of solar disinfection (up to 35^{o} of latitude north or south),
6. The effect of seasons and weather (the intensity of solar radiation varies with the time of the day, date, geographic location and weather),
7. The influence of water quality and depth (turbidity <30 NTU and a maximum water layer of 0.1 m),
8. The lack of bacterial and viral regrowth,
9. The increase in the methods' efficiency when the bottles' lower half (lengthwise) is painted black.

Other factors such as bacteria type, growth phase, water pH, turbidity and presence of ions or other pollutants might dramatically affect the results (Villén et al., 2006). For instance, fast-growing cells were more sensitive to the stresses than slow-growing cells (Saitoh and El-Ghetany. 2002).

1.1.2. Action mode of solar disinfection

i) Optical Inactivation

Although sunlight may cause direct damage to biomolecules, it is more common for solar UV and visible light to cause indirect damage, being absorbed by photosensitizer molecules (endogenous, like porphyrins, or exogenous, synthetic ones), which are then raised to an excited state (Reed, 2004).

An excited photosensitizer may then react directly with cellular biomolecules (type I reaction), or more commonly, with molecular oxygen (type II reaction). The type II, briefly described, leads to the production of various reactive oxygen species (ROS) including singlet oxygen, superoxide and hydroxyl radicals, along with hydrogen peroxide. ROS generated by solar irradiation will then react with cellular constituents, including DNA, proteins and cell membrane components of the outer surface, leading to the inactivation of the cell because of the alterations in membrane permeability (Reed, 2004).

ii) Thermal inactivation

The infrared region of light is mainly responsible for the temperature increase and the subsequent inactivating action (Reed, 2004). For instance, Blaustein et al., (2013) have mentioned the lethal effect of temperature on bacterial kinetics as it is increased, by the denaturation of cells' proteins and other vital components; as SODIS has been applied in bottles, the lethal temperature range is a desired target. Also, heating water up to a temperature of 65°C and exposing the water sample to direct solar radiation for 2 to 3 h at the same time could be an alternative to thermal treatment with solar rays (Saitoh and El-Ghetany. 2002).

iii) Interaction between optical and thermal effects

Several research studies have reported a synergy between optical and thermal inactivation (e.g. McGuigan et al., 1998). Temperatures around 45°C offer also solid ground for synergistic effect, along with the radiation (Gelover et al., 2006). Also, it was suggested that the backs of solar disinfection containers should be painted black, to increase the thermal effect (Sommer et al., 1997, Wegelin and Sommer, 1998). Inactivation of *E. coli* can be enhanced by a factor of almost two-fold by adding an aluminum foil backing to the containers to reflect UV and visible light, thereby enhancing the optical component of the process (Kehoe, 2001).

The difference between the two alterations of the methods is that absorptive, black-backed containers might be expected to give the best effects in full-strength sunlight, where thermal effects are likely to raise the water temperature to 45°C and above, whereas reflective, foil-backed containers might be more effective in suboptimal sunlight and cloudy conditions, where thermal effects will be greatly reduced and where optical (UV-mediated) inactivation is most important (Dalrymple et al., 2010).

1.2. Parameterization of solar disinfection

1.2.1. Light quality and intensity

When it comes to field-scale real-water or wastewater disinfection applications, one of the most crucial factors is the availability of light (Fabriccino and d'Antonio, 2011). In some cases, areas with poor water supplies are provided with a large number of sunny days per year (more than 3000 hours) (Blesa and Litter, 2007), but for instance, solar-UV power is dependent on the clarity of the sky and the absence of clouds. The solar-only disinfection is very susceptible to changes in solar irradiation, and therefore, only takes place at higher irradiation intensities (Sichel et al., 2007).

There is a general consensus that effective solar disinfection requires around 3–5 hours of strong sunlight at intensity above 500 W/m^2 (Oates et al., 2003; Reed, 2004). Once the lethal solar dose has been received, the efficacy is not particularly enhanced by any further increase. A greater effectiveness of applying a high UV intensity for a short time is preferred than applying a lower intensity for a longer period of time (Sommer et al., 1998). Authors suggest that this effect may be due to the action of repair enzymes in the cell which are more negatively influenced by high UV intensities (Sommer et al., 1998). Consequently, the solar UV dose is not a good parameter to accurately predict and standardize the impact of the solar photocatalytic process on bacteria (Rincon and Pulgarin, 2004a).

Hence, studies have been made to assess the potential impact that this process has on disinfection (Rincon and Pulgarin, 2003) and the effects of intermittence in light supply on the solar disinfection process (Misstear et al., 2013). Even in the sunniest areas in the world, there is no guarantee that the UV supply will be continuous; therefore, there is a need to further investigate the mechanisms and possible implications of intermittence in the overall efficiency of the process. Although some works have demonstrated indifference of the effect of light intermittence on some matrices (Lanao et al., 2012), this is not the rule for all microorganisms and all light waves (Velez-Colmenares et al., 2011). However, there is a general consensus that the intermittent process deviates from the behavior expected in a normal test; hence, this could be attributed to the disinfection installations as well.

A very common method of solar disinfection is the compound parabolic collector (CPC) reactors (Malato et al., 2004), which recirculate the sample around an illuminated surface and a dark storage tank. Therefore, technical aspects can affect the process, causing intermittence, such as the storage of water in the dark tank (Rincon and Pulgarin, 2007a; Moncayo-Lasso, 2009; Fernandez et al., 2005; 2009). Sciacca et al. (2011) with a minimum dark storage volume (83% illuminated volume), reported different results while performing solar CPC intermittent tests, compared to the equivalent batch tests, stating that there are actions that intervene (such as shear forces or oxygenation of the sample) and modify the final outcome. Finally, Ubomba-Jaswa et al. (2009), concluded that the continuous manner of irradiation has greater inactivation potential, compared to the interrupted manner of solar UV light supply.

1.2.2. Temperature

In general, the thermal efficiency of solar disinfection is at a minimum for partially cloudy, low ambient temperature days in windy areas (Saitoh and El-Ghetany, 2002). The synergy of temperature and solar rays only occurs between 40-50°C. Below this temperature, it doesn't affect solar disinfection (Reed, 2004). However, bacteria and viruses do not demonstrate the same behavior; for *E. coli*, between 12-40°C, the kinetics remain unchanged, whereas for some viruses the inactivation rate increases as temperature rises from 20 to 50°C (Wegelin et al., 1994). Finally, it is possible that the water temperature (between 6 and 10°C) in winter increases the susceptibility of bacteria to photocatalytic treatment (Rincon and Pulgarin, 2004a). Authors have reported that *E. coli* subjected to low-temperature storage results in an increase in susceptibility to the subsequent environmental stresses (Ingraham, 1999).

1.2.3. Organic compounds

There is a conflict on the effect of the organic compounds contained on water disinfection by solar radiation. While Reed (2004) suggests that the presence of dissolved organic compounds, such as humic acids could result in the enhancement of solar inactivation as a consequence of their action as photosensitizers, Marugan et al. (2008) have shown that low concentrations of humic substances inhibit the disinfection process, whereas the same concentration of sucrose does not affect at all. In natural waters, the possible inhibitory effects of such dissolved organic compounds and their absorption of sunlight will be the drawback of the enhanced ROS production, again because of their existence.

1.2.4. Inorganic compounds

Several studies have demonstrated a synergistic interaction between dissolved salts and solar illumination (Davies and Evison, 1991; Vicars, 1999), though this is most pronounced at the high salt concentrations found in sea water and is likely to be less significant than organic compounds at the salt concentrations found in most natural fresh waters (Reed, 2004).

Rincón and Pulgarin (2004b) and Gomes et al., (2009a) showed that the addition of some inorganic ions affects the sensitivity of bacteria to sunlight. However, the versatility in the concentrations required to demonstrate effect on the microorganisms among the different anions disables a safe result on the kinetics (Marugan et al., 2008).

Inorganic compounds could affect the pH of the water to be treated. If the inorganic compounds lead to alkaline conditions, it was shown that it increases the susceptibility of fecal bacteria to sunlight. This could be attributed to membrane damage, thereby affecting intracellular pH homeostasis (Curtis et al., 1992a; 1992b)

1.2.5. Dissolved oxygen

Photooxidation, with the resultant production of ROS, is the principal reason for the rapid decrease in bacterial counts in water of low turbidity. Disinfection can be 4–8 times faster in oxygenated water as compared with deoxygenated water (Reed, 2004). On a practical level, this could be achieved by the agitation of small-scale systems, either by hand or by using an air pump (Reed, 1997b).

1.2.6. Turbidity

It has been proved (Acra et al., 1984; 1990; Wegelin et al., 1994; Kehoe, 2001) that the water setting candidacy for solar disinfection must be quite clear. Waters with turbidity greater than 300 NTU should be filtered prior to disinfection for transmission reasons discussed earlier. However, in some cases in turbid waters there was a slightly bigger release of dissolved oxygen (Reed, 1997a). Also, due to the presence of particles, the absorption of rays can speed up the heating of water. This effect is still lesser than the need for transmission of rays.

1.3. Solar water disinfection on various microorganisms

SODIS is shown to be effective against the vegetative cells of a number of emerging waterborne pathogens (Boyle et al., 2008). Typical inactivation curves show an exponential decrease in the bacterial count against time, often with an initial shoulder or delay period, lasting 0.5–2 hours. After this initial shoulder, the inactivation kinetics generally follows a single-exponential decay function, giving a straight line on a log-linear graph (Reed, 2004). The same kinetics is observed for high initial bacterial populations, and higher inactivation rate constants are observed (Gomes et al., 2009b).

Most of the disinfection studies use fecal bacteria for model microorganisms and proved its efficiency. For example, Martin-Dominguez et al. (2005) have suggested that total coliforms (TC) are more difficult to eliminate than fecal coliforms (FC), such as E. coli, and require a much larger amount of irradiation to become inactivated.

Heaselgrave and Kilvington (2011) experimented with Acanthamoeba, Naegleria, Entamoeba and Giardia and exposure to solar light. It resulted in significant inactivation of these organisms. Sciacca et al. (2011) tested wild Salmonella, using surface water with high turbidity. Their treatment was efficient in completely inactivating Salmonella sp. Lonnen et al. (2005) tested SODIS in a variety of microorganisms, such as protozoa (the trophozoite stage of Acanthamoebapolyphaga), fungi (Candidaalbicans, Fusariumsolani) and bacteria (Pseudomonas aeruginosa, Escherichia coli). The results are summarized in Table 1.2.1.

Table 1.2.1. – Effectiveness of SODIS over multiple microorganisms (Lonnen et al., 2005).

Pathogen	SODIS	
	Reduction (log units)	*Time (h)*
A. Polyphaga (Trophozoites)	- 4.2 ± 0.2	6.0
A. Polyphaga (Cysts)	0.0 ± 0.1	8.0
E. coli DH5a	- 5.5 ± 0.3	2.5
P. aeruginosa	- 5.0 ± 0.2	2.0
B. subtilis (spores)	- 1.7 ± 0.4	8.0
C. albicans	- 5.4 ± 0.2	6.0
F. solani (conidia)	- 5.5 ± 0.2	8.0

1.4. Field applications of solar disinfection of drinking water

It is clear that SODIS is an efficient and a reliable method especially in the places where normal treatment of water is impossible, either for technical or economic reasons. This main advantage was exploited in many real-life applications, in Central and Latin America, Africa and East Asia. The results were quite promising and boosted the hopes of researchers to keep the ongoing studies and evolve the processes, utilizing the new findings in their practices (Gill and Price, 2010). To date, the most complete review has been provided by McGuigan et al. (2012). Some indicative results of field SODIS applications are presented below.

In Maasai villages in Kajiado province, Kenya, children who drank solar-disinfected water showed a 10% reduction in the incidence of diarrheal disease and a 24% decrease in severe diarrhea only 3 cholera cases were seen from 155 young children (5 years or under) who drank solar disinfected water as compared with 20 cases out of 144 young children in the control group (Martín-Domínguez et al., 2005).

Solar disinfection proved to be effective in the elimination of coliform bacteria, improving the water quality of the supply sources of the study zone. This makes it possible to ensure that its use would guarantee water free of pathogenic bacteria (Martín-Domínguez et al., 2005).

A field study was carried involving seven different developing countries (Bolivia, Burkina Faso, China, Colombia, Indonesia, Thailand, and Togo). After 1 year the number of households using solar disinfection had risen to over 10,000, with 84% stating that they intended to continue using this approach after the project had ended (Wegelin and De Stoop, 1999).

Finally, in more recent studies, the use of CPC reactors was implemented in the field, in order to increase the volume of the treated water. Although Sciacca et al. (2011) were focusing on the post-irradiation sterile conditions, they proved that SODIS in real application offered potable water in larger amount than the PET. Also, McGuigan et al. (2014) performed a long term evaluation of a 25-L CPC system, achieving total inactivation of the target microorganisms and Ndounla et al. (2014) in another 25-L CPC setup studied the effects of photo-Fenton reactants. The limiting step of the PET/borosilicate bottles is slowly overpassed, thus increasing freshwater available quantities.

1.5. Solar disinfection of wastewater

1.5.1. Initial considerations

Over the years, there have been published works demonstrating application practices, such as Davies-Colley et al. (1999) and Craggs et al. (2004) in waste stabilization ponds; they have indicated the efficiency of sunlight in disinfecting wastewater as well. However, the high retention times make them less attractive than catalytic processes as far as the application point of view is concerned. Nevertheless, developing countries benefited a lot from SODIS and can possibly benefit from solar disinfection of wastewater. Sanitation conditions in many African countries are marginally non-existent and untreated or poorly treated sewage end up polluting the drinking water supplies (Mwabi et al., 2011). It also occurs that the pre-mentioned regions are areas with a vast number of sunny days per year, so an application of the disinfecting action of light without other technological means could be attractive.

Solar wastewater disinfection follows the same principles as water disinfection; the effect of light against pathogens is the same, but practically, one of the major differences lies in the conditions microorganisms find in this water matrix. The presence of ions and nutrients, organic matter etc. provide solid ground for their survival and growth (Marugan et al., 2010). The process depends on several parameters (such as dissolved oxygen, pH), which complicate the study more than the drinking water one. Another important aspect is the temperature conditions that are present during the treatment. SODIS applications have reported elevated temperatures and synergistic actions of light and UV (Wegelin et al., 1994; McGuigan et al., 1998), in otherwise simpler water matrices. Reed et al. (2004) highlighted, among others, the presence of organic substances in SODIS water; the case of wastewater is an even enhanced one.

In parallel, many studies have initiated a cycle of investigations over the efficacy of solar disinfection for wastewater. This field was relatively unexplored and several aspects needed to be studied; this knowledge area welcomed works conducted by Kositzi et al., (2004) and Polo-Lopez et al., (2012) and Rizzo et al. (2014), that have investigated several aspects of solar photolytic and photocatalytic treatment in different microorganisms (*E. coli*, *Fusarium*). Interest was also given in the enhancement of the process by technical means, such as compound parabolic collector (CPC) solar photoreactors (Polo-Lopez et al., 2011; Bichai et al., 2012), with special focus given to the application and reuse of wastewater.

Furthermore, photolytic and photocatalytic methods have been used to target the microorganisms present within this matrix (Bichai et al., 2012; Ortega-Gomez et al., 2013; Giannakis et al., 2013, Rizzo et al., 2014). Studies performed by Wegelin et al. (1994) or McGuigan et al. (1998), set the milestones for solar disinfection (SODIS) of water. More specific studies have followed throughout the years, which highlighted the important parameters of the process, as the UVA dose, boosting efficacy and rendering SODIS a safe practice (Rincon and Pulgarin, 2004a; Boyle et al., 2008; Ubomba-Jaswa et al., 2009), by explaining the acute inactivation of microorganisms after a few hours of exposure to sunlight.

1.5.2. Modeling of solar disinfection of wastewater

Among researchers, the need to study and design applications of solar disinfection led to the modification of existing methods and models, in order to predict the outcome of the experiments. Modeling of bacterial inactivation was reviewed recently by Dalrymple et al. (2010) for photocatalysis of water, and its mechanisms are well explained; in this work the evolution was presented starting with the Chick model, the modification known as Chick-Watson Model, the delayed Chick-Watson Model, the Hom model and others; all were pre-cursors of the most sophisticated models to follow in the next years. For instance, the approaches of Geeraerd et al. (2000) or Mafart et al. (2002), or the modifications Marugan et al. (2008) have introduced for photocatalysis, all contributed in understanding the process in depth, while being application specific.

In fact, the photocatalytic models have been found to resemble the simple photolytic ones, as stated by Block et al. (1997) and Gomes et al., (2009). Although the disinfectant source changes, the formula remains similar; hence the use of the same model for photolysis and photocatalysis is valid. The change in the water matrix to wastewater, is however rather unexplored. Marugan et al. (2010) have stated the modification of disinfection potentials when the chemistry of the matrix is altered, Salih (2003) marked the importance of consideration of contamination load, the exposure to sun, Sichel et al. (2007) and Rincon and Pulgarin (2004a) highlighted the idea of minimum dose for inactivation and the importance of irradiation conditions on photolysis and Malato et al., (2009) in their review mention the importance of light dispersion. These are factors that all co-exist in wastewater and affect the process more than drinking water.

1.5.3. Field applications of solar wastewater disinfection

The efforts to implement field application of solar wastewater have been reported in works in tropical regions in Africa (Maïga et al., 2009), Brazil (von Sperling, 1999), New Zealand (Davies-Colley et al., 1997), and more, with success in terms of removal rates for bacteria, viruses and other microorganisms. The most extensive review belongs to von Sperling et al., (2005) who have reviewed the data of 186 facultative and maturation ponds around the world. Geographically speaking, the majority of these data were extracted from applications in Brazil and tropical regions.

Typically these applications are in the form of: primary facultative ponds, secondary facultative and maturation ponds (von Sperling, 2005). In another work, the use of lagoons was studied, with decreasing efficiency in the inactivation efficiency, as the series evolve (Xu et al., 2002). Finally the use of waste stabilization ponds for the reduction of effluent pollution was implemented (Davies-Colley et al., 1995) and the ecologically engineered high rate ponds with mixing (Craggs et al., 2004) are some of the forms in which solar wastewater disinfection was implemented. In most of the cases the limits of discharge for irrigation were achieved, but it requires long exposure times which discourage the application.

1.6. Regrowth of microorganisms

The greatest disadvantage of UV disinfection of wastewater, either from UV lamps or solar, is its point efficiency, which lacks residual effect (White, 2010). The effluent of the process will include inactive (completely decayed microorganisms), injured (not lethally damaged, potentially dangerous if healed) and microorganisms that escaped the process. The absence of the residual disinfecting factor could possibly allow the reactivation of injured microorganisms, if favorable downstream regrowth conditions are presented (Hijnen et al., 2006; Hallmilch and Gehr, 2010). The remaining bacteria could increase their numbers while being in the treated effluent, due to a variety of reasons; for example, the existence of nutrients and related chemicals in wastewater could provide an abundant food source for the bacteria, allowing them to metabolize and reproduce (Marugan et al., 2010). Hence, the main three factors that are responsible for bacterial regrowth are (Guo et al., 2011): i) the growth of injured microorganisms ii) the reactivation and iii) the regrowth of the reactivated microorganisms.

Bacterial viability and survival after the UV disinfection has been a subject of big debate for decades among the scientific community, with varying explanations and percentage distribution among the reasons for regrowth. The main misleading factor was the reduction of cultivable count numbers in the plates enumerating the bacteria after the process. It was believed that the reduction of colonies could mean direct and permanent reduction in the actual bacterial number.

Long after regrowth as a phenomenon was observed, the ‘‘viable but non-cultivable’’ (VNC) hypothesis was developed to explain the absence of bacterial counts at the end of the treatment, but the re-appearance after a time period, and supported by various researchers (Xu et al., 1982; Roszak and Colwell, 1987). This hypothesis suggests that not all the bacteria are destroyed by the action of light, but there is a significant number that is not able to reproduce themselves.

This ability was measured by the enumeration of colonies in bacterial plates of various mediums. Reed (2004) in his work reports a number of experiments conducted that mislead the conclusions, due to use of selective medium agars; the use of non-selective media led to bigger bacterial counts, concluding that non-selective mediums must be used e.g. for SODIS experiments. Barer et al. (1993), detected the excess numbers by metabolic activity methods and verified the difference in the bacterial numbers.

DNA is one of the main targets of both direct and indirect actions of UV light, through the direct dimerization of thymines or indirect attacks by ROS (Pigeot-Remy et al., 2012), and the generated ROS, especially hydroxyl radicals, interact with the intracellular components of the cell. Bacteria possess the ability to repair a number of their DNA damages through two main mechanisms, light-dependent ones, namely photoreactivation, and light-independent (dark repair) which help them recover from the damages inflicted during phototreatment.

The repair of the UV-induced DNA damage, namely cis-syn-cyclobutane pyrimidine dimers (CPDs) (Hallmich and Gehr, 2010) that leads to reactivation of the microorganisms is demonstrated by various methods that include photoreactivation (light mediated repair) and dark repair mechanisms (nucleotide and base excision repair). The light-induced DNA repair is based on the activity of the key enzyme photolyase, which binds to complementary DNA strands and efficiently breaks pyrimidine dimers. However, this enzyme only functions as a DNA repair mechanism when visible light is available for activation (preferentially in the violet to blue range of the spectrum).

In contrast, the nucleotide and base excision repair includes numerous molecular steps such as damage recognition by specific proteins, assembly of a DNA repair complex, incision of the DNA backbone on either side of the damage, removal of the damaged strand, and filling of the remaining gap by DNA polymerase followed by attachment of the replacement DNA to the rest of the strand with a DNA ligase (Britt, 1996; Amsler, 2008). The count of viable organisms can increase by several log values due to photoreactivation, thus representing an obstacle to reaching safe disinfection levels and a potential disadvantage for application of UV disinfection (Hallmich and Gehr, 2010).

1.6.1. Photoreactivation (PHR)

It wasn't observed until the 50's that the visible light, which withstands long wavelengths, is able to heal the biological effects of the UV rays. This discovery, of photoreactivation (PHR), identified a very common DNA repair mechanism, which was interpreted very quickly; PHR was responsible to reverse the damage inflicted to nucleotides by short wavelength UV (Cleaver, 2003).

Photoreactivation is a process where microorganisms utilize light in the 310-480 nm wavelength range, spanning from near-UV to blue light to activate a specific enzyme, photolyase, in order to recover activity through the repair of pyrimidine dimers in the DNA and occurs in conditions of prolonged exposure to (visible) light (Hijnen et al., 2006; Nebot Sanz et al., 2007; Shang et al., 2009). This bacterial ability is a heritage of evolution through time, to protect themselves from the natural ultraviolet rays from the sun (Quek and Hu, 2008). PHR is inversely related to UV doses; higher doses are followed by low reactivation rates. Low doses are expected to demonstrate higher repair rates (Nebot Sanz et al., 2007).

Systematic quantitative study of photoreactivation, the more important of the two mechanisms, has suggested a two-step reaction scheme (Harm, 1980):

Step 1: Formation of a complex between a photoreactivation enzyme (PRE) and the dimer to be repaired (Nebot Sanz et al., 2007).

Step 2: Release of PRE and repaired DNA. The restoration of the dimer to its original monomerized form is absolutely dependent upon light energy intensity (Nebot Sanz et al., 2007); energy is needed to repair damage (Guo et al., 2011).

1.6.2. Dark Repair (DR)

Like photoreactivation, a quite related process but in different conditions is dark repair. The dark repair mechanism, as its name suggests, can repair the damaged DNA without light. This mechanism is a multi-enzyme repair process involving the excision of dimers (Harm, 1980). It also called nucleotide excision repair and requires coordination of over a dozen proteins to excise and repair the damaged DNA segment (Shang et al., 2009). The dark repair methods are regulated by the expression of recA, a critical gene in the bacterial cell, with well-known properties (Sinha and Hader, 2002; Jungfer et al., 2007). The nucleotide and base excision repair, includes numerous molecular steps, including identification of the damage, assimilation of a repair complex, incision and removal of the damaged strand and filling with DNA polymerase, finalized by attaching the replaced DNA with the rest of the strand with a ligase. (Britt, 1996; Amsler, 2008; Shang et al., 2009).

Dark repair has been demonstrated in almost all bacteria. Although spores have no active metabolism, the repair starts upon germination. Dark repair has been demonstrated in viruses, too; however, since viruses have no metabolism, they cannot repair damage to their genome themselves. Nevertheless, several viruses have been shown to use the repair enzymes of the host cell (Hijnen et al., 2006). Finally, it seems that it is crucial to monitor the effluent after treatment with UV, mostly because the organic matters present could be favorable conditions for dark repair (Rincon and Pulgarin, 2007a).

Generally, rates of PHR are greater than dark repair ones, fact that makes the latter almost negligible under some cases. On the other hand, dark repair is less predictable and varies among different species' strains and conditions (Shang et al., 2009).

1.7. Factors affecting bacterial regrowth after UVC irradiation

Bacterial regrowth has been widely studied for UVC disinfection, a fact that provides a relevant starting point to address regrowth after solar disinfection, which has been only scarcely studied. Accordingly, a review of regrowth after UVC treatment is presented below.

1.7.1. Effect of temperature

The influence of temperature is of great importance, especially when it comes to real-world applications and case studies; modeling of real situations is often manifested by fluctuations in temperature. The reactivation of *E. coli* is possible when the treated effluent is released in natural water bodies, but it is dependent on temperature among other factors.

Chan and Killick (1995) performed a series of experiments that proved the correlation between temperature and regrowth potential. Lower temperatures could reduce the regrowth dynamics of both photoreactivation and dark repair to a certain extent. These findings were verified and extended by Shang et al. (2009) that stated the elasticity of the regrowth dynamics response between 10 and 35 °C, observing the minimization of the potential under 10°C.

Also, comparing the two mechanisms within the same temperature range, it was shown by Chan and Killick (1995) that the reactivation was more profound due to photoreactivation than dark repair and reached a higher level over the nine hour period of study when compared with dark repair rates.

1.7.2. Effect of salt and nutrient contents

UV-C radiation appears to be a potential alternative to chlorination, if it is employed in plant with continuous flow of water. However, the storage of UV-treated water in tanks during its passage through different stages of the plant could permit bacterial reactivation and recovery. Determination of micronutrients could be helpful to draw conclusions about the bacterial after-growth dynamics (Munshi et al., 1999). The experiments of Munshi et al. (1999) proved that given the proper conditions the bacteria recover within 24h. Within the same framework, it was shown (Shang et al., 2009) that especially for reactivation by light the supply of nutrients demonstrated higher numbers, attributed both to PHR and regrowth.

In an effort to predict the behavior in sea water, which is a highly saline receiving environment for incoming populations, it was concluded that the same samples diluted in varying salinity levels present favor over less saline solutions. Above a 30% of the salinity of synthetic sea water the ability of the *E. coli* to photoreactivate declines sharply and levels off at 70% of the maximum salinity. For those cells in a saline environment reactivation was slower and a lower maximum recovery was obtained. Dark repair rates were

extremely limited in those cells exposed to the saline environment which was produced from synthetic sea water. Also, in such environments, the temperature plays a secondary role, a lesser one compared to isotonic conditions (Chan and Killick, 1995).

1.7.3. Effect of UV source, dose and intensity

As described in previous chapters, low pressure lamps produce a monochromatic, single wavelength peak, which affects only the DNA (Nebot Sanz et al., 2007). The medium pressure lamps produce a broad spectrum of UV wavelengths that inflict irreparable damage not only on cellular DNA, but on other molecules, such as enzymes (Kalisvaart, 2004). Hence, since the bacteria are severely damaged the reactivation is lower in medium pressure (MP) lamps than in low pressure (LP) ones. A quantification is presented by Shang et al. (2009) and a comment on the intensity; the extent of photoreactivation remained similar at the same UV dose (12 mJ/cm^2) but different UV intensities (0.12 and 0.2 mW/cm^2). However, in higher doses, as 40 mJ/ cm^2, Halmilch et al. (2010) in their work stated a number of experiments which proved that both in vitro and in vivo, the photoreactivation was similar between the two types of lamps.

The explanation on this is provided by Lindenauer and Darby (1994), who state that at the higher UV doses, no further UV inactivation occurs with increasing UV dose. The increase of the dose, will not affect the shielded microorganisms, but will only inflict more damage to the irradiated ones, reducing the reactivation potentials, without reducing the actual number of microorganisms present in water.

1.7.4. Effect of other water quality parameters

It is obvious that there are other water quality parameters that could affect the outcome of the experiments but some consideration has to be made, mostly in terms of dose and transmittance. There are a lot of substances present in wastewater that can absorb light waves. This effect is true, for both UV rays of sterilization and photoreactivating light. However, the effect on shadowing within the water is much more important in the efficiency of UV rays as a critical parameter in the following bacterial regrowth.

To begin with, in terms of dose, regardless of the substances or clarity, low UV doses lead to low inactivation rates and less damage. Subsequently, photoreactivation increases, as long as the dosage is low and the damage is sub-lethal. This is not surprising and if the transmittance is taken into consideration, which is a key parameter in UV disinfection, it could be concluded that as suspended solids rise, the dimer formation decreases and photoreactivation rate is greater (Lindenauer and Darby, 1994).

Suspended solids will influence both initial inactivation and subsequent photoreactivation directly and indirectly: An organism may be directly shielded from UV light by being embedded within a bigger particle. However a cell may also be protected indirectly by the fact that the actual average UV intensity in the

reactor is decreased either by scattering (i.e. longer light travel path required) or by absorption by organic particles (Lindenauer and Darby, 1994).

Theoretically, non-turbid, clear waters demonstrate bigger transmittance levels while the reverse could be true for poor water quality. Nevertheless, it was shown (Lindenauer and Darby, 1994) that the water quality parameter had a greater impact in inactivation than in PHR levels, leading to lower inactivation rates. Finally, according to the same source, all the above are true for low UV doses; for high doses, the effects of water quality were negligible.

1.7.5. Effect of initial bacterial population

The philosophy behind the way the initial population is considered has changed over the last years. Although Lindenauer and Darby (1994) supported that no significant correlation exists between photoreactivation and the initial number of coliform in wastewater, at any dose; they found out that in low doses, the surviving coliforms affected the reactivation. Craik et al. (2001) explained this noting that if the initial population is high, there is a big chance that there will be a part of it going through unharmed due to shielding (by each other) and bad mixing. Gomes et al. (2009b) confirmed these findings, discovering high energy requirements to disinfect such samples. As far as photoreactivation is concerned, its fractions for values below 100.000 CFU/100ml, the required energy increases (Halmich and Gehr, 2010). Dark repair hasn't demonstrated some special behavior and probably falls in the category Craik et al. (2001) mentioned.

1.7.6. Effect of pre-, simultaneous or extended illumination by visible light

Solar radiation consists of a wide range of wavelengths including visible and UV light, which can activate repair enzymes and cause cell damage, respectively. Consequently, both inactivation and repair can occur at the same time (Yoon et al., 2007).

Pre-illumination with non-coherent monochromatic 446, 466, 570 and 685 nm radiation, as well as with polychromatic red and IR radiation at room temperature, leads to increased cell survival after subsequent irradiation with UV light. This increase in survival from UV irradiation could be due to infrared heat-shock response; the increased survival rate can affect the downstream numbers of bacteria able to regrow (Lage et al., 2000). For example, if the samples are exposed to UV irradiation and visible light at the same time, the recovery of the microorganisms by the photoreactivating light is halved compared to UV irradiation when applied alone (Halmich and Gehr, 2010). However, if the samples remain for an extended period under irradiation, they get even more inactivated than photoreactivated, leading to smaller numbers and less regrowth (Yoon et al., 2007).

1.8. Studies on the factors affecting survival and regrowth of solar-treated bacterial strains

The application of solar treatment systems requires two main axis of caution: disinfection and post-irradiation events. Over the years, solid knowledge concerning the exploitation of solar power to reduce microorganisms in water has been accumulated, which could be extrapolated to wastewater (Lonnen et al., 2005; Berney et al., 2006; McGuigan et al., 2011), in various treatment methods, such as PET bottles (Ndounla et al., 2013), CPC reactors (Sciacca et al., 2011) or, the most feasible in the context of developing countries, in superficial flow constructed wetlands (Kivaisi, 2001) or waste stabilization ponds (Sinton et al., 2002).

The second axis deals with the fate of microorganisms, once disinfection is over. In natural aquatic environments carbon availability and temperatures are much lower and therefore, the expected specific growth rates of enteric bacteria are lower (Berney et al., 2007). There are a number of works concerning the occurrence of microorganisms in natural waters, such as rivers (Avery et al., 2008), lakes (Haller et al., 2009), estuarine (Chandran and Hatha, 2005; Kay et al., 2005) or brackish water (Mezrioui et al., 1995) and seawater (Noble et al., 2004; Darakas et al., 2009).

However, only few studies deal with the microbial post-irradiation fate of microorganisms when treated wastewaters are discharged in these water matrices (for instance after UVC: Chan and Killick, 1995; Sinton et al., 1999, after solar UV exposure). What is mostly discussed is the fate of microorganisms occurring in different water types, while others include the simultaneous application of solar irradiation; Yukselen et al. (2003) have studied the inactivation of bacteria in seawater, Jenkins et al. (2012) the die-off in pond waters etc., thus providing information on the concurrent action of adaptation and illumination.

1.8.1. Effect of ions, salts and nutrient content

Rincon and Pulgarin. (2004a) observed that after solar illumination and reproduction of the same experiments in the laboratory, almost all samples that were based on natural waters, which contain even lower concentration of dissolved organic carbons, presented regrowth in dark conditions. This was unexpected, since low organics concentration should have limited the regrowth dynamics, as Tassoula (1997) showed, because low COD values lower survival dynamics. Natural water bodies as a receiving medium are interesting, because it is believed that enteric bacteria may survive in natural waters but are not able to multiply themselves (Roszak and Colwell, 1987). In natural aquatic environments carbon availability and temperature are much lower and, therefore, the expected specific growth rates of enteric bacteria are lower (Berney et al., 2007).

1.8.2. Effect of the bacterial strain

Rincón and Pulgarin (2004c) experimented with seeded and natural microorganisms (*E. coli*) and significant differences between their behavior in dark repair; the differences in photolysis, resistance and subsequent dark recovery process between pure *E. coli* culture and bacterial consortia present in wastewater, illustrates the difficulty to extrapolate pure-culture survival data to bacterial response in a real natural polluted water. Therefore, experiments with lab strains and conditions can show essential mechanisms and significant trends, but a straightforward translation to field conditions would be risky.

1.8.3. Effect of storage conditions

Sciacca et al. (2011), have highlighted details on the storage conditions affecting bacterial regrowth. It has been mentioned that the use of non-sterile containers can result to bacterial regrowth, compared to its prevention, when sterile ones were used instead.

1.9. Regrowth modeling

1.9.1. UVC disinfection and post-irradiation modeling

Historically, the first attempt in mathematical representation of the bacterial life cycle was made by Verhulst in 1838 to interpret biological population growth. The models used to describe the repair rate are relatively simple, representing the repair potential ex ante.

$$S = \frac{N_t}{N_o} 100$$

Where:

N_t is the concentration of *E. coli* at time of exposure for time t in the repair conditions.

N_0 is the concentration of *E. coli* immediately after UV disinfection (logCFU/mL), and

S is the repair rate after UV disinfection (%)

However, the analyses that took place in recent years by Nebot Sanz et al. (2007) followed the model proposed by Kashimada et al. (1996), described by the following equation:

$$\frac{dS}{dt} = k_1(S_m - S)$$

Where:

S_m is the maximum survival ratio (N_m/N_o) x 100 (%),

N_m is the maximum bacterial population and

k_1 the first-order reactivation rate constant.

Nebot Sanz et al. (2007) modified the Kashimada model, because it didn't fit their experimental data, mainly at the beginning of the curve, when an induction period was observed. The new proposed model is represented by the following equation:

$$\frac{dS}{dt} = k_2 \cdot (S_m - S) \cdot S$$

where k_2 is the new growth second-order reactivation rate constant.

The model has the advantage that both kinetic parameters: S_m and k_2, have a clear physical significance. On the one hand, S_m is the maximum limit of the microorganisms' survival by reactivation, and on the other hand, k_2 represents the rate at which that value is reached.

By integration of this equation and solution for S, they produced this form:

$$S = \frac{S_m}{1+\left(\frac{S_m}{S_o}-1\right)\cdot e^{-k_2 \cdot S_m \cdot t}}$$

The experimental data acquired for dark repair kinetics, did not fit this equation. Therefore, they introduced a zero-order kinetic for the decay process they noticed, $\frac{dS}{dt} = -M \cdot t$, where M, mortality, is a zero-order decay rate constant.

With the introduction of this constant to their initial modification, the proposed model has the form:

$$S = \frac{S_m}{1+\left(\frac{S_m}{S_o}-1\right)\cdot e^{k_2 \cdot S_m \cdot t}} - M \cdot t.$$

In a more recent work (Velez-Colmenares et al., 2012) a model has been proposed, which describes the photoreactivation kinetics after UVC disinfection, as an improvement of the Kashimada model.

$$S_t = S_i \cdot e^{-M_s t}$$

t: is the time in minutes,

S_t is the survival after ultraviolet disinfection at time *t*,

S_i is the survival of the decay phase at an initial time *t* and

M_s is the solar decay rate constant (min^{-1}) that only depends on the solar radiation to which the sample is exposed.

Grouping the corresponding expressions for the growth and decay phases, the equation that defines the solar reactivation kinetic model:

$$S_t = (S_m \cdot e - M_s \cdot t) - (S_m - S_o) \cdot e^{-(k_s + M_s)\cdot t}$$

k_s is the growth rate constant of solar reactivation (min^{-1}).

1.9.2. Solar disinfection and post-irradiation modeling

Apart from UVC disinfection, there are not enough systematically obtained data in order to model the bacterial kinetics in the solar post-irradiation period. Bacterial regrowth has been assessed in some works as an indicator of the quality of disinfection (Rincon and Pulgarin, 2004a; 2007a), but except for the biological aspects which are very well understood (Sinha and Häder, 2002), the prediction of the phenomenon is rather fuzzy. Many authors in their works have studied the regrowth after the phototreatment of water (Rincon and Pulgarin, 2007a; Polo-Lopez et al. 2012), while some monitored the survival in wastewater (Bichai et al., 2013; Giannakis et al., 2013). The presence of nutrient sources in wastewater pose a direct threat of re-contamination of the water, so the prediction models should turn their attention on the phenomenon and the suggested pre-treatment conditions.

1.10. Thesis aims and objectives

The review of the main parameters affecting bacterial removal by solar light in water and wastewater, as well as the ones that influence bacterial regrowth after UV disinfection, has made clear that the process is a complex dynamic system with interactive factors. Despite having modeled the majority of the involved driving forces, i.e. growth kinetics and solar-assisted bacterial inactivation for a long time, there are still efforts to explain the events taking place. By isolating factors and testing the interactions among them, one can draw valuable conclusions that build the knowledge base and influence the actual design and reuse practices.

In solar wastewater disinfection, it is crucial to predict the disinfection efficiency. The majority of the knowledge base comes from the pond applications and similar theoretical assessments. Some studies implemented simulation of the involved physicochemical parameters (Curtis et al., 1992a,b; Ouali et al., 2013) or the hydrologic (Persson et al., 2003) and hydraulic aspects (Olukani and Ducoste, 2011), in order to efficiently predict the outcome of the designed process. The interaction between the parameters has often challenged research and the action mode/pathway of inactivation. In the same philosophy, von Sperling et al. (2005) have reviewed the bacterial die-off rates for the creation of equation modeling in ponds. Optimization of the treatment conditions was often under question (Bracho et al., 2006) and the practical problems often led to efforts to upgrade the existing pond applications (Craggs et al., 2003). Less studied, but a valid question is the tuning of the treatment conditions in technical means of solar wastewater disinfection (Polo-Lopez, 2011; Bichai et al., 2012) in order to re-use the reclaimed water.

However, literature has significant gaps concerning the understanding of crucial matters on the behavior of solar-treated wastewater microorganisms during and after treatment. Significantly, very limited research has been performed on the inactivation kinetics in solar disinfection of secondary effluent, particularly on the variables affecting this process. Even more, the effect of the solar disinfection conditions on the post irradiation period has been hardly explored. In accordance to the complexity of the process, the critical question of bacterial regrowth after solar disinfection has not been systematically assessed. Dark repair, photoreactivation and long-term monitoring of the bacterial survival after solar wastewater disinfection are some of the questions the present work is putting under question.

1.10.1. Main objective

The main focus of this Thesis is to explore the fundamental aspects governing the solar disinfection of wastewater, as well as the subsequent, post-irradiation events. The investigation is therefore split into two major parts, namely solar treatment and bacterial regrowth. More specifically, an extensive investigation in the internal and external parameters affecting solar wastewater disinfection is attempted in order to predict

the success of the treatment and the quantification of the bacterial dark repair (mainly) and photoreactivation.

1.10.2. Specific objectives

The specific goals of the Thesis are:

- To intensively study the effect of intensity, initial bacterial concentration and treatment temperature on the overall inactivation efficiency of the process. Also, to measure the subsequent dark repair and to predict the short and long term survival of bacteria.
- To assess the importance of classic standardization indicators of solar water treatment, in wastewater (e.g. dose effects).
- To model the two distinct processes; the acquisition of a disinfection model, as well as regrowth prediction.
- To estimate the survival of solar-treated bacteria after their disposal in various environmental water matrices and light conditions (DR and PHR).
- To assess the implications possibly encountered by temporal weather changes and mechanical applications, as well as the enhancement of the treatment by AOPs (photo-Fenton and high frequency ultrasound) towards bacterial regrowth elimination.

1.10.3. Thesis Organization

In order to effectively accomplish the goals set in the objectives section, the experimental parts are elaborated in accordance to the presented subchapter. The experimental conditions, the performed tests, their analyses and the conclusions of each part are explained in detail in the next chapters.

In Chapter 2, the methods that were common in all experiments are presented, to set the framework of the work, in terms of microbiology and simulation conditions. The preparation of the microorganisms, the wastewater matrix employed in all experiments, as well as details on the solar simulator are given.

Afterwards, a systematic study on the effects and interactions of the fundamental parameters governing solar disinfection was performed, whose results are presented in Chapter 3. Firstly, a multilevel design of experiments is shown, focusing on the disinfection events. An evaluation of the regrowth, in both short and long term is performed, as a second evaluation criterion, and finally, considerations on the role of solar dose are expressed. The chapter closes with modeling of solar disinfection in various intensities and an assessment on the prediction of bacterial regrowth.

Chapter 4 deals with the post-irradiation events, and the microbial fate in various environmental conditions. The regrowth as a function of the temperature and four different dilution media is presented, followed by a study on the photoreactivation potential of solar-treated wastewater. Five different monochromatic and one

polychromatic fluorescent lamps were employed to investigate the regrowth dynamics of the phototreated microorganisms.

In Chapter 5, the effects of interrupted, non-continuous irradiation on disinfection efficiency are assessed, either when high or of low frequency intermittent light was employed. Simulation of CPC disinfection was performed and the use of AOPs for the complete exploitation of the recirculating water was studied. Photo-Fenton and ultrasound were the subject AOPs, as means of eliminating the regrowth risk.

Finally, the Thesis closes with the overall conclusions deriving from this investigation in Chapter 6. An evaluation of the tests described before is performed; an overall vision of the effectiveness of solar disinfection and the potential regrowth are given as final remarks.

Chapter 2. Generally employed materials and methods

In this chapter, the general experimental methods and techniques common to all studies in chapters 3 to 5 are described. For each specific study, the methodological approach and its materials and methods are presented later, in the beginning of the corresponding chapter or subchapter.

2.1. Microbial methods

2.1.1 Selected microorganism

Instead of analyzing a variety all microorganisms currently present in secondary wastewater effluents, the use of an indicator microorganism was preferred. *Escherichia coli* is currently the most studied microorganism in genetics, is commonly found in the human intestine and indicates probable upstream water pollution, if found. Although its suitability as a fecal indicator bacterium has been questioned (Berney et al, 2006; Sciacca et al. 2010 and more), there are strong facts supporting its use in such studies (Odonkor and Ampofo, 2013). More specifically, in this work the *E. coli* K-12 strain was used. The specific is non-pathogenic, consists a reliable indicator already used in a vast number of works in solar disinfection, because it approximates well the Gram-negative wild type (Spuhler et al., 2010). Its simplicity in laboratory cultivation have established it as a valuable tool in similar works, although its response might differ slightly among the various strains.

2.1.2. Preparation protocol

The *E. coli* strain K-12 (MG1655 was supplied by the "Deutsche Sammlung von Mikroorganismen und Zellkulturen". Luria-Bertani (LB) broth (10 g BactoTM Tryptone, 5 g Yeast extract, 10 g NaCl, per liter) was prepared for each experimental series by suspension in Mili-Q water and heat-sterilization by autoclaving. One colony was picked from the pre-cultures and inoculated into a 50 mL sterile falcon, containing 5 mL of LB broth. The flask was then incubated at 37°C under stirring at 180 rpm in a shaker incubator. Further dilution was made after 8 h in 1% v/v and the new solution was incubated under the same conditions for 15 more hours.

Cells were harvested during the stationary phase by centrifugation from batch culture for 15 minutes at 5000 rpm and at 4°C, in a universal centrifuge. After centrifugation the bacterial pellet was re-suspended

and washed for 5 minutes under the same centrifugation conditions. Rinsing was repeated twice and the final pellet was re-suspended into the initial volume. Washing and re-suspension was done in heat-sterilized pure saline solution (NaCl 8g/L and KCl 0.8 g/L, neutral pH, regulated with NaOH). The above described procedure resulted in a bacterial pellet of approximately 10^9 colony forming units per milliliter (CFU/mL).

2.2. Microbial enumeration

Bacterial colonies were enumerated by the pour-plating method on 9-cm petri dishes containing plate count agar. Samples were properly diluted to maintain measurable counts on the plastic Petri dishes (15-150 colonies per plate). The detection limit for diluted samples is 10 CFU/ml, and 1 CFU/mL for the undiluted. In all cases, even under 15 colonies per dish, the actual reading of CFU/mL is reported here. In each measurement, 0.5-1.5 mL was drawn, plating was done in duplicates, and 5% difference (maximum 10% in low numbers) was obtained, or results were discarded.

2.3. Composition of the synthetic wastewater

The preparation of the synthetic wastewater was made by dissolving 160 mg/L peptone, 110 mg/L meat extract, 30 mg/L urea, 28 mg/L K_2HPO_4, 7 mg/L NaCl, 4 mg/L $CaCl_2 \cdot 2H_2O$ and 2 mg/L $MgSO_4 \cdot 7H_2O$ in distilled water, as instructed by OECD (1999). The COD of the solution was 250 mg/L. As done in other works (e.g. Velez-Colmenares et al., 2011) in order to better approximate the values of secondary effluent, a 10% dilution was used. 1 mL of concentrated (10^9) bacterial solution per liter was added in the solution, to reach an initial population of 10^6 CFU/mL. The transmittance levels approach the real secondary effluent ones.

Figure 2.3.1: The synthetic wastewater used in the present Thesis. A slight yellow-ish color is visible.

Chemicals were acquired from the following suppliers: Peptone from I^2CNS, Switzerland, meat extract, NaCl, $CaCl_2 \cdot 2H_2O$, $MgSO_4 \cdot 7H_2O$ and $FeSO_4 \cdot 7H_2O$ from Fluka, France, urea from ABCR GmbH, Germany, K_2HPO_4 and H_2O_2 from Sigma-Aldrich, Germany.

2.4. Simulated solar light specifications

The light source was a bench-scale Suntest CPS solar simulator from Hanau, employing a 1500 W air-cooled Xenon lamp (model: NXe 1500B), with effective illumination surface of 560 cm^2. A portion of 0.5% of the emitted photons fall within a range shorter than 300 nm (UVB) and 5-7% in the UVA area (320-400 nm). After 400 nm, the emission spectrum follows the visible light spectrum. The solar simulator also contains an uncoated quartz glass light tube and cut-off filters for UVC and IR wavelengths. The intensity levels employed were monitored by a pyranometer and UV radiometer (Kipp & Zonen, Netherlands, Models: CM6b and CUV3). Measurements took place at the beginning of each experiment to ensure the desired emission levels, and lamps are changed every 1500 h, in all different Suntest apparatus used in the research period.

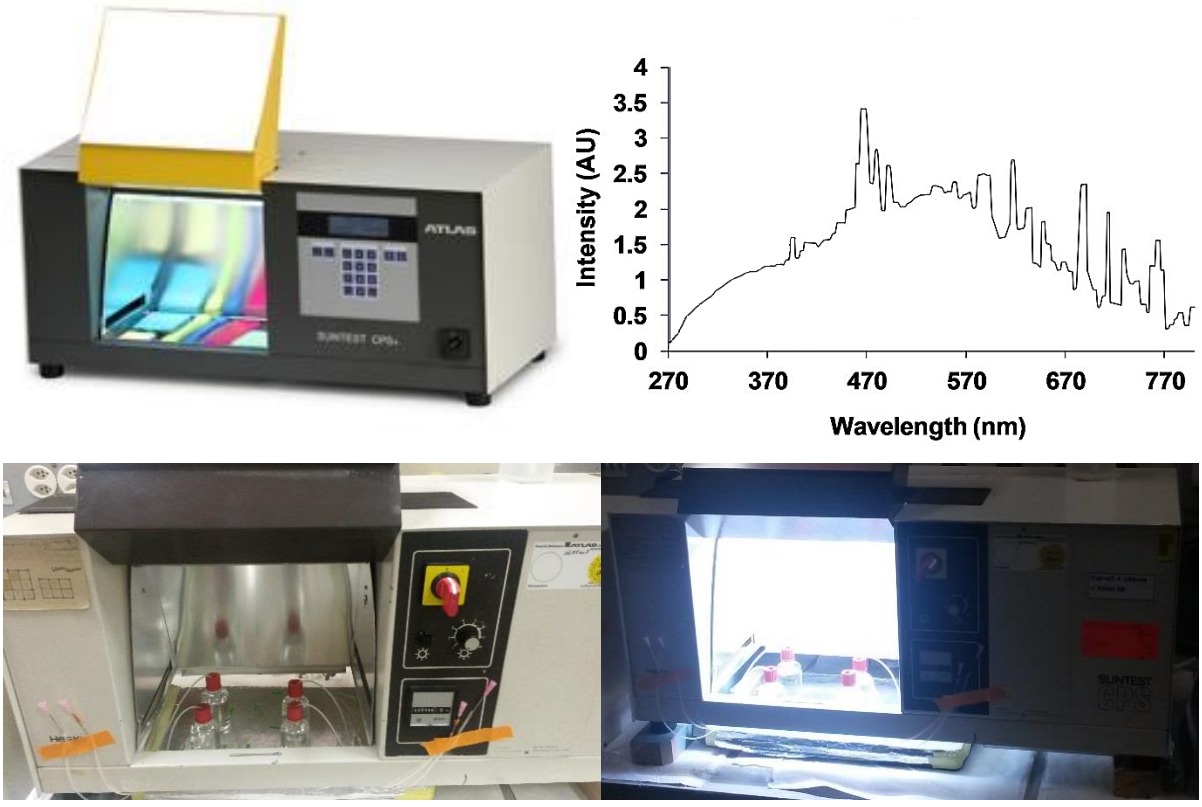

Figure 2.4.1: The Suntest solar simulator: image, lamp output spectrum and operation.

Chapter 3. Variables affecting solar disinfection and post-irradiation dark repair in secondary treated wastewater

3.1. Methodological approach

The current chapter focuses on the disinfection of wastewater by solar light alone and a statistical approach has been done, to investigate the behavior of microorganisms in synthetic secondary wastewater, when exposed to sunlight. In summary, a full factorial design has been employed to further investigate the effects of basic parameters on *E. coli*, in batch tests simulating solar disinfection of secondary treated wastewater. A full factorial design of 240 experiments (DOE) was employed to investigate the effects of i) exposure time (1, 2, 3 and 4 h), ii) treatment temperature (20, 30, 40, 50 and 60˚C), iii) initial bacterial concentration (10^3, 10^4, 10^5 and 10^6 CFU/mL) and iv) sunlight intensity (0, 800 and 1200 W/m^2) on *Escherichia coli* disinfection and survival for a subsequent 48-h dark control period. Also, the importance of dose was investigated and its correlation with the control variables. Finally, the effects of sunlight intensity were modeled, with respect to disinfection and post-irradiation events, in experiments without temperature control.

Temperature and irradiation were varied in order to obtain a range of conditions. Some of the conditions tested are hardly feasible in natural conditions, but achievable, for instance, with mechanical assistance by CPCs or solar collectors. The experimental set-up allowed controlling the temperature at desired levels. The point of this experimental sequence was to investigate the potential synergies and antagonistic effects that temperature would create and influence, during solar disinfection. In any case, with this method of artificial temperature control, the possible combined effects are expected to be observed, positive or negative, according to the potential acquired temperatures in a solar disinfection application.

3.1.1. Simulated solar light specifications

Concerning the applied intensities of the temperature controlled experiments, 800 W/m^2 is a feasible value of solar irradiance, in the areas candidate for solar disinfection, in general. On the other hand, 1200 W/m^2 is a relatively high value chosen in purpose, defining i) a neighboring value to the highest intensity able to reach earth's crust and ii) a value with profound results, in order to stress the modifications in bacterial

kinetics; an initial investigation (data not shown) indicated that values around 1000 W/m^2 had the desired effect, but not as obvious as the presented ones.

3.1.2. Reactor configuration

The batch tests that withheld the bacterial samples during temperature-controlled experiments were cylindrical double-wall Pyrex glass bottle reactors (outer diameter 7.5 cm, inner diameter 6.5 cm, height 9 cm, irradiation surface 20.41 cm^2), which allow control of the temperature and UVB transmission, as well as mild stirring with magnetic stirrer. Water was taken from the body of the irradiated sample, still under stirring.

3.1.3. Bacterial enumeration

Viable bacterial counts after solar treatment were assessed by pour-plating on non-selective agar as suggested by Reed (2004) and Rizzo et al. (2004), in order to obtain all viable counts, after proper dilution in sterile saline solution to achieve measurable counts on the dishes (15-150 colonies). Experiments were performed with duplicate plating in three consecutive dilutions.

Hourly measurements of the bacterial numbers took place for the temperature-controlled experiments, and approximately 1 mL was drawn; during the systematic intensity research, sampling was made each 30 min, or 20 min for intensities > 1000 W/m^2. Regrowth tests were conducted 24 and 48 h after sampling; samples remained in the dark covered by aluminum foil in room temperature (~25˚C).

3.1.4. Experimental design set-up

Full factorial DOE was chosen to investigate the influence of the important parameters of treatment time, temperature and initial bacterial population, on the disinfection process and their possible synergies and/or interactions. When a full factorial DOE is chosen, the responses are measured at all the combinations in the different experimental levels. Combining the different factor levels reflects the conditions in which the various responses are measured by the actual experiments. It was chosen over fractional factorial design to prevent confounding and data credibility loss. Table 3.1.1 presents the parameters under study and their respective levels.

Table 3.1.1. – Design of experiments' parameters, levels and respective units.

Parameters	Levels		Units
Time	4	1, 2, 3, 4	h
Initial Population	4	10^3, 10^4, 10^5, 10^6	CFU/mL
Temperature	5	20, 30, 40, 50, 60	˚C
Light Intensity	3	0, 800, 1200	W/m^2

MINITAB for Windows was used for the data analysis. The DOE was configured as a Multilevel Full Factorial Design, because of the different levels within the parameters. The timespan of the experiment was 4 h, initial bacterial population was chosen to vary from 10^3 to 10^6 CFU/mL and temperature was analyzed for five levels, from 20 to 60˚C. Data analyses are presented grouped by light intensity levels: i) 0, ii) 800 and iii) 1200 W/m^2. Table 3.1.2 summarizes the DOE for each intensity level. The control (response) variables were process efficiency and regrowth after 24 and 48 h. Although the disinfection kinetics are monitored and presented, the main focus when Process Efficiency is used as a control variable, is to evaluate the combination of the defined disinfection parameters in an unambiguous indicator, which is the number of bacteria inactivated in a pre-set time. Finally, the statistical evaluation of the results through Minitab was simplified, since kinetics comparison would not be feasible.

The results of the control variables are shown with the aid of Time vs. Population graphs, contour and main effects plots. The sampling intervals are 1h in all cases except for 60°C (30 min used). Through MINITAB, the contour plots produced represent the possible interaction between three parameters in a 2-D scheme. In this manner, the sampling intervals, the discrete temperatures and their respective results are presented. The results are connected through the areas set by the contours by either the distance or the Akima's polynomial method (the 1st was mainly chosen); close values are grouped in the different levels and the intermediate values among the DOE levels are estimated through these methods, hence more dense presentation can be offered.

Also, MINITAB was used to display both the sequential sums of squares (Seq SS) and adjusted sums of squares (Adj SS), after the presentation of the Degrees of Freedom (DF). Since the model is orthogonal and does not contain covariates, these two SS values will be the same. The SS quantifies the variability between the groups of interest, here being the values of the first column, one of the control variables (process efficiency %). In other words, the difference between the source means and the grand mean is represented.

Variation between individual scores and the mean of every group is presented by the values; the greater this value is, the bigger the effect of changing that factor on the control variable is.

Table 3.1.2. – Design of Experiments set-up.

Run	A	B	C	Run	A	B	C	Run	A	B	C	Run	A	B	C		
1	1	1	1	**21**	2	1	1	**41**	3	1	1	**61**	4	1	1		
2	1	1	2	**22**	2	1	2	**42**	3	1	2	**62**	4	1	2	**Factors**	3
3	1	1	3	**23**	2	1	3	**43**	3	1	3	**63**	4	1	3	**Replicates**	2
4	1	1	4	**24**	2	1	4	**44**	3	1	4	**64**	4	1	4		
5	1	1	5	**25**	2	1	5	**45**	3	1	5	**65**	4	1	5	**Base Runs**	80
6	1	2	1	**26**	2	2	1	**46**	3	2	1	**66**	4	2	1	**Total Runs**	160
7	1	2	2	**27**	2	2	2	**47**	3	2	2	**67**	4	2	2		
8	1	2	3	**28**	2	2	3	**48**	3	2	3	**68**	4	2	3	**Base Blocks**	1
9	1	2	4	**29**	2	2	4	**49**	3	2	4	**69**	4	2	4	**Total Blocks**	1
10	1	2	5	**30**	2	2	5	**50**	3	2	5	**70**	4	2	5		
11	1	3	1	**31**	2	3	1	**51**	3	3	1	**71**	4	3	1	**No. of levels**	**A;B;C;=4;4;5**
12	1	3	2	**32**	2	3	2	**52**	3	3	2	**72**	4	3	2	**A**	Time (h)
13	1	3	3	**33**	2	3	3	**53**	3	3	3	**73**	4	3	3	**B**	Initial Population (CFU/mL)
14	1	3	4	**34**	2	3	4	**54**	3	3	4	**74**	4	3	4	**C**	Temperature (˚C)
15	1	3	5	**35**	2	3	5	**55**	3	3	5	**75**	4	3	5		
16	1	4	1	**36**	2	4	1	**56**	3	4	1	**76**	4	4	1	**where:**	
17	1	4	2	**37**	2	4	2	**57**	3	4	2	**77**	4	4	2	**A**	1,2,3,4 (h)
18	1	4	3	**38**	2	4	3	**58**	3	4	3	**78**	4	4	3	**B**	10^3,10^4,10^5,10^6 (CFU/mL)
19	1	4	4	**39**	2	4	4	**59**	3	4	4	**79**	4	4	4	**C**	20,30,40,50,60 (˚C)
20	1	4	5	**40**	2	4	5	**60**	3	4	5	**80**	4	4	5		

3.1.5. Modeling of bacterial disinfection and regrowth without temperature control

In order to model the bacterial response under the solar light stress without temperature control, the GInaFiT freeware add-on for Microsoft Excel was used (Geeraerd et al., 2005). Between the models tested to fit the curves, Model 1: a Shoulder log-linear (Geeraerd et al., 2000), Model 2: the Weibull frequency distribution model (Mafart et al, 2002) were used.

3.1.5.1. Employed models

1) Shoulder log-linear inactivation model:

$$N = N_0 * \exp(-k_{max} * t) * (\exp(k_{max} * Sl))/(1 + (\exp(-k_{max} * Sl) - 1) * \exp(-k_{max} * t))) \quad (1)$$

For identification purposes reformulated as:

$$log_{10}(N) = log_{10}(N_0) - k_{max} * \frac{t}{\ln(10)} + log_{10}(\frac{\exp(k_{max} * Sl)}{1+(\exp(k_{max} * Sl)-1) * \exp(-k_{max} * t)}) \quad (2)$$

Where:

- N: the bacterial population at any given time (CFU/mL)
- N_0: the initial bacterial population (CFU/mL)
- t: the investigated time (s)
- k_{max} and Sl (shoulder length): shoulder-log linear model-specific constraints

The shoulder log-linear model was first suggested as two separate equations (Geeraerd et al., 2000).

$$\frac{dN}{dt} = -k_{max} * N * \left(\frac{1}{1+C_c}\right) * \left(1 - \frac{N_{res}}{N}\right) \quad (3)$$

$$\frac{dC_c}{dt} = -k_{max} * C_c \quad (4)$$

C_c is related to the physiological cell state, k_{max} is the rate of inactivation (1/time unit), and N_{res} is the residual density of the bacterial population (CFU/mL). By changing Cc with $e^{kmaxSl}-1$ with Sl (time units) being the shoulder length, the final versions (1) and (2) are obtained.

This model is not a fundamental description of the bacterial metabolic process, rather than a mathematical way of integrating in an equation two well-known phenomena in solar disinfection: 1) the initial shoulder demonstrated, corresponding to the initial resistance/adaptation time required for the light to inflict damage on a minimum number of bacterial sites (Berney et al., 2006) and 2) the well-known subsequent log-linear decay. Furthermore, this equation doesn't integrate the irradiation power as a variable, so specific parameters need to be estimated for each irradiation level. On the right side of the equation, the first two terms would represent a log-linear decay from the very start of irradiation. However, the third term adds a delay (Sl) to the log-linear decay and sets $N=N_0$ constant along the shoulder, and a smooth transition to the log-linear decay phase. So, this model provides a formal way to calculate the length of the shoulder phase, and the kinetic constant of the log-linear decay.

2) Weibull inactivation model:

The Weibull model is the Mafart et al. (2002) suggestion to adapt the cumulative probability density function to microbial inactivation. The effort is "to reduce naturally" the classic log-linear model, and is as follows:

$$\frac{N}{N_0} = 10^{\left(-\left(\frac{t}{\delta}\right)^p\right)} \quad (5)$$

For identification purposes reformulated as:

$$log_{10}(N) = log_{10}(N_0) - (\frac{t}{\delta})^p \quad (6)$$

Where:

- N: the bacterial population at any given time (CFU/mL)
- N_0: the initial bacterial population (CFU/mL)
- t: the investigated time (s)
- δ and p: Weibull model-specific constraints (scale and shape parameters).

δ is a scale parameter and marks the time for the first decimal reduction (if p=1). For p<1 concave curves are described and p>1 describes convex shapes. Finally, δ and p are not independent; there is a strong correlation existing, as suggested by Van Boekel (2002) and Mafart (2002), and it is due to the model structure. Through scaling and shaping, the Weibull curve can be fitted to UV/solar disinfection kinetics. However, the shoulder length and a classical kinetic parameter cannot be estimated from curve fitting.

3.1.5.2. Experimental specifications

In order to model the effect of solar intensity on bacterial disinfection and regrowth, in the experiments without temperature control, discrete intensities were used (500, 600, 700, 800, 900, 1000, 1200, 1400 and 1600 W/m^2). The temperature was monitored and never exceeded 40˚C. The analytical nature of this investigation aims to quantify the contribution of several discrete intensity levels in solar wastewater disinfection. The intensity threshold is set according to the guidelines of SODIS (www.sodis.ch) considering that candidate countries for water would fulfil the standards for wastewater as well. The upper end reaches an exclusive artificially-induced level of irradiance, encountered in technical applications, such as compound parabolic collector reactors (CPCs) (Malato et al., 2007) with concentration ratios higher than 1; this approach will investigate the potential use of such solutions in wastewater disinfection.

The vessels used were Pyrex glass reactors (of total volume 65 mL) were used, containing 50 mL of *E. coli*-spiked wastewater. The sampling manner, plating and enumeration methods of cultivable bacteria was similar to the specific ones described in subchapters 3.1.2 and 3.1.3. For intensities until 1000 W/m^2 sampling was performed semi-hourly, while for 1200, 1400 and 1600 W/m^2, 20-min intervals were employed to follow bacterial inactivation kinetics.

3.2. Disinfection of wastewater: application of a systematic study on solar-inflicted inactivation

In this section, a systematic study on the variables affecting solar disinfection of a synthetic secondary effluent are presented and discussed. More specifically, the effects of initial bacterial load, temperature and light intensity on disinfection are assessed here. The details of the DOE and experimental conditions were given in sections 3.1.1 to 3.1.4, and the corresponding results are analyzed here.

3.2.1. Dark experiments (0 W/m^2) - Effects of reaction time, temperature and initial population in absence of light

Figure 3.2.1a presents the evolution of bacterial population over time, within the varying initial population and the corresponding temperature conditions. The figure can be split into two major groups of curves showing clearly different behavior and their respective sub-groups: i) for temperatures 20-40˚C and ii) 50-60˚C. In absence of light, the driving force of the reaction is temperature alone. The initial bacterial population sets the bar from which the initiation of the thermal impact is observed. The contour plot of the removal (Figure 3.2.1b, % Process Efficiency) over time and provides an overview with a clear ineffective area (20-40˚C) and a thermal effect one. However, the main effects plot (Figure 3.2.1c.) does not clearly present the effect of the different temperature ranges and provide a false, rather masked image by the overall means; time for instance seems to be biased by the different efficiencies noticed in (Figures 3.2.1a and b and presents quite mild influence in the process, which is not true. Therefore, the graphs are presented divided according to the temperature range they belong, in Figure 3.2.2.

For the first group of graphs, in Figure 3.2.2a (20-40˚C), it can be noticed that there is a slight increase in the bacterial count. The water matrix supporting the bacterial population is synthetic wastewater and, due to the existing nutrient sources, growth is expected. This observation is valid for all initial bacterial levels and within this increase, there are two tendencies present: Firstly, there is a correlation between the temperature of the reaction and the final bacterial numbers. The 40˚C traces are always higher than the 30˚C traces and them, always higher than the 20˚C traces. This behavior agrees with the fundamental findings of Johnson and Levin (1946) that attribute higher cell division rates in higher temperatures. Secondly, there is a statistical observation presented in Table 3.2.1 that generally, higher initial numbers lead to larger percentile increases of population, when the critical temperature is reached.

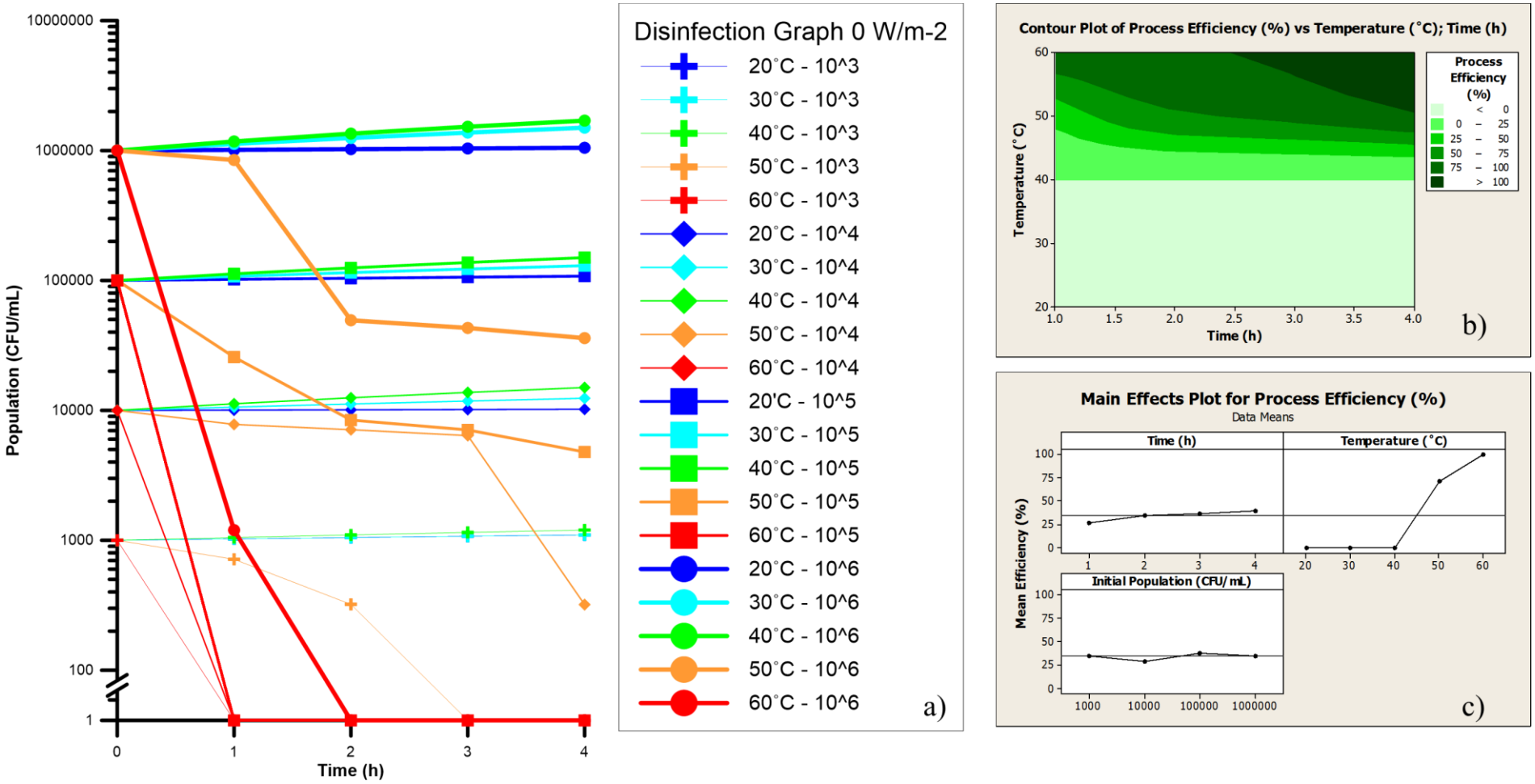

Figure 3.2.1: Main results of non-irradiation experiments for synthetic secondary effluent at different temperatures and initial *E. coli* populations. (a) Disinfection kinetic curves. (b) Contour plot of process efficiency vs. temperature and time. (c) Main effects plot (control variable: Process Efficiency)

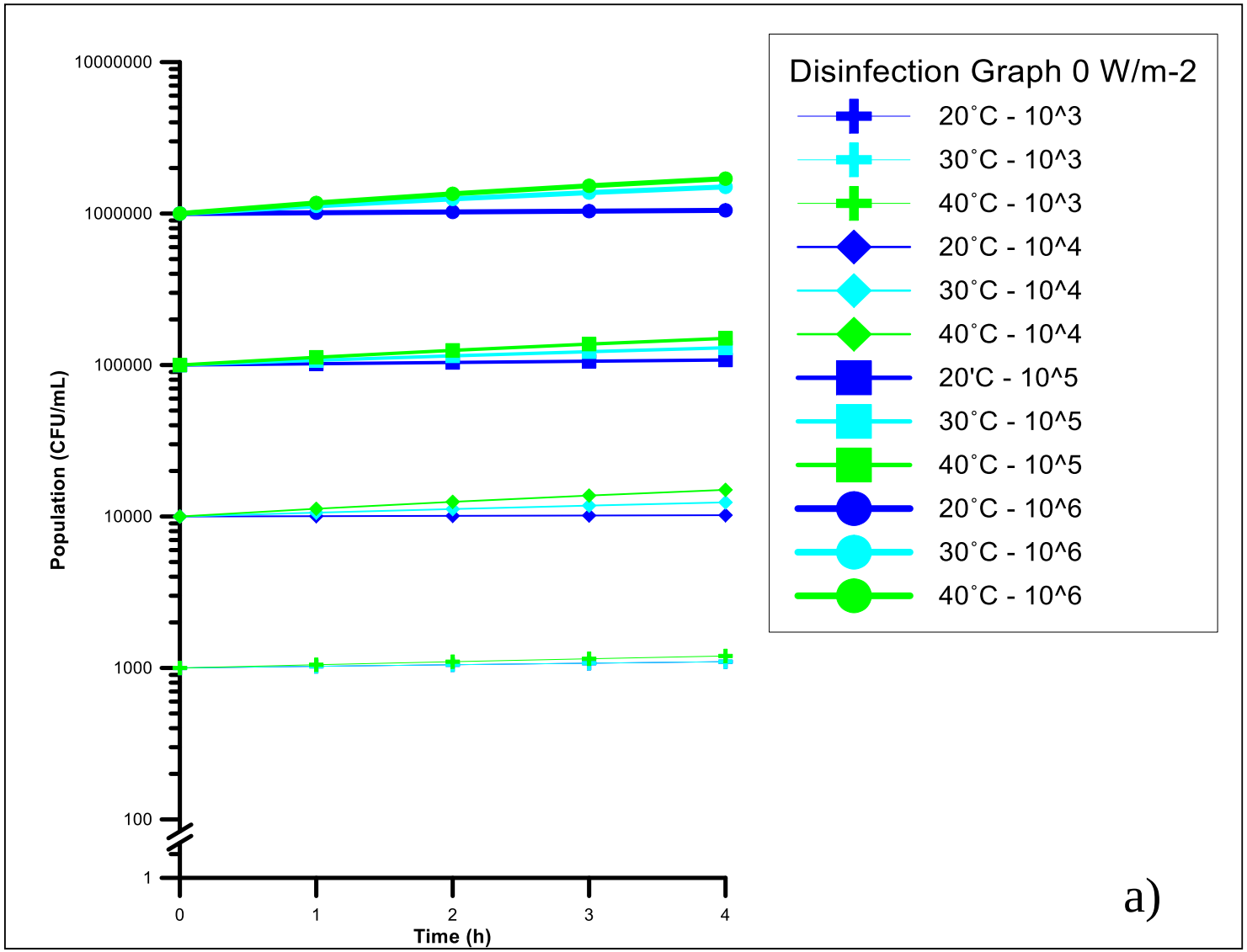
Disinfection Graph 0 W/m-2
20˚C - 10^3
30˚C - 10^3
40˚C - 10^3
20˚C - 10^4
30˚C - 10^4
40˚C - 10^4
20'C - 10^5
30˚C - 10^5
40˚C - 10^5
20˚C - 10^6
30˚C - 10^6
40˚C - 10^6
Population (CFU/mL)
10000000
1000000
100000
10000
1000
100
1
0
1
2
3
4
Time (h)
a)

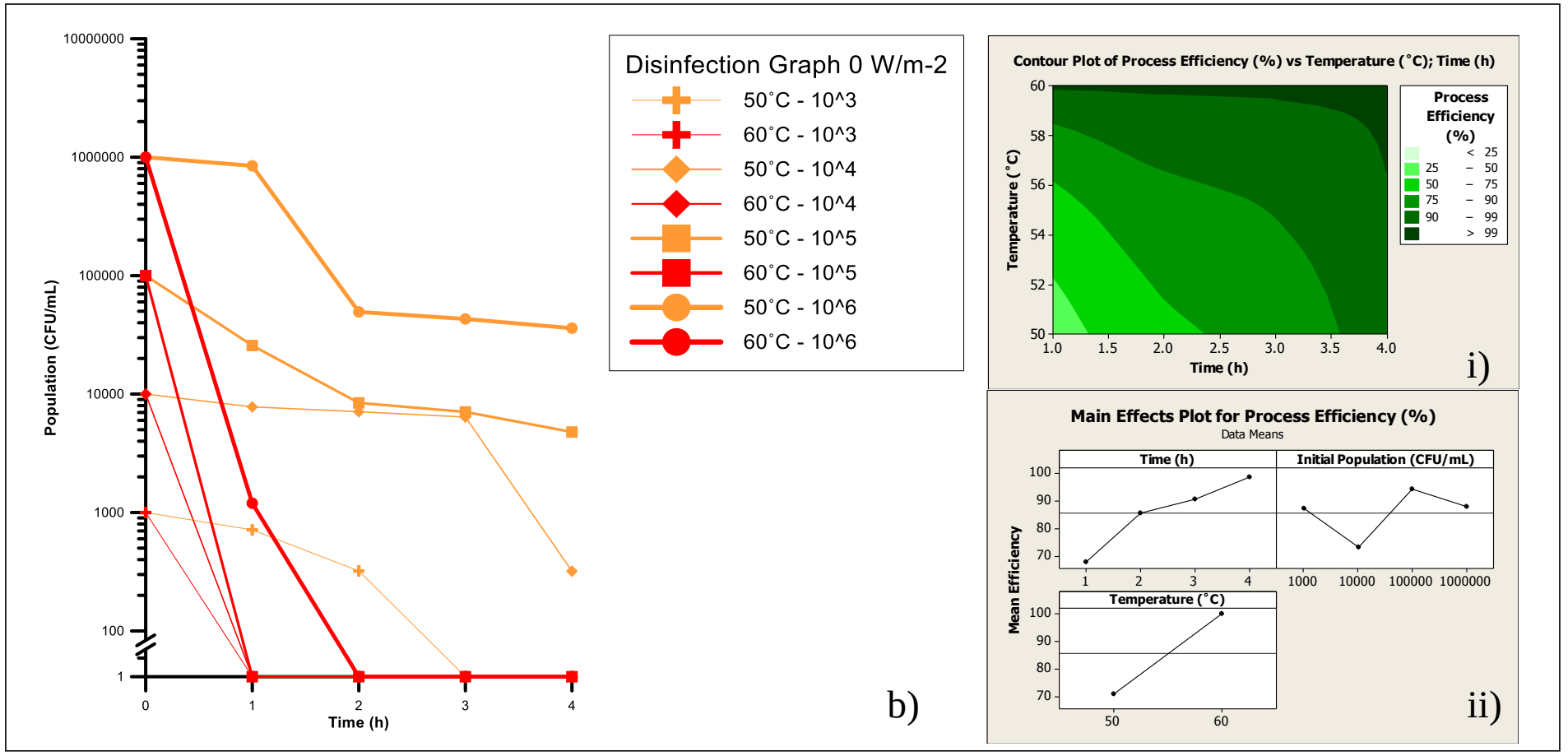

Figure 3.2.2: Main results of non-irradiation experiments for synthetic secondary effluent at different temperatures and initial *E. coli* populations. (a) 20-40˚C kinetic curves. (b) 50-60˚C kinetic curves. b-i) Contour plot of the changes in process efficiency vs. temperature and time from 50-60˚C. b-ii) Main effects plot for temperatures 50-60˚C (control variable: Process Efficiency)

Table 3.2.1. – Percentile change of bacterial concentration after 4 h treatment in absence of solar light.

Temperature/Initial Concentration	10^3	10^4	10^5	10^6
20˚C	10	2	8	5
30˚C	10	24	30	50
40˚C	20	50	50	70
50˚C	*-100*	*-96.8*	*-95.2*	*-95*
60˚C	*-100*	*-100*	*-100*	*-100*

This behavior changes radically above 40˚C. In the same table (Table 3.2.1.), the curves indicate bacterial inactivation instead of bacterial growth. *E. coli* are mesophilic microorganisms, that typically thrive between 20-45˚C (Fotadar et al., 2005). Above this temperature, there is a thermal stress applied to the cells, altering the cell wall plus damaging the proteins and nucleic acids, leading to easier bacterial death (Blaustein et al., 2013). This effect becomes more visible (Figure 3.2.2b) as temperature increases from 50˚C to 60˚C. Treating *E. coli* within high temperatures can result in total inactivation, as it can be seen for low initial populations, but slightly more difficult when the initial population is high. Also, temperatures as high as 60˚C lead to fast inactivation. This is attributable to the increased degradation of the vital components of the cell, by the decomposition mechanisms characterized many decades ago (Johnson and Levin, 1946; Marr and Ingraham, 1962).

As far as the efficiency of the process is concerned, in terms of removal percentage, a variation in Figure 3.2.2c is seen, which demonstrates the modification of the process, when temperature is increased from 40 to 60˚C. Maximum efficiency is achieved at 60˚C after 1 h and as the time passes, the thermal threshold is lower, reaching 51˚C, for a 4-h period of treatment. An increase of 10˚C achieves dramatic enhancement in removal rates (up to 75%) and the last 10˚C increase ensures total inactivation (Figure 3.2.2d). The significance of temperature is verified by the P values of the ANOVA table (Table 3.2.2) produced by all data from MINITAB, which validates the previous results; in order of significance, temperature is the most important factor that influences the outcome, then treatment time, while the initial population is the least significant among the three.

3.2.2. 800-W/m^2 experiments - Effects of reaction time, temperature and initial population for intensity of 800 W/m^2

The second group of experiments utilizes solar energy to inactivate *E. coli*, with the irradiance of the solar simulator set at 800 W/m^2. The same batch test configurations were used as the control experiments, to

ensure comparability among the conditions. Many authors have demonstrated that there is a synergistic action between light and temperature in different media and microorganisms (Wegelin et al., 1994; Petin et al., 1997; McGuigan et al., 1998; Rincon and Pulgarin, 2004b). This test investigates the light-temperature interaction in synthetic secondary effluent.

Table 3.2.2. – ANOVA table for each intensity level.

Process Efficiency	*DF*	Intensity 0 W/m^2	*SS*	*MS*	*F*	*P*	Intensity 800 W/m^2	*SS*	*MS*	*F*	*P*	Intensity 1200 W/m^2	*SS*	*MS*	*F*	*P*
t	3		1662	554	2.82	0.045		7710.6	2570.2	13.41	0		29034.5	9678.2	31.09	0
T	4		147130	36783	187.52	0		44260.2	11065	57.72	0		15212.1	3803	12.22	0
C	3		772	257	1.31	0.278		5106.4	1702.1	8.88	0.2		549	183	0.59	0.625
Error	69		13534	196				13228.1	191.7				21480.2	311.3		
Total	79		163098					70305.3					66275.9			

Figure 3.2.3a demonstrates in overall the evolution of bacterial population over time, grouped by initial numbers and temperature of the process. Within 4 h of treatment, samples that were processed at 20˚C demonstrated a continuous decrease of the population. However, as temperature rises to 30˚C the remaining populations are somewhat equal or higher than the respective ones at 20˚C. The phenomenon is even clearer at temperatures around 40˚C, where insignificant removal rates are demonstrated and presented in Table 3.2.3. Figure 3.2.3b presents an overview of the efficiency of the process, in which a gap is visible, around 40˚C. There is a descending trend until 40˚C and then an increase in the efficiency, which is verified in Figure 3.2.3c; temperature is dominating the process and modifies the outcome of the experiment. Therefore, once again the two clear groups of graphs are distinguished, according to the large temperature groups, below and over 40˚C.

Within this system there are two opposing forces present that determine the outcome so far. Compared to the 0-W/m^2 experiments, first of all, Figures 3.2.3a and 3.2.4a-b light changes the growth phenomenon observed before. What appears in Figure 3.2.3b-i) as an "island" of low efficiency among the average ones, is attributed to the 40˚C area, which provides with increased metabolic rates and thereby higher remaining populations. On the one hand, the disinfecting action of light exists, which tends to inactivate bacteria as seen in 20˚C curves (Figure 3.2.4a), with the number of inactivated bacteria vs. initial population increasing when initial population is increased. On the other hand, submitting the population to temperatures around 37˚C, in a nutrient-enhanced matrix as the wastewater, mesophiles, such as *E. coli*, tend to present their highest reproduction rates (Dawes and Sunderland, 1976). *E. coli* belongs to this category and is encountered in the human gut (Levine, 1975), with the normal human body temperatures being the most favorable for their growth. Normally, *E. coli* are inactivated by exposure to 55ºC for 1 hour or 60ºC for 20 minutes (Charkraborty, 1998). Hence, as temperature is raised in the disinfection process, the two concurrent actions tend to balance in favor of the reproduction rates, around 40˚C.

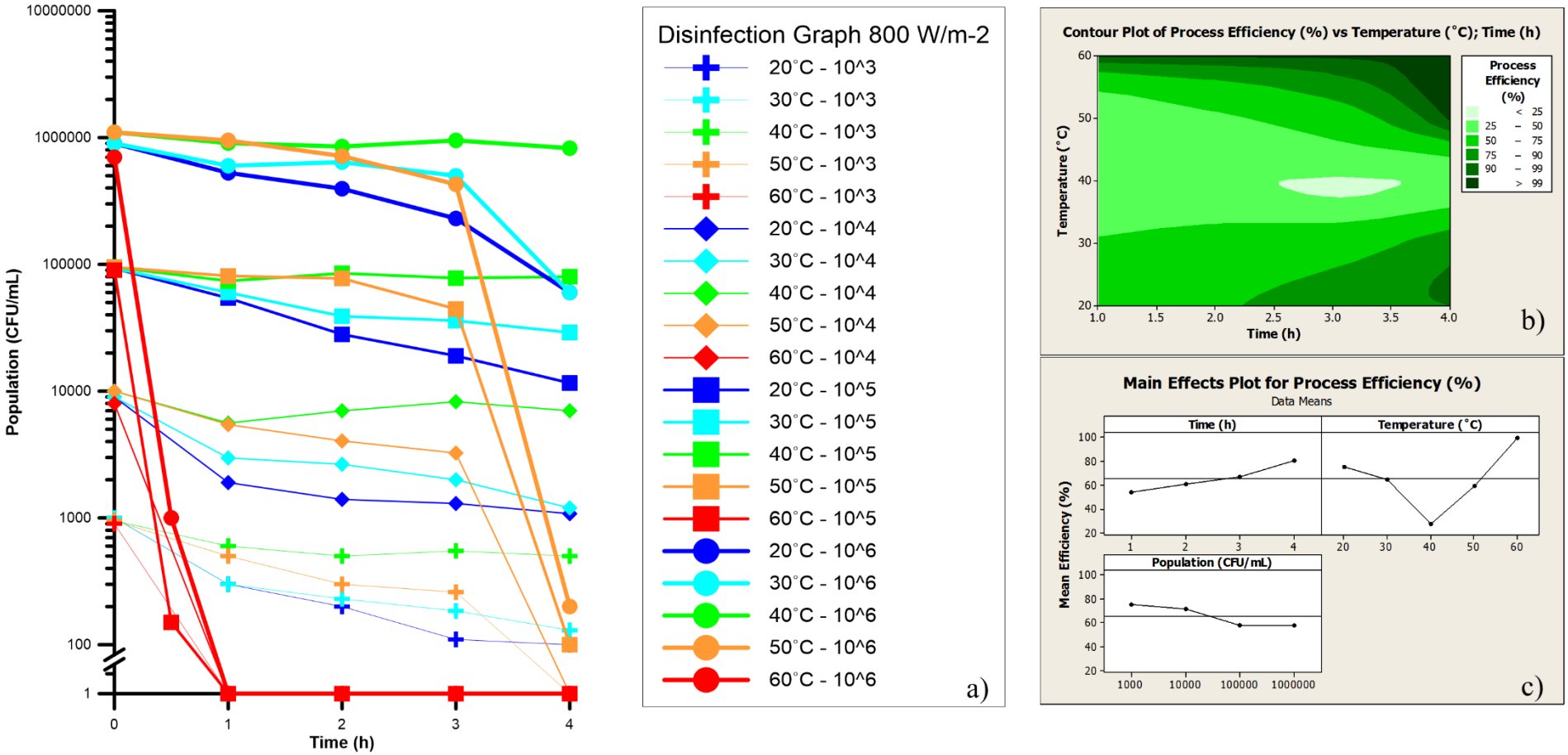

Figure 3.2.3: Main results of 800 W/m^2 experiments for synthetic secondary effluent at different temperatures and initial *E. coli* populations. (a) Disinfection kinetic curves. (b) Contour plot of process efficiency vs. temperature and time. (c) Main effects plot (control variable: Process Efficiency)

Table 3.2.3. – Percentile removal of bacterial concentration after 4h treatment under 800 W/m^2 light.

Temperature (˚C)/Initial Concentration (CFU/mL)	10^3	10^4	10^5	10^6
20˚C	90.0	88.0	87.5	93.3
30˚C	87.0	86.7	68.8	93.3
40˚C	47.4	30.0	15.8	25.0
50˚C	100.0	100.0	99.9	99.9
60˚C	100.0	100.0	100.0	100.0

However, a temperature increase over 45˚C would affect *E. coli* metabolic cycles, and lead to cell death. Indeed, as it is observed, the 50˚C curves (Figure 3.2.4b) after an initial shoulder, a common observation at solar disinfection processes (Harm, 1980; Sinton et al., 1999; Berney et al., 2006), then present total (10^3 and 10^4 curves) and almost total inactivation (10^5 and 10^6 curves). In addition, increasing the treatment temperature up to 60˚C leads to total inactivation of the microorganisms before 60 min, regardless of the initial bacterial population.

Furthermore, one can notice the synergy between light effects and temperature increase at the graphs, by comparing Figure 3.2.2 with 3.2.4: First of all, at 50˚C without light, only samples with 10^3 initial population were inactivated, whereas in presence of light 10^3 and 10^4 were totally inactivated and 10^5 and 10^6 presented a 3 or 4 $\log_{10}$U reduction instead of 1 or 2 $\log_{10}$U. Secondly, 60˚C treated samples were totally inactivated in less than an hour, slightly faster than in absence of light. Consequently, in the latter case thermal treatment is the main disinfecting force and light is only complementary.

Speaking in terms of efficiency, Figures 3.2.4a-i and 4b-i, provide information about the effect of each parameter over the total inactivation capability of the process. In the 20-40˚C interval, lower temperatures seem to favor inactivation with the peak appearing between 20 and 25˚C, while treatment time increases the potentials; the 4th hour contributes in the greatest proportion, adding on the inactivation side of the balance. Comparing with the equivalent graphs for 50-60˚C, temperature increase leads to percentile inactivation enhancement, while statistically in both cases, initial bacterial population does not seem to significantly affect the percentage of inactivated bacteria in the process. However, the same actions manage to inactivate lower bacterial numbers more efficiently (in percentage) but in absolute numbers, removal increases with higher populations, due to larger numbers' correspondence of the removal percentage.

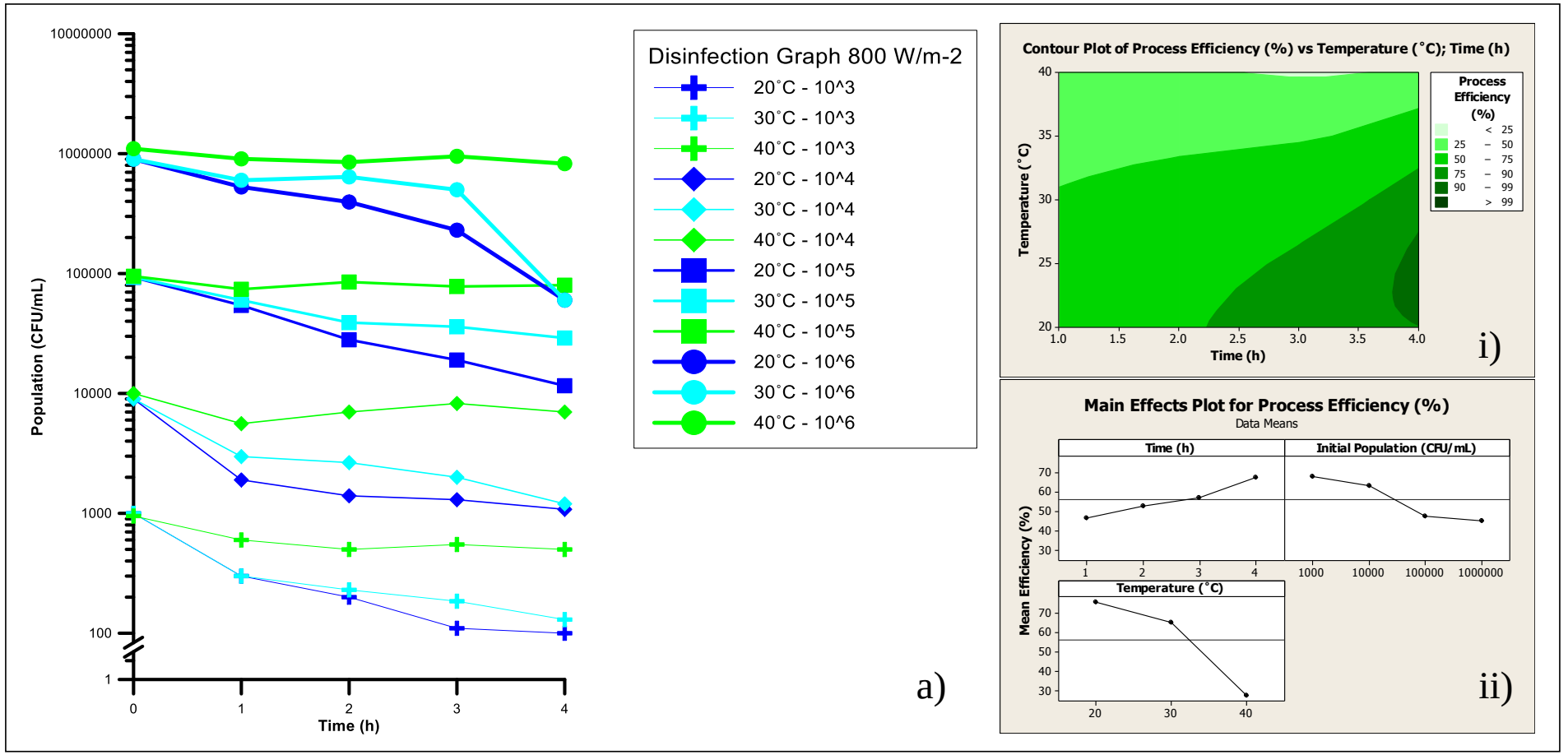
Population (CFU/mL)
10000000
1000000
100000
10000
1000
100
1
0
1
2
3
4
Time (h)
Disinfection Graph 800 W/m-2
20˚C - 10^3
30˚C - 10^3
40˚C - 10^3
20˚C - 10^4
30˚C - 10^4
40˚C - 10^4
20˚C - 10^5
30˚C - 10^5
40˚C - 10^5
20˚C - 10^6
30˚C - 10^6
40˚C - 10^6
a)
Contour Plot of Process Efficiency (%) vs Temperature (˚C); Time (h)
Temperature (˚C)
Time (h)
Process Efficiency (%)
< 25
25 – 50
50 – 75
75 – 90
90 – 99
> 99
i)
Main Effects Plot for Process Efficiency (%)
Data Means
Time (h)
Initial Population (CFU/mL)
Temperature (˚C)
Mean Efficiency (%)
ii)

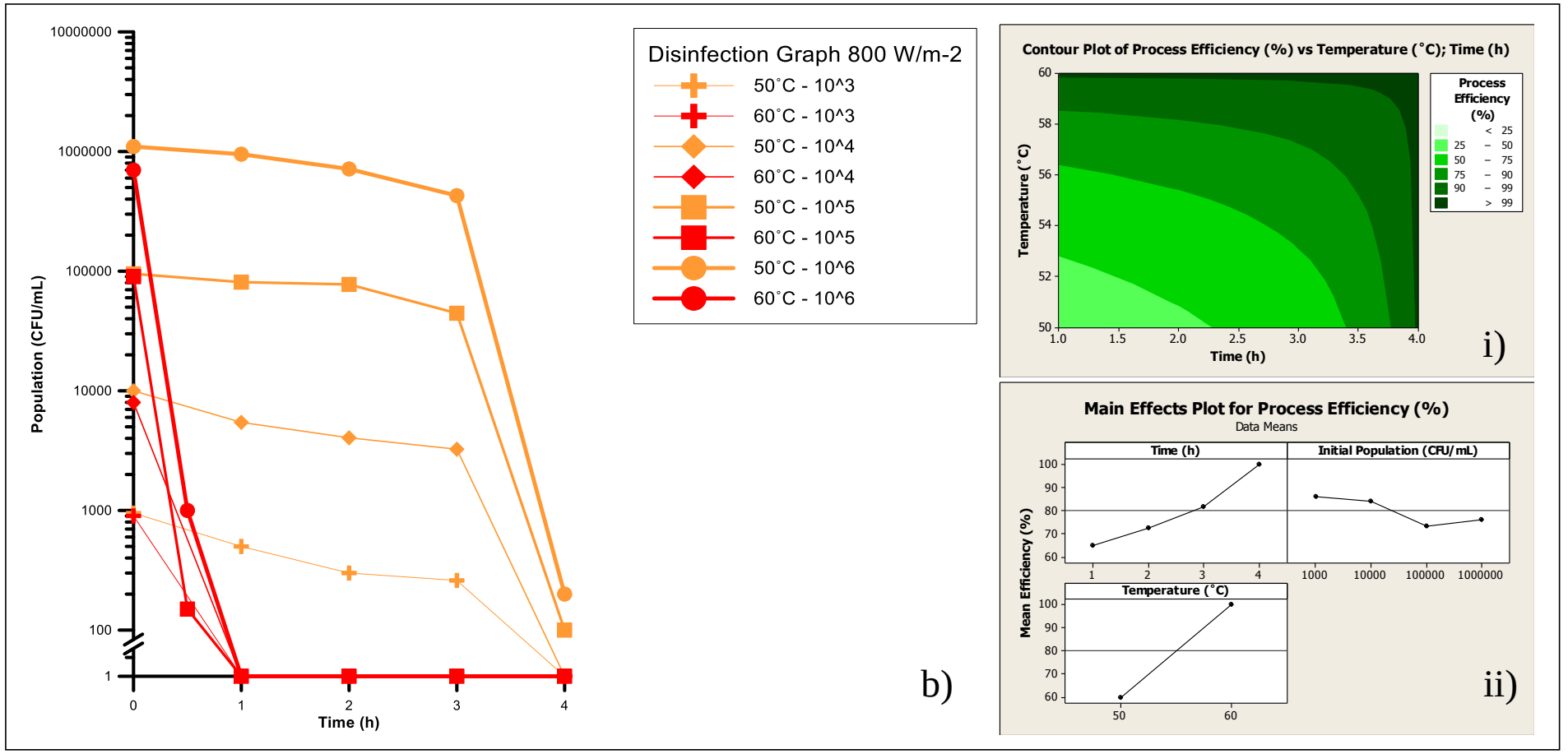

Figure 3.2.4: Main results of 800 W/m^2 experiments for synthetic secondary effluent at different temperatures and initial *E. coli* populations. (a) 20-40˚C Disinfection kinetic curves, a-i) 20-40˚C contour plot of process efficiency vs. temperature and time, a-ii) 20-40˚C Main effects plot (control variable: Process Efficiency). (b) 50-60˚C Disinfection kinetic curves, b-i) 50-60˚C contour plot of process efficiency vs. temperature and time, b-ii) 50-60˚C Main effects plot (control variable: Process Efficiency).

Finally, the ANOVA table reveals the important contribution of time and temperature and the milder one from initial bacterial population. The P values presented in Table 3.2.2 are also verified by Figures 3.2.4a-ii and b-ii. It is observed that time almost proportionally increases the total efficiency, while initial population fluctuates around the average inactivated bacteria. What is more important, is the temperature effect on efficiency, which presents what was in detail described before; temperature increase enhances bacterial inactivation, as literature suggested for other water matrices, but only above 40˚C. Otherwise, the disinfection process is delayed by the excessive growth of the microorganisms.

3.2.3. High irradiance experiments (1200 W/m^2) - Effects of reaction time, temperature and initial population for high intensity irradiation conditions

The final experimental part consists of the runs that utilized high intensity illumination. Higher supply of photons in the system could result in higher possibility of effective hits in the number of crucial areas of the cell, as described by Harm (1980).

Figure 3.2.5a presents an overview of the disinfection reactions of the varied initial population. The main and most profound difference between this set-up and the previous ones, is that all samples regardless of initial population and treatment temperature have been inactivated within the time frame of 4 h. The action of light was more intense and influenced the outcome of the experiments in cases that was not sufficient before. Bacteria have now to cope with higher concurrent light and thermal action, which is expressed by more acute kinetics in the final hour. When the samples were treated at lower temperatures, the disinfection curves again present a lag-phase or shoulder, but considerably lower, varying from 30 to 120 min, compared to the minimum 3-h shoulder presented under 800 W/m^2 irradiance. Figures 3.2.5b and c, present once more the erratic behavior around 40ºC, demonstrated as a lower efficiency area (Figure 3.2.5b) or a mean decrease (Figure 3.2.5c), however mitigated, compared to the equivalent of 800 W/m^2 or even the increase in numbers observed in null intensity experiments.

What is more, the main effects plot of this high irradiation also adds direct information over the main overall efficiency. All parameters concerned, the addition of light initially increased the efficiency from 35% to 65% (from 0 to 800 W/m^2), to reach 80% when high intensity is applied. This is a good indicator of the robustness of the system, predicting, at some extent, the success of the group of trials. Finally, it is also shown that the biggest contribution in bacterial inactivation derives from the 1st hour of illumination and the least, but most important from the application point of view, during the 4th hour. Plus, the drop in efficiency around 40˚C is also visible, like each previous case but less intense; high irradiance illumination compensates for the inactivation difference.

Observing Figure 3.2.6a, it is clear that, at 1200 W/m^2, the equilibrium between the disinfecting action of light and the growth-stimulating effect of increasing temperatures changes within the 20-40˚C range. After a 2-3-h shoulder, bacterial numbers fall sharply to total disinfection at the fourth hour. This means the

disinfecting action becomes higher than the growth force and, as far as the cell is concerned, indeed, the growth action is present but is no longer in favor of their survival. Also, the contour plot of efficiency over time (Figure 3.2.6a-i) has a clear area of total inactivation, after 3.5 h, while temperature increase has a mitigated effect of delay in inactivation, compared to all other cases till now.

For higher temperatures, it is shown that at 50˚C, compared to 0 and 800 W/m^2, the same process at 1200 W/m^2 is completed faster, compared with the cases it was completed before, and in total, all cases resolved to total inactivation. As shown in Figure 3.2.6b, the disinfection kinetics at these particular conditions (1200 W/m^2, 50ºC) is very sensitive to the initial bacterial concentration, probably attributable to shielding (Craik et al., 2001) playing a critical role in these runs. At 60˚C and 1200 W/m^2, complete disinfection is achieved faster than at 0 or 800 W/m^2. Where in absence of light inactivation time was around an hour, at 800 W/m^2 slightly less, and now is even less than 30 minutes. Finally, this outcome is common for all initial populations; all result in total inactivation faster than their respective 800 W/m^2 curves.

The contour plots of the process efficiency (Figure 3.2.6b-i) indicate clearly the bigger "effective" area of >99%, and the relatively higher rates; no area lies under 50% bacterial inactivation even after only 1 h. As treatment time increases the efficiency increases as well, however, the same cannot be observed for temperature. For instance, at 50˚C, only 2.5-3 h are sufficient to achieve total inactivation, demonstrated in Figure 3.2.6b-ii. Also, from the ANOVA table (Table 3.2.2) it is concluded that the efficiency is highly correlated only with treatment time and temperature.

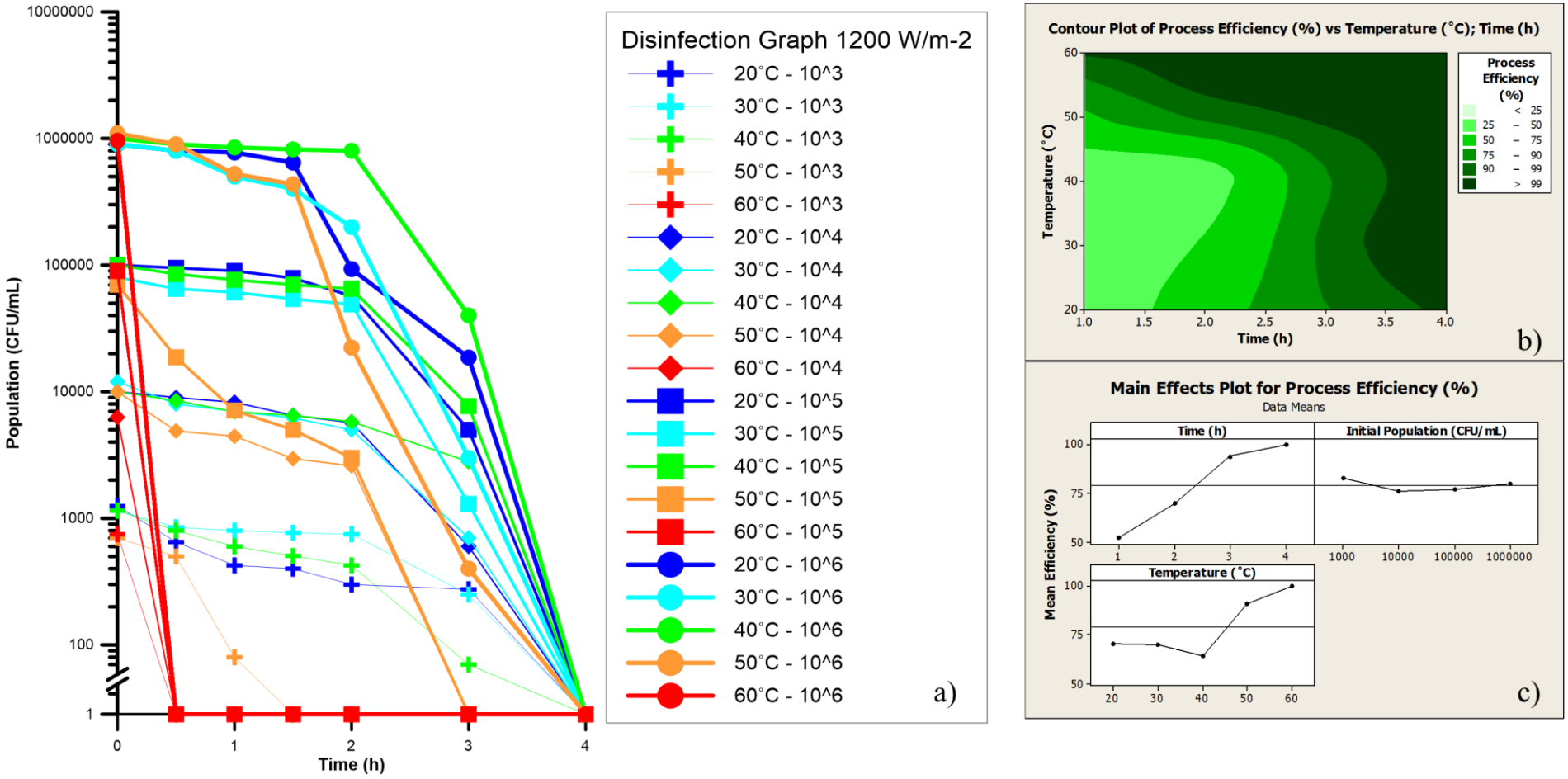

Figure 3.2.5: Main results of 1200 W/m² experiments for synthetic secondary effluent at different temperatures and initial *E. coli* populations. (a) Disinfection kinetic curves. (b) Contour plot of process efficiency vs. temperature and time. (c) Main effects plot (control variable: Process Efficiency)

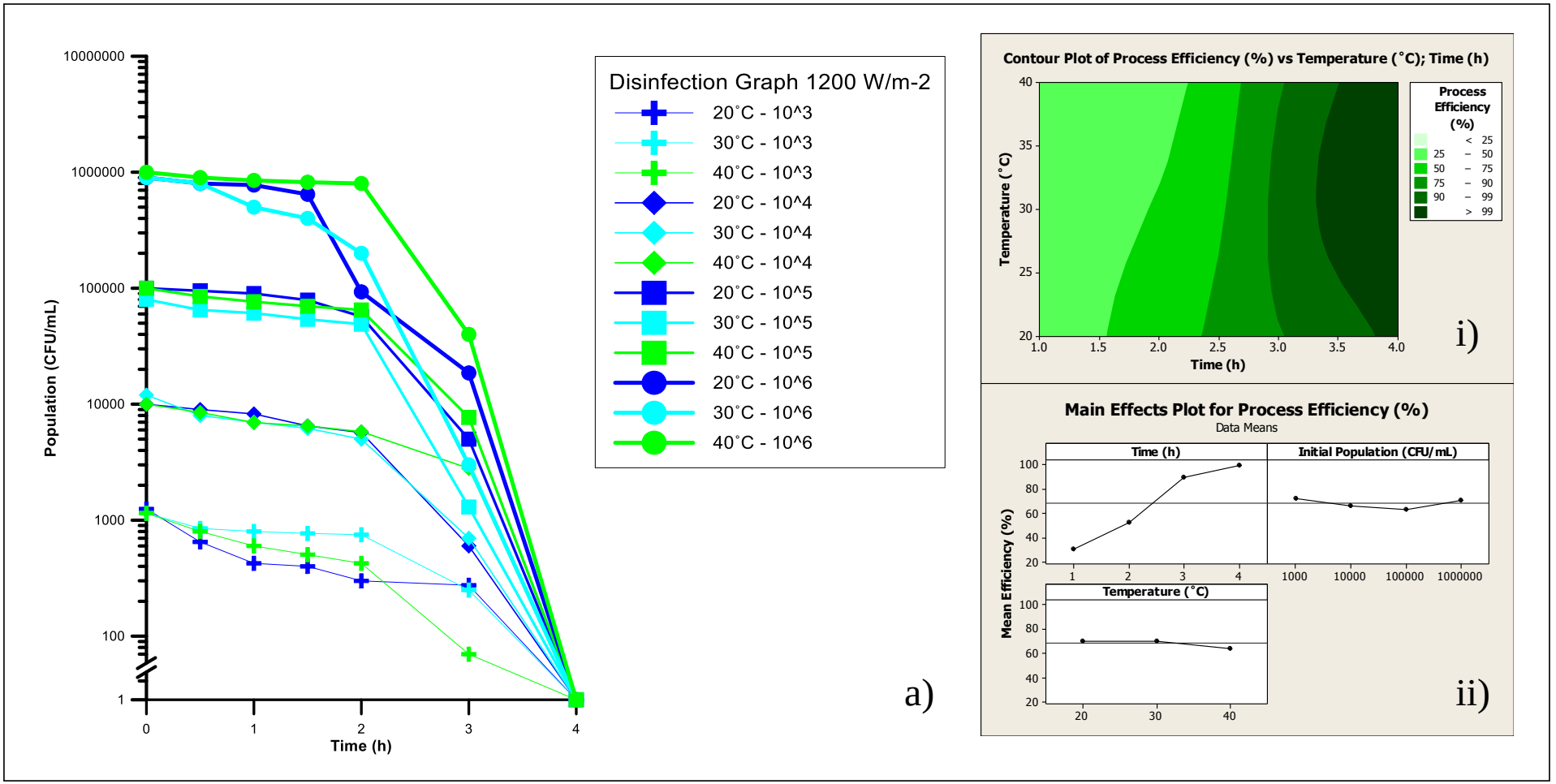
Population (CFU/mL)
10000000
1000000
100000
10000
1000
100
1
0
1
2
3
4
Time (h)
Disinfection Graph 1200 W/m-2
20˚C - 10^3
30˚C - 10^3
40˚C - 10^3
20˚C - 10^4
30˚C - 10^4
40˚C - 10^4
20˚C - 10^5
30˚C - 10^5
40˚C - 10^5
20˚C - 10^6
30˚C - 10^6
40˚C - 10^6
a)
Contour Plot of Process Efficiency (%) vs Temperature (˚C); Time (h)
Temperature (˚C)
Time (h)
Process Efficiency (%)
< 25
25 – 50
50 – 75
75 – 90
90 – 99
> 99
i)
Main Effects Plot for Process Efficiency (%)
Data Means
Time (h)
Initial Population (CFU/mL)
Temperature (˚C)
Mean Efficiency (%)
ii)

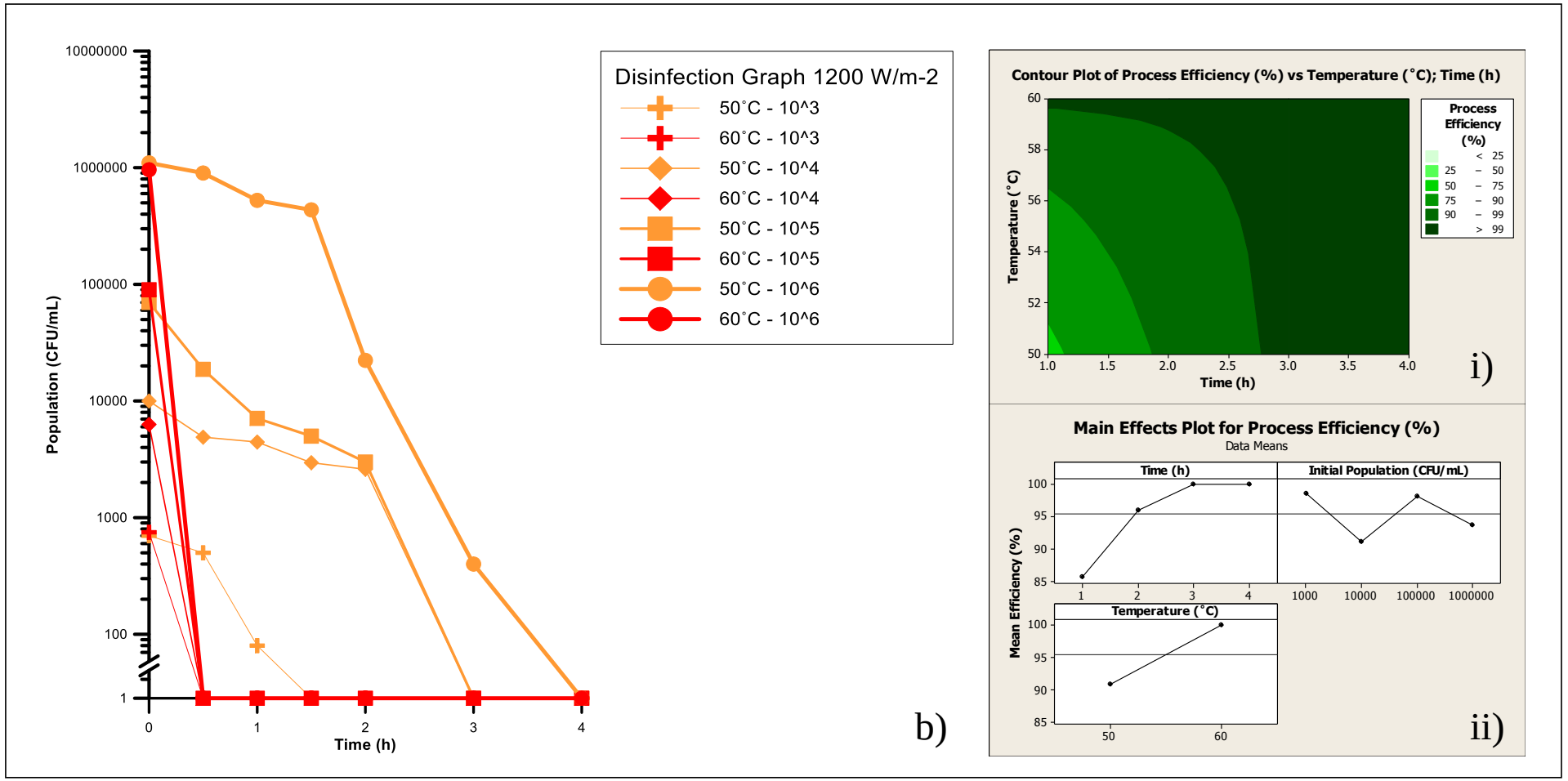

Figure 3.2.6: Main results of 1200 W/m^2 experiments for synthetic secondary effluent at different temperatures and initial *E. coli* populations. (a) 20-40˚C Disinfection kinetic curves, a-i) 20-40˚C contour plot of process efficiency vs. temperature and time, a-ii) 20-40˚C Main effects plot (control variable: Process Efficiency). (b) 50-60˚C Disinfection kinetic curves, b-i) 50-60˚C contour plot of process efficiency vs. temperature and time, b-ii) 50-60˚C Main effects plot (control variable: Process Efficiency).

3.2.4. Modeling solar disinfection of secondary treated wastewater with temperature control

As a result of the statistical interpretation of the experimental data, a simplified model can be proposed. Through the statistical software of MINITAB, a model is suggested, which relates the response factors with the parameters of the process, in order to further analyze the experimental concept, and help facilitate all these experimental runs (Rodrigues-Chueca et al., 2012).

In these experiments, the parameters involved in the process were treatment time, temperature, initial population and light intensity. Furthermore, in order to achieve a decent fitting model, the interactions of the parameters were used; the first-order model (20-60˚C) without interactions yields R^2 =51.17% (model not shown). The ANOVA tables have indicated initial population as relatively insignificant; however, it is chosen to model all the experiments in one equation and include it in the model, expressed as follows:

Process Efficiency (%) = -41.60 - 8.43 t + 1.76 T - 2.20e-005 C + 0.02 I + 0.27 t*T + 5.03e-006 t*C + 0.036 t*I + 3.77e-007 T*C - 7.26e-005 T*I + 6.21e-009 C*I – 6.85e-008 t*T*C - 0.001 t*T*I - 3.42e-010 T*C*I + 4.67e-011 t*T*C*I

S = 24.4245, R^2= 65.10%, R^2-(adj) = 62.93%, PRESS = 150725, R^2-(pred) = 60.81%

Figure 3.2.7a demonstrates the level of approach. The R^2, as a general indicator of the success of the fit, gives a 65% of match. In addition, the coefficients and ANOVA table for the model are presented (Table 3.2.4.), confirming the small contribution of the initial population to the model. This figure represents the 240 experiments conducted in these conditions and X axis presents the order of experimental runs, from 1 to 240. Each X value corresponds to an Efficiency value, shown in Y axis. The difference between the experimental and the calculated value (linear model values) is shown by the distance among the two corresponding marks. The trends are similar; the values follow the same tendency and are relatively close.

However, following the same principle noticed in the disinfection experiments, splitting the data in two sets, of lower and equal to 40˚C and to higher than 40˚C is proposed. Even though the use of interactions suggests the introduction of the synergies (especially light and temperature) in the model, there exists a possible danger of over-fitting and un-necessary complexity in a simple concept, like the general linear model. For the above reasons, a temperature-dependent linear model, without the use of interactions between the parameters is proposed.

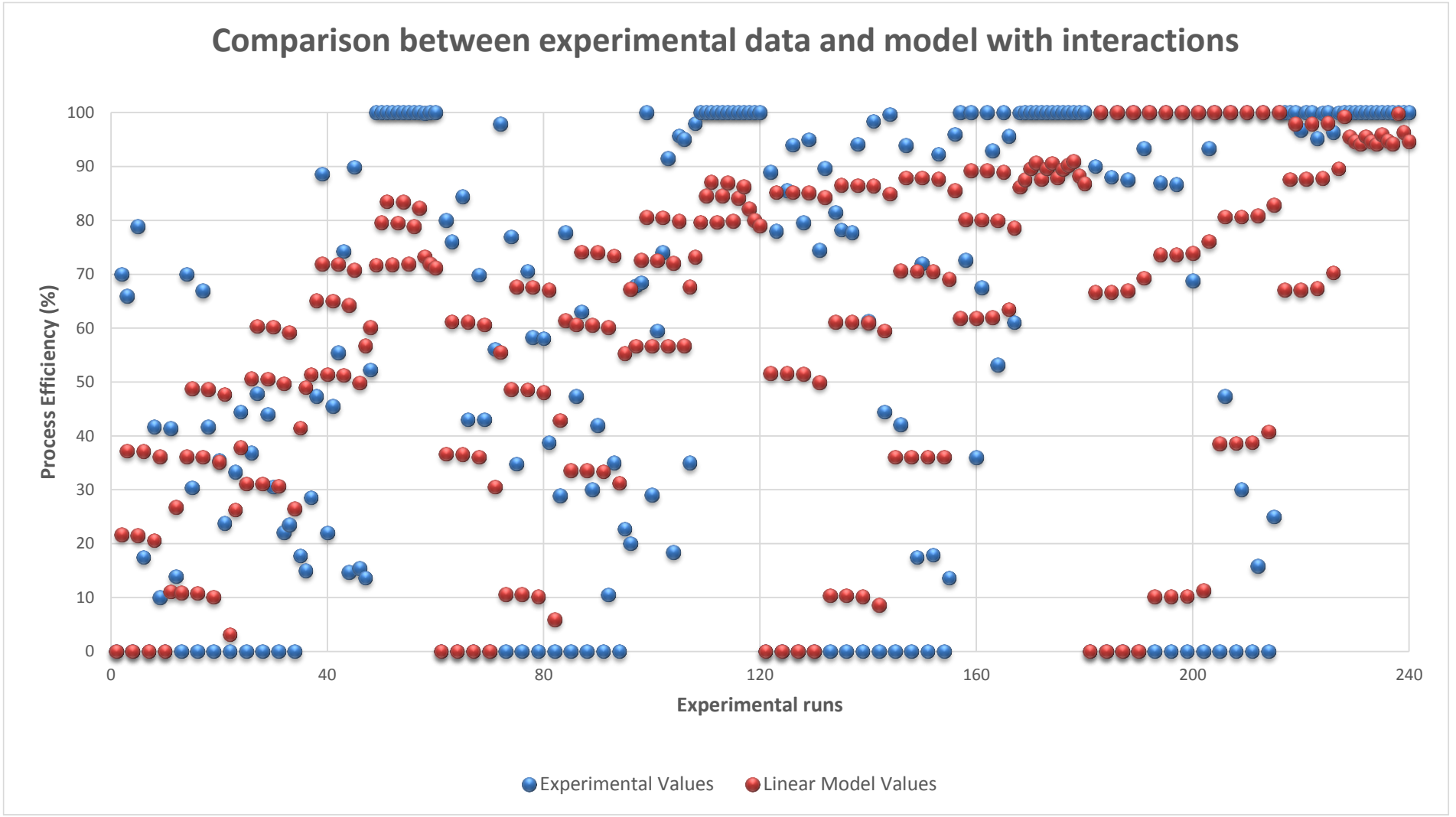
Comparison between experimental data and model with interactions
Process Efficiency (%)
0
10
20
30
40
50
60
70
80
90
100
0
40
80
120
160
200
240
Experimental runs
Experimental Values
Linear Model Values

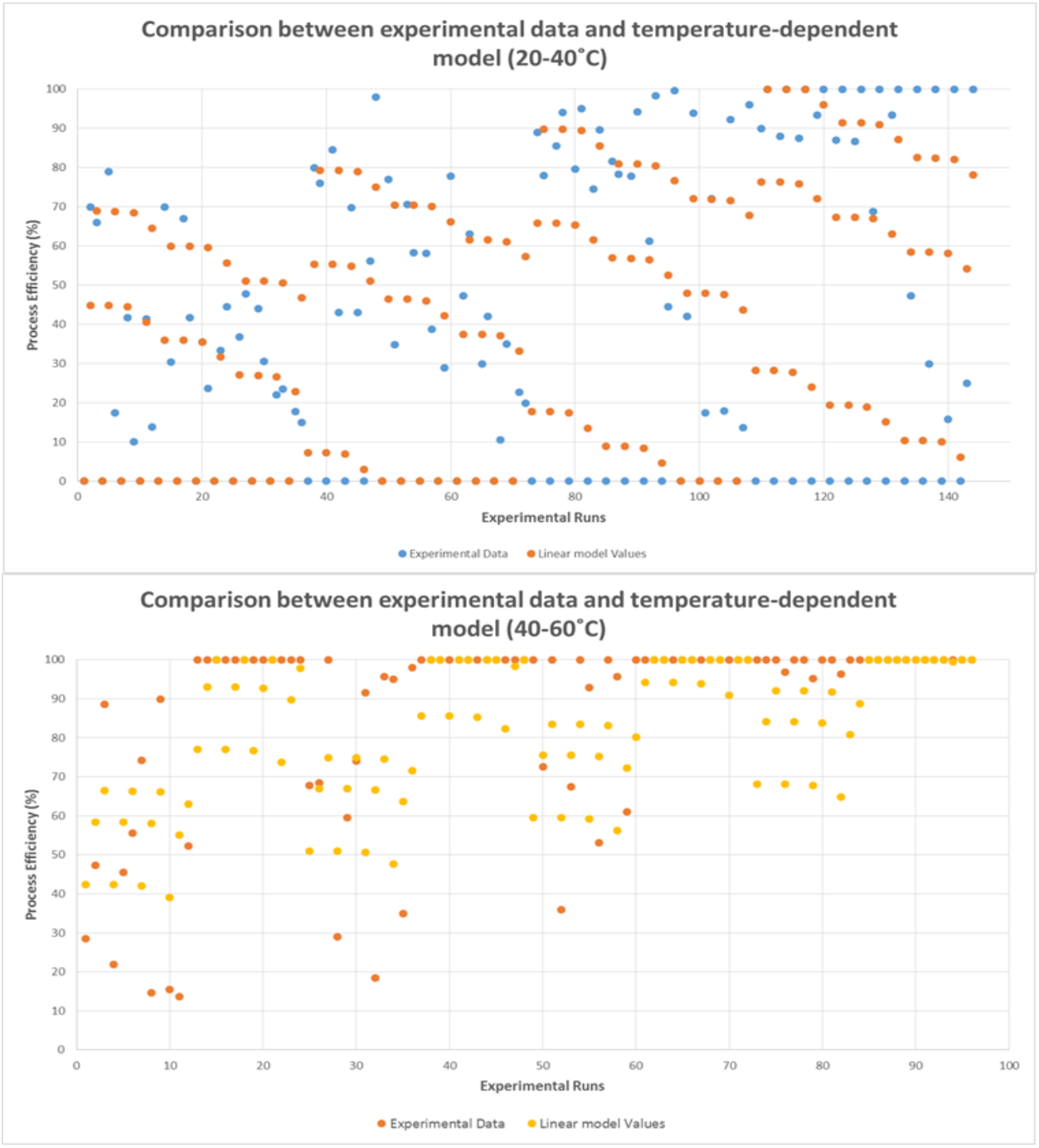

Figure 3.2.7: Fitting of the linear models to the experimental data. a) Linear model with interactions.b) Temperature dependent model (20-40˚C). c) Temperature dependent model (40-60˚C).

$$\textbf{Process Efficiency}\ (\%) = \begin{cases} 4.21 + 10.47\ \mathrm{t} - 0.89\ \mathrm{T} - 4.29 * 10^{-6}\ \mathrm{C} + 0.06\ \mathrm{I}, \textbf{for } \mathbf{20 \leq T \leq 40^{\circ}C} \\ -139.68 + 8.57\ \mathrm{t} + 3.47\ \mathrm{T} - 3.34 * 10^{-6}\ \mathrm{C} + 0.02\ \mathrm{I}, \textbf{for } \mathbf{40 < T \leq 60^{\circ}C} \end{cases}$$

First of all, the coefficients are included in Table 3.2.4. The new model has more advantages than the formerly suggested; the regression standard error (S) is lower, it does not use 2nd level interactions and in addition, it yields higher R^2 values. Therefore, it is a simpler and more accurate model, describing in better extent the evolution of the process efficiency. Figures 3.2.7a and b present in separate plots the experimental values acquired versus the predicted ones from the model (40˚C plotted in both figures for better demonstration of the temperature evolution). All things considered, this temperature-dependent model is a good indicator of the tendencies present in solar disinfection of wastewater or an estimating tool concerning the remaining population within some range, rather than an actual predictor of the efficiency.

Table 3.2.4. – Summary of the statistical parameters of the full interaction model.

Coefficients					Analysis of Variance					
Model 1	**Coef**	**S**	**T**	**P**	**DF**	**Seq SS**	**Adj SS**	**Adj MS**	**F**	**P**	**Summary of Model**
Constant	-41.6006	21.2256	-1.9599	0.0510	14.0	250386.0	250386.0	17884.7	29.9798	0.0000	S = 24.4245
t	-8.4277	7.5979	-1.1092	0.2690	1.0	28413.0	734.0	734.0	1.2304	0.2685	PRESS = 150725
T	1.7565	0.5057	3.4736	0.0010	1.0	83168.0	7198.0	7197.9	12.0658	0.0006	R^2 = 65.10%
C	0.0000	0.0000	-0.6980	0.4860	1.0	402.0	291.0	290.6	0.4872	0.4859	R^2-(adj) = 62.93%
I	0.0178	0.0241	0.7418	0.4590	1.0	84823.0	328.0	328.3	0.5503	0.4590	R^2-(pred) = 60.81%
t*C	0.0000	0.0000	0.4976	0.6190	1.0	656.0	148.0	147.7	0.2476	0.6192	
t*T	0.2726	0.1815	1.5023	0.1340	1.0	1801.0	1346.0	1346.3	2.2568	0.1344	
t*I	0.0355	0.0085	4.1911	0.0000	1.0	7360.0	10479.0	10478.5	17.5650	0.0000	
T*C	0.0000	0.0000	0.4779	0.6330	1.0	26.0	136.0	136.2	0.2283	0.6332	
T*I	-0.0001	0.0006	-0.1257	0.9000	1.0	37360.0	9.0	9.4	0.0158	0.9001	
C*I	0.0000	0.0000	0.2742	0.7840	1.0	83.0	45.0	44.8	0.0752	0.7842	
t*T*C	0.0000	0.0000	-0.2630	0.7930	1.0	15.0	41.0	41.2	0.0691	0.7928	
t*T*I	-0.0007	0.0002	-3.1913	0.0020	1.0	6122.0	6075.0	6075.4	10.1841	0.0016	
T*C*I	0.0000	0.0000	-0.5146	0.6070	1.0	107.0	158.0	158.0	0.2648	0.6073	
t*T*C*I	0.0000	0.0000	0.2936	0.7690	1.0	51.0	51.0	51.4	0.0862	0.7693	
Error					225.0	134225.0	134225.0	596.6			
Total					239.0	384611.0					
Model 2 (≤40˚C)	**Coef**	**S**	**T**	**P**	**DF**	**Seq SS**	**Adj SS**	**Adj MS**	**F**	**P**	**Summary of Model**
Constant	4.2149	7.7882	0.5420	0.5890	4.0	151682.0	151682.0	151682.0	94.3	0.0	S = 20.0507
t	10.4743	1.4945	7.0086	0.0000	1.0	19748.0	19748.0	19748.0	49.1	0.0	PRESS = 60045.2
T	-0.8980	0.2046	-4.3882	0.0000	1.0	7742.0	7742.0	7742.0	19.3	0.0	R^2 = 73.08%
C	0.0000	0.0000	-1.0770	0.2830	1.0	466.0	466.0	466.0	1.2	0.3	R^2-(adj) = 72.30%
I	0.0588	0.0034	17.5428	0.0000	1.0	123726.0	123726.0	123726.0	307.8	0.0	R^2-(pred) = 71.07%
Error					139.0	55882.0	55882.0	402.0			
Total					143.0	207564.0					
Model 2 (>40˚C)	**Coef**	**S**	**T**	**P**	**DF**	**Seq SS**	**Adj SS**	**Adj MS**	**F**	**P**	**Summary of Model**
Constant	-139.6750	12.3560	-11.3042	0.0000	4.0	144740.0	144740.0	36185.0	75.3	0.0	S = 21.9270
t	8.5700	1.6343	5.2435	0.0000	1.0	13219.0	13219.0	13219.0	27.5	0.0	PRESS = 71869.3
T	3.4670	0.2238	15.4915	0.0000	1.0	115385.0	115385.0	115385.0	240.0	0.0	R^2 = 68.41%
C	0.0000	0.0000	-0.7650	0.4460	1.0	281.0	281.0	281.0	0.6	0.4	R^2-(adj) = 67.50%
I	0.0210		5.7425	0.0000	1.0	15855.0	15855.0	15855.0	33.0	0.0	R^2-(pred) = 66.03%
Error					139.0	66831.0	66831.0	481.0			
Total					143.0	211571.0					

3.2.5. Specifications concerning solar disinfection of wastewater

Solar disinfection experiments were conducted under a solar simulator that emits all spectrum from 290 nm and above, excluding infrared wavelengths, due to the existence of cut-off filters. Therefore, the actions expected should be attributed UVB, UVA and visible light. In this subsection, a discussion is done of how these light fractions and some environmental conditions can determine the observed results

3.2.5.1. Inactivation mechanism: Light source and bacterial damage

i) UVB irradiation:

Malatana-Surget et al, (2012) have stated the double action of UVB irradiation; in general, UVB damage is considered to mainly cause direct DNA damage, through the creation of photoproducts (cyclobutane pyrimidine dimer and the pyrmidine (6–4) photoproducts) (Hallmich and Gehr, 2010). They also mention the creation of internal and external reactive oxygen species (ROS) such as hydrogen peroxide (H_2O_2), and more profoundly, the creation of singlet oxygen (Regensburger et al., 2011). These ROS attack nucleic acid, proteins and cell lipids (Storz and Imlay, 1999). However, UVB is very often overlooked, although it has a relatively high contribution in bacterial inactivation. The important impact of UVB inactivation of bacteria has been stated since 1974 (Setlow et al. 1974), there are very few works that add up to this wavelength band to attribute part of the bacterial inactivation. Of course, this happens due to the sensitivity of UVB to meteorological phenomena, but this is far from the present case, and a force two or three orders of magnitude higher than UVA cannot be overlooked (Opezzo, 2012; Mbonimpa et al, 2012). Also, the peak of UVB germicidal activity, roughly among 300 and 310 nm, is clearly within the employed range (Mbonimpa et al., 2012) and according to previous reports, UVB radiation of 313 nm demonstrates an interaction with the 365 nm, to enhance DNA transformation (Peak et al., 1975; Tyrell and Peak., 1978). Hence, there is a double UVB action, of DNA strand break, and the creation of ROS which have been identified to be implicated in bacterial inactivation through oxidative stress.

ii) UVA irradiation/near-UV visible light

UVA-induced loss of bacterial cultivability is attributed to the catalysis of the formation of ROS. It is the least effective irradiation range to damage bacterial DNA directly, but its proven efficiency (Robertson et al., 2005) comes from the biological effects of internal and external ROS attacks, such as protein destruction or adducts of nucleic acid with membrane proteins with the bacterial envelope escaping key damage, towards cell inactivation (Pigeot-Remy et al., 2012). One of the first attacks is the respiratory chain and the cell's potential to produce ATP (Bosshard et al., 2010a). Other attacks include internal photo-Fenton reaction (Spuhler et al., 2010) due to loose cell iron sources, disruption of normal internal ROS suppression mechanism (SOD, catalase etc.) (Chiang et al., 2012) and others, all related by the ROS production inside and outside the cell. ROS are normal by-products of bacterial respiratory chain, and bacteria possess a big number of suppressive mechanisms (Mishra and Imlay, 2012). Hence, UVA damage is an internal/external

oxidative damage, plus the internal/external photo-Fenton contribution, with measurable effects; an increase in dose can inflict greater damage (Polo-Lopez et al., 2011).

3.2.5.2. Inactivation mechanism: Influence of the water matrix

There is no disagreement that the majority of the solar disinfection experiments were conducted in distilled or drinking water, making the inactivation mechanism clear and well established. The main difference of this synthetic secondary effluent is the added salts and organic components. Marugan et al. (2010) have explained that during bacterial osmotic stress among the first released ions are calcium and magnesium ones, while Caballero et al. (2009) stated the importance of organic substances as nutrient sources for bacteria; therefore, bacterial survival/growth is favored in this matrix. Given the absence of light in the first group of experiments, growth is normal and expected, and as temperature rises, with a peak around 35-39˚C (according to the discreet choice, 40˚) growth will be increased. However, this behavior is expected to change when the irradiation is present and light is applied to the sample. The presence of organic substances can induce an indirect stress. They can either be endogenous, like porphyrins, co-enzymes or cytochromes, or exogenous, synthetical ones, which lead to either internal or external photosensitized matter. After receiving UV irradiation, this effect can cause indirect photolysis, while the photosensitizers are in an excited, high energetic state (Matthews, 1991; Dunkel, 1992; Reed, 2004). Other works however, have demonstrated reduction of cell inactivation, when inorganic and organic compounds were present (Sichel et al., 2007; Alrousan et al., 2009; Dunlop et al., 2011).

3.2.5.3. Temperature influence and evolution of experiments

As demonstrated in the experimental part, temperature altered the outcome of the inactivation assays in great extent, from level to level. For this reason, the experiments were divided in two parts, below and over 40˚C degrees. Wegelin et al, (1994) reported no differences between 12 and 40˚C in water, and Reed (2004) explained this behavior by the double effect of temperature range. When temperature is increased, growth is favored, and inactivation as well: Thermally-driven growth is cancelled by oxygen depletion, due to its lower solubility at higher temperatures. In the experiments presented, growth was favored to a point that the synergic effect was cancelled, depletion of oxygen did not occur (samples under mild stirring) and eventually, until the intensity was increased over 1000 W/m^2, light alone could not overcome the rapid growth. Rincon and Pulgarin (2003) suggested the increase in intensity to efficiently remove *E. coli*, and also, the effects of physiological bacterial state; the same techniques are adopted to ensure reproducible results.

When low temperatures were applied, metabolic activity was at its minimum, so the same actions of light battled against less targets. This, however was not the case in temperatures around 40˚C, where excessive

growth was observed, thus providing more targets for incoming photons or ROS. In addition, this excess growth can lead to extensive shielding from one cell to another (Craik et al., 2001), inducing higher inactivation rates for increased populations. In the first steps of each experiment, a shoulder is observed, and this latency effect is due to initial self-defense mechanisms (Rincon and Pulgarin, 2003). As time passes and new generations of bacteria appear due to high reproduction rates, the new generations are more resistant to the disinfecting action of light, having endured the exposure of the original cells towards the actions of light. It has been stated that a greater effectiveness of applying a high intensity for a short time is demonstrated and preferred, rather than applying a lower intensity for a longer period of time (Sommer et al, 1998).

3.3. Bacterial regrowth: the effect of disinfection conditions on the subsequent dark repair

All samples submitted to 4-h solar exposure tests and presented in section 3.2 were subsequently stored for 24 and 48 h for dark repair evaluation. The experimental conditions of the dark repair tests were presented in section 3.1.2 to 3.1.4. The results are presented and discussed herein, with a focus on the effect of disinfection conditions on post-irradiation dark repair.

3.3.1. Post-processing events: Parameters affecting dark survival and/or regrowth after null irradiation experiments

As far as the post-treatment events are concerned, the behavior of *E. coli* is divided into two groups: treated under mild temperatures (20-40˚C) or treated in higher temperatures than 40˚C. The first group of graphs presenting the experiments performed in lower temperatures (Figure 3.3.1a), demonstrates a high increase of the bacterial population, influenced by the pre-treatment conditions. It is clear that the samples treated at 40˚C, present higher dynamics of growth and relatively higher final counts after 24 and 48h. Also, there is visible influence of the initial population, by which higher initial populations result in higher reproduction rates after 48 h. In addition, one can notice a gradual decrease in growth rates between the 1st and the 2nd day of storage, probably interpreted by the stress caused by some initial nutrient shortage, due to the overgrown bacterial numbers.

Figures 3.3.1b and c are the contour plots that visualize all regrowth tests, performed by hourly sampling in all temperatures and initial population rates. They reveal that there is a correlation between the treatment temperature and the regrowth after 24 or 48 h (expressed by C_{24}/C_0 and C_{48}/C_0). These fractions reveal the regrowth of the bacterial numbers higher than the initial one; if the ratio is <1, then survival is observed, instead. Lower temperatures present suppressed rates, compared to higher ones. Also, the difference between the bacterial number after 24 h and 48 h is noticeable, being influenced by the disinfection conditions, which is expressed in orders of magnitude. Plus, temperatures that initially seemed safer against regrowth (around 25˚C), demonstrate equally high rates. In Figures 3.3.1d and e, the correlation between treatment time and regrowth is presented; the prolongation of the experiment has a profound effect in the bacterial numbers observed after 2 days. However, initial concentration cannot be attributed to a direct effect. In the last sub-graphs which present the main effects of the temperature on regrowth, elevating temperature during treatment is observed to have a strong and rather linear impact only over 30˚C for the regrowth after one day, and stronger for after two days.

The samples treated under higher temperatures (Figure 3.3.2a) do not present any recovery of the population; the population, if any bacteria still existed, continued the decay during dark storage. For the bacterial samples treated at 50˚C, although total inactivation was not observed, after 24h no viable counts

were observed. As it seems, the thermal damage rendered bacteria unable to reproduce; no repair mechanism was observed to act. The remaining samples, after their treatment at 60˚C, presented the same behavior. Higher temperatures accelerated inactivation, which was total within the 4-h timespan, and no regrowth was observed thereafter.

Contour plots in Figures 3.3.2b and c, present the survival rates after 24 and 48 hours, for all hourly samples taken during disinfection. First of all, high regrowth risk (C_{24}/C_0 and $C_{48}/C_0 \geq 1$) is observed around 50˚C and for 60-90 min of treatment. The survival pattern for the rest of temperatures and time is consistent, for the two post-treatment days, and slightly more elevated numbers are observed after 2 days. The main effects plots (Figures 3.3.2 d and e) demonstrate the inverse effect that high-temperature treatment has on regrowth; as time passes, survival capability is diminishing, and as temperature increases, the same effect is observed. However, initial population follows a similar pattern from the first to the second day.

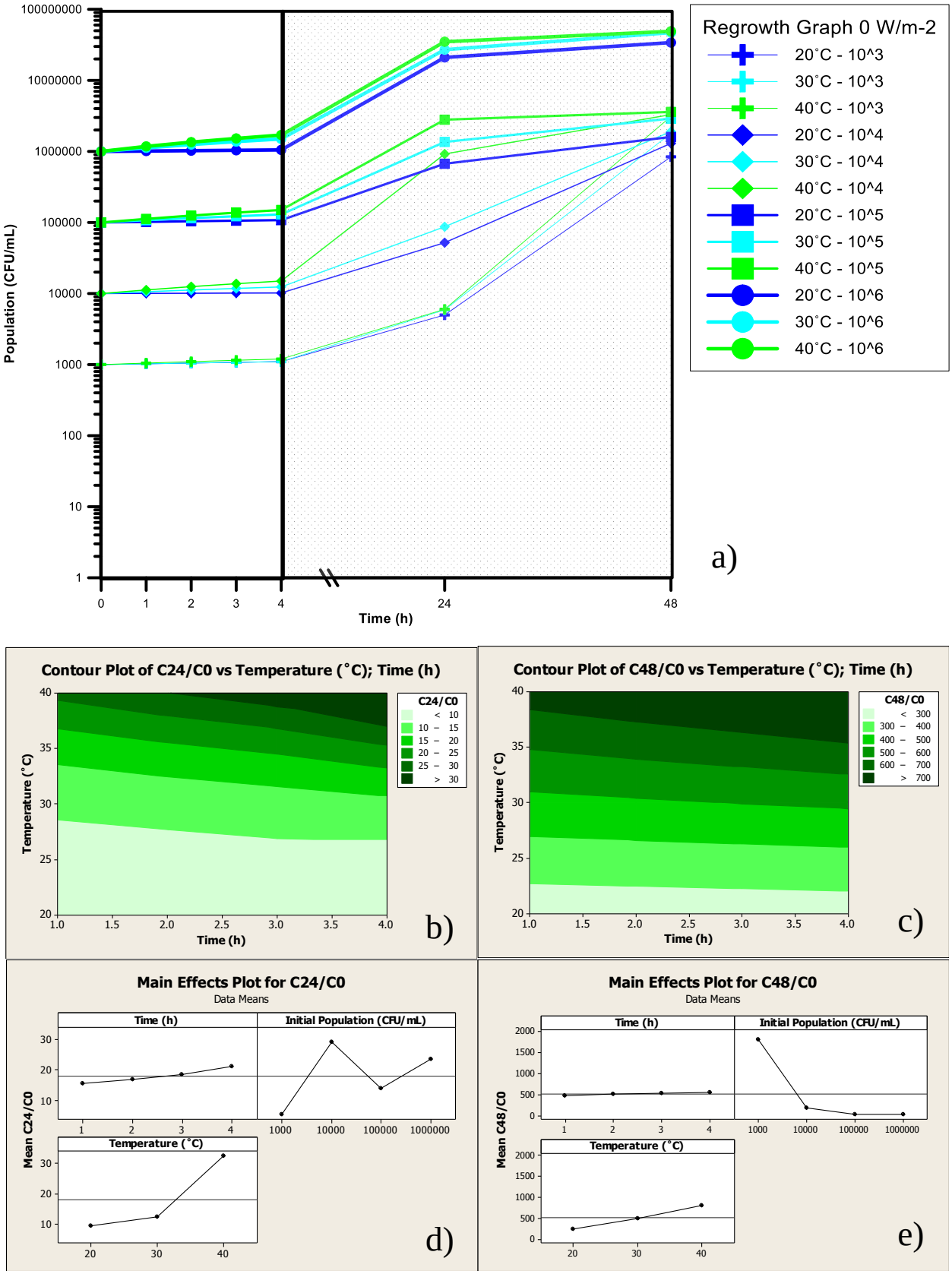

Figure 3.3.1: Main results of non-irradiation experiments for synthetic secondary effluent at among 20-40˚C and all initial *E. coli* populations. (a) Post-treatment regrowth curves. (b) Contour plot of regrowth after 1 day vs. temperature and time. (c) Contour plot of regrowth after 2 days vs. temperature and time. (d) Main effects plot (control variable: Regrowth after 1 day). (e) Main effects plot (control variable: Regrowth after 2 days).

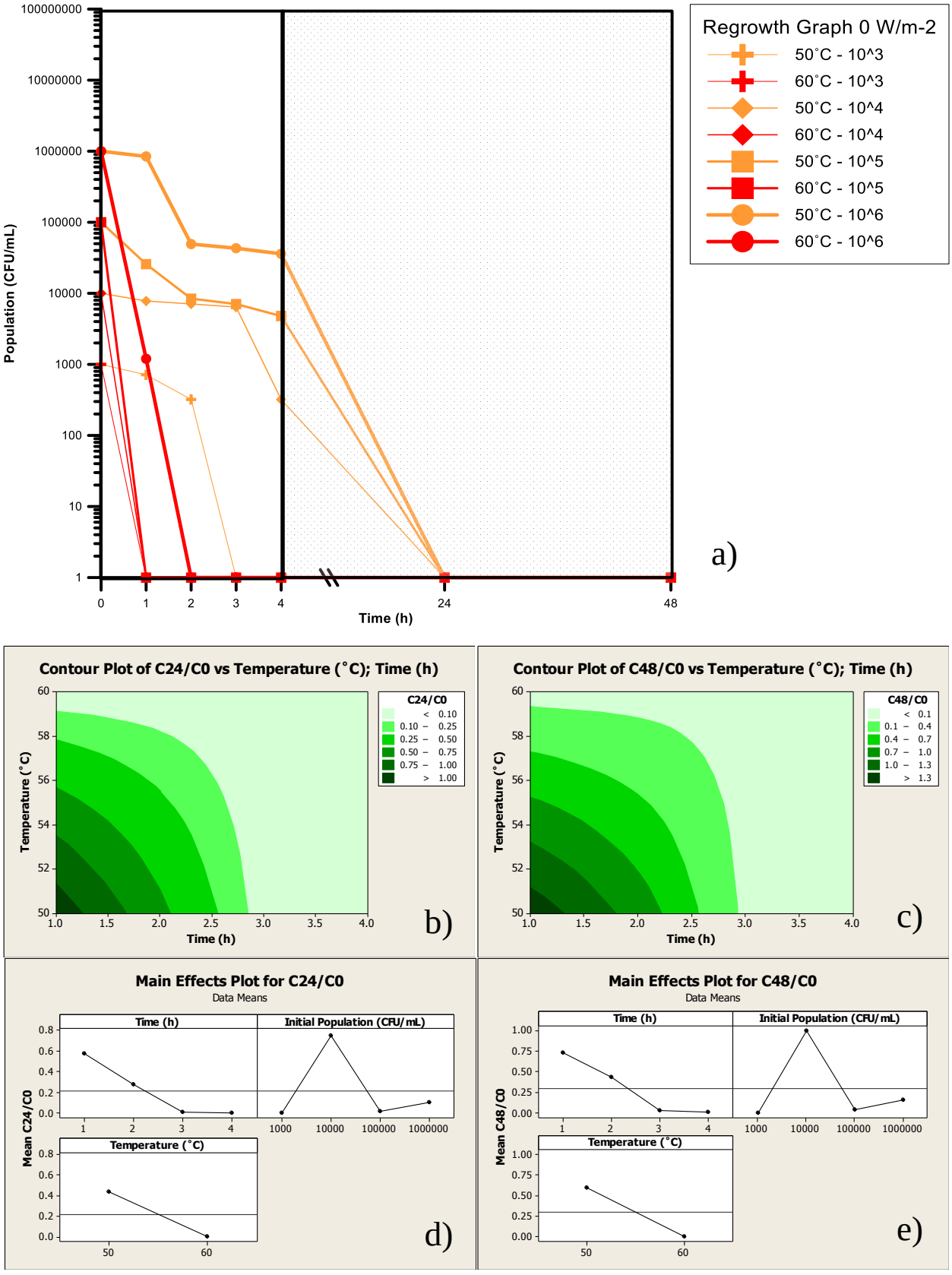

Figure 3.3.2: Main results of non-irradiation experiments for synthetic secondary effluent at among 50-60˚C and all initial *E. coli* populations. (a) Post-treatment regrowth curves. (b) Contour plot of regrowth after 1 day vs. temperature and time. (c) Contour plot of regrowth after 2 days vs. temperature and time. (d) Main effects plot (control variable: Regrowth after 1 day). (e) Main effects plot (control variable: Regrowth after 2 days).

3.3.2. 800-W/m^2 experiments: Effects of 800-W/m^2 intensity illumination on the parameters affecting survival and/or regrowth

Figures 3.3.3 and 3.3.4 present the extension of monitoring the bacterial population for 48 more hours after 800-W/m^2 intensity irradiation is complete. Results are grouped per temperature range (20-40˚C and 50-60˚C) and initial concentration of bacteria. It can be deduced that post-irradiation survival is more complex, compared to the experiments in absence of light.

The first temperature range (20-40˚C, Figure 3.3.3) presents elevated (re)growth/survival rates; since there is no total inactivation taking place (i.e. zero viable counts), the recovery of the bacterial numbers could be attributed to i) live bacteria that continued replicating, ii) bacteria that recovered their DNA lesions by dark repair methods, and growth of the revived bacteria (Guo et al., 2011).

The contour plots (Figure 3.3.3b and c) demonstrating the bacterial population after 24 or 48 h, reveal an interesting behavior, as far as the influence temperature is concerned. Although the temperature range of 40-50˚C includes a breaking point, where bacterial disinfection is drastically changing, it appears that 30˚C is the most critical for regrowth. First of all, after 24 h, regrowth is not probable, and only occurred from samples treated around 3-4 h and 30-40˚C. Samples that were treated in low temperatures and for short time, present low counts after 24 h.

Normally bacteria in samples that remain for longer time under illumination tend to get more inactivated, as it is shown in Figure 3.3.3a. However, prolonging their treatment in this favorable temperature promotes multiplication and therefore, new strains, that gain resistance against solar irradiation in conditions of exposure to (visible) light (Hijnen et al, 2006; Nebot Sanz et al, 2007; Shang et al, 2009). This bacterial ability is a heritage of evolution through time, to protect themselves from the natural ultraviolet rays from the sun (Quek and Hu, 2008).

As a consequence, higher remaining populations led to higher survival rates from the bacteria. Although Lindenauer and Darby, (1994) supported that no significant correlation exists between regrowth and the initial number of coliforms in wastewater, at any dose; they found out that in low doses, the surviving coliforms affected the reactivation rates. Craik et al. (2001) explained this noting that if the initial population is high, there is a big chance that there will be a part of it going through unharmed due to shielding (by each other) and bad mixing.

After 48 h, a change in the effect takes place; in Figure 3.3.4c, samples treated in lower temperatures and for shorter times, demonstrate higher regrowth rates and samples presenting regrowth in the first 24 h, showed 5-fold lower rates during the second 24-h period. This is clearly demonstrated in the main effects plot, where treatment times reveal inverse action, and 30˚C reveal their statistical significance in regrowth. This can be explained, mostly by the action of light; samples that were treated for a short time accumulated a relatively low dose, and were able to recover their cultivability, whereas samples that were treated in high

temperatures (and showed high regrowth), remained for a long time under illumination, and their repair capabilities were diminished.

The behavior of bacteria that were treated in high temperatures is more straightforward (Figure 3.3.4). First of all, almost no regrowth is observed; all values for C_{24}/C_0 and C_{48}/C_0 are <1. Hence, it can be deduced that it is crucial to obtain null bacterial counts at the end of the experiments (total inactivation) in order to avoid their re-appearance. The combined action of light and temperature, and the joint actions are proven to be not only more efficient, but hinder re-population as well. Regarding the Figure 3.3.4b and c, that picture bacterial survival after 24 and 48 hours, there is one point worth commenting; the highest survival rates have appeared around 1.5-2 h, but low for sure. This is explained by the influence of the type of concurring actions in the batch tests employed in this study: there is an equilibrium between growth and inactivation, and it appears to bend in favor of inactivation, at this time point, for 50˚C. Beyond this time mark, inactivation is higher, and as inactivation negatively influences regrowth, lower rates are observed. Finally, in the main effects plot in Figures 3.3.4d and e, temperature and time have a straightforward effect, where prolongation of treatment equals to regrowth suppression; this is considered normal, since higher experimental times assists both bacterial protein damage and light inactivation.

3.3.3. High intensity experiments (1200 W/m^2): Effects of high intensity illumination on the parameters affecting survival and/or regrowth

In Table 3.3.1 the total inactivation achieved after 4 h in all samples has been demonstrated, in all temperature ranges and initial population, at 1200 W/m^2. As it seems, apart from the contribution of temperature the beneficial effect of switching from thermal to light/thermal treatment was verified, now it is evident that light has a significant, additional role in bacterial inactivation (Ubomba-Jaswa et al., 2009); for the same temperature levels and initial bacterial population in the samples, the outcome was altered when intensity was increased from 800 to 1200 W/m^2. The synergy of light and temperature has reached the maximum inactivating action (among the presented cases), leading to null bacterial counts, at the end of the treatment, for another 2 days.

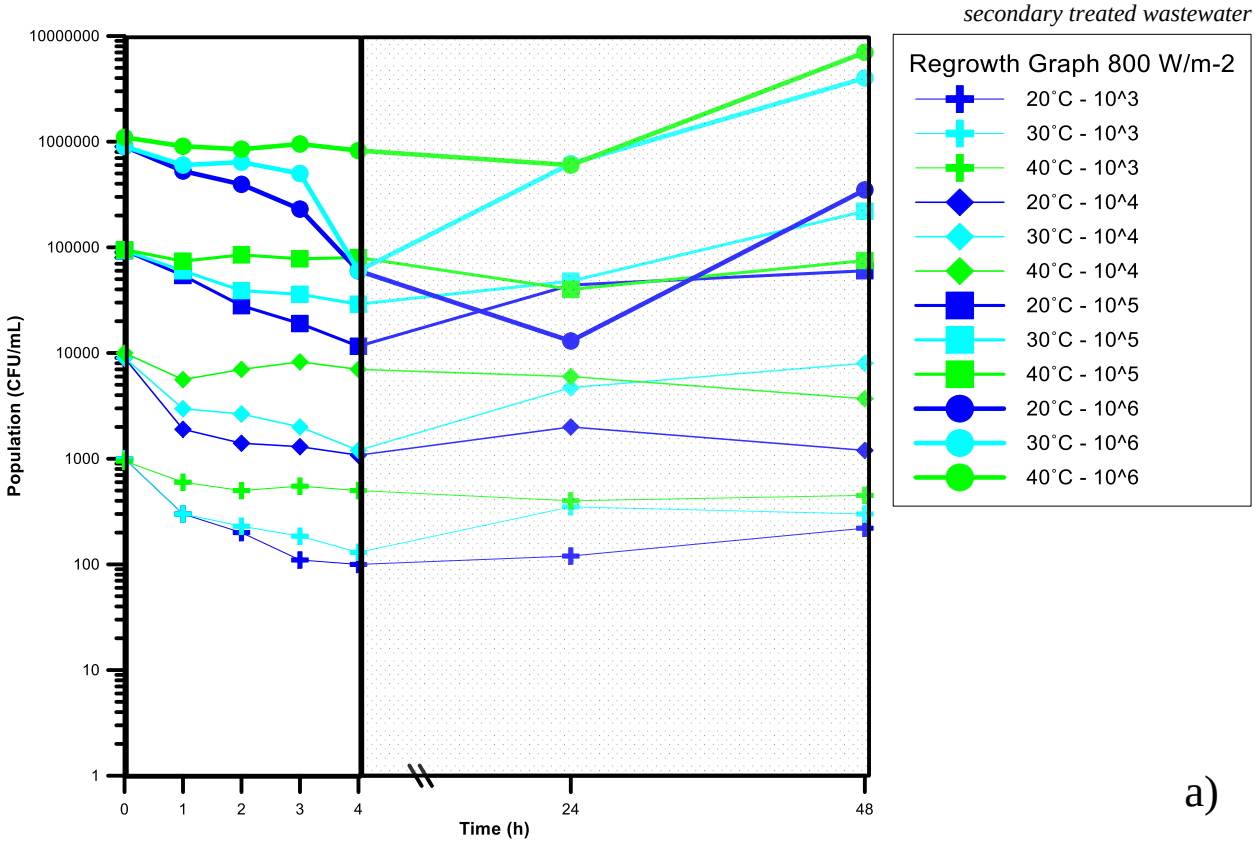

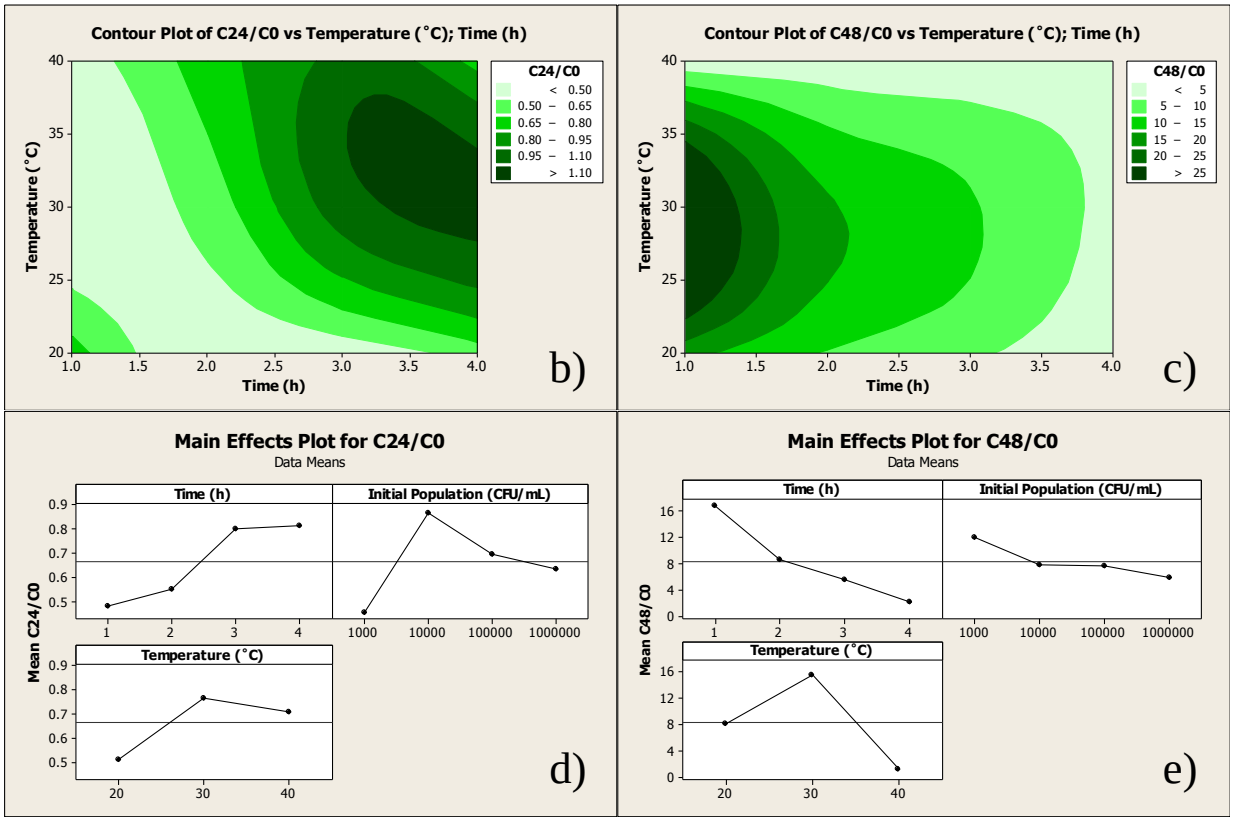

Figure 3.3.3: Main results of 800 W/m^2-irradiated experiments for synthetic secondary effluent at among 20-40˚C and all initial *E. coli* populations. (a) Post-treatment regrowth curves. (b) Contour plot of regrowth after 1 day vs. temperature and time. (c) Contour plot of regrowth after 2 days vs. temperature and time. (d) Main effects plot (control variable: Regrowth after 1 day). (e) Main effects plot (control variable: Regrowth after 2 days).

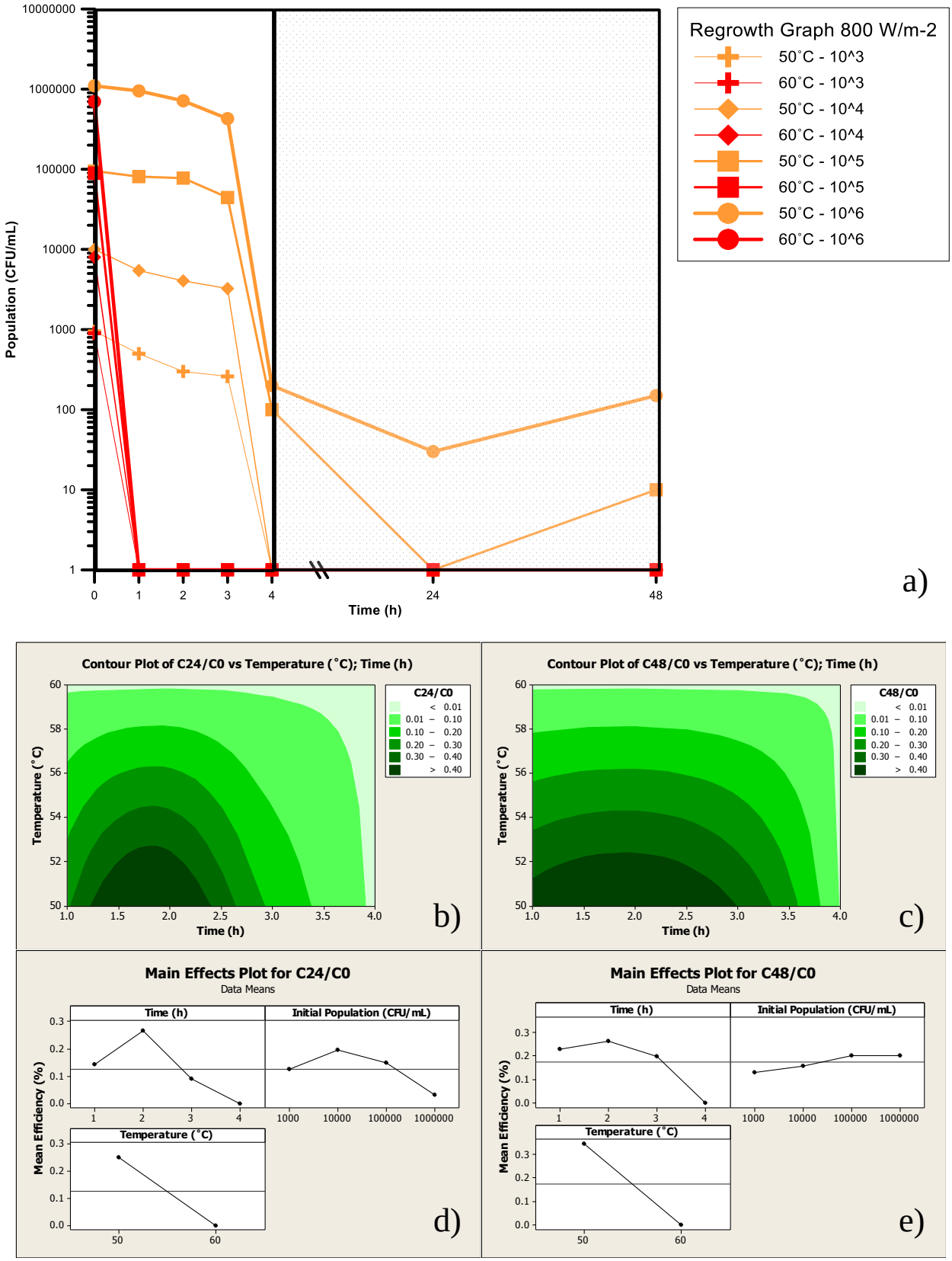

Figure 3.3.4: Main results of 800 W/m^2-irradiated experiments for synthetic secondary effluent among 50-60˚C and all initial *E. coli* populations. (a) Post-treatment regrowth curves. (b) Contour plot of regrowth after 1 day vs. temperature and time. (c) Contour plot of regrowth after 2 days vs. temperature and time. (d) Main effects plot (control variable: Regrowth after 1 day). (e) Main effects plot (control variable: Regrowth after 2 days).

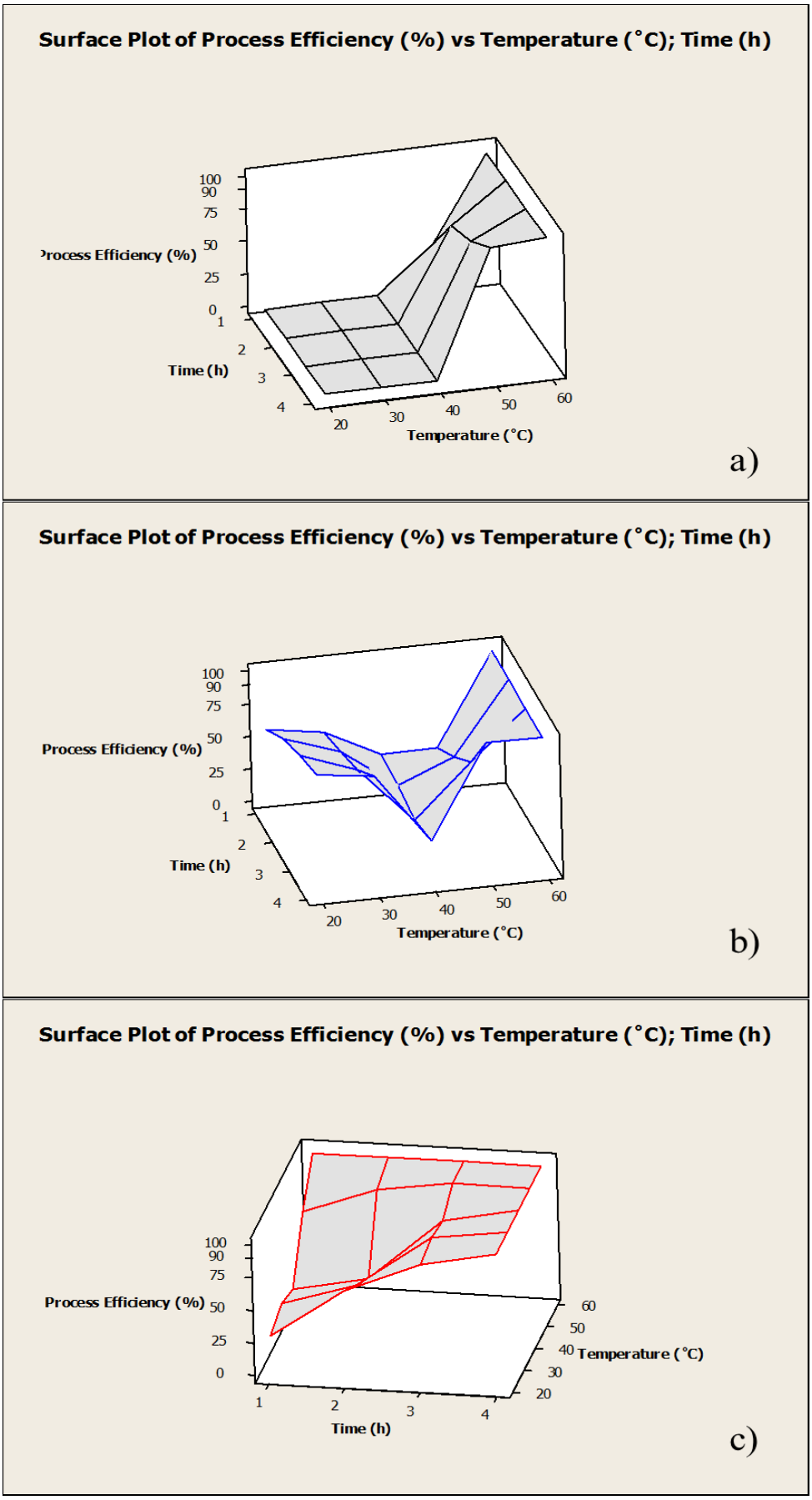

Figure 3.3.5: Overview of disinfection experiments. Process efficiency vs. treatment time and temperature is plotted. a) 0 W/m^2. b) 800 W/m^2. c) 1200 W/m^2

Table 3.3.1. – Inactivation efficiency % (at the end of each treatment method).

Intensity	Population (CFU/mL) / Temperature (˚C)	10^3	10^4	10^5	10^6
0 W/m^2	20˚C (% growth)	*10*	*2*	*8*	*5*
	30˚C (% growth)	*10*	*24*	*30*	*50*
	40˚C (% growth)	*20*	*50*	*50*	*70*
	50˚C	100	96.8	95.2	95
	60˚C	100	100	100	100
800 W/m^2	20˚C	90	88	87.5	93.3
	30˚C	87	86.7	68.8	93.3
	40˚C	47.4	30	15.8	25
	50˚C	100	100	99.9	99.9
	60˚C	100	100	100	100
1200 W/m^2	20˚C	100	100	100	100
	30˚C	100	100	100	100
	40˚C	100	100	100	100
	50˚C	100	100	100	100
	60˚C	100	100	100	100

When moderate light (800 W/m^2) was applied and the conditions favored disinfection (all cases of 60˚C treatment and 10^3–10^4 at 50˚C) no regrowth was observed. Common denominator in all cases was a null bacterial count active at the end of the process. Therefore, it is expected that no regrowth will be observed. Figure 3.3.6a demonstrates the post-treatment phenomena, after the illumination of the varied population samples subjected to the different process temperatures.

In the previous cases, only the outcome after the end of the treatment is plotted, for clarity. However, the contour plots of C_{24}/C_0 and C_{48}/C_0 (Figure 3.3.6a, b, 3.3.7a,b) contain information, for the fate of the microbial population at each hour and level of population and temperature. There are only two combinations that led to regrowth, deriving from samples that were irradiated for only 1 h, around 20 and 40˚C and of high risk are the next 30 min for all temperatures. In this case, there is shortage of dose accumulation from the cells, so the reactivation is highly probable. This is reflected in the regrowth rates in day 2, with the excess growth effects around 40˚C playing the most important role in regrowth appearance.

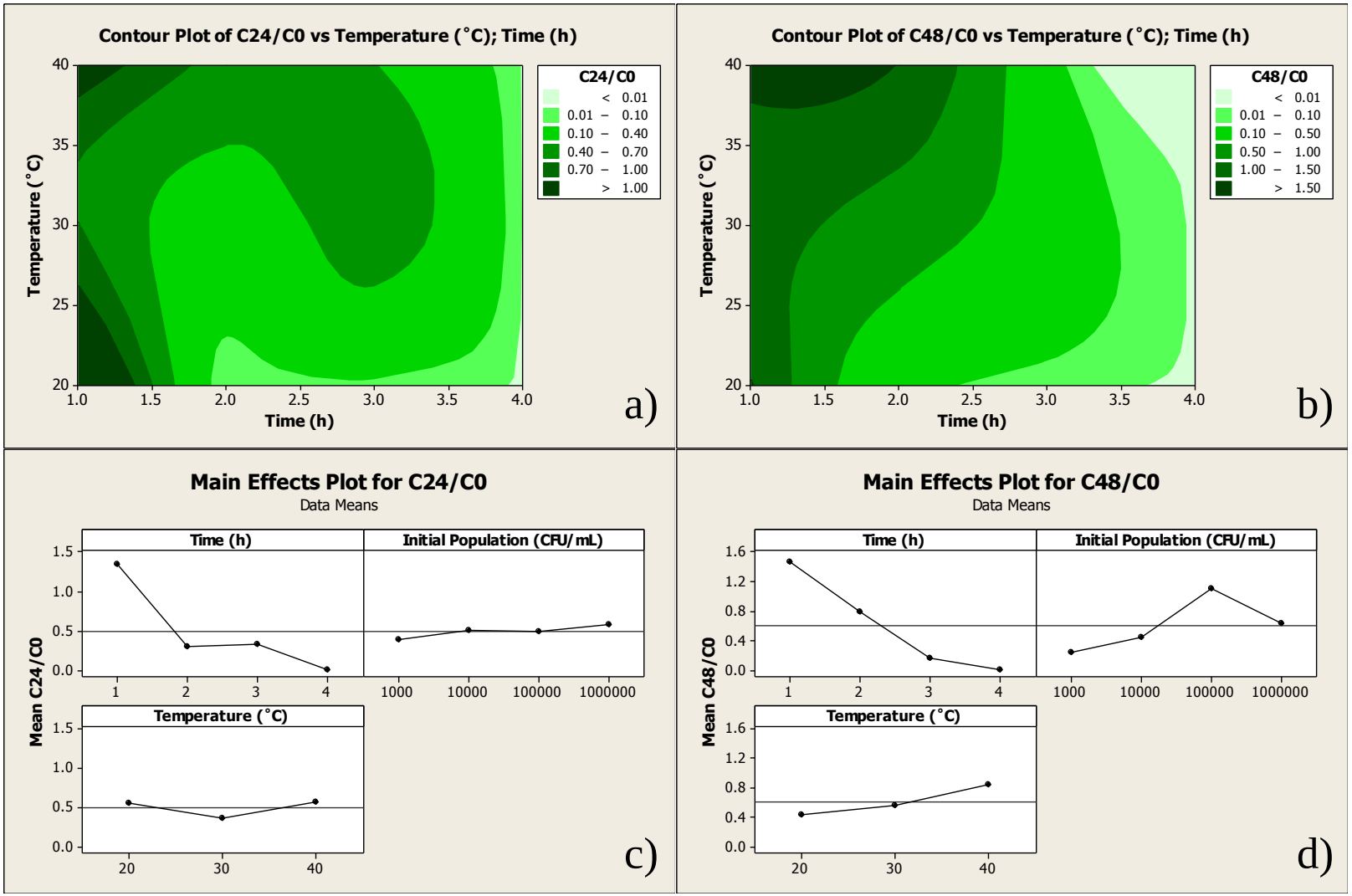

Figure 3.3.6: Overview of the 1200 W/m^2-irradiation experiments, among 20-40˚C and all initial *E. coli* populations. (a) Contour plot of regrowth after 1 day vs. temperature and time. (b) Contour plot of regrowth after 2 days vs. temperature and time. (c) Main effects plot (control variable: Regrowth after 1 day). (d) Main effects plot (control variable: Regrowth after 2 days).

The effect of time, demonstrated in the main effects plots (Figure 3.3.6c and d) is in favor of bacterial inactivation; firstly, prolonging the samples in such high intensities renders bacteria unable to recover or deploy defense mechanisms, because the incoming photonic rate is very high to cope with. Also, after 2 h of treatment, C_{24}/C_0 and C_{48}/C_0 are less than 1, and therefore, no regrowth is observed. Finally, temperature produces the same obstacles stated in the previous section, against inactivation, but high intensities overcome this effect.

The most effective combination, of high intensity and elevated temperatures, is demonstrated in Figure 3.3.7, and shows a very low survival potential and also, for the first time, it is decreasing from day to day. The surviving populations are very low in and in condition unable to recover neither their numbers nor their cultivability and decay day by day. The main effects plots (Figure 3.3.7c and d) demonstrate the negligible differences time and temperature have in survival. However, both main effects plot between 20˚C-40˚C and 40˚C-60˚C allow a good comparison on the effect of light intensity, if compared with the respective ones of 800 W/m^2 and 0 W/m^2. It is clear that although temperature has a strong effect, it affects (re)growth indirectly, through cell growth effects and thermal inactivation. Temperature on the other hand shows that it is the main active force leading to suppressed risk of bacterial re-appearance. For 800 W/m^2, repair was possible, whereas for 1200 W/m^2, even after 1-2 h of exposure, bacteria have lost their ability to perform dark repair of their damage.

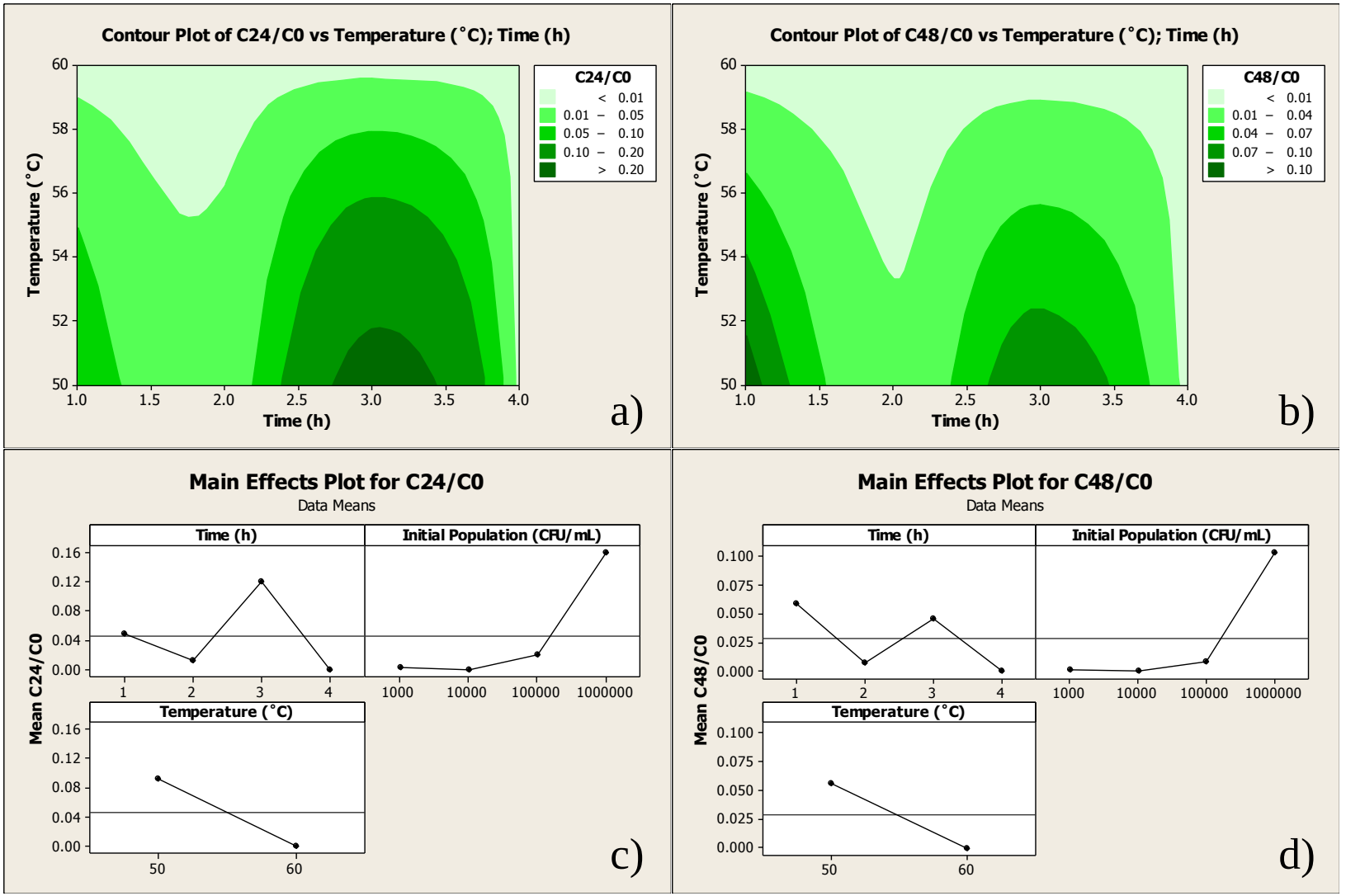

Figure 3.3.7: Overview of the 1200 W/m^2-irradiation experiments, among 50-60˚C and all initial *E. coli* populations. (a) Contour plot of regrowth after 1 day vs. temperature and time. (b) Contour plot of regrowth after 2 days vs. temperature and time. (c) Main effects plot (control variable: Regrowth after 1 day). (d) Main effects plot (control variable: Regrowth after 2 days).

3.3.4. Disinfection efficiency vs. bacterial regrowth

Among others, Guo et al. (2011) and Craik et al. (2001), have suggested the possible states of bacteria in the post-treatment periods, i.e. either non-cultivable bacteria or intact ones that escaped irradiation (and an intermediate state). In any case, when bacteria are present in the dark part of post-treatment period, they can recover their numbers through the dark repair mechanisms. This work has employed plating to measure cultivable bacteria, therefore regrown or surviving bacteria are treated as one, cultivable entity. Also, it was rather avoided suggesting an influence of the initial bacterial population, because of the lack of a straightforward correlation or tendency. Each population level withholds its own special effect; for instance, initial population of 10^3 bacteria encounter more available nutrients per cell and initial population 10^6 offer higher chances of aggregation and shielding; in both cases, surviving bacteria are offered an enhanced possibility of (re)growth. Therefore, in order to be able to correlate the influence of starting bacterial population in the regrowth period, some statistical indicators were used. A main target was to homogenize results, regardless of initial population, to aid the overall robustness of the treatment.

First of all, Figures 3.3.8a and b demonstrate the correlation between the efficiency of the disinfection process, for all possible treatment times (1 to 4 h) and the consequent regrowth, for samples that have been treated in low (20˚C≤T≤40˚C) or high temperatures (40˚C<T≤60˚C). The ▲ traces reveal the population after 24 h while the ▲ traces, after 48 h, expressed as the fraction of bacteria/initial population, for homogenization of the 20˚C≤T≤40˚C results, regardless of initial bacterial numbers. It is observed that in overall, the population after 48 h is tending to be higher than the population after 24 h. It also appears that as efficiency increases, the samples without regrowth are increasing (line indicating $C_{24,48}/C_0$ ratio=1), and a tendency to reduce their regrowth potential, according to the percentage of efficiency increase. However, for higher temperatures, the significant absence of regrowth after 24 h (trace:✚) (line indicating $C_{24,48}/C_0$ ratio=1) and the suppression of growth after 48 h (trace:✚), compared to the lower temperatures is observed. Hence, treating in higher temperatures is detrimental in both short and long-term storage of the treated samples.

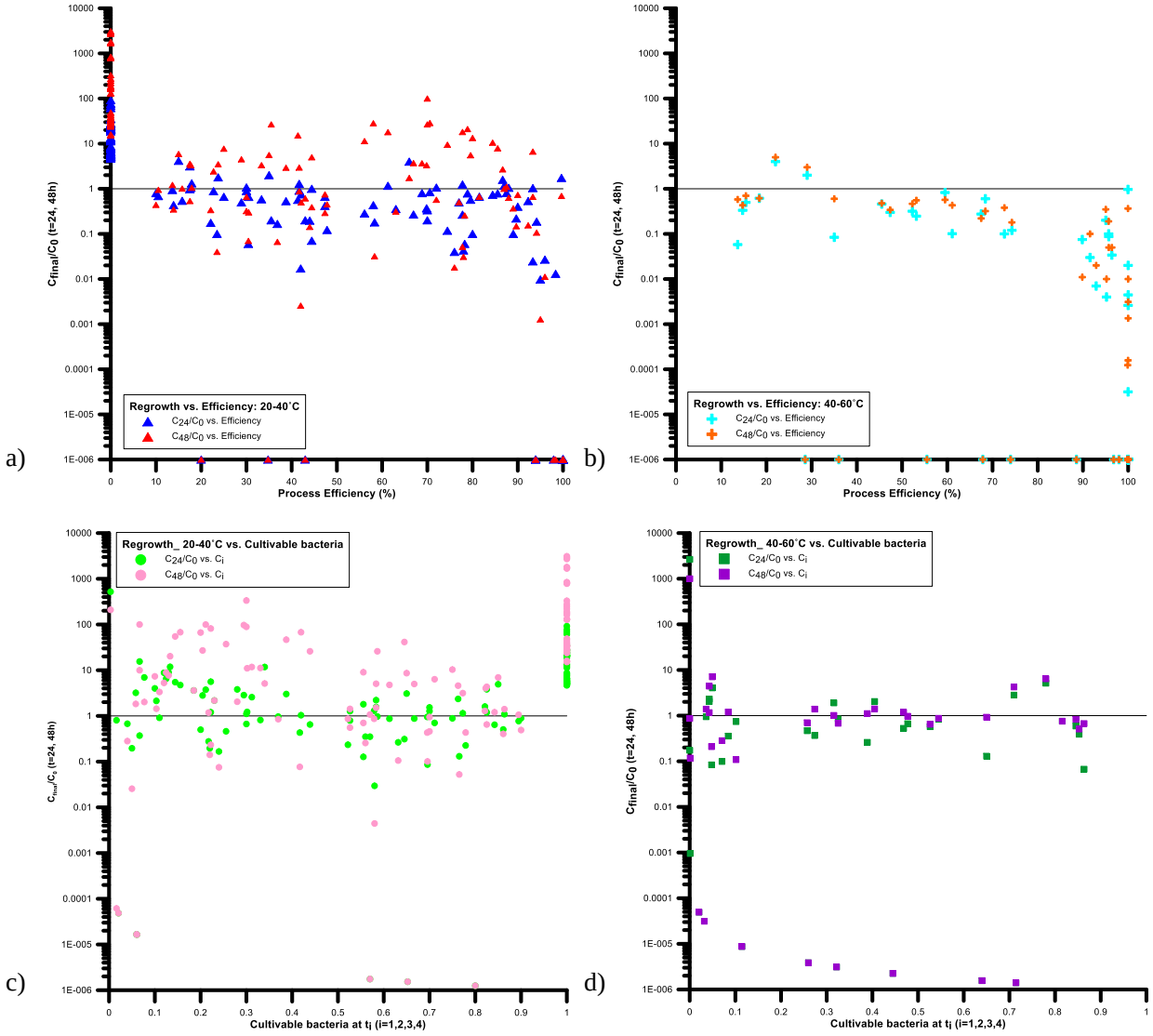

Figure 3.3.8: Statistical interpretation of regrowth vs. disinfection efficiency. (a) Efficiency vs. Regrowth after 1 day. (b) Efficiency vs. Regrowth after 2 days. (c) Cultivable bacteria at the end of the treatment period (1-4 h) vs. Regrowth after 1 day. (d) Cultivable bacteria at the end of the treatment period (1-4 h) vs. Regrowth after 2 days.

Furthermore, the cultivable fraction of bacteria left at the end of the process is calculated and plotted against the population after 24 and 48 h, for both low (Figure 3.3.8c) and high temperatures of pre-treatment (Figure 3.3.8d). Figure 3.3.8c demonstrates a constant live bacteria/initial population ratio fluctuating around 1 after 24 h of treatment (trace:●), but the bacterial numbers after 48 days (trace:●) seem to decrease, as the live fraction increases; lower populations would be expected when the live fraction is lower. This is interesting, for it indicates that the correlation between the pre-treatment and regrowth is not limited to the cultivable fraction at the end of the given treatment time (1 to 4 h), but is linked to the treatment method. This indicates that the correlation between the pre-treatment and regrowth is not limited to the cultivable fraction at the end of the given treatment time (1 to 4 h), but is linked to the treatment method. For instance, a low surviving fraction, deriving from a short-treatment time in low intensity is very susceptible to regrowth. The opposite statement, for higher light intensities and low temperatures to expect low regrowth, is validated as well. Special mention should be made at the non-treated samples (live fraction = 1) that always present regrowth. In contrast, in Figure 3.3.8d plotting the higher temperature experiments, there is no live fraction encountered at 100%, but less regrowth after 24 (trace:■) and 48h (trace:■) is observed. Also, a higher number of experiments present near-zero regrowth, compared with the low-temperature experiments. Even samples that presented 90% live bacterial fraction present diminished numbers, with obvious positive effects of high temperature in suppressing regrowth.

Finally, Figure 3.3.9 presents an estimation of the bacteria carried from the end of the treatment time after 24 h and from these ones, after 48 h. On X axis the final live fraction of bacteria after 24 h is plotted, due to the bacteria at the end of time i (i=1-4 h) per initial concentration and on Y axis the respective ones for 48 h storage. This ratio assesses the transferability of bacterial growth from day 1 to day 2 and expresses the fate at the end of the treatment time; i.e. values >1 indicate higher numbers after 48 h, due to the live fraction in 24 h. Mathematically, this ratio is $\frac{C_{24}/C_0}{C_i/C_0}$ *or* $\frac{C_{48}/C_0}{C_i/C_0}$, and is expressed as C_{24}/C_i or C_{48}/C_i, respectively. As it seems, the transferability from day 1 to day 2 is strongly influenced by the treatment temperatures during the experiment; for low temperatures 20˚C≤T≤40˚C, the same fraction of cultivable bacteria after 1 day can yield higher fractions after 48h (trace:●) than the respective 40˚C<T≤60˚C ones (trace:●). For example, 24-h ratios of 1 or 10 can result in much higher ratios (up to 1000) after 48 h. It is shown that i) there is no repair on the damages inflicted by temperature and ii) the synergistic action of light and temperature ensures low transferability from the surviving fraction. The dominant trend existing in regrowth is also expressed by the logarithmic equations and the possibility of increased appearance after 2 days is reflected by the constants of the equations which describe that trend.

In overall, there is a lighter regrowth risk when high temperatures of treatment are applied. However, this condition is not always applicable, when it comes to the existing solar disinfection techniques. In that case, either higher light intensities must be accounted for, low (around 20˚C) ambient temperatures or maybe, prolongation of the exposure time can compensate the risk of remaining bacteria in the solution. In this manner, either light action will be enhanced, bacterial division will not be favored or extended damage will

be inflicted, to ensure low live fractions at the end of the treatment; it was proved that this condition, regardless the pre-treatment condition, is a precursor of the bacterial numbers in short or long term storage of water.

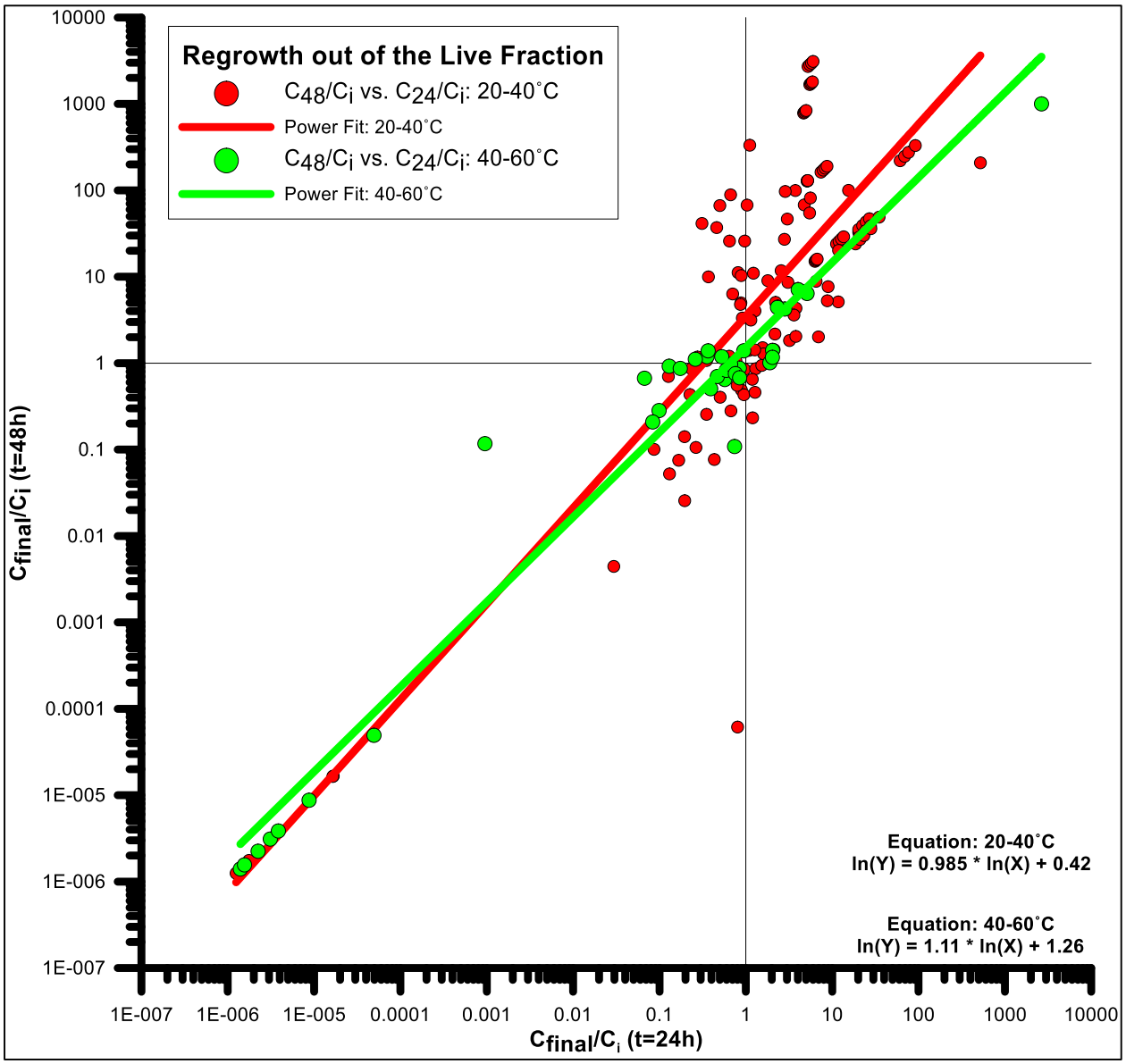

Figure 3.3.9: Transferability of live bacteria through the post-irradiation treatment period. Regrowth after 24 h out of the live fraction subjected to i hours of treatment (i=1-4 h) vs. Regrowth after 48 h.

3.4. Relevance of dose in solar disinfection of wastewater

The experimental results of sections 3.2 and 3.3 are processed here to obtain curves base on irradiation dose, in order to evaluate the significance of dose and the reciprocity law for both inactivation and subsequent dark repair. When examining the disinfection results in more depth, the importance of considering temperature as a key factor in intensity and dose studies is necessary.

3.4.1. Dose influence and disinfection in temperature controlled experiments

Figures 3.4.1 (a-h) demonstrate the disinfection curves for each initial temperature range and each temperature level, as a function of dose. A stepwise increase of temperature, for all initial population levels, reveals the following:

- At 20˚C treatment temperature: the same dose is more efficient if it derives from lower irradiation intensities (continuous vs. dashed line).
- For treatment temperatures around 30˚C the same tendency in the experiments is observed (exception: 30˚C-10^6 CFU/mL, probably a statistical error, 1 case out of 240 or 0.42% deviation).
- At 40˚C: the disinfection kinetics starts to change. There is faster initial inactivation rate for low intensities, but as dose increases, for the same dose, higher intensities are more effective; for a given dose lower intensities cannot cope with the growth observed in the matrix.
- At 50˚C treatment temperature: Higher intensities, for the same dose, seem to inactivate bacteria faster than the respective dose, resulting from lower intensities.
- At 60°C: initially, the reciprocity law seems to be applicable. However, it is not possible to fully evaluate the reciprocity law, because there is only two points per curve, both yielding total inactivation. The exact dose required for total inactivation cannot be calculated, because the sampling time (30 or 60 min, because of the chosen levels of the design) resulted too long to notice the real difference in an almost purely thermal-driven system.

Normally, the reciprocity law should be applicable, according to Peak and Peak (1982), because all our intensities were higher than 750 W/m^2. Even, Bosshard et al. (2009) validated reciprocity law for less than 750 W/m^2 (400 W/m^2), but for *Shigella flexneri* and *Salmonella typhimurium*. Also, Berney et al. (2006), working in our high-temperature range, did validate the reciprocity law. However, this study has shown very different results, with significant deviations from reciprocity at low and high temperatures, but in opposite directions.

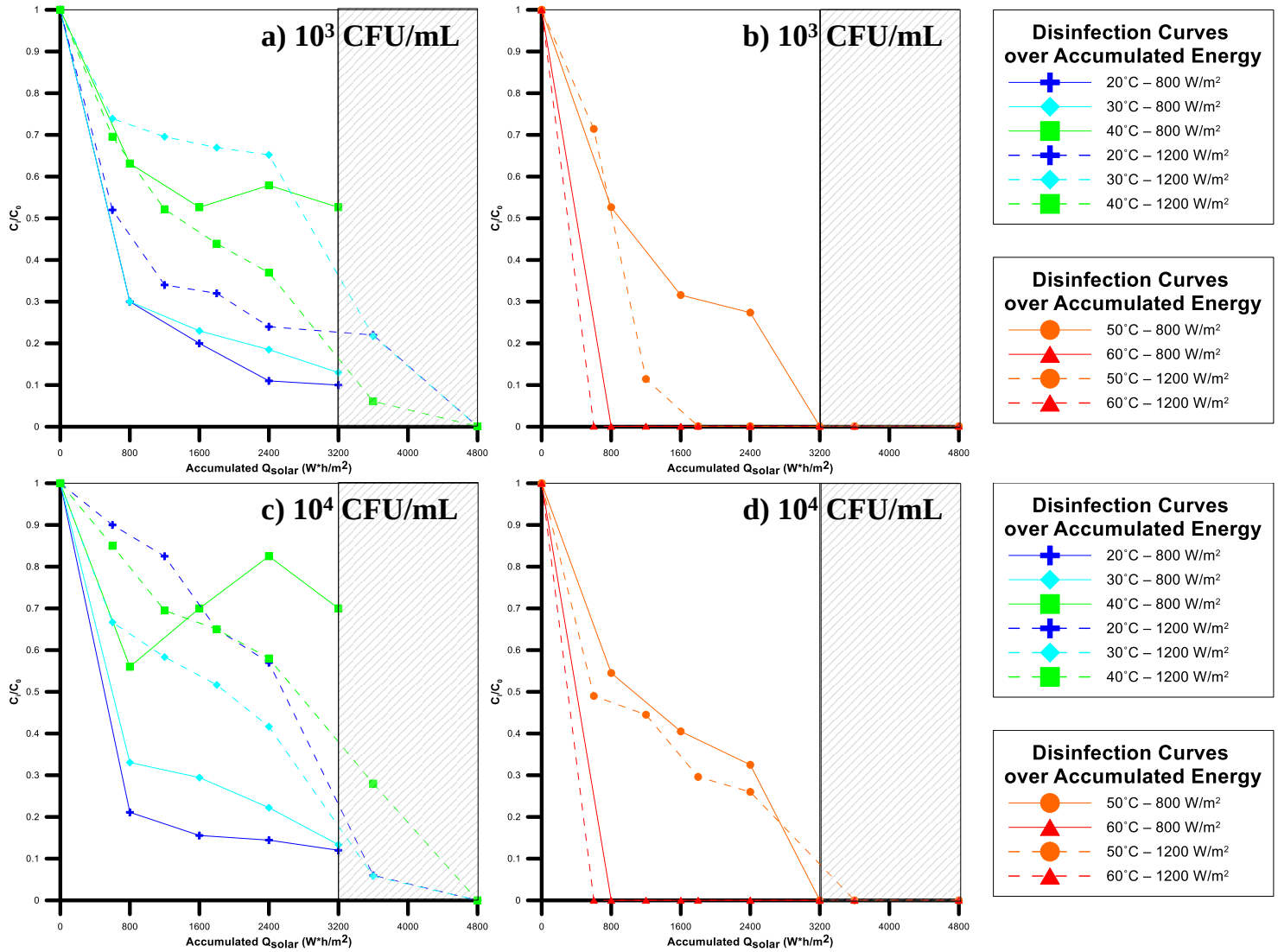
a) 10³ CFU/mL
b) 10³ CFU/mL
c) 10⁴ CFU/mL
d) 10⁴ CFU/mL
C/C₀
Accumulated Q_solar (W*h/m²)
Disinfection Curves over Accumulated Energy
20°C – 800 W/m²
30°C – 800 W/m²
40°C – 800 W/m²
20°C – 1200 W/m²
30°C – 1200 W/m²
40°C – 1200 W/m²
50°C – 800 W/m²
60°C – 800 W/m²
50°C – 1200 W/m²
60°C – 1200 W/m²

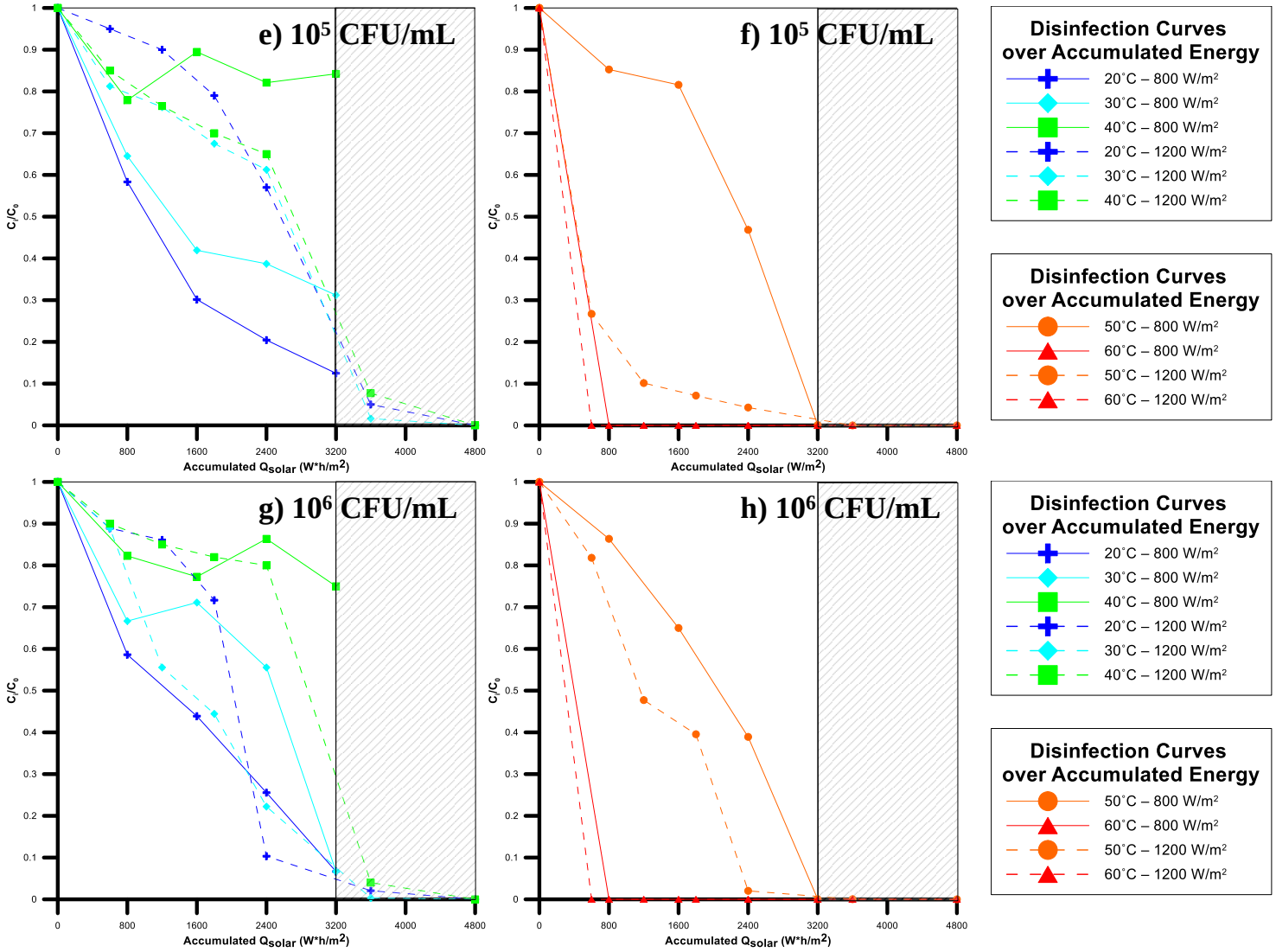

Figure 3.4.1: Overview of the disinfection experiments. On the left side: experiments with 20≤T≤40˚C and 40<T≤60˚C on the right. (a) and (b): 10^3 CFU/mL. (c) and (d): 10^4 CFU/mL. (e) and (f): 10^5 CFU/mL. (g) and (h): 10^6 CFU/mL.

3.4.2. Dose influence and regrowth in temperature controlled experiments

Trying to summarize these effects and extend beyond disinfection, to regrowth, in Figures 3.4.2 (a-f) the effects on disinfection and regrowth are presented, according to the dose and the respective intensity that produced it. However, having noticed this dual, temperature-dependent behavior in disinfection and regrowth, results are presented per temperature range (Figures 4.3.2a, 2c and 2g for 20-40˚C, 2b, 2d and 2h for more than 40˚C). In fact, the tendencies observed were worth analyzing one step further: for low treatment temperatures (Figure 3.4.2a) dose has different effect when it derives from high fluence or low one. It was noted that for the same dose, generally lower intensities were more efficient. However, it is observed here that in very high doses, this difference is party mitigated. Figure 3.4.2b demonstrates the changing effect temperature has in efficiency. Doses which were achieved from low irradiation intensities, do not differ significantly from the ones acquired from high intensities, but are clearly more efficient (differences along X axis).

Concerning the regrowth of the microorganisms, the results are more significant; in Figure 3.4.2c the effect intensity has on short-term storage is presented; low dose-high intensity experiments seem to result in higher bacterial numbers than low dose-low intensity experiments, for treatment temperatures between 20-40˚C. This is consistent with the disinfection trend observed at low temperature. Moreover, these results partly agree with the findings of previous researches, where UVA-irradiated cells were not able to regrow (Bosshard et al., 2009; Oates et al., 2003 and more), because the inflicted dose was non-lethal. However, samples that were fully inactivated did not demonstrate regrowth. In higher temperatures (above 40˚C), thermal action seemed to mitigate this effect, presenting much lower bacterial survival rates, which decrease normally when dose increases and are also slightly higher for low intensities. As far as long term storage (48-h) is concerned, consistent behavior in the two temperature levels was demonstrated: the same dose was more effective in suppressing bacterial growth when it derived from higher intensity levels. However, when samples were treated at low temperatures, the regrowth potential was considerably higher.

Summarizing the aforementioned analysis, it seems both axes, of disinfection and regrowth have to be taken into consideration in solar treatment studies, respecting the behavior of the involved microorganisms. Since it is relatively difficult to achieve high intensities in real applications, the lower margin is of higher practical interest. The disinfection part is more straightforward: it is positive that even lower intensities were efficient in inactivating bacteria. However, regrowth suppression would require higher doses, to counterbalance the loss of efficient regrowth suppression inflicted by heat.

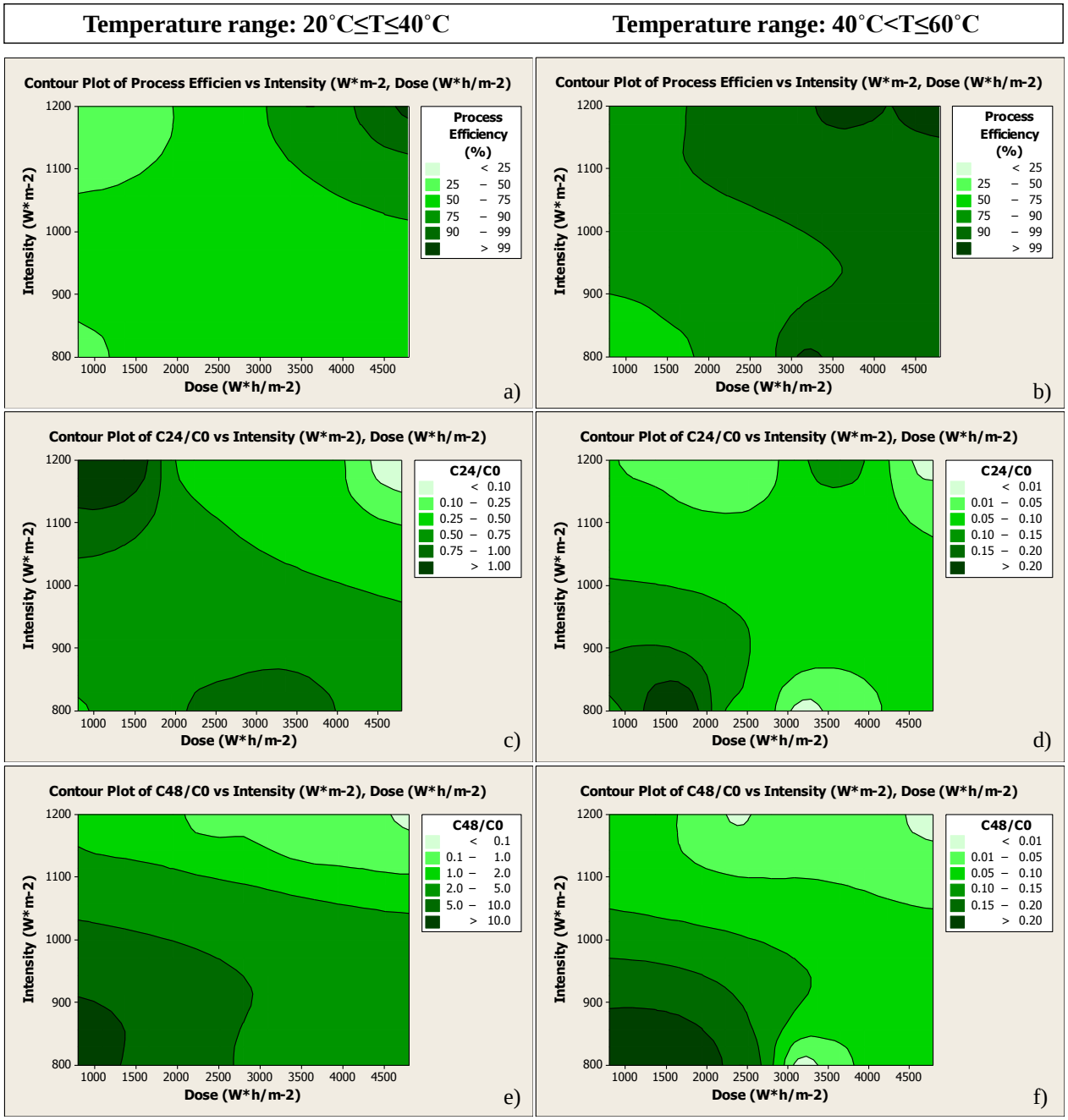

Figure 3.4.2: Overview of the experimental results under the prism of dose/intensity. (a) Contour plot of the Process Efficiency vs. Intensity and Dose, for 20≤T≤40˚C. (b) Contour plot of the Process Efficiency vs. Intensity and Dose, for 40<T≤60˚C. (c) Contour plot of the Regrowth after 24 h vs. Intensity and Dose, for 20≤T≤40˚C. (d) Contour plot of the Regrowth after 24 h vs. Intensity and Dose, for 40<T≤60˚C. (e) Contour plot of the Regrowth after 48 h vs. Intensity and Dose, for 20≤T≤40˚C. (f) Contour plot of the Regrowth after 48 h vs. Intensity and Dose, for 40<T≤60˚C.

3.5. Modeling bacterial disinfection and dark repair assessment

In this section, the experimental results presented in subchapters 3.1.5 are elaborated, which assess the effect of irradiance and time on disinfection and dark repair; the findings are discussed here and mathematically modeled. A systematic investigation of the effects of 9 intensity levels and their corresponding kinetics, as well as the subsequent survival/regrowth are presented in detail.

3.5.1. Simulated solar light disinfection experiments: Bacterial inactivation as a function of the light intensity

Figure 3.5.1 (i) illustrates a synopsis of all the disinfection experiments conducted under simulated solar light. Batch tests were conducted, exposing *E. coli* dispersed in wastewater to solar light in a range of intensities from 500 to 1600 W/m^2.

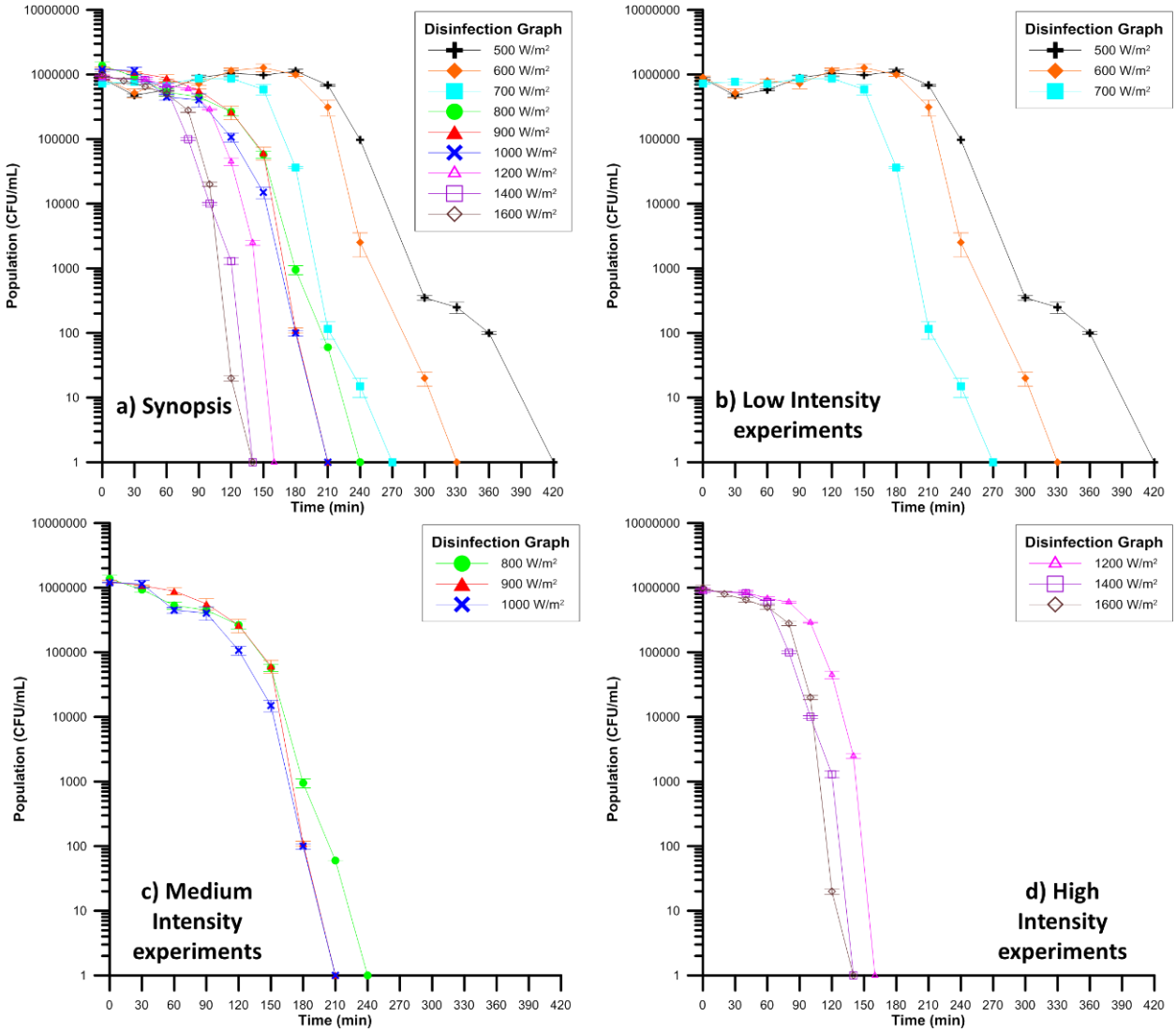

Figure 3.5.1: Solar disinfection experiments under discrete irradiation intensities at laboratory scale. (a) Synopsis of the experiments. (b) Low intensity experiments (500-700 W/m^2). (c) Medium intensity experiments (800-1000 W/m^2). (d) High intensity experiments (1200-1600 W/m^2).

For analysis and clarity reasons, intensity levels will be divided as low (Figure 3.5.1-ii), medium (Figure 3.5.1-iii) and high (Figure 3.5.1-iv) intensity levels. Figure 3.5.1-ii) sums the low intensity experiments, where some distinct phases can be observed. First of all, the bacterial population does not decrease until the 3rd hour of continuous illumination, presenting an initial shoulder, as it was proposed by many works (Berney et al., 2006; Ndounla et al, 2013; Giannakis et al., 2013). In addition, in the pre-mentioned works, this shoulder was not (or was mildly) accompanied by an increase in bacterial population. A fluctuation is visible, reducing with increasing intensity. Literature suggests that this phenomenon is attributed to i) photoactivation of previously non-cultivable bacteria (Rincon and Pulgarin, 2007b), ii) an initial adaptation phase for bacterial population in the new dilution medium and iii) the growth of bacteria which is supported by this medium (Caballero et al., 2009; Marugan et al., 2010); the presence of nutrients and ions enhances bacterial growth, and bacteria which have not been lethally damaged by the action of light are able to reproduce and compensate for the lost numbers.

Afterwards, the initial shoulder is followed usually by a linear (in logarithmic plot of results) decay period. This phase fits to the behavior suggested by Geeraerd et al. (2000). Within the log-linear inactivation phase, there is a second delay phase towards its middle, which has been encountered again in literature (Fabriccino and D'Antonio, 2010). The authors suggested that the synergy between temperature and light action (McGuigan et al., 1998) was able to inflict the final damage and totally inactivate bacteria. This second delay is decreasing with increasing intensities, fact that leads us to believe that it is dose related, since temperature was always lower than 40˚C in these trials, and neither thermal inactivation nor synergetic actions are expected. Finally, a clear correlation between the exposure time needed for total inactivation and the intensity can be seen, with higher intensities decreasing significantly the demand for exposure up to 55% for a 200 W/m^2 increase in intensity.

What is introduced here, in Figure 3.5.1-iii, as medium intensities, are the most desirable real solar intensities expected in field disinfection applications. Firstly, compared to the low intensity experiments, it is seen that the shoulder length is greatly reduced to 90-120 min. Higher photon flux in the same system leads to more efficient disinfection, according to the multi-hit theory of Harm (1980). There is a certain "n" number of hits a cell must receive in specific critical points in order to get inactivated. Berney et al. (2006) have identified the targets, and therefore, the intensity increase is linked to increasing effective hits in the system. Also, the second lag period is almost (800 W/m^2) and totally (900, 1000 W/m^2) suppressed. There is a possibility of an adaptation of the bacterial strains that grow under low irradiation conditions (Berney et al., 2007) which could be linked with the demonstration of the second lag phase. However, increasing intensity at these levels is lethal, rather than beneficial. Finally, increasing intensity from 800 to 1000 W/m^2 influences the exposure time necessary for total inactivation, with approximately 22% less require time visible. So far, increasing from doubling the intensity (500 to 1000 W/m^2) leads to halving the exposure time (420 to 200-210 min).

The last sub-graph (Figure 3.5.1-iv) presents the highest end of intensities employed in the study, from 1200 to 1600 W/m^2. Increasing intensity continued to decrease the shoulder length, to a minimum of approximately 80 min, followed by acute log-linear decrease within the next 60 min after the shoulder is finished. In this case, the equilibrium set between the growth forces and the disinfecting action of light is turned against survival very fast, indicating a possible minimum dose required for initiating the decay phase, as also suggested by Sichel et al. (2007) and Ubomba-Jaswa (2009). In total, increasing the intensity from 500 W/m^2 to 1600 W/m^2 has inflicted dramatic change to the necessary exposure time, with the initial 420 min being reduced to (approximately) 130 min, which equals to 70% less time necessary. This decrease is very important, if the residence times for an application are concerned, and would lead to smaller, more feasible constructions, if high intensities were achieved.

3.5.2. Modeling of the inactivation data

Table 3.5.1 presents analytical data concerning the parameters of the models. The two models were explained and presented in Chapter 3.1.5.1. In order to diminish any small differences in initial population, data were normalized prior to fitting. As far as the shoulder log-linear model is concerned, the fit approximation is very good (average R^2: 97.3%) with very low MSE. Also, the decreasing tendency in the length of the shoulder (Sl) is confirmed while in the same time k_{max} is increasing, and a systematic underestimation of the initial population is noticed, which does not affect the results significantly. For the Weibull model, a decreasing delta value is also seen, which is related with the delay of the decay phase. The results of the fit are equally good (average R^2: 96.9%), and the MSE is also low (0.13).

When explaining the experimental results, a decrease in the shoulder length was noted and the inactivation time in total, as intensity increased. This change is reflected to the selected models as well. Figure 3.5.2 presents the changes intensity causes to the shoulder length, to k_{max}, to delta and p values of the two models. First of all, in Model 1, plotting the shoulder length versus intensity provides details on their almost linear dependence. In every case a linear fit proves this correlation for the suggested fit parameters in terms of intensity, although in the case of k_{max} and p the actual measurements fluctuate around the calculated value, suggested by the fit.

The most important suggestion these linear models provide us with, is the correlation between the fitting parameters and the intensity levels. Since all the parameters in the fits can be expressed as a function of the intensity, the survival models can become bi-parametric functions of the exposure time and the intensity, thus simplifying the conception of the models, while correlating directly with the experimental conditions. When setting up an experiment, there is an initial population subject to a certain time of solar exposure at an intensity. Even if these constraints are not constant, the accumulated dose could be a good alternative to be inserted and generalize the mathematical expressions.

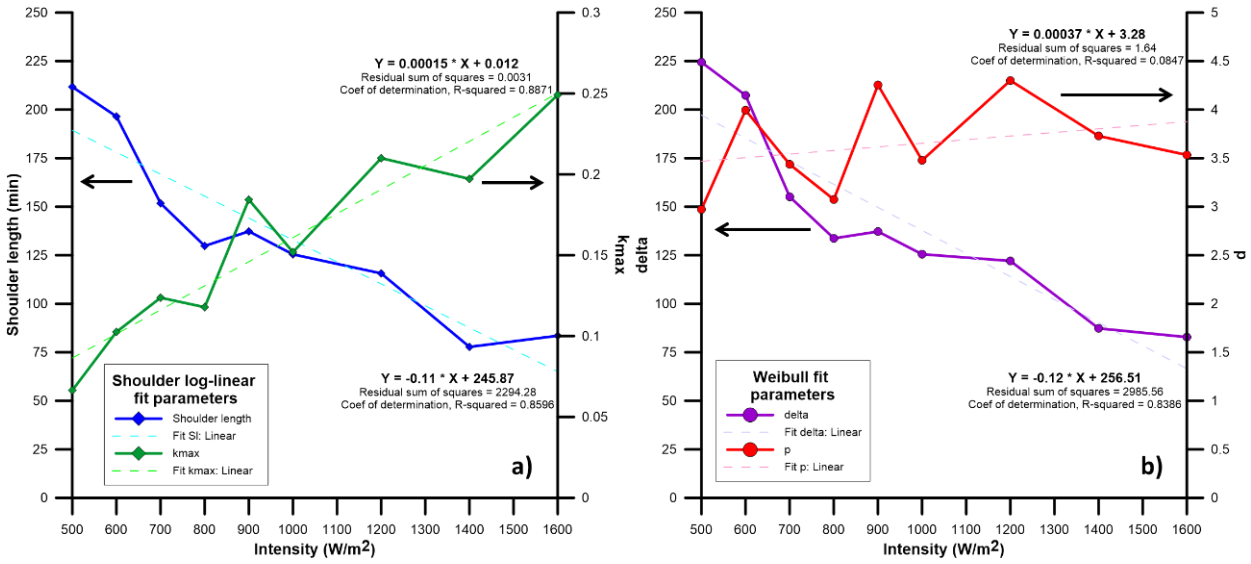

Figure 3.5.2: Modification of the shoulder (a) log-linear and (b) Weibull distribution models' parameters, Sl, k_{max}, delta and p, as a function of the irradiation intensity.

Table 3.5.1. – Modeling details and analysis of fit for the shoulder log-linear and Weibull distribution model.

Shoulder log-linear survival model								Weibull distribution survival model						
Intensity	**Sl**	**k_{max}**	**$LogN_0$**	**MSE**	**RootMSE**	**R^2**	**R^2-(adj)**	**δ**	**p**	**$LogN_0$**	**MSE**	**RootMSE**	**R^2**	**R^2-(adj)**
500	211.72	0.07	5.98	0.0764	0.2764	0.978	0.9754	224.45	2.97	6.1	0.1824	0.427	0.9475	0.9413
600	196.49	0.1	5.99	0.0548	0.2341	0.9856	0.9837	207.36	3.99	6.08	0.1417	0.3764	0.9628	0.9578
700	151.76	0.12	6.05	0.0571	0.239	0.9873	0.9854	155.1	3.44	6.22	0.2381	0.488	0.9471	0.939
800	129.77	0.12	5.67	0.0456	0.2137	0.9874	0.9853	133.7	3.07	5.87	0.0551	0.2347	0.9848	0.9823
900	137.31	0.18	5.76	0.0896	0.2993	0.9754	0.971	137.21	4.25	5.93	0.0974	0.3121	0.9733	0.9684
1000	125.45	0.15	5.69	0.0996	0.3155	0.9725	0.9676	125.53	3.48	5.89	0.0455	0.2132	0.9875	0.9852
1200	115.64	0.21	5.89	0.2971	0.5451	0.9272	0.911	122.06	4.3	5.95	0.1198	0.3461	0.9706	0.9641
1400	77.77	0.2	5.91	0.1893	0.435	0.9596	0.9481	87.32	3.73	5.97	0.0525	0.2291	0.9888	0.9856
1600	83.52	0.25	5.83	0.0868	0.2946	0.9852	0.981	82.81	3.53	6.02	0.2293	0.4789	0.9609	0.9498
Average	***136.6***	***0.16***	***5.86***	***0.1107***	***0.317***	***0.9732***	***0.9676***	***141.73***	***3.64***	***6***	***0.1291***	***0.345***	***0.9693***	***0.9637***
St. Dev.	***45.21***	***0.06***	***0.14***	***0.0817***	***0.1073***	***0.0195***	***0.0243***	***48.08***	***0.47***	***0.11***	***0.0745***	***0.1062***	***0.016***	***0.0182***

3.5.3. Solar wastewater disinfection and dose dependence without temperature control

The analysis of the kinetic models fit before have indicated the mathematical expressions describing solar disinfection of wastewater, according to the intensity acquired in the solar simulator. There is however a need to standardize somehow the photon energy that the system needs in order to be sterilized. Rincon and Pulgarin (2004a) have spoken about the need to standardize the results in order to achieve comparable results among the researches in field trials for drinking water. They have put the dose under question, and decided that it is not an appropriate indicator for efficiency. In the same wavelength, Ubomba-Jaswa et al. (2009) in drinking water, Ndounla et al. (2014) in photocatalysis and many others, have all conducted experiments at different times during the day and have concluded, in summary, that in general, the same dose has the same effect when it is a result of high intensities. This suggests a shorter exposure at higher irradiance to achieve better disinfection results.

In these experiments, since the irradiation is constant and the measurements are frequent, the kinetic figures can be converted to Population vs. Dose ones. Figure 3.5.3 presents the normalized disinfection results presented in Figure 3.5.1, but in terms of dose. In Figure 3.5.3a, it is noticed that all the range of intensities requires approximately the same amount of energy from the sun in order to achieve total disinfection (i.e. zero viable counts) around 3200 Wh/m^2 (range: 3100-3700). Since the sampling intervals were 30 min under 1000 W/m^2 and 20 min over 1200 W/m^2, there are some differences observed, mostly due to the long intervals between sampling. In any case, in 8 of 9 conditions total inactivation is achieved with a dose between 3150 and 3500 Wh/m^2. The 500, 600 and 700 W/m^2 plots originally present a fluctuation over and under the initial population. Since the percentage of removal is presented in Figure 3.5.3b, the results (time periods) over the initial population are negative, and therefore excluded from the graph.

Modeling with GInaFiT provides also information for the estimated time for 4-log reduction (99.99%) necessary for every model. Table 3.5.2 summarizes the necessary times for this removal, where for both models the times are very close. In fact, as intensity increases the models estimate closer required 4-log inactivation times. Knowing the intensity that caused the inactivation, the necessary dose for 99.99% disinfection can be calculated. As it seems, the final dose is affected by the sampling interval, but in general, a dose around 3000±200 Wh/m^2 results in 4-log reduction of the population.

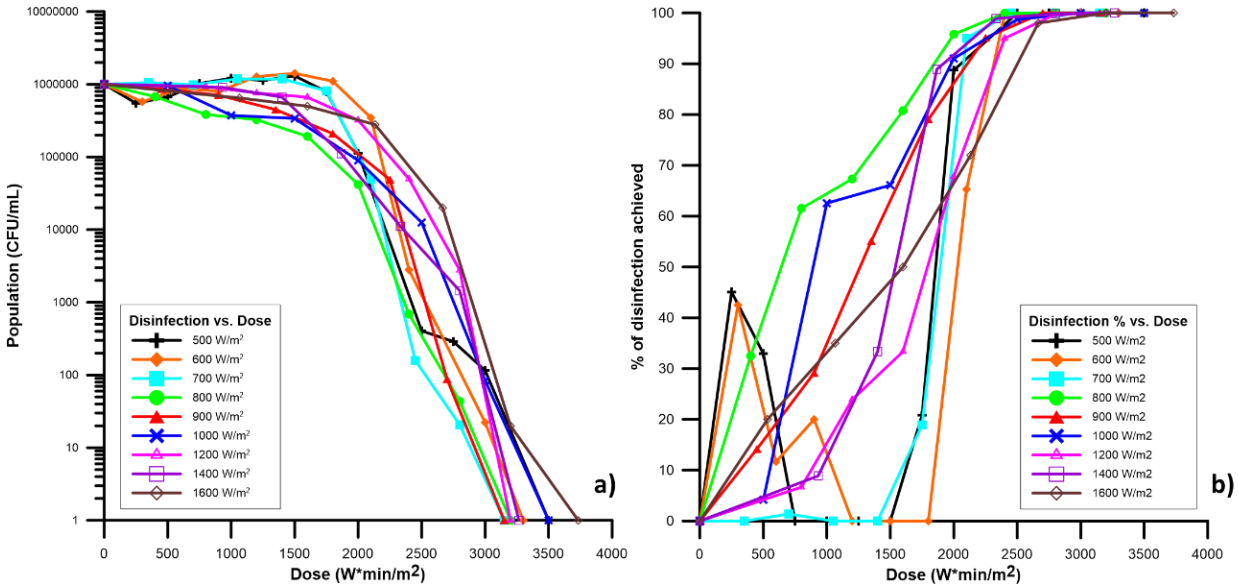

Figure 3.5.3: Normalized solar disinfection results, over the accumulated dose per intensity level. (a) Population vs. Dose and (b) Disinfected population percentage vs. Dose

These findings contradict with the literature suggestions for photocatalytic doses, as well as the natural measurements for solar water disinfection. The constant supply of light leads to adaptation of the population on the stress conditions (Berney et al., 2007). Also, there is promoted growth due to the support offered by the water matrix, and new generations of bacteria that derive from stressed ones are more prone to survive the light impact (Quek and Hu, 2008). However, this effect is diminished as intensity increases.

In Figure 3.5.3b the percent of bacteria eliminated due to each intensity level versus the dose are shown. Although most of the kinetic curves display directly a reduction in the bacterial numbers since the beginning of the process, the curves of 500, 600 and 700 W/m^2 present a decrease in numbers, then reverse effects and, afterwards, continuous and monotonous inactivation, as explained in the fluctuations in Figure 3.5.1. However, even in these low intensities, there is an energy threshold that initiates permanent inactivation, around 1500 Wh/m^2.

Beyond this point, all kinetic curves demonstrate consistent inactivation, with even increasing inactivation rates. First of all, it is known that the accumulation of photoproducts in the bacterial cell leads to cell death (Rincon and Pulgarin, 2004c). Then, there is a certain number of targets solar light can attack, such as respiration chain (Bosshard et al., 2010a), or the double DNA strand, but bacteria can heal this damage through a light-induced enzymatic process, known as photoreactivation. Under this scope, the accumulation of a certain amount of energy is necessary to cause permanent effects on bacteria (Bosshard et al., 2010b) or to throw them in a viable, but not cultivable state (Rincon and Pulgarin, 2007b).

Table 3.5.2. – Required time and dose for 4-log (99.99%) removal per intensity and model.

Intensity (W/m^2)	Shoulder Model (min)	Weibull Model (min)	Shoulder: Dose Required (Wh/m^2)	Weibull: Dose Required (Wh/m^2)
500	353	361	2942	3008
600	287	293	2870	2930
700	227	232	2648	2707
800	209	211	2787	2813
900	189	191	2835	2865
1000	187	189	3117	3150
1200	152	154	3040	3080
1400	125	127	2917	2963
1600	122	123	3253	3280
		Average Dose:	***2934***	***2977***
		St. Dev.:	***181***	***176***

3.5.4. Bacterial regrowth in the dark: Dark repair kinetics

The second part of the investigation deals with the post-irradiation period, while storing the synthetic wastewater in the dark for a consequent period of 48 h. For clarity reasons, the results will be split, according to the intensity levels, in Figure 3.5.4 (a-c, low intensity), Figure 3.5.5 (a-c, medium intensity) and Figure 3.5.6 (a-c, high intensity). In all figures, the same color line represents the same sampling interval, for instance 120 min of treatment followed by dark storage is red line, and every intensity level is with a different trace. Also, for each intensity level six representative kinetic curves are shown (four in high intensities), according to the behavior of the microorganisms (growth or decay). Finally, no regrowth was observed when total inactivation was observed.

Figure 3.5.4 represents the low intensity experiments, here 500, 600 and 700 W/m^2. As it can be observed, regrowth of the bacterial population changes as the inflicted intensity is changed. When intensity is increased, the same sampling intervals present different behavior. A general trend indicates a decrease in the population as intensity increases. For instance, samples retrieved at 150 min, at 500 W/m^2 present growth after 48 h, are marginally stationary (slight decrease) at 600 W/m^2 and clearly decrease, when exposed to 700 W/m^2.

For the medium intensity experiments (800-1000 W/m^2), in Figure 3.5.5 the response in the same sampling intervals, from 30 to 180 min. It is found that one of the most visible changes is the behavior of the samples irradiated for 180 min, are now completely decaying within the first 24 h. The damages accumulated differ from one intensity level to another, and after the extent of damage in disinfection, the differences in the inability to recover the damage done within 48 h are noticeable. However, the differences among the three levels are relatively small, and some changes are visible only in long term; for instance, samples drawn between 90-150 min are presenting fluctuations in the bacterial numbers but the kinetic curves shape shifts from concave to convex, indicating the pre-determined decay.

Finally, similar observations can be made for the high intensity regrowth curves, presented in Figure 3.5.6. It is seen that increasing the intensity causes a change in the bacterial ability to heal their damages, as from 60-80 minutes only, the damage seems more than their potential healing abilities. Also, as few as 20 minutes, in such high intensities can cause change in the long term behavior; for instance, the 60-min kinetic curve, which turned into a clear decay curve.

3.5.5. Investigation on the effective bacteriostatic dose

Further analysis of the regrowth data, can provide with observations on the role of the dose. It was observed before, in mathematic terms, a change in the post-irradiation curves from concave to convex ones, as intensity increased; formerly regrowth lines are later representing decay ones. As the time of the sampling is not modified, but intensity is, then the received dose during disinfection is increased and as a consequence, the post-irradiation behavior.

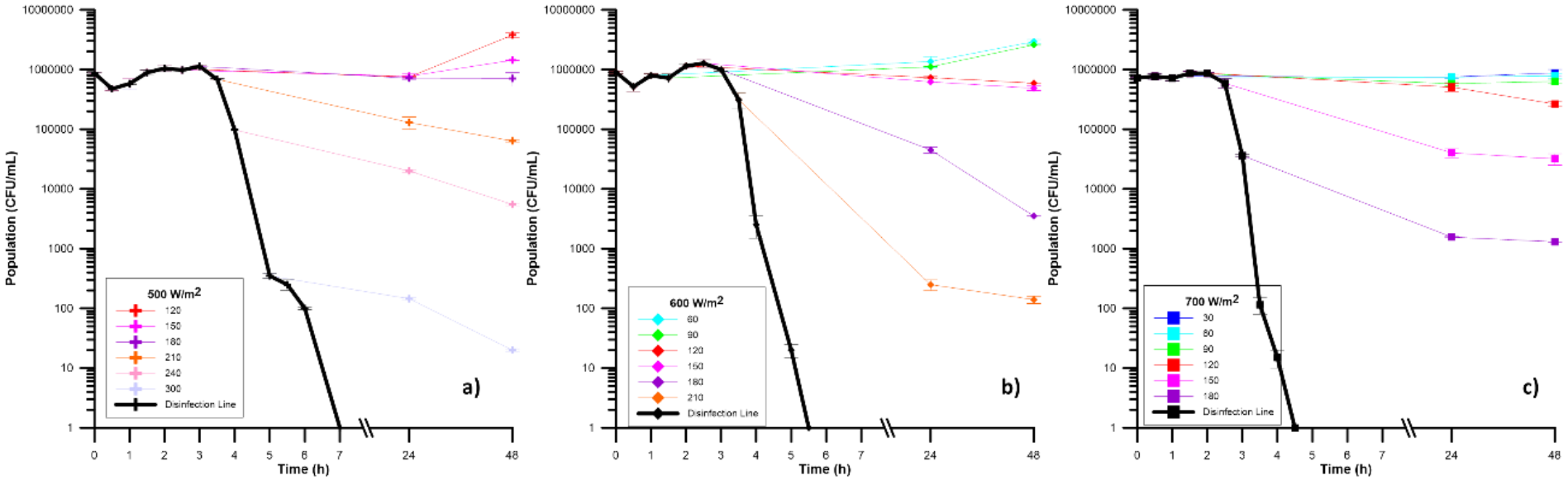

Figure 3.5.4: Post-irradiation events after 30-min sampling, during 48 h, for the low intensity experiments (500-700 W/m^2). (a) 500 W/m^2. (b) 600 W/m^2. (c) 700 W/m^2.

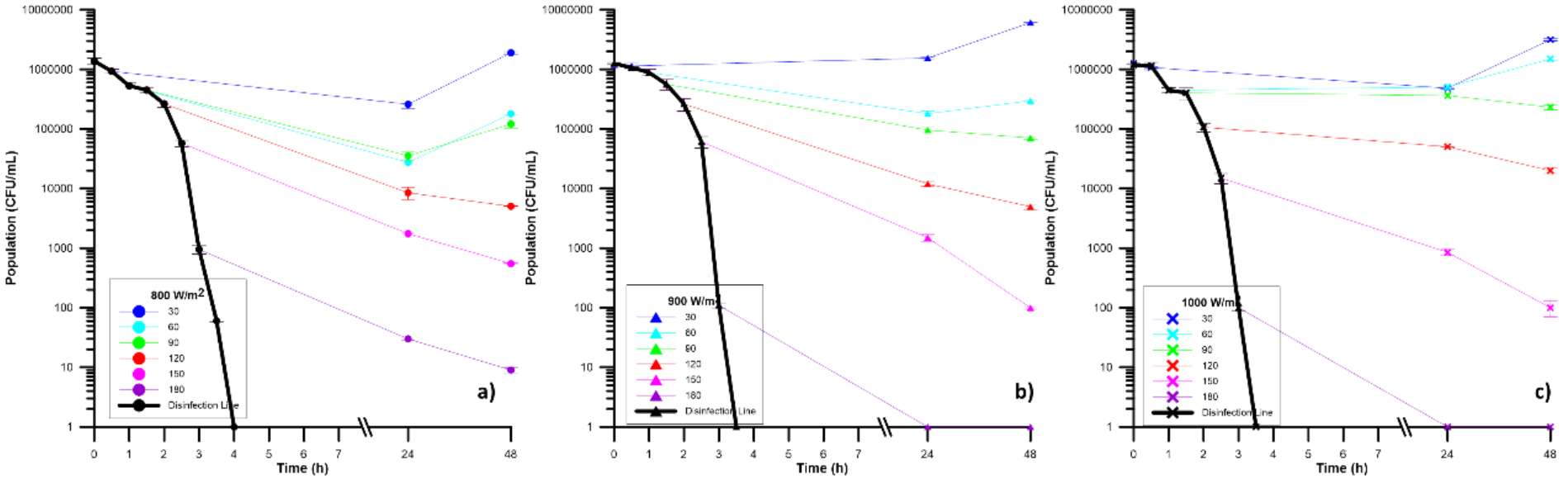

Figure 3.5.5: Post-irradiation events after 30-min sampling, during 48 h, for the medium intensity experiments (800-1000 W/m^2). (a) 800 W/m^2. (b) 900 W/m^2. (c) 1000 W/m^2.

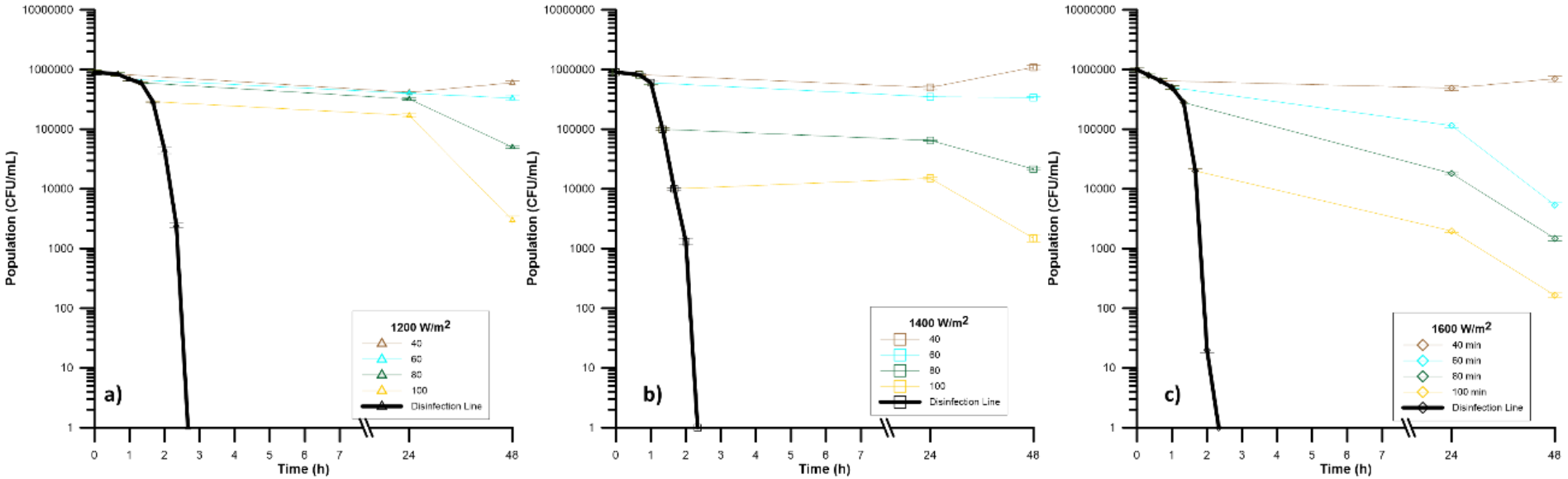

Figure 3.5.6: Post-irradiation events after 20-min sampling, during 48 h, for the high intensity experiments (1200-1600 W/m^2). (a) 1200 W/m^2. (b) 1400 W/m^2. (c) 1600 W/m^2.

These changes in behavior are summarized in Table 3.5.3. The observations of the kinetic curves provide the information on the response during the dark period. Having taken samples in relatively short intervals, the curves presented as "GROWTH" are the curves that in overall or long term presented increase of the population and "DECAY" the ones that show permanent or long term decrease of the population. As it seems, this change is not linear; increasing the intensity does not lead to infinite decrease of the ability to recover. As a matter of fact, along with the increase of the intensity, the same system receives more dose, and if the light action mode against bacteria (Harm, 1980; Berney et al. 2006) is considered, the possibility of inflicting damage in critical areas is increased. However, as suggested by (Sichel, 2007), in experiments conducted in solar light, increasing the dose did not result to great enhancement of disinfection; this was also the case for the disinfection experiments and as it is seen now, is also true for regrowth.

Furthermore, if virtual 5-min intervals are interpolated between the sampling times, and combined with the present data from the regrowth curves, there can exist an analysis on the point when bacteria change their behavior from "GROWTH" to "DECAY". For instance, in 500 W/m^2, the 120-min curve presents growth, the 150-min as well, but less and the 180-min curve presents decay. By interpolation through the bacterial population data, it is suggested that the time point that changed the bacterial curve from growth to decay was around 155-160 min. In the same manner, this point in every curve is found and the details are summarized in Table 3.5.4.

As it can be seen, the effective bacteriostatic dose (EBD) has proved to be a well-defined threshold: when it is crossed, it determines the bacterial fate. The analysis of each curve provides with an EBD between 1120 and 1280 Wh/m^2. The sampling intervals, as above for total inactivation times, inflict minor changes in the results, as well as the estimation of the time points, especially at high intensities. In overall, an average dose of 1200±70 Wh/m^2 has a bacteriostatic effect in long term. It is also observed that this energy threshold is very close in all intensities, resulting in a direct estimation of the theoretical exposure time required for total inactivation. Finally, along with the estimation of the population done before, one can predict the behavior of the microorganisms only by the dose received, which allows to foresee the growth or the decay of the bacteria in long term.

Table 3.5.3. – Summary of the post-irradiation changes in bacterial behavior according to the inflicted intensity.

Time (min)/ Intensity	500 W/m^2	600 W/m^2	700 W/m^2	800 W/m^2	900 W/m^2	1000 W/m^2	1200 W/m^2	1400 W/m^2	1600 W/m^2
0	GROWTH	GROWTH	GROWTH	GROWTH	GROWTH	GROWTH	GROWTH	GROWTH	GROWTH
20	GROWTH	GROWTH	GROWTH	GROWTH	GROWTH	GROWTH	GROWTH	GROWTH	GROWTH
30	GROWTH	GROWTH	GROWTH	GROWTH	GROWTH	GROWTH	GROWTH	GROWTH	GROWTH
40	GROWTH	GROWTH	GROWTH	GROWTH	GROWTH	GROWTH	GROWTH	GROWTH	GROWTH
60	GROWTH	GROWTH	GROWTH	GROWTH	GROWTH	GROWTH	DECAY	DECAY	DECAY
80	GROWTH	GROWTH	GROWTH	GROWTH	GROWTH	DECAY	DECAY	DECAY	DECAY
90	GROWTH	GROWTH	GROWTH	GROWTH	DECAY	DECAY	DECAY	DECAY	DECAY
100	GROWTH	GROWTH	DECAY	DECAY	DECAY	DECAY	DECAY	DECAY	DECAY
120	GROWTH	DECAY	DECAY	DECAY	DECAY	DECAY	DECAY	DECAY	DECAY
140	GROWTH	DECAY	DECAY	DECAY	DECAY	DECAY	DECAY	DECAY	DECAY
150	GROWTH	DECAY	DECAY	DECAY	DECAY	DECAY	DECAY		
160	GROWTH	DECAY	DECAY	DECAY	DECAY	DECAY	DECAY		
180	DECAY	DECAY	DECAY	DECAY	DECAY	DECAY			
210	DECAY	DECAY	DECAY	DECAY	DECAY	DECAY			
240	DECAY	DECAY	DECAY	DECAY					
270	DECAY	DECAY	DECAY						
300	DECAY	DECAY							
330	DECAY	DECAY							
360	DECAY								
390	DECAY								
420	DECAY								

Table 3.5.4. – Investigation on the effective bacteriostatic dose (EBD).

Intensity (W/m^2)	Time min (min)	Time max (min)	Dose min (Wh/m^2)	Dose max (Wh/m^2)	Average
500	155	165	1291.7	1375	1333.3
600	110	120	1100	1200	1150
700	100	110	1166.7	1283.3	1225
800	90	100	1200	1333.3	1266.7
900	75	85	1125	1275	1200
1000	65	75	1083.3	1250	1166.7
1200	50	60	1000	1200	1100
1400	45	55	1050	1283.3	1166.7
1600	40	50	1066.7	1333.3	1200
Average	***81.1***	***91.1***	***1120.4***	***1281.5***	***1200.9***
St. Dev	***37.1***	***37.1***	***88.0***	***59.6***	***68.5***

3.5.6. Reciprocity law in thermally non-controlled experiments

In 1964, the reciprocity law was suggested (Zetterberg, 1964) to interpret the behavior of different photochemical applications, indicating that the same dose will have the same effect on the various targets. In terms of energy, it suggests that the same light dose has the same effect, if it is a result of low irradiation intensity for a long time or if it is produced by high intensities for a short time. Since the first statement of the law, there have been many works that do not comply with this formulation, reviewed also in 2003 by Martin et al. As it was suggested, the main reason for failing is very high or very low intensities. What is considered "high" or "low" will be discussed later.

Even in more recent years and strictly on water disinfection, there are a number of applications in which reciprocity law seems to fail, for instance photocatalysis by TiO_2 (Rincon and Pulgarin, 2004c;2007b), by the photo-Fenton reaction (Ndounla et al., 2014) or even without catalysts (Ubomba-Jaswa et al., 2009). For each application there is an explanation to the failure; in photocatalysis for instance, the mode of action by TiO_2 produces a number of hydroxyl radicals big enough to cause recombination to H_2O_2 which is not equally active, and therefore cause decrease in efficiency. In solar-only applications, the effect is not the same until a threshold required for inactivation is achieved (Ubomba-Jaswa et al., 2009). No application however deals with this problem in a rich nutrients matrix, such as wastewater.

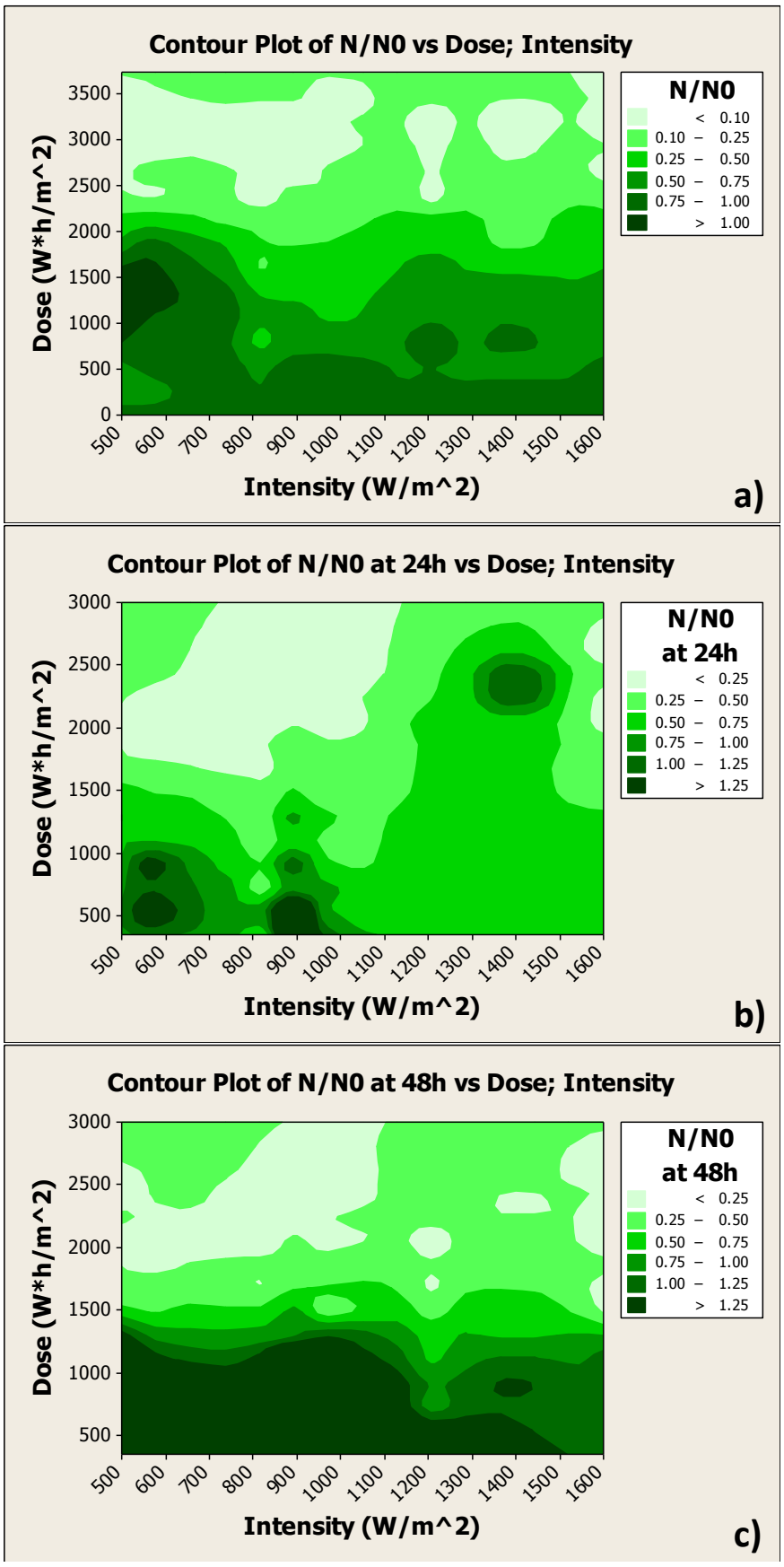

Figure 3.5.7: Overview of the experimental results by contour plots. (a) Contour plot of the bacterial inactivation (N/N_0) vs. Intensity and Dose. (b) Contour plot of the normalized bacterial regrowth after 24 h. (c) Contour plot of the normalized bacterial regrowth after 48 h.

A wide range of intensities was investigated, from 500 to 1600 W/m^2, in order to have really dense data, to create a link between intensity and dose and their results. A convergence is observed around 3000 Wh/m^2 for 99.99% disinfection efficiency, with the equivalent for inflicting enough damage to inactivate bacteria in long term (effective bactericidal dose) being around 1200 Wh/m^2. These levels, with a small deviation, were found to be accurate for all intensities, low or high. The only practical problem was the ability to attribute the exact minute these phenomena take place and estimate the dose safely, due to the sampling intervals chosen (20 or 30 min).

In Figure 3.5.7, an overview of normalized disinfection and regrowth results for all intensities and the corresponding doses is presented. What is observed, is the compliance with the reciprocity law, but not as a fundamental principle; for the same dose, results are similar, but moving horizontally in specific intensity levels will not result in exactly the same effect. Therefore, it is suggested that for solar wastewater disinfection, the reciprocity law is valid, under some restrictions; for the same dose, the same effect is observed, but for relatively close intensities. For stepwise increases of dose, the results improve. In regrowth tests, after 24 h minor differences are observed, but it is noted that the highest values appear in low doses from low intensities. After 48 h, the behavior is similar for different dose levels, with slightly better results in high intensities. Also, the growth support provided by the wastewater matrix influences the deviations, because the excess growth of bacteria creates more targets for inactivation, with the same applied dose.

As it can be concluded, very low or very high intensities, as defined in these experiments, can present some deviations from the reciprocity law. But what is globally, and most importantly, perceived as low intensity for bacteria, is possibly different. The philosophy behind the choice of 500 W/m^2 as a minimum intensity level is inspired by the SODIS practices which suggest a similar minimum intensity for at least 6 h for cloudless skies. However, in 400 W/m^2, for instance, total disinfection could be achieved, after many hours of constant irradiation, to achieve the energetic equivalent needed.

3.6. Conclusions

Non-irradiated samples of synthetic secondary effluent treated at 20-40°C showed slight growth during treatment. Significantly, thermal inactivation predominated at 50°C and was total at 60°C. Irradiation at 800 W/m^2 was sufficient to suppress growth at 20-40°C, but not for providing proper disinfection in 4 h of treatment, with efficiency decreasing with rising temperatures and showing a minimum around 40°C. Synergy between light and temperature above 40°C was evident, with all 60°C samples undergoing total disinfection in just 1 h, or, at 50°C, high disinfection efficiencies after 4 h of treatment. Irradiation at 1200 W/m^2 resulted in total disinfection (no bacterial counts) in 4 h (20-40°C), in 1.5-4 h (50°C) or in just 0.5 h (60°C), showing again the light-temperature synergy.

The profound actions of UVB and UVA irradiation demonstrated different results, according to the experimental temperature range, with the cases of very low and very high demonstrating the best results, due to either lower metabolic rhythm or synergy between temperature and light, plus thermal modifications of cells' proteins.

A 4-factor, multilevel, complete factorial design of experiments has proved a powerful, useful tool to evaluate the main variables governing disinfection. A linear model with interactions (R^2=65.1%, S=24.42) has been initially proposed and improved, when it was modified to a temperature dependent one. The new model is simpler (no interactions needed), as well as more accurate (S = 20.0507, R^2= 73.08%, for 20<T≤40°C and S = 21.9270, R^2= 68.41% for 40<T≤60°C). While unrelated to any fundamental modeling of the process, it has allowed to statistically determine the significant factors and interactions in the process.

In terms of regrowth: non-irradiated samples of secondary effluent treated at 20-40°C showed slight growth during treatment, and high post-treatment regrowth (ratios of 250-1000). Significantly, thermal inactivation with no regrowth predominated at 50°C and was total at 60°C.

At 800 W/m^2, bacterial regrowth only occurred in incompletely disinfected samples, which are linked to lower irradiation, shorter times or high initial microorganism populations. No regrowth was observed in samples presenting no bacterial counts at the end of the treatment. An erratic behavior was observed when treatment temperature was among 20-40˚C, where prolongation of treatment resulted in higher long term re-appearance of bacteria in the samples, related to growth issues after 30˚C.

High intensities revealed almost no regrowth (special cases: 1-h treatment), for low temperatures, revealing the detrimental effect of elevated light intensities, whereas the combination of high temperatures with high intensity resulted in no regrowth and survival diminishing, as well, due to the very high levels of synergetic action between light and temperature.

When present, regrowth was directly connected to the enumerated leftover bacteria. The lower temperature region promoted bacterial regrowth (max. in 30°C) and high temperatures suppressed the reappearance,

both in short and long term storage. Also, the lower temperature set demonstrated higher rate of transferring their live bacteria from the end of the treatment time towards the next days, than high temperatures.

The employed temperature range for light-temperature synergy (above 40°C) is well above the common pond temperatures in shallow ponds, even in tropical countries, while the maximum sustained intensity lies around 800-900 W/m$^{2.}$ It is suggested that contact times longer than the 4 h observed here, would be required at field conditions. Other field factors, like shielding by particles (residual suspended solids, algae) would extend required contact time to days, as is common practice in shallow ponds.

The reciprocity law was tested and verified for very few cases of temperature controlled experiments, such as high temperature experiments (mainly 50°C). In fact, when temperature is taken into consideration, doses must be divided in low and high-temperature ones, then study the effect of high and low intensities and how they can shape up the same dose. Disinfection kinetics revealed different inactivation rates for the same dose, being higher for low intensities at low temperatures (except for 40˚C) and lower for higher intensities at higher temperatures. Bacterial growth has interfered in the normal evolution of the process.

For regrowth, temperature seemed to dominate the probability of reappearance of bacteria in wastewater, resulting in high ratios in low temperatures (although increasing towards 30-40˚C) and low ratios in samples treated in warmer water. Short term storage could be dangerous if treated for a short time in high intensities, while long term one is more susceptible to present regrown numbers in low doses deriving from low intensities.

These results can significantly influence natural solar treatment methods of wastewater, because they indicate the feasibility of applying such a method, without the need to achieve high temperatures. Even at low temperatures as 20˚C, low intensities could result in total disinfection, if the exposure is prolonged. Therefore, reciprocity law is a rather simplified image of the real bacterial response to phototreatment and this study indicates that there are more factors affecting this generalized rule.

Also, in all simulated solar light wastewater disinfection experiments without temperature control, the decay period was presented with a lag, namely shoulder phase. Increasing the intensity decreased the length of the lag period, as well as the fluctuations in the population, induced by the growth support of the matrix. Above 700 W/m^2 the second (minor) lag phase towards the end is diminished and beyond 900 W/m^2, no fluctuations are observed whatsoever.

The models used to fit the experimental data were the Shoulder Log-Linear, the Weibull distribution and the Biphasic model (with shoulder). Since the second lag phase disappeared Biphasic model did not yield sufficient fit, the results were processed only through the first two models. Through the fit, the shoulder length was identified, along with its correspondence with the inflicted dose. Also, intensity was related with the efficient energy to inactivate 99.99% (4-log) of the total population.

One of the most significant findings was the constant, coherent character of the required dose, as far as disinfection without temperature control is concerned. For any given intensity, the dose required to inactivate 99.99% was nearly constant (2975±179 Wh/m^2), while total inactivation required almost constant dose of 3200 Wh/m^2 (range: 3100-3700). This gives indications for standardization of the required dose, when a solar wastewater disinfection unit will be studied.

When it comes to regrowth, no regrowth was observed in the cases that total inactivation was reached. It was also found that there is a certain energy threshold in each discrete intensity level, after which regrowth turns into decay. This point was shown to be delayed as intensities dropped. However, the total accumulated dose to cause a bacteriostatic effect was the same in every case. There exists an energy threshold, once achieved, one can estimate decay for the surviving population.

As far as a potential application is concerned, the recommended practice would be to acquire the highest irradiation times possible for the given regional climatological constraints. Given the fact that real applications will be temperature-limited, the design practices should be oriented to acquiring prolonged exposure to sunlight, since extension of the treatment always favored bacterial disinfection.

In conclusion, the estimations of the bacterial kinetics during irradiation and the post-irradiation events were well correlated with simple mathematical concepts. The link between the bacterial behavior during and after irradiation and the dose, allows the estimation of a bacterial life cycle, to say, according to their initial population and the treatment conditions. Finally, since the dose was found to have relatively the same effect, the reciprocity law seems to comply with minor deviations. However, the hypothesis of constant irradiation is far from the real context, and before definite results, even at laboratory scale, more trials need to test the bacterial response in variable intensities, in randomized manner, for the proper generalization of the solar wastewater disinfection process.

Chapter 4. Photoreactivation and dark repair studies in different matrices

4.1. Methodological approach

In this chapter, an investigation on the fate of bacteria was undertaken, from the moment they enter the disinfection system, the effect of solar dose and the introduction into several water matrices. While keeping the solar dose at same levels, solar-treated secondary effluent is first kept in the dark in a range of temperature (4, 20 and 37°C), so as to test regrowth dynamics as a function of temperature. In another context, pre-illuminated samples are lead into untreated wastewater (synthetic *E. coli*-free), lake water, sea water and distilled water, in order to assess the effect of the receiving water body on the regrowth potential, the survival and the mortality rate. The same assessment was carried out in a series of dilutions (50%, 10% and 1%), with the aim of systematically investigating the effects of different osmotic conditions and nutrient content. The aim is to locate the ability of bacteria to adapt in the environment while being pre-stressed by solar light and the variation of the environmental conditions on the required dose for safe handling of the treated samples.

In order to assess the dark repair events, every 30 min a sample was taken and was kept in the dark for the total duration of the monitoring period. Temperature control experiments were stored for 72 h (3 days), while dilution experiments were kept for 120 h (5 days). Monitoring of the bacterial population was made by sampling from the stored samples every 24h after the initial acquisition time. A graphical representation is given in Figure 4.1.1. Temperature experiments were done at 4, 20 and 37˚C (refrigeration, ambient temperature and incubator temperatures), but dilution experiments were made in ambient temperature in absence of light. Dilutions (50%, 10% and 1%) were made in sterile synthetic wastewater, in Lake Leman water, synthetic seawater and Mili-Q water. The last groups of tests in Mili-Q water represent a control experiment, rather unlikely to achieve in real environmental context, but will offer great insight on the way osmotic pressure and presence/absence of food acts on pre-stressed bacteria.

Also, a series of tests has been conceived to assess the PHR and DR risks, after simulating solar exposure of *E. coli*-spiked synthetic secondary effluent. Photoreactivation was intensely studied, aiming to attribute the bacterial recovery in specific wavelength bands, by the use of 6 different fluorescent colored lamps, plus the relationship between the applied wavelengths and the final bacterial numbers. Finally, the ability to alter the normal DR potential by the pre-illumination tests and an assessment of *E. coli* PHR is also under study.

For photoreactivation estimation, the experimental sequence took place as follows: i) solar disinfection, ii) exposure to mono/polychromatic photoreactivating light and iii) dark storage for 48 h. The simulated solar disinfection part consisted of 0-4 h of illumination, whose evolution was monitored by semi-hourly measurements of the bacterial population. Each sample was exposed to 4 different conditions, namely 2, 4, or 8 h of photoreactivating light (followed by dark storage), or directly dark storage as a blank experiment. During photoreactivation, samples were plated at 2, 4 and 8 h to monitor the bacterial numbers during the process. Finally, in order to assess the dark repair events taking place in the bacteria of these samples (as a reference), the samples were kept in the dark for 48 h after the completion of the irradiation period. Every 30 min, a solar irradiated or a photoreactivated sample was drawn and kept in the dark, and the corresponding population was measured every 24 h. There were two sets of experiments under the same conditions, for comparison and verification of the findings.

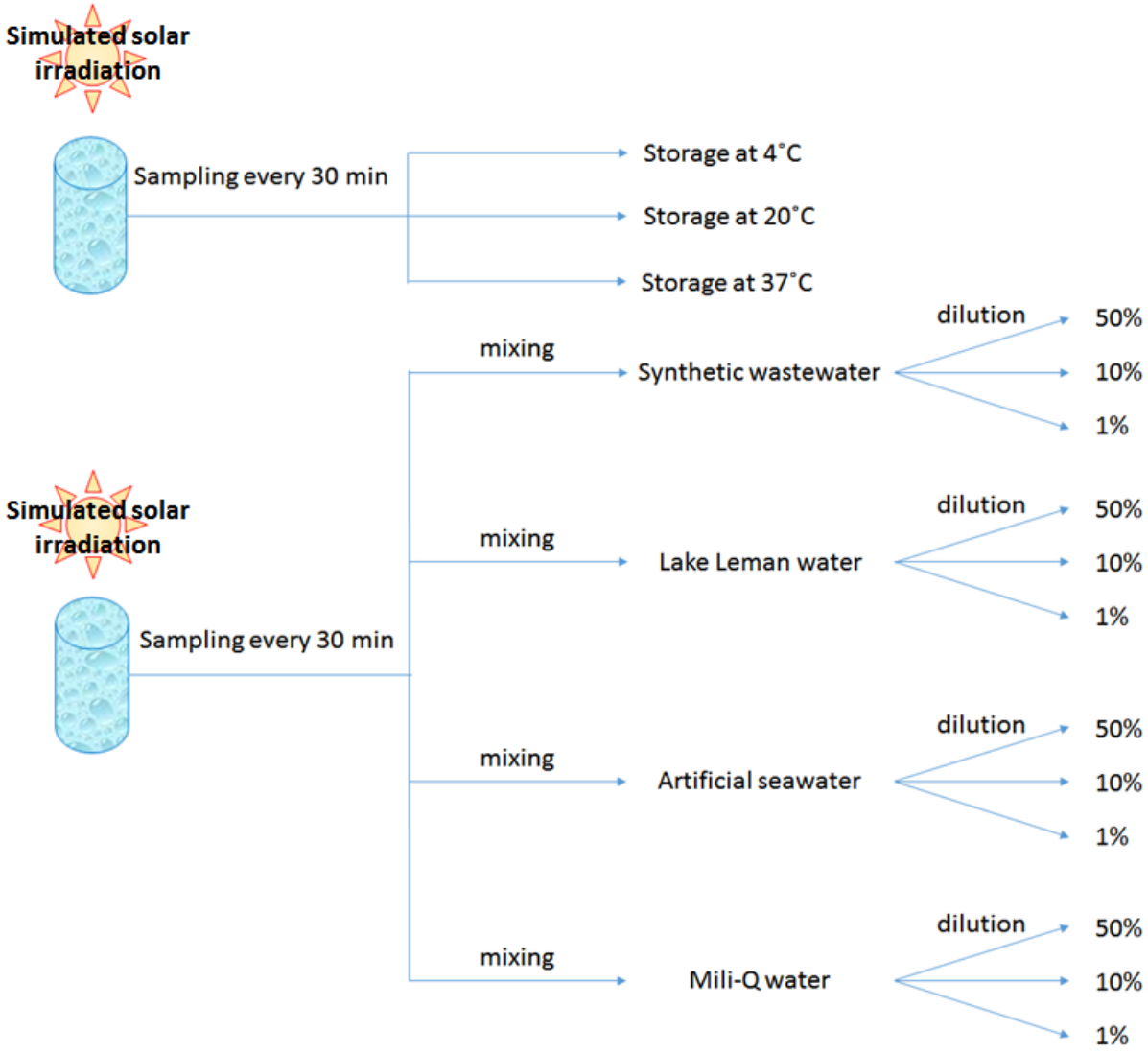

Figure 4.1.1: Schematic representation of the experimental strategies. An irradiated batch was split to three samples for temperature control, and another batch was divided into the four matrices and the subsequent dilutions.

4.1.1. Employed water matrices

The physicochemical characteristics of Lake Leman water and the composition of synthetic seawater are presented in Table 4.1.1 and 4.1.2. Mili-Q water is characterized by 0.0555 μS/cm at 25 °C. Lake water was heat-sterilized to avoid the effects of indigenous microorganisms, while artificial seawater and Mili-Q water were sterilized prior to use, to avoid contamination.

4.1.2. Reactors and experimental conditions

Bacterial inactivation tests took place in 50 mL batch tests, in Pyrex glass reactors of 65 mL total capacity, while being mildly stirred with a magnetic stirrer (approx. 150 rotations per minute). 50 mL of wastewater were first illuminated with a Suntest solar simulator, followed by exposure to monochromatic or

polychromatic lamps for 2-8 h and finally 48 h in the dark. Samples were drawn semi-hourly for the solar exposure part, at 2, 4 and 8 h for the photoreactivating light part and daily for the final dark storage sequence.

4.1.3. Monochromatic and visible light lamps

The monochromatic lamps (18 W blacklight blue, actinic blacklight, blue, green and yellow) were acquired from Philips, while the visible light lamps were purchased from Osram. Their specifications are given in Table 4.1.3. Figure 4.1.2 presents the chromaticity diagram, explaining the color designation found on the X and Y coordinates of the lamps in Table 4.1.3. An apparatus bearing 5 lamps of 18 W nominal electrical value was used, and samples were placed 15 cm away from the light source. Eventually, less than 80 W/m^2 of global irradiation was reaching the body of the sample.

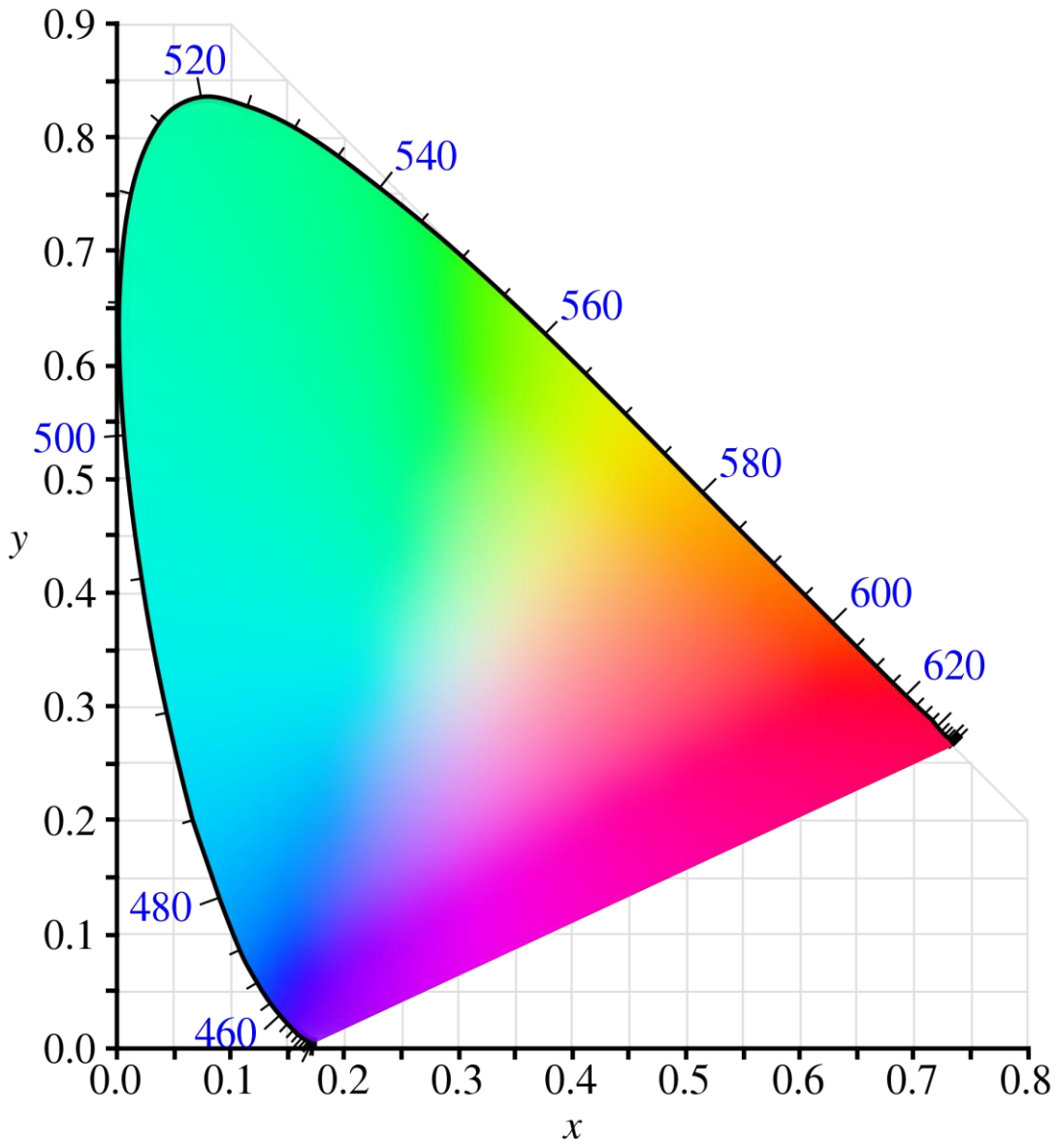

Figure 4.1.2: CIE chromaticity diagram.

Table 4.1.1. – Physicochemical characteristics of Lake Leman water (yearly min, max and average).

Parameter	Unit	Min	Max	Average	Parameter	Unit	Min	Max	Average
Turbidity	*NTU*	0.32	0.88	0.64	**Nitrates**	*mg/L*	1.7	2.5	2.1
Temperature	*°C*	5.7	8	6.3	**Fluorides**	*mg/L*	0	0.1	0
pH		7.82	8.1	7.94	**Nitrites**	*mg/L*	0	0.016	0.005
Conductivity	*µS/cm*	269	278	274	**Ammonium**	*mg/L*	0.005	0.156	0.033
Acid Consumption	*mmol/l*	1.79	1.92	1.87	**Aluminum**	*mg/L*	0.016	0.025	0.021
Hydrogen Carbonates	*mg/L*	106.14	114.07	110.9	**Total Iron**	*mg/L*	0.011	0.026	0.018
Hardness	*mg $CaCO_3$/L*	89	96	93	**Total Manganese**	*mg/L*	0.001	0.001	0.001
Total Hardness	*mg $CaCO_3$/L*	133	139	137	**Phosphorus direct**	*mg p/l*	0.003	0.047	0.018
Active CO_2	*mg/L*	-0.4	1.1	0.4	**Silica**	*mg/L*	0.8	0.9	0.8
Saturation Index		-0.16	0.08	-0.06	**Copper**	*µg/L*	1.3	1.3	1.3
Dissolved Oxygen	*mg/L*	8.5	10.5	9.5	**Zinc**	*µg/L*	3	4.7	3.9
% saturation	*%*	75.7	88.4	83.4	**Cadmium**	*µg/L*	0	0	0
$KMnO_4$ Oxydability	*mg/L*	2.3	2.8	2.5	**Lead**	*µg/L*	0.1	0.3	0.2
Absorbance 254 nm	*/m*	1.143	2.061	1.557	**Chromium**	*µg/L*	0.3	1.2	0.8
Total Organic Carbon	*mg C/l*	0.61	1	0.72	**Cobalt**	*µg/L*	0	0	0
Calcium	*mg/L*	43.8	45.5	44.8	**Nickel**	*µg/L*	0.3	0.5	0.4
Magnesium	*mg/L*	5.7	6.1	5.9	**$CHCl_3$**	*µg/L*	0	0	0
Sodium	*mg/L*	6.1	7.5	6.7	**$CHCl_2Br$**	*µg/L*	0	0	0
Potassium	*mg/L*	1.6	1.7	1.6	**$CHClBr_2$**	*µg/L*	0	0	0
Chlorides	*mg/L*	9.2	9.7	9.4	**$CHBr_3$**	*µg/L*	0	0	0
Sulfates	*mg/L*	48.4	49.6	48.8	**Trihalomethanes**	*µg/L*	0	0	0

Table 4.1.2. – Synthetic wastewater and sea water composition.

Wastewater Composition		Seawater Composition	(Jonkers et al., 2013)
Peptone	160 mg/L	**NaCl**	27.35 g/L
Meat Extract	110 mg/L	**KCl**	0.8 g/L
Urea	30 mg/L	**$CaCl_2 \cdot 2H_2O$**	1.5 g/L
K_2HPO_4	28 mg/L	**$MgSO_4 \cdot 7H_2O$**	6.9 g/L
NaCl	7 mg/L	**$MgCl_2 \cdot 6H_2O$**	5.1 g/L
$CaCl_2 \cdot 2H_2O$	4 mg/L	**Salinity**	3.5 %
$MgSO_4 \cdot 7H_2O$	2 mg/L		

Table 4.1.3 – Color distribution of the employed fluorescent lamps.

Fluorescent Lamp	Color Designation	Code	Coordinate X	Coordinate Y	UVA	UVB/ UVA	Provider/ Model
Blacklight blue	Blacklight Blue	108	-	-	3.9 W	0.20%	Philips TL-D 18W
Actinic blacklight	Actinic	10	222	210	5.0 W	0.20%	Philips TL-D 18W
Blue light	Blue	180	157	75			Philips TL-D 18W
Green light	Green	170	246	606			Philips TL-D 18W
Yellow light	Yellow	160	495	477			Philips TL-D 18W
Visible light	LUMILUX Cool White 2700K	840	0.38	0.38	UVA < 150 mW/klm	0.13%	OSRAM 827 Lumilux Interna

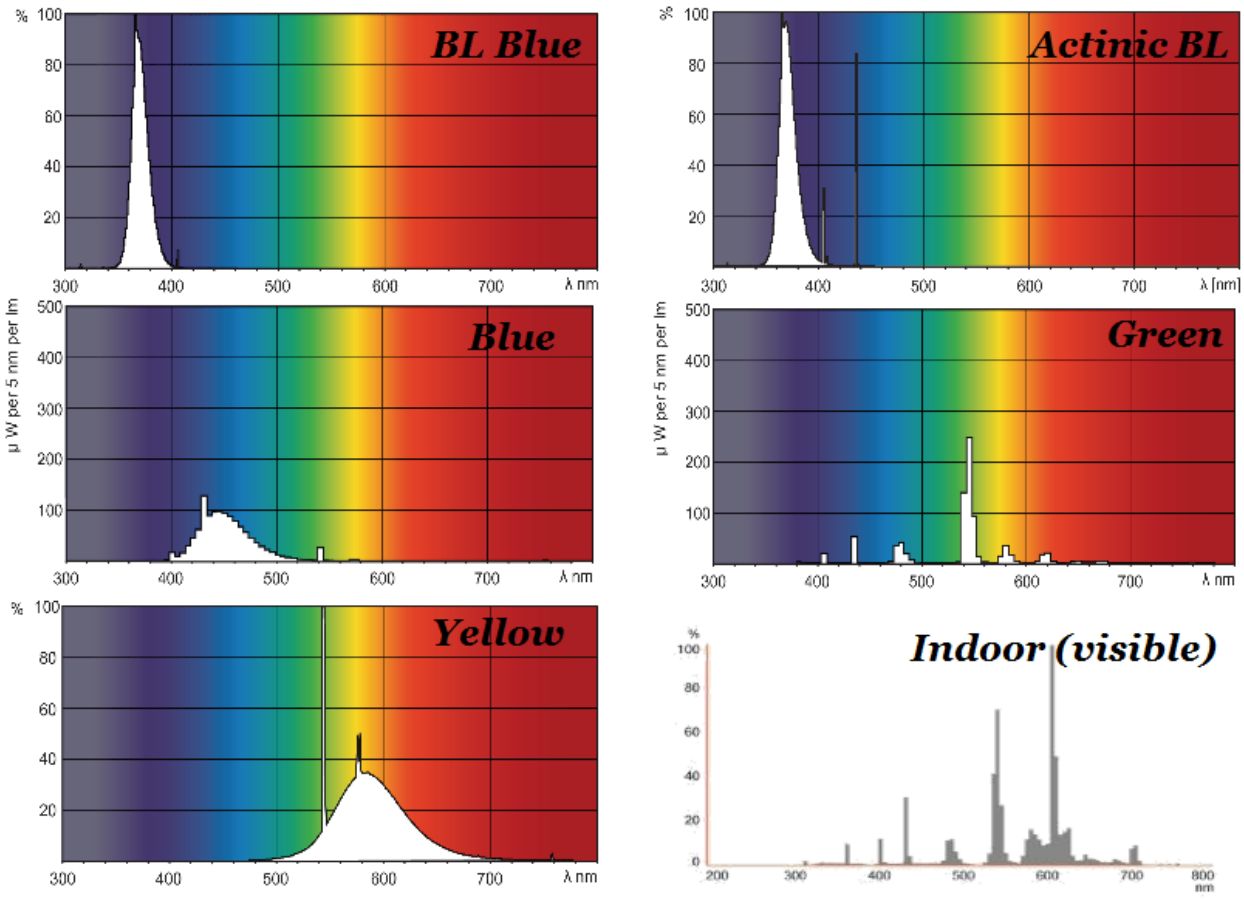

Figure 4.1.3: Emission spectra of the monochromatic and visible light lamps.

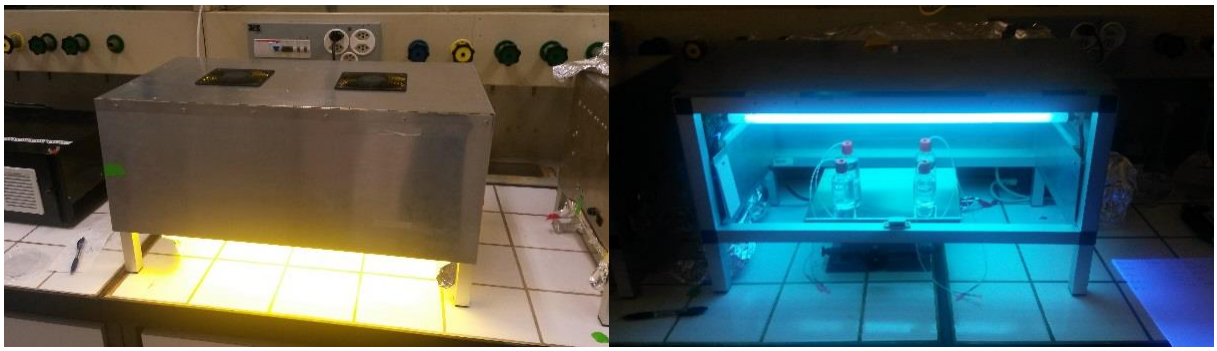

Figure 4.1.4: The light apparatus bearing the monochromatic and visible light lamps. On the left, the yellow light at work and on the right, the actinic blacklight. The spatial distribution of the reactors is also visible.

4.2. Temperature experiments: post-irradiation modification of storage temperature and its effects on bacterial repair

The first set of experiments studies the modification of storage temperature conditions for the solar-treated samples. The samples were exposed in simulated solar light, with the intensity set at 1000 W/m^2, an achievable solar intensity in real context.

In this approach, there are some constraints to be considered, such as the nature of the target microorganism: *Escherichia coli* is a typical mesophilic microorganism, that usually thrives around 35-39˚C, presenting a maximum growth rate around these temperatures. Lowering temperature will result in deceleration of their metabolic rhythm (Blaustein et al., 2013), while the expected behavior at 4˚C would be a stabilization in the minimum metabolic activity required to sustain life. Also, the chemical composition of the matrix is of high importance, considering the abundance of nutrients and salts present within it. Marugan et al. (2010) have underlined the importance on Mg and K salts for the maintenance of bacterial life and Caballero et al. (2009) highlighted the aid nutrients provide in the growth of bacteria in water matrices. Therefore, optimal support conditions for bacterial development is expected, as seen in previous work with this matrix (Giannakis et al., 2013).

In Figure 4.2.1 it is observed that the disinfection kinetics of illuminated samples reveal a shoulder-lag phase, followed by log-linear decay until the end of a 4-hour period that was required to fully inactivate microorganisms. In reality, almost 90% of bacteria were inactivated in 3 h and the excess 1-h dose ensured zero counts at the end of the experiment. Post-treatment storage of the samples drawn every 30 min took place in three different conditions, 4, 20 and 37˚C, in order to recreate the conditions usually encountered by microorganisms. It also presents the monitoring of the bacterial population for three days after the sampling time. First of all, the effects the exposure (UV dose) has on bacterial survival are demonstrated. Generally, increasing the dose decreases bacterial survival. It can be also seen that until the corresponding dose of 90-min exposure to sunlight, bacteria still maintain their ability to recover their damage and, after a lag phase, once again increase their population. Conversely, from 120 min of treatment and more, damage is permanent; bacterial population is lowering, as days pass, indicating cells that are unable to recover their damage and probably, cellular senescence is taking place (Stephens, 2005). It is known that the accumulation of photoproducts inside the cell (Hallmich and Gehr, 2010), makes bacteria unable to sustain normal life functions, through the damages in the respiratory chain (Bosshard et al., 2010a), in DNA (Hallmich and Gehr, 2010) etc.

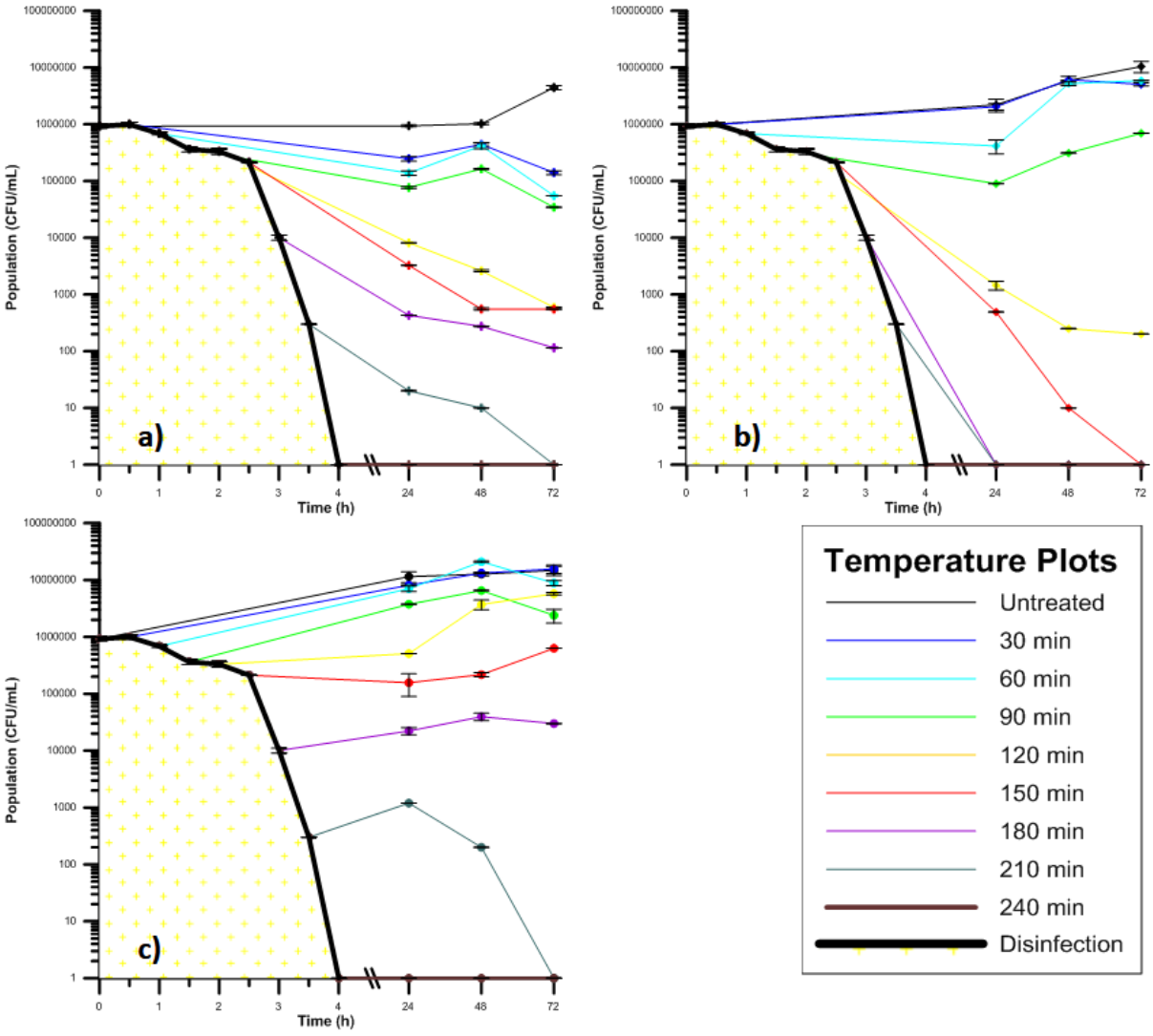

Figure 4.2.1: Post-irradiation monitoring of synthetic secondary effluent at different temperature levels. Samples were kept for three days at: (a) 4˚C. (b) 20˚C. (c) 37˚C.

Considering the above, it is interesting to observe the differences low (unfavorable) and high (favorable) temperatures inflict on bacterial survival. In Figure 4.2.1a, the deceleration of bacterial metabolism is visible. Since the samples have been subjected to the same irradiation energy, under the same experimental conditions, it is normally expected to have the same evolution, when it comes to their survival. However, i) suspended growth rates in lightly or non-irradiated samples and ii) prolongation of the bacterial survival is observed, compared to the situation at 20˚C. For instance, the kinetic curves that correspond to 150, 180 and 210 min of pre-treatment, reveal a significant delay towards their respective 20˚C ones. This is attributed to the formation of more resistant forms of cell structure as a defense against low temperature, which includes low metabolism rates and nutrient uptake. As it seems, either repair of photoinduced damage or, along with delayed metabolic action, a delayed programmed cell death (Sat et al., 2001) triggered by light exposure is observed.

In contrast, cells that remained at 37˚C, present altered kinetic curves compared to their respective ones in lower temperatures. Firstly, in Figure 4.2.1c, significant changes are visible in low-dose treatment times, where growth is orders of magnitude higher than the respective one at 4˚C. But even in high irradiation doses, samples that were treated for 180 min presented different behavior: at 4˚C slightly decreased their numbers, decayed shortly after treatment stopped when metabolism was increased (20˚C), even present a mild growth at 37˚C. At this temperature the conditions for growth are favorable, and bacterial survival is promoted. Another possibility, since no total disinfection was achieved, is that the live fraction of bacteria compensated for the fatally injured ones, in terms of numbers. In the existence of a declining number due to damage and a growing one, due to comfortable conditions, the numerical balance is in favor of growth. Finally, in all experiments, whenever total inactivation was reached during the illumination period, no regrowth was observed in any samples, thus indicating the permanent nature of the inactivation due to light exposure.

4.3. Post-irradiation modification of the receiving aqueous matrix and long-term monitoring of bacterial survival

4.3.1. Dilution in fresh (synthetic) wastewater

Figures 4.3.1 (a-c) present in a summarized way the results of bacterial monitoring for a period of five days after the irradiation. The inset presents the disinfection experiment from which sample is taken every 30 min, followed by the dark storage. Figures 4.3.1a to 4.3.1c represent a dilution of the original disinfected sample of 50, 10 and 1% respectively, over the untreated effluent. This dilution in wastewater serves a double purpose: first of all, after the treatment there is a remaining bacterial population, which is then submitted to halving, 10-fold and 100-fold reduction. In this manner, three different cases of initial population can be assessed and the kinetics response in this case. Since the medium remains the same, normally growth pattern is expected to remain similar. Also, the second aspect of the dilution concerns the replenishment of organic substances which are subject to degradation due to solar treatment of the sample, according to Dahlen et al. (1996).

Therefore, in Figures 4.3.1a to 4.3.1c the kinetic curves of bacteria in five consecutive days, after their exposure to sunlight, are presented. Their kinetics are generally described as growth, which is then subjected to certain variations. In Figure 4.3.1a the exponential growth of almost all samples is visible, with the exception of the 180-min treated sample; after 3 hours of irradiation it is impossible for bacteria to heal the injuries caused by exposure to simulated sunlight and they rather survive until their complete decay after four days. All samples (except for the untreated) seem to grow their numbers, but after an initial delay of 24 h. This observation is clear in samples treated for a significant portion of time (60-150 min).

The effect of dilution is visible, passing from 50% to 1% Figures, mainly in the lag and decay phases. The initial sample is diluted in 3 different proportions, thus resulting in three different initial numbers of active bacteria. This difference is visible at time 0, and as it seems it affects the growth curves, presenting longer lag phases, when growth is observed, or faster decay in the case of 180-min pre-treatment. This is explained by the statistical probability to acquire less active or heavier injured cells from the initial sample. As light is inflicted on the sample, some bacteria are able to escape irradiation through shielding or scattering (Lindenauer and Darby, 1994) and therefore, when the amount of the original sampled proportion is increased, the possibility of acquiring healthier cells is also rising. This probably explains the different behavior of the 150-min treated sample, which switched from growth to decay.

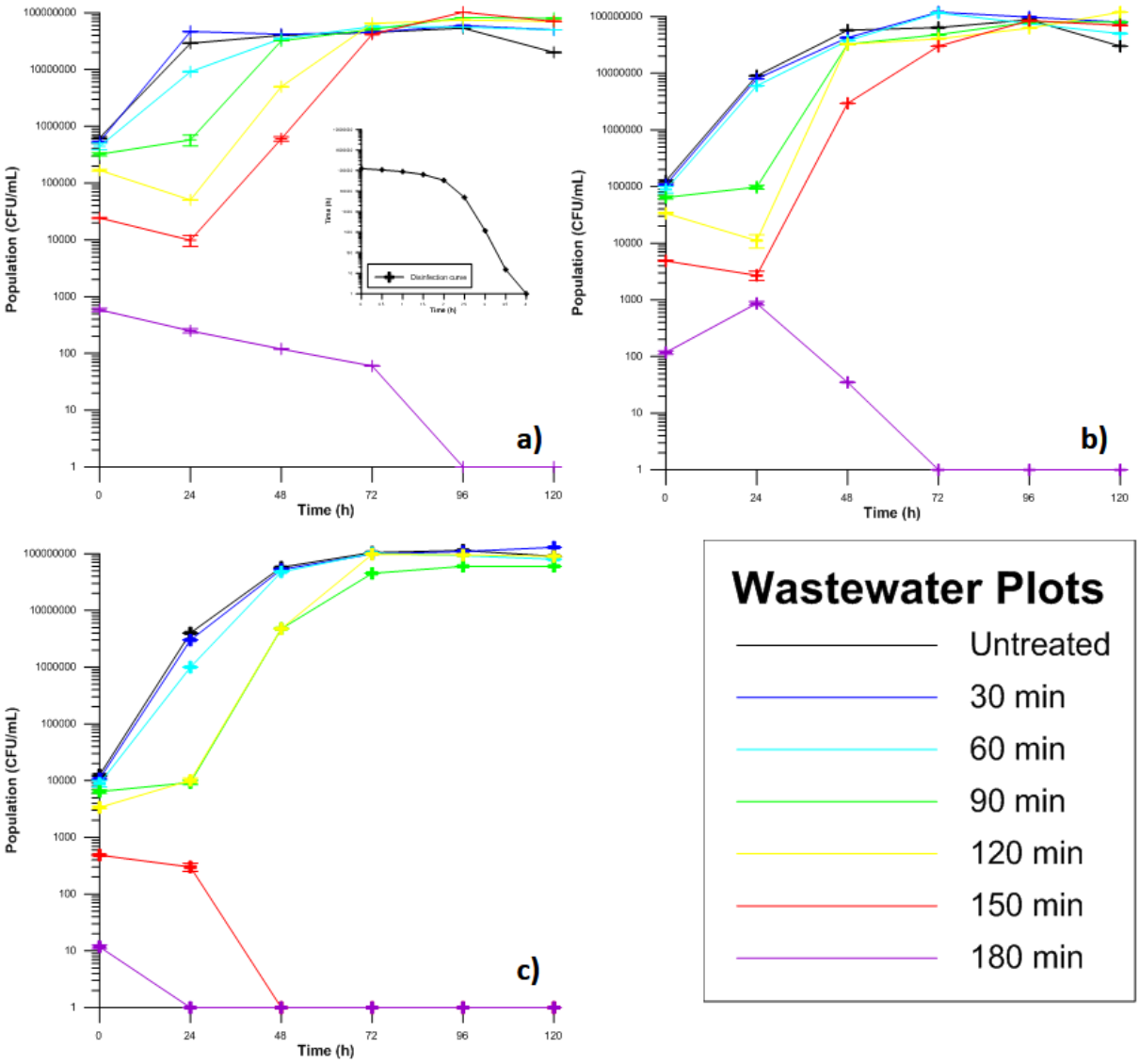

Figure 4.3.1: Overview of the 5-day monitoring period of the irradiated sample diluted in wastewater. (a) 50% dilution. (b) 10% dilution. (c) 1% dilution.

Finally, when the dilution rate is high (1%), the availability of nutrients per cell is higher than the other two cases. Knowing that degradation of organics affects the availability of nutrients for bacteria, a dilution in fresh wastewater will be beneficial for their survival. Therefore, in this case, there is less competition among the cells, resulting to excessive growth and their population reaches the same plateau (peak) as the previous cases with higher initial population, in the same time period (2-3 days), plus the stabilization towards the end of monitoring period versus the slight decreases observed in lower dilution rates.

4.3.2. Dilution in Lake Leman water

The second tested matrix was water acquired from Lake Leman. The water was unfiltered, to permit the occurrence of natural suspended solids, but heat-sterilized prior to experiments to avoid the effects of competition between seeded *E. coli* and indigenous microorganisms or predators (Flint, 1987). Figures

4.3.2a to 4.3.2c demonstrate the results of a 5-day long monitoring of bacterial survival. In this matrix, survival of unharmed bacteria is expected for a relatively long time; there are reports for the occurrence of bacteria in water for weeks (Darakas, 2001), even months in lake sediments (Haller et al., 2009a). However, there are no records on the responses of previously phototreated bacteria.

In Figure 4.3.2a, the impact that solar dose has on bacterial survival after 50% dilution is demonstrated. It can be seen that bacteria can retain their cultivability for doses less than 120-min exposure to sunlight, while longer exposure causes decay, faster with increasing doses. There is a lag phase visible in mid-ranged doses (60-120 min of pre-treatment); however, after 4 days all doses from 0 to 120 min result in almost similar concentrations, indicating a growth "ceiling" for these conditions.

Applying 10% dilution modifies the bacterial survival, as it can be seen in Figure 4.3.2b. As far as the matrix conditions are concerned, there has been a change in the availability of nutrients and baro-protective salts. This change is reflected to the kinetic curves especially of 90 and 120 min solar treatment, which change from growth to decay form. Also, 150 and 180-min curves reach a minimum 48 h earlier than 50% dilution, while 0 to 60-min treatment curves present no significant alteration. This can be explained by the injury state of the cells from each dose group: it seems that cells which suffered the same amount of damage, in the higher presence of nutrients respond better and present growth instead of decay.

Finally, Figure 4.3.2c presents the survival curves for 1% dilution of the original sample, clearly representing the effect of initial population decrease, as well as the shortage in nutrients. First of all, the curves are significantly lower, and growth is limited at the end of the monitoring period in lower numbers than the respective ones of 50% and 10%. Both untreated and relatively mildly treated samples initiate in lower numbers and result in lower or even null counts. For instance, the 60-min curve is now decaying more rapidly, and the 90-min one is reaching total inactivation. After all, apart from the nutrient source, mild osmotic forces are suspected to be accelerating bacterial death due to pressure differences inside and outside the cell. This stress adds up to the already solar-damaged cells to result in faster decay rates.

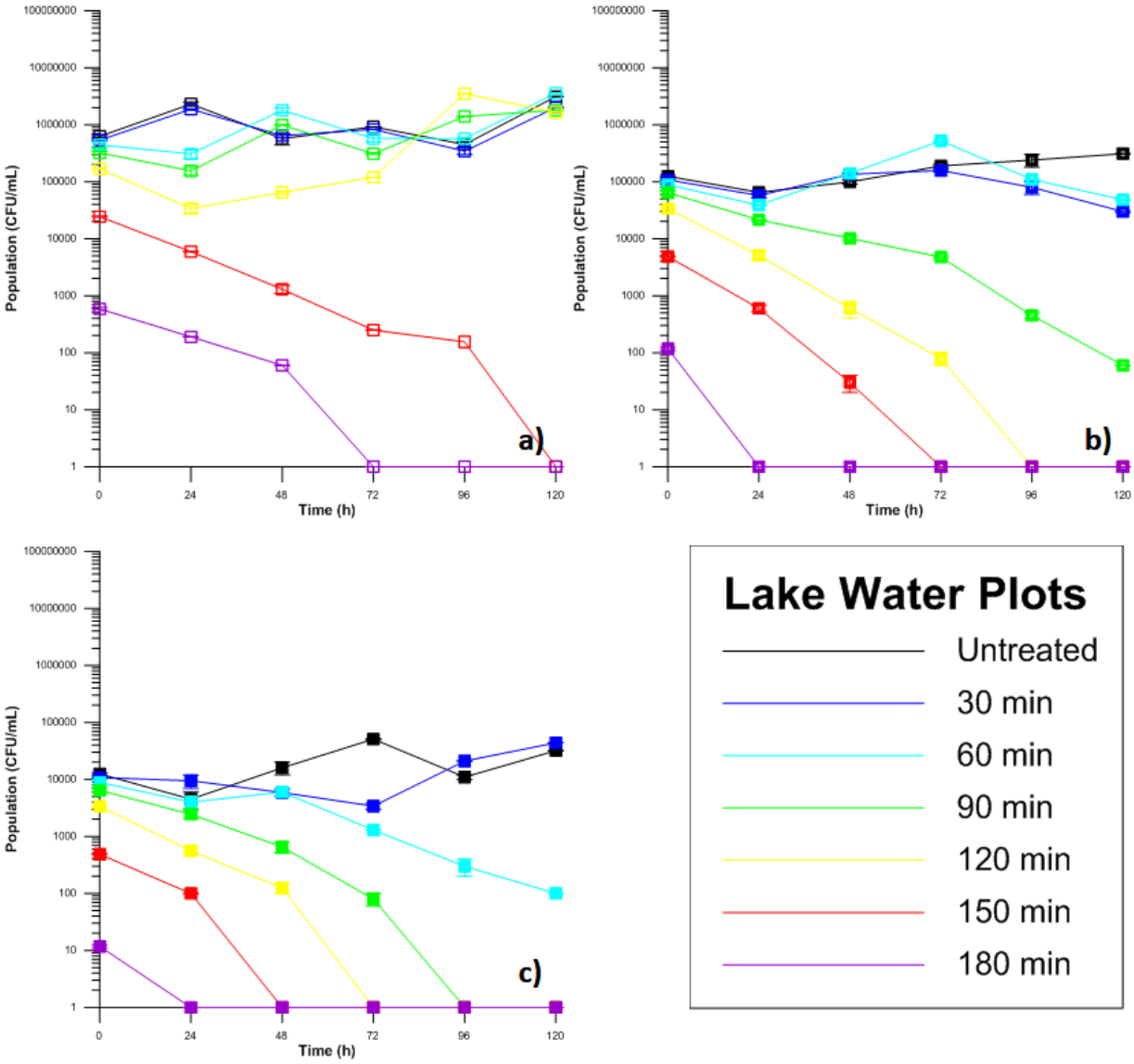

Figure 4.3.2: Overview of the 5-day monitoring period of the irradiated sample diluted in Lake Leman water. (a) 50% dilution. (b) 10% dilution. (c) 1% dilution.

4.3.3. Dilution in (synthetic) seawater

Seawater, as a receiving medium for wastewater, has been a subject of interest for a very long time and some practices have tried to model the survival (Darakas, 2001) and growth (Tassoula, 1997) of microorganisms within it. There have been significant findings, and bacterial decay has been attributed to solar light, the co-existence with predators and the osmotic difference between the cell contents and the seawater (Yang et al., 2000; Darakas, 2002). Bacteria are being lysed usually after they release their intracellular fluids. Also, there have been many works studying the most common phenomenon of solar disinfection in estuarine or sea water (Yukselen et al., 2003), taking into account the action of the sun. It has been stated that bacteria have even developed anti-irradiation mechanisms in order to maintain their integrity and continue replication. This bacterial response is a result of bacterial gene evolution, to protect themselves from the solar ultraviolet rays (Quek and Hu, 2008). Keeping all the above into consideration,

the ability of bacteria to survive after they have been exposed to simulated solar light, and therefore, sterile synthetic seawater has been used is studied, in order to exclusively quantify the amount of physicochemical stress applied on the cells.

Figure 4.3.3a demonstrates the survival kinetics for five days in 50% diluted wastewater. Although it is known from literature that the change in osmotic pressure is a fatal stress, decay is observed only in cells previously irradiated for 150 min and beyond. All other samples present a lag and then a growth phase, which is proportional to the dose received. There is a certain extent of osmotic difference to be achieved, in order to visualize its detrimental effects. This dilution is not very hostile, since only weak cells are subject to decay. The adaptation phase is finished in three days and then a mild growth phase initiates until the end of the study period.

After 10% dilution of the samples, (Figure 4.3.3b) almost all treated samples present decay. It is clear that even non-lethal irradiation doses are able to lead to bacterial decay within the studied time. Once again, *E. coli* succumb to their solar-inflicted wounds once the environment is relatively hostile. Bacteria that managed to retain their cultivability are now subject to greater stress and are lead to decay (60-120 min). The untreated, healthy cells continue to multiply and grow, as well as the 30-min treated ones; after a 3 day survival phase, they retain their ability to grow once more, since there is 10% of the original, nutrient-rich medium.

Finally, Figure 4.3.3c demonstrates the fatal effect unfavorable osmolarity has on the bacterial cells. Contrary to every other case, all bacterial samples present decaying kinetic curves, even the healthy ones. The curves that presented decay in the previous (10%) case, are declining even faster, revealing the deleterious effect of high salinity. Nutrient sources are also scarce and the first totally negative survival conditions are presented in this dilution rate.

4.3.4. Dilution in Mili-Q water

Figure 4.3.4a represents a 50% dilution in Mili-Q water and the subsequent survival in a 5-day monitoring period. The results here represent a relatively steady survival state; the same curves that decayed right away (150 and 180 min) in the previous water matrices, also do so in this case. Conversely, all others present a survival over the five days, with untreated and 30-min treated samples passing directly to a growth phase, and the curves from 60-120 min present an increasing lag over the accumulated dose, and then a growth phase.

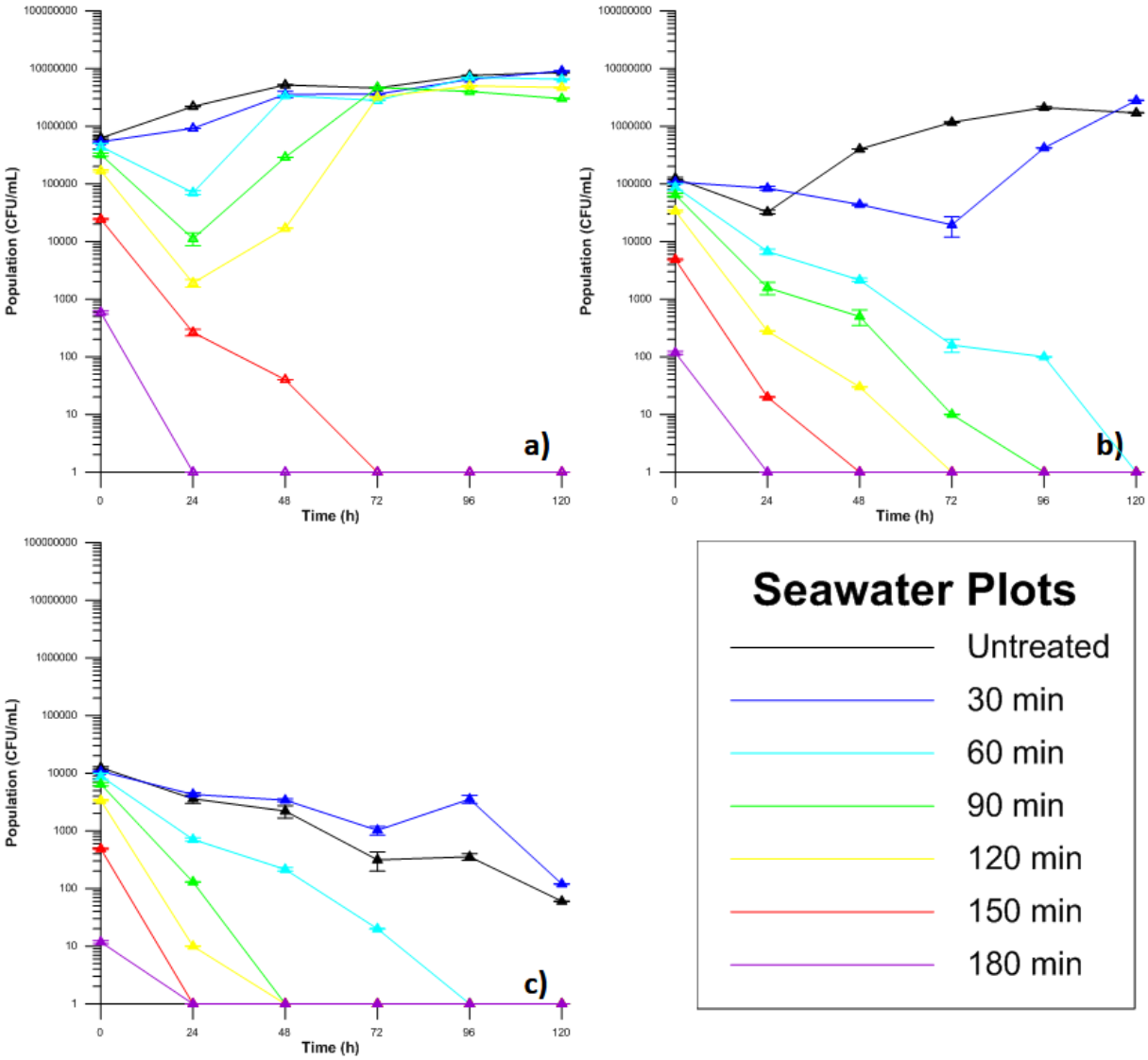

Figure 4.3.3: Overview of the 5-day monitoring period of the irradiated sample diluted in synthetic seawater. (a) 50% dilution. (b) 10% dilution. (c) 1% dilution.

Further dilution of the treated samples reveals steady survival kinetics for 0, 30 and 60-min treatment, and decay for all other curves. In Figure 4.3.4b, initial population is decreased 5-fold and alongside, nutrients are becoming scarce. The kinetics have definitely been modified, and the loss of the osmotic balance is affecting all survival curves. The response is similar to the other water matrices, when bacteria were subjected to combined stress by environmental change and injury due to sunlight.

Even more, in Figure 4.3.4c another 10-fold decrease in wastewater content is inflicted. The most optimistic estimation is a prolonged decay phase; no growth is observed in any sample. Also, the increase of stress conditions has shortened the survival times significantly. A decrease of 24 h has been observed in all cases, while the untreated, 30-min and 60-min treated samples seem to be adapting better in this environment than the heavily injured cells.

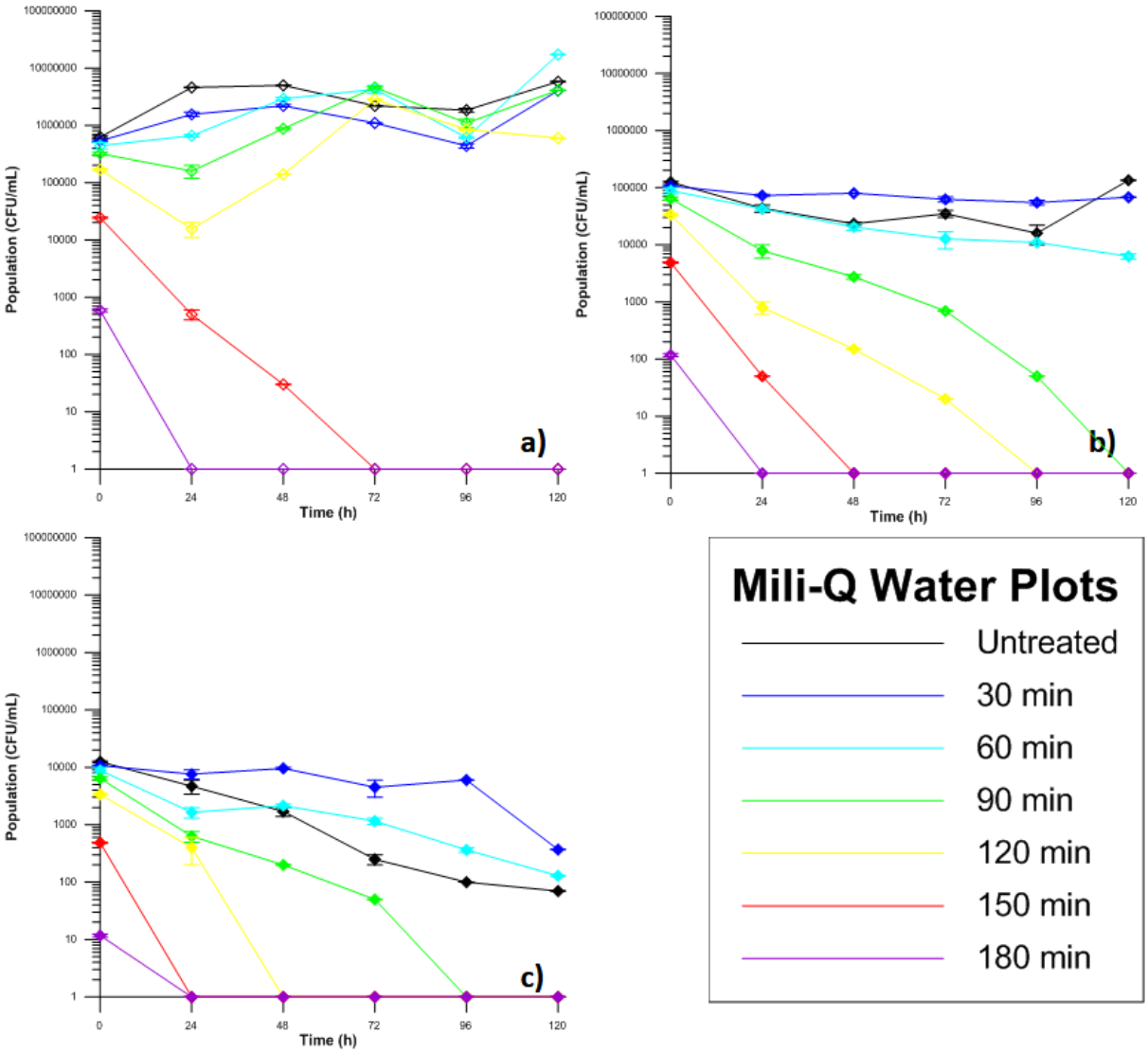

Figure 4.3.4: Overview of the 5-day monitoring period of the irradiated sample diluted in Mili-Q water. (a) 50% dilution. (b) 10% dilution. (c) 1% dilution.

4.4. Bacterial response to environmental changes

In a system designed to disinfect effluent by solar light, according to the availability of sunlight and the climatic constraints, the temperatures that can be approached do not normally exceed 40˚C in tropical regions (FAO, 1987) and normally, 4˚C as representative in near-freezing values. Having analyzed the temperature influence as an environmental factor, the prolongation of bacterial survival due to reduced metabolic activities is noticed, and therefore longer lifespan. Moreover, the risks of overgrown bacterial numbers due to optimal growth conditions are visible. Also, having stressed the bacteria in different light doses prior to the exposure to a variety of temperatures, one can estimate the essential exposure times to achieve a state of permanent bacterial damage, instead of the classic approach of total disinfection times. It appears that taking into consideration the dose along with temperature could lead to more accurate design estimations of the minimum treatment conditions. In that sense, apart from the studies on retention time for disinfection, studies on the temperature variations must be conducted in order to avoid miscalculation of the final bacterial numbers.

An interesting result of this research, considers the various stresses applied to the bacteria in "chronological" order. There have been reports of altered bacterial responses in various stresses, such as Mezrioui et al. (1995), which observed different survival modes when bacteria left stabilization ponds. High survival activity in ponds was followed by low resistance in brackish water and vice versa. In the majority of the experiments and almost in all dilution rates, the samples that were treated for 30 min result in the highest bacterial numbers in long term, even higher than the untreated samples. This phenomenon is attributed in two different factors. First of all, an explanation has been given by Rincon and Pulgarin (2007b), who attributed such effects to photoactivated bacteria. Also, it is given to understand that bacteria which have the initial illumination period, are more resistant to the other stresses that follow irradiation, namely dilution and starvation. Trousselier et al. (1998) have explained this paradoxical phenomenon with the action mode of the RpoS gene (RNA polymerase, sigma S), which is responsible for activating several anti-stress responses, such as osmo-protection, even if stresses are a result of different causes. The authors highlight that initially pre-stressed bacteria are more likely to survive potential following stresses. This behavior could influence the design of solar treatment systems, so as bacteria to receive only the necessary dose (as defined in the previous paragraph) before they are introduced in the receiving water bodies.

Considering the applied dose, Table 4.4.1 summarizes its effects on bacterial survival as a function of the dilution rate and receiving medium. In the rows, the kinetic curves that reflect a recovery in the cultivability of bacteria are shown, in relation with dilution per medium. Literature suggests that the lack of nutrients inflicts the smallest vital changes, in short term. However, when microorganisms have to cope with a combined stress of food source deprivation and, for instance, hyperosmotic adaptation, cells' energy capacities are depleted and membrane transport is limited (Trousselier et al., 1998). The experimental findings are in accordance with the literature, supported by the data in Table 4.4.1. It is also true that sunlight

leads to restriction of cell division due to a loss of cultivability, so the initially inflicted stress leaves bacteria unable to repopulate.

Table 4.4.1. – Summary of kinetic curves presenting post-irradiation growth.

Medium/Dilution ratio	50%	10%	1%
Wastewater	0-150 min	0-150 min	0-120 min
Lake Water	0-120 min	0-90 min	0-30 min
Seawater	0-120 min	0-30 min	-
Mili-Q Water	0-120 min	0-60 min	-
Temperature	**4˚C**	**20˚C**	**37˚C**
Undiluted Wastewater	0 min	0-90 min	0-180 min

Nevertheless, the loss of the ability to be cultivated, even in non-selective media, is a questionable method to judge whether cell division can take place (Trousselier et al., 1998), knowing that cultivability can be lost first by other alterations in cell physiology (Roth et al., 1988; Genthner et al., 1990). It is deducted from these experiments that samples with theoretically active and cultivable bacteria find it difficult to survive in hostile environments, such as high dilution in lake or seawater. It is concluded that cells do not lose their cultivability before 150 min of exposure in this intensity, being the highest value demonstrating repopulation of the sample. Adaptation is impossible and the energy reserves are devoted to cell integrity maintenance, as stated by Trousselier et al. (1998).

In accordance to temperature alterations, profound differences are also visible, but due to other causes. For instance, at low temperatures, only the untreated bacteria are able to increase in numbers, at 20˚C the ones that received treatment from 0-90 min and in the most favorable temperature, 0 to 180-min treated samples present growth. It has been reviewed lately, that temperature influences bacterial survival (Blaustein et al., 2013). The findings in the same matrix, by the same pre-treatment method and with bacteria bearing equal light-mediated injuries, support the temperature preference of bacteria. In addition, they reveal the positive effects that favorable conditions have on bacterial self-reparation capacities; when bacteria are in osmotic friendly environment, temperature can dominate survival kinetics, causing regrowth instead of simple survival and adaptation to the new conditions.

Certain behavioral patterns were correlated here, as a function of the osmotic difference and the availability of nutrients in the matrix. The order of increasing hostility against bacteria reflected in survival times, is as follows: sea water<Mili-Q water<lake water<wastewater. Wastewater and its dilutions, demonstrate growth in all cases, while the negative osmotic influence of lake water induces prolonged survival, and less growth than wastewater. Sea water, especially in high dilution rates, is an unfriendly matrix and presents a deterministic decay regardless the pre-induced damage. The stressed microorganisms have to deal with

acclimatization (initial shock) issues, which were visible in the kinetic curves and the initial stress. This shock can modify the adaptation capacities. Findings like these, have influenced propositions of introducing wastewater in deep outfalls into the sea with little treatment (Yang et al., 2000). Finally, lake water and Mili-Q water as receiving media demonstrated mitigated hostile effects, when they received wastewater diluted in high rates, compared to seawater. This behavior could influence outfall designs especially in lake shores, and stricter pre-treatment rules should be applied in these cases. It is known that bacteria enter aquatic systems in dormant states (Roszak and Colwell, 1987) and are lead to non-cultivable phases. The results are in agreement with literature. However, it was shown that cultivability is not exclusively a function of dose, neither of dilution nor the medium alone. Temperature has also significant influence, because metabolic dormancy (Avery et al., 2008) can easily be disrupted and result to bacterial repopulation and prolonged survival in such waters (Haller et al., 2009a).

4.5. Photoreactivation experiments

This section presents and discusses the results of photoreactivation experiments on previously solar-irradiated synthetic secondary effluent samples. The experimental design and conditions are given in the general 4.1 section and the specific details, concerning photoreactivating lights are given in subchapters 4.1.2 and 4.1.3.

4.5.1. Blacklight blue and actinic blacklight effects

Figure 4.5.1 presents the results of the post illumination exposure of the bacterial samples to blacklight (BL) blue and actinic blacklight wavelengths. The Figures 4.5.1-i to 4.5.1-iv demonstrate the hourly change of bacterial kinetics, after none until up to 3-h exposure to solar light, respectively. Sampling was made semi-hourly; for reasons of clarity the events are presented in 4 distinct phases of solar treatment, such as untreated (0 h), mildly treated (1-2 h) and heavily damaged (3 h of exposure In the case of 4-h exposure to solar light, total disinfection was reached (zero bacterial counts), and zero counts were observed too through the photoreactivation experiments. So, these results are not shown. The difference between the two lamps lies in the wavelength distribution: in the actinic BL lamp, there is an extra narrow wavelength emitted, not present in the BL blue one, which falls closer to the far end of UV that causes ROS production and peripheral damage to the cell.

Figure 4.5.1a presents the effect 2, 4 or 8 h of exposure to BL blue and actinic BL have on bacterial survival, on previously untreated sample. The samples untreated and not submitted to PHR light (dark control) show a slight growth (in logarithmic terms), nearly doubling its population in 8 hours. Free of solar-light damage and kept in the dark, unharmed and in a favorable medium, the bacteria should keep growing, as it is observed. 2 h of exposure in the BL lamps do not modify greatly the bacterial population and have a rather mild inactivating effect 24 and 48 h after the treatment, in dark storage. This effect is enhanced by 4-h exposure time; there is a slight inactivation presented directly and a significant 90% decrease of the bacterial numbers in long term. However, 8 h of exposure under the same lights directly impacts bacterial viability. The employed wavelengths fall into the UV region, damaging the cell constituents, with the low intensity being the limiting step; 2 or 4 hours of illumination are not enough to impact directly the population. The cells are damaged by the energy accumulated in 8 hours.

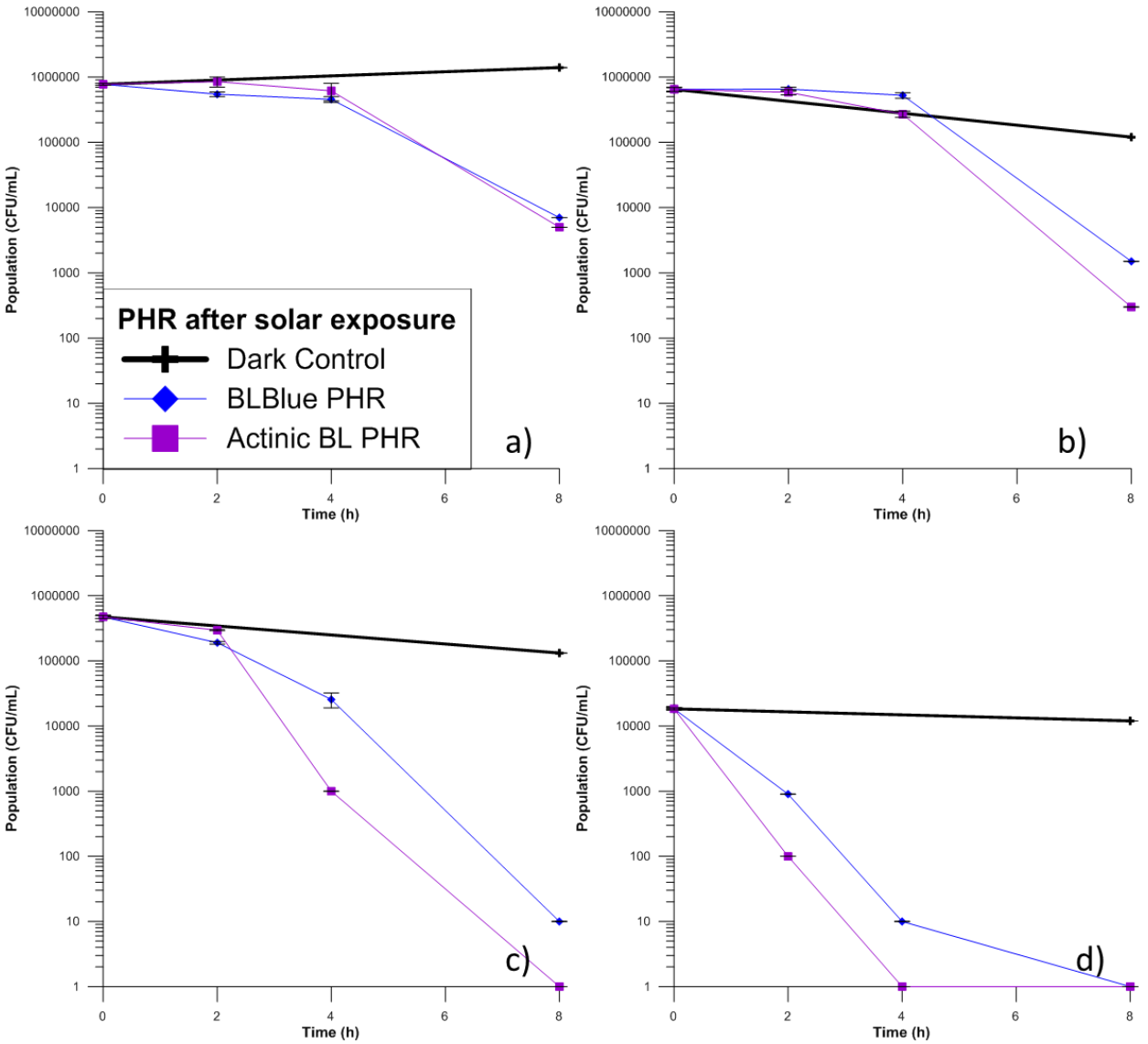

Figure 4.5.1: Results of the exposure of wastewater in PHR lamps: BL Blue and Actinic BL. a) PHR without solar pre-treatment. b) PHR after 1 h solar pre-treatment. c) PHR after 2 h solar pre-treatment. d) PHR after 3 h solar pre-treatment.

Pre-illumination of the samples before their exposure to BL blue and actinic BL light, greatly modifies the survival kinetics. There are two aspects that are modified, compared to the untreated samples, one being the greater susceptibility to direct damage and the second, the inability to sustain viable counts for longer times. Figure 4.5.1b to 4.5.1d show that increasing pre-treatment times of solar illumination renders the same BL blue and actinic BL doses more effective. From the nearly invisible effect in untreated samples of Figure 4.5.1a, to the lethal doses of 4 and 8 h (for actinic and blue, respectively) in Figure 4.5.1d. In all cases, the effect of BL blue light was lower than the respective actinic BL ones. As far as the disinfection kinetics are concerned, samples that remained more time under the solar light, when transferred under the blacklight, their kinetics differed significantly. In Figure 4.5.1a, until the beginning of the dark storage, the disinfection kinetics were similar, while in 4.5.1d the respective kinetic curves are significantly different. However, Oguma et al. (2002) took notice in their work that UVA has been long known to photoreactivate

cells, due to a process called non-concomitant reactivation (Jagger, 1981), which doesn't corroborate with these findings, indicating the multiple attack of solar light against the bacteria, and not limited to CPD formation.

4.5.2. Blue and green light effects

The second experimental part involves subjecting the pre-illuminated samples to exposure under blue or green light. Figure 4.5.2 demonstrates the inflicted changes these monochromatic wavelengths have on bacterial viability. More specifically, in Figure 4.5.2a the untreated sample is subjected, to illumination by the monochromatic lights (for 2, 4 and 8 h). In both cases the light effect is not detrimental to the bacterial survival, and only slightly reduces the counts of the samples under blue light. Also, dose has an important effect on the survival kinetics, for the changes observed before are demonstrated only after high periods of exposure to the light.

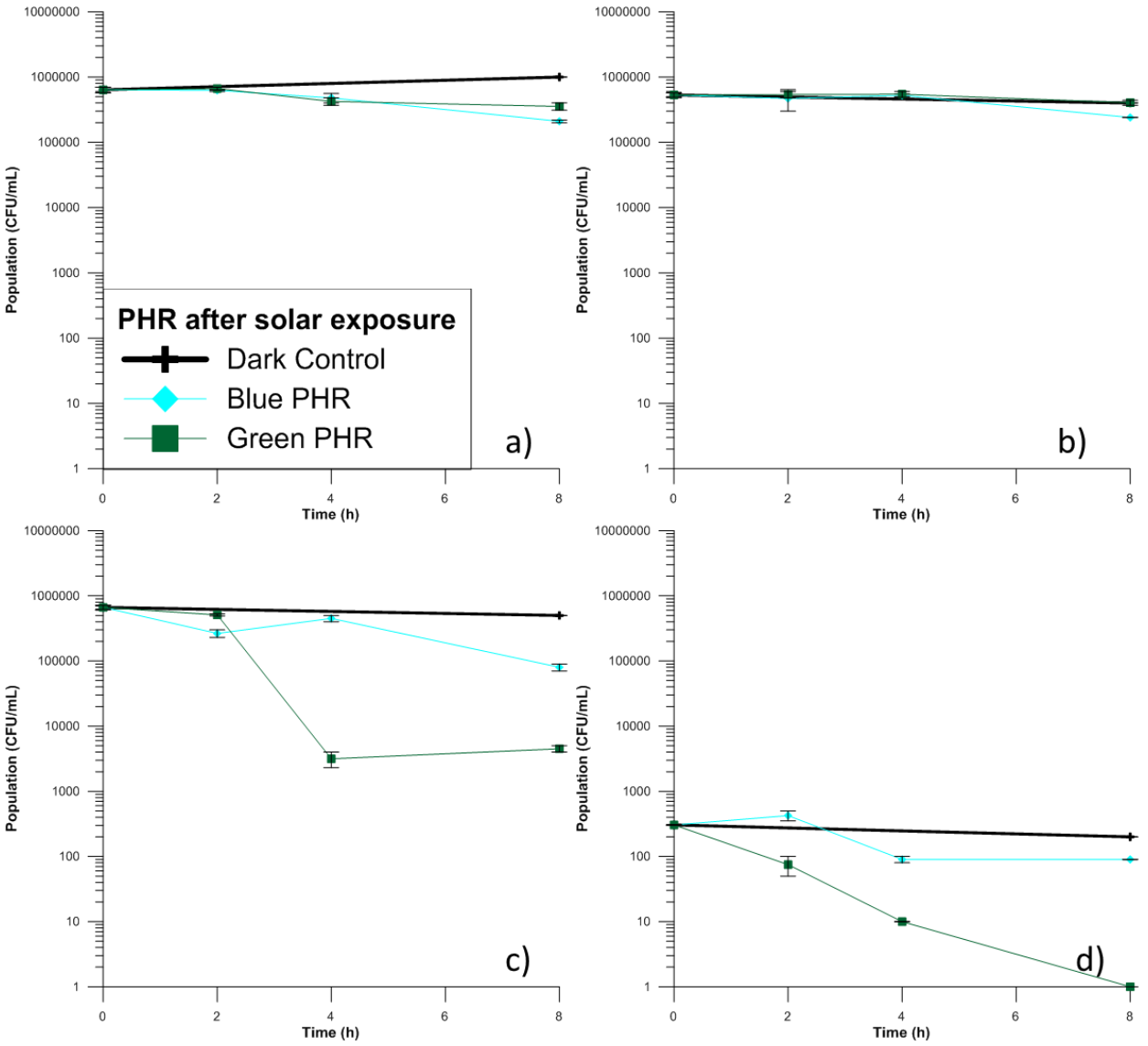

Figure 4.5.2: Results of the exposure of wastewater in PHR lamps: Blue and Green light. a) PHR without solar pre-treatment. b) PHR after 1 h solar pre-treatment. c) PHR after 2 h solar pre-treatment. d) PHR after 3 h solar pre-treatment.

Similarly, lightly treated samples (1 h of pre-exposure to solar light) do not alter their survival kinetics in great extents, as seen in Figure 4.5.2b. In this case, the solar pre-treatment for 1 h modified the kinetics of the blank experiments, and shifted their behavior from growth to survival. However, 2, 4 or 8 h of exposure to blue or green light do not influence greatly bacterial viability in short term. On the contrary, 2 h of blue or green light result in higher cell counts than the sample not subjected to the monochromatic light; the beneficial photoreactivating effect is observed, the healing process of the solar inflicted damages in the cell.

Two hours of solar pre-illumination demonstrate different kinetics, when they are followed by exposure to monochromatic blue or green light. The dark controls are able to survive, while the first impacts of accumulated damage start to be demonstrated. Blue light in low doses maintains survival but results in noticeable reduction in high doses, whereas green light is detrimental to these samples, stabilizing its effect in high doses. After 4 h, no significant change is observed in the bacterial counts.

Figure 4.5.2c presents once more the negligible effect of 2-h exposure under monochromatic blue or green light, but 4 h differ significantly. Although blue light does not affect the bacterial viability, green light seems to reduce the counts up to 3 logarithmic units ($log_{10}U$). In long term, the effects are reversed. Further irradiation does not inflict more damage for the green light, but enhances inactivation for the blue light.

Finally, severely damaged cells from solar light demonstrate (Figure 4.5.2d) the most definite alterations in their kinetics among the two colored lamps. Blue light is identified as less inactivating than the green one, and even causes increase of the population in low doses (2 h of exposure). This is in agreement with the photolyase activation spectrum, but increasing the dose of PHR light has little effect on the bacteria exposed in blue light. On the contrary, green light after 8 h results in total inactivation of more than 2 $log_{10}U$ of bacteria that remained after 3 hours of solar pretreatment.

4.5.3. (Monochromatic) yellow and visible light lamps' effects

The last experimental part involves the exposure of the pre-illuminated bacterial samples under lamps emitting yellow light and visible light (fluorescent) lamps. Since the two experiments took place in different batches, both control experiments will be presented for reference. Figure 4 demonstrates the main results of the investigation. Figure 4.5.3 demonstrates the main results of the investigation. In Figure 4.5.3a, the effects low intensity yellow and visible light has on non-illuminated bacteria are shown. First of all, there is growth in the dark, similarly to the other two experimental parts. The application of yellow light has no immediate effect; the kinetic curves of 2, 4 or 8-h exposure are very similar, as well as very close to the original, non-irradiated samples. Healthy cells are not affected by the wavelength emitted by the monochromatic lamps, regardless of dose. The kinetics of the bacteria under visible light are close to identical with those under the yellow light ones, being the closest approximation to each other's wavelengths.

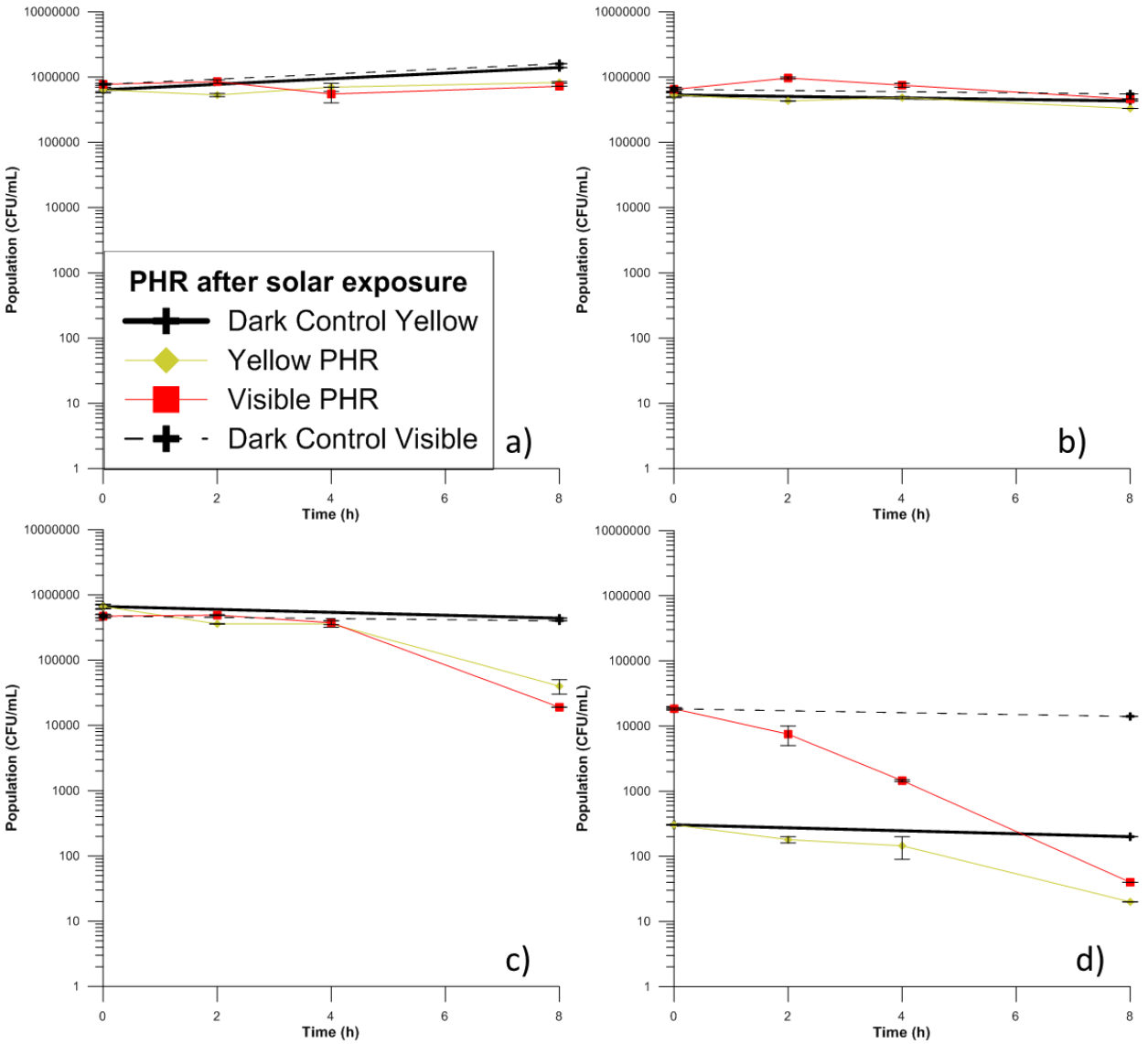

Figure 4.5.3: Results of the exposure of wastewater in PHR lamps: Yellow and Visible light. a) PHR without solar pre-treatment. b) PHR after 1 h solar pre-treatment. c) PHR after 2 h solar pre-treatment. d) PHR after 3 h solar pre-treatment.

Pre-illuminating the samples for 1 h has almost no effect (Figure 4.5.3b), when followed by exposure in low yellow light doses. On the other hand, visible light in low doses seems to favor bacterial recovery, causing increase of the population after 2-h exposure. These results are different in Figure 4.5.3c, which demonstrates the kinetics after 2 h of solar illumination and exposure to yellow and visible light. The main difference is observed in the bacterial response in high yellow and visible light doses, by prolonging their stay in these conditions; extended illumination time has greater impact on previously more stressed bacterial cells (8-h kinetic curves) and the probability of photoreactivation is reducing significantly. There are few cases only, mainly in yellow light, which bacteria managed to maintain their viability in the previous levels.

Finally, the response of bacteria that are determined to decay in the dark after some time (Figure 4.5.3d, 3-h treatment), yellow light or visible spectrum irradiation cannot change the outcome. In both batches, the already weakened bacteria cannot demonstrate photoreactivation, neither short nor long term. The

inactivation kinetics continue and their effects are immediate. Pre-stressed bacteria close to full disruption of the living functions seem to be incapable of full inactivation by neither yellow nor visible light.

4.6. Photoreactivation and the subsequent bacterial survival

4.6.1. Post-irradiation dark repair assessment – control experiments

Figure 4.6.1 presents the disinfection kinetics, when wastewater samples are exposed to 1000 W/m^2 global irradiation. After an initial shoulder (Sinton et al., 1999; Berney et al., 2006; Giannakis et al., 2013) which presents mild fluctuations due to promoted growth in the supporting matrix, the population is decreasing log-linearly, with 99.99% inactivation reached in 3.5 h and total inactivation in 4 h.

Each regrowth/survival curve does not represent the same post-irradiation behavior. The untreated samples present growth directly, the 30 to 90-min irradiated samples fall between growth and preservation in numbers, and after that point, the kinetics describe a decay. The growth of the untreated sample is normally expected, but the slightly treated samples (30 min) present an increase, which is supported by the dark repair mechanisms that are enzymatically correcting the DNA lesions (Sinha and Hader, 2002), or the respiratory chain ROS scavengers, such as catalase (Bosshard et al., 2010a), that suppress the potential indirect damage. As the receiving dose is increasing, the capability of the cells to self-heal their photoinduced damage is declining. After the transition of 30-120 min of treatment, a definite damage has caused decay. The cells have initiated programmed cell death (PCD) by the accumulation of photoproducts (Rincon and Pulgarin, 2004c).

4.6.2. Modification of dark repair kinetics due to pre-illumination conditions: BL blue and actinic BL lamps

In Figure 4.6.2 the alteration of post-irradiation bacterial kinetics in the dark is presented, according to the degree of pre-treatment with solar light. Figures 4.6.2a-d present the effects of 0, 1, 2 or 3 h illumination prior to exposure to monochromatic BL blue or actinic BL. The application of low intensity monochromatic light strongly modifies the normal regrowth potential of microorganisms.

Firstly, the exposure to low doses of BL blue or actinic BL was found to marginally reduce the bacterial cells, until the application of an 8-h equivalent light dose, which inflicts a 3 $\log_{10}$U reduction of the population. However, after 24 h hours from stopping the illumination, the remaining population is nearly equal, for 2-h and 4-h. The only difference is presented in long term, where the 8-h irradiated samples under BL blue maintain partly their viability while the actinic BL ones demonstrate total inactivation. This difference is attributed to the emission of the extra wavelength band in the actinic lamp. The wavelengths closer to the UVB region mostly cause DNA damage, and nucleotide excision repair would be responsible for its recovery. In the present case, the effects are cumulative and according to the degree of pretreatment, a corresponding difficulty to repair the damage is observed.

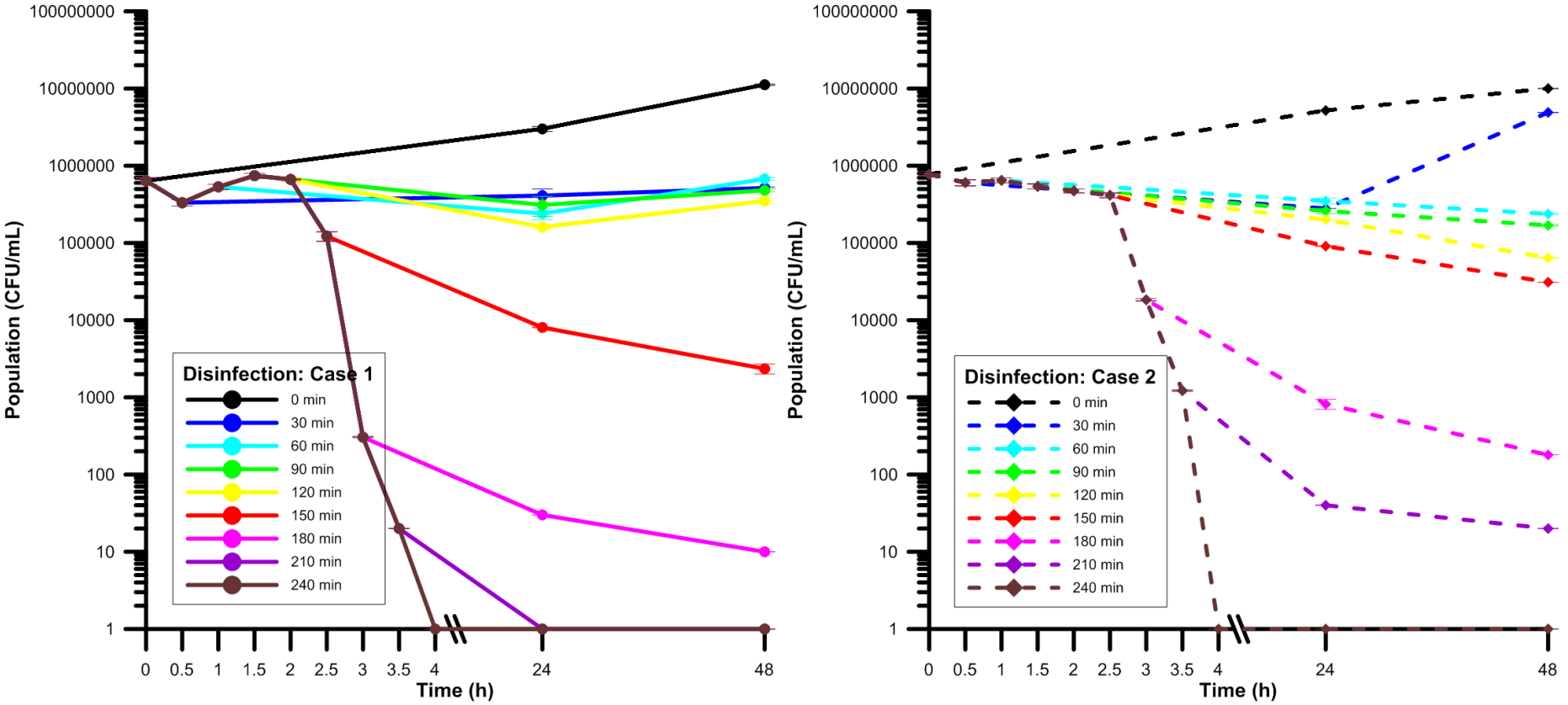

Figure 4.6.1: Blank experiments. Results of the 48-h long dark storage of solar treated wastewater. a) Case 1. b) Case 2.

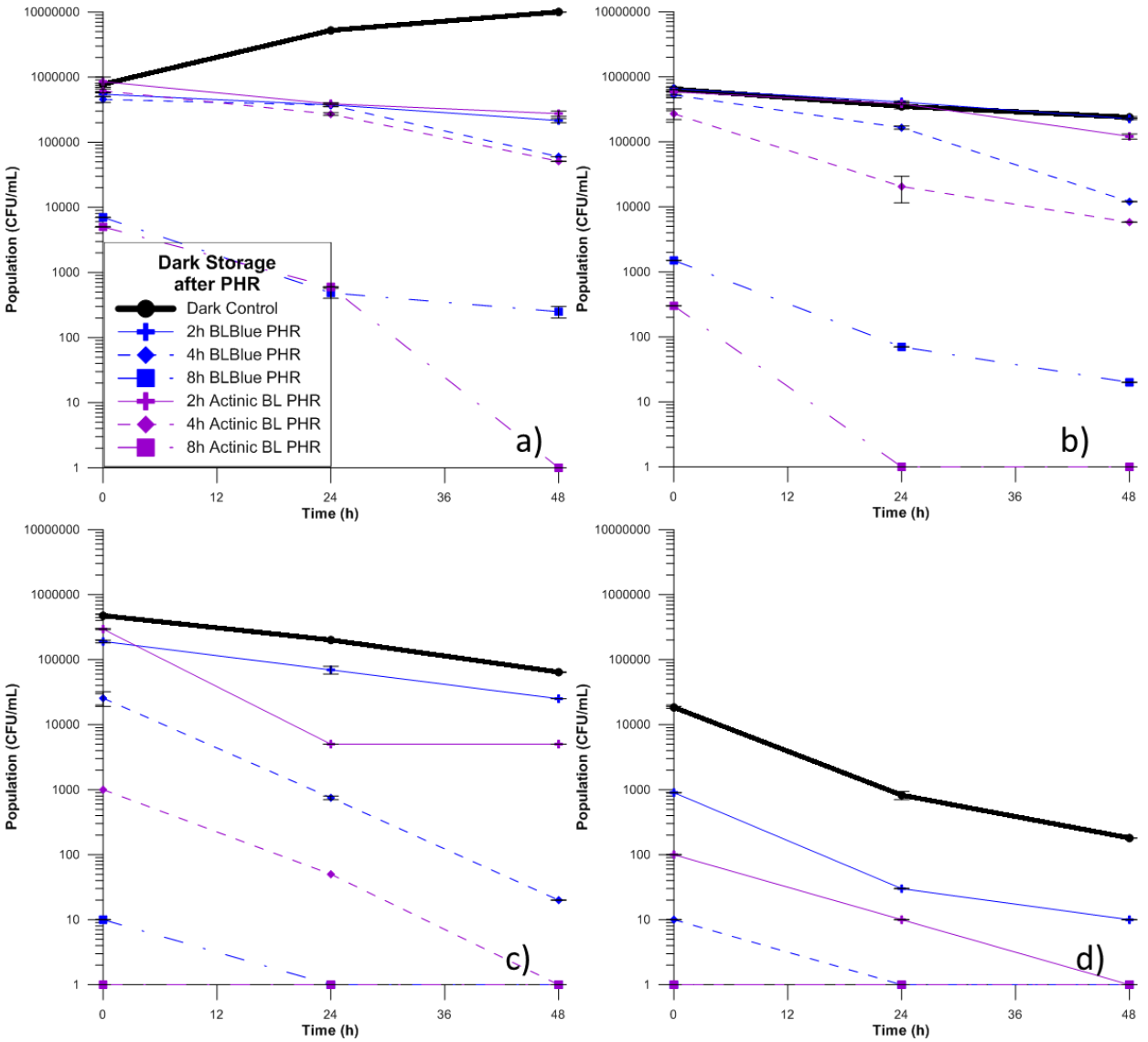

Figure 4.6.2: Results of the 48-h long dark storage after 0, 2, 4 and 8 h of PHR with BL Blue and Actinic BL light. a) DR without solar pre-treatment. b) DR after 1 h solar pre-treatment. c) DR after 2 h solar pre-treatment. d) DR after 3 h solar pre-treatment.

Finally, as far the long term dark storage is concerned, the untreated samples presented growth. This ability is disrupted after 1-2 h of solar exposure and diminished after 3 h. The application of the blacklight lamps after the solar light exposure, never favored regrowth (photoreactivation) or survival of the microorganisms, but on the contrary enhanced the continuing inactivating profile inflicted by solar light. This behavior was also enhanced as the blacklight exposure times were increased; high doses apply more acute decreases during dark storage times than low ones, and in all cases, actinic BL inflicted more acute inactivation than the respective BL blue light doses. These facts lead to the conclusion that the extent of damages by solar illumination modifies, or predetermines a more vulnerable and non-recurring profile of kinetics, when followed by these two specific wavelengths applied.

4.6.3. Modification of dark repair kinetics due to pre-illumination conditions: Blue and green light

Figure 4.6.3 summarizes the effects of 2, 4 or 8-h long exposure of the previously solar treated samples to blue and green light. Starting from the healthy cells of untreated samples, the infliction of blue and green light in all the used doses, has similar effect in bacterial kinetics. The initial population of this observation stage (population after the PHR light) is very close to the initial samples. The untreated bacteria are able to continue reproducing in the dark and increase their numbers over 48 h. In contrast, even 2 h of exposure under monochromatic light is enough to disrupt the normal reproductive rates, and lead to slightly decreased population after 48 h. However, increasing the exposure times has almost no effect; the resulting numbers are very similar. This is an indication of the action of light on bacterial rates, which either does not accumulate or gets mitigated by self-defense mechanisms of the cell.

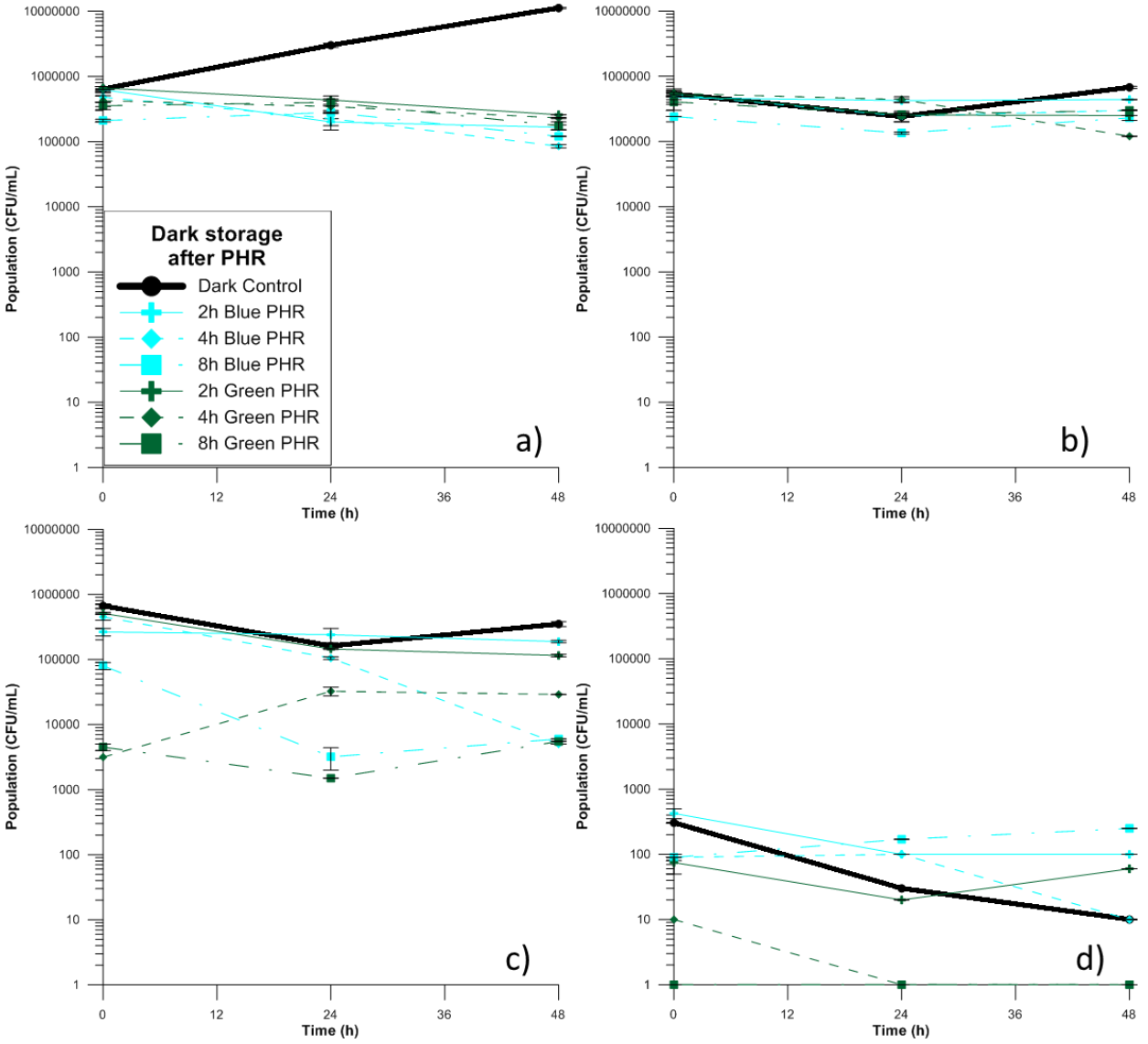

Figure 4.6.3: Results of the 48-h long dark storage after 0, 2, 4 and 8 h of PHR with Blue and Green light. a) DR without solar pre-treatment. b) DR after 1 h solar pre-treatment. c) DR after 2 h solar pre-treatment. d) DR after 3 h solar pre-treatment.

The samples that have been illuminated for 1 h prior to photoreactivation (Figure 4.6.3b) can recover their damage and demonstrate regrowth. However, all samples that have been exposed to the monochromatic blue and green lamps are no longer able to express regrowth. In long term, the control sample results in higher population than the other phototreatment pathways. When 2 hours of treatment were followed by PHR light, the effects differed significantly than the corresponding 1-h treatment. In 24 and 48 h, there is noticeable regrowth (Figure 4.6.3c) in the samples that were exposed to green light, which indicates the non-detrimental effect of the photoreactivating light. However, the final population has reached its minimum and after 48 h the bacterial counts are similar, for the same dose of PHR light. This indicates that the exposure to these wavelengths has not diminished their replicating ability completely.

Finally, Figure 4.6.3d demonstrated the effects of the sequence 3-h solar light, and different PHR light and dose. Compared with the bacterial samples that did not go through monochromatic blue light exposure, the resulting numbers were higher in all cases, and very close to the population before blue light. It seems that the cells are benefited more than harmed from this wavelength. On the contrary, only mild (2-h) exposure to green light seems to have a beneficial long term effect; all other doses inflict total inactivation in 24 h (4-h green light dose) or directly (8-h green light dose). In the case of total inactivation due to green light, there is no regrowth observed in the dark, similarly to the case of the efforts to photoreactivate totally inactivated bacteria, after 4 h of solar illumination.

4.6.4. Modification of dark repair kinetics due to pre-illumination conditions: (Monochromatic) Yellow and visible light

Figure 4.6.4 summarizes the results of long term storage of previously illuminated samples by solar light, followed by yellow or visible light. In untreated samples (subfigure a) the dark control samples demonstrate the normal growth kinetics, as well as the samples that went through exposure to PHR light. Growth was suppressed compared to the dark control, but in 48 h hours the final population is almost the same. Visible light has more or less the same effect but i) the recovery in 2 days is higher than the one demonstrated in yellow lamps and ii) closer to the untreated samples, when exposure was prolonged.

Application of 1 h solar stress followed by PHR yellow or visible light allows very few combinations of photorecovery of the populations; in Figure 4.6.4b only small doses of visible light are able to increase the bacterial counts. Another difference in high doses is the relative evolution through the 48 h; when the sample was exposed for 8 h under yellow light, a temporary decrease was observed, followed by recovery of the numbers in long term. The kinetics are shifted only after the dark storage of 2-h damaged samples. All kinetics are declining in long term (Figure 4.6.4c). In short term, visible light doses leave bacteria slightly stressed, but the tendency after 48 h in the dark reveals a minor decrease in the total number of cultivable cells. Compared to the untreated cells (only 1-h of solar illumination), the tendency of dark repair is changed.

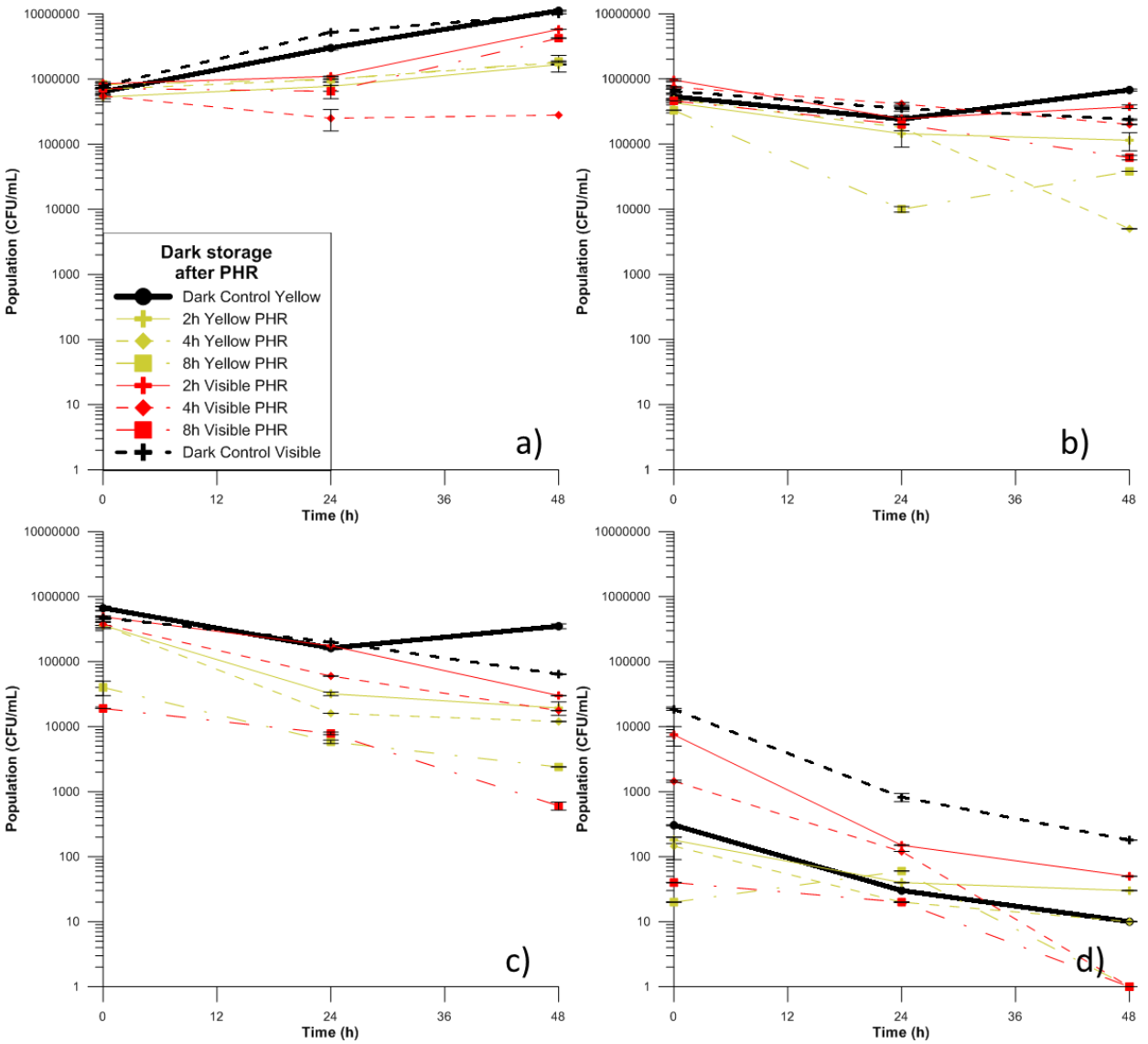

Figure 4.6.4: Results of the 48-h long dark storage after 0, 2, 4 and 8 h of PHR with Yellow and Visible light. a) DR without solar pre-treatment. b) DR after 1 h solar pre-treatment. c) DR after 2 h solar pre-treatment. d) DR after 3 h solar pre-treatment.

Finally, heavily damaged bacteria are unable to perform dark repair after their exposure to any dose of yellow or visible light. Figure 4.6.4d reveals the impact of these wavelengths in long term survival in the dark. In fact, under high doses of visible light exposure, even low intensity one, after 48 h of storage there are no longer cultivable bacteria. Also, in both cases the kinetic curves all fall below the dark control experiments. In the specific case of yellow light, the difference is only a bit less, with the curves being closely related to the dark control.

4.7. Quantitative and qualitative assessment of bacterial photoreactivation

4.7.1. PHR light exposure and modeling of the bacterial response

The analysis of the experimental part has revealed a trend over the response of previously phototreated samples, when exposed to monochromatic or visible light. In overall, for the analyzed solar doses and the subsequent PHR ones, the populations tended to decrease, with some exceptions. At this point, it is important to interpret the bacterial response under the prism of a general response to the stress applied and the risks of PHR demonstration due to these actions.

In order to estimate the amount of PHR induced and relationship between the doses, the different phases of the bacterial population are divided into C_0, C_{24} and C_{48}, being the population after solar exposure and PHR light, plus 24 and 48 h of dark storage, respectively. For this analysis, all data were used (semi-hourly measurements) without separating the data according to the color of the PHR lamps. The total of 216 tests were evaluated to point out the statistical significance of the findings.

The first step was the Pearson test, which reveals the correlation between the parameters under investigation: i) exposure to solar light, ii) exposure to PHR light (dose), iii) $\log C_0$, iv) $\log C_{24}$ and v) $\log C_{48}$. The results were obtained through analysis by MINITAB 16 for Windows and are summarized in Table 4.7.1. The independent variables (exposure to solar or PHR light) have no correlation, while solar exposure significantly affects the outcome in short ($\log C_0$) or long term, having absolute values higher than 0.8. The negative sign indicates the negative influence of solar light against bacterial survival. Furthermore, the PHR dose is shown as negative but with insignificant correlation. this result is influenced both by the majority of the cases which present further reduction of the bacterial numbers by the PHR light, as well as by the existence of cases of growth; actual PHR modifies the statistical result to “light negative correlation” between PHR dose and survival. However, the most important influence is derived through the remaining bacterial populations at the end of each stage (solar and PHR exposure, 1-day dark storage), with the Pearson values being greater than 0.8, plus indicating the positive influence of the remaining bacteria in their survival, from one day to another.

Table 4.7.1. – Pearson Correlation and null hypothesis values.

	Solar Dose	PHR Dose	$logC_0$	$logC_{24}$	Cell Contents
PHR dose	0				*Pearson correlation*
	1				*P-Value*
$logC_0$	-0.823	-0.278			
	0	0			
$logC_{24}$	-0.848	-0.259	0.961		
	0	0	0		
$logC_{48}$	-0.827	-0.29	0.923	0.972	
	0	0	0	0	

The outcome of the whole sequence can be expressed as a general linear model, with independent variables the solar and PHR light doses and the effects summarized in $logC_0$, $logC_{24}$ and $logC_{48}$, as before. Regression analysis provided three models for the three cases of short or long term survival. The Gauss-Newton algorithm was used for the acquisition of the parameters (max iterations=200, tolerance 0.00001).

$$logC_0 = Initial\ population - 0.00107 * Solar\ Dose - 0.00108 * PHR\ Dose$$

$$logC_{24} = Initial\ population - 0.00124 * Solar\ Dose - 0.00134 * PHR\ Dose$$

$$logC_{48} = Initial\ population - 0.00127 * Solar\ Dose - 0.00179 * PHR\ Dose$$

Where initial population is in CFU/mL, and solar and PHR dose are in W/m^2.

Finally, the acquired models were tested to estimate the goodness of their fit to the experimental data. Figure 4.7.1 presents an overview of the fit of theoretical (modeled) values to the existing measurements. The fits of $logC_0$, $logC_{24}$ and $logC_{48}$ are presented in Figures 4.7.1a, 4.7.1b and 4.7.1c respectively. The assessment indicates the good fit of the models, (R^2: 72-77%) with details on the residual errors and R^2 values being summarized in Table 4.7.2. The weakness of the models is located in the acute and probably non-linear accumulation of damage from hour 4 to hour 8, during the exposure to photoreactivating light. However, the models fit adequately and non-selectively for the 6 types of lamps used in this study.

4.7.2. Correlation between bacterial response and the applied PHR light wavelength

Although the lamps used in this study cover a significant part of the wavelengths of the solar spectrum that reaches Earth's surface, the action modes of each light cannot be attributed to a single wavelength. Fluorescent lamps emit a relatively broad spectrum, whose peak corresponds to the final output, the selected color. For this reason, in this part the different lamp colors are correlated with their effect.

Table 4.7.2. – Models evaluation and goodness of fit.

$LogC_0$		$LogC_{24}$		$LogC_{48}$	
RSE	0.7238	**RSE**	0.7789	**RSE**	0.8265
R^2	0.7369	**R^2**	0.774	**R^2**	0.7588
R^2-(adj)	0.7356	**R^2-(adj)**	0.773	**R^2-(adj)**	0.7577
F	599.2	**F**	733	**F**	673.3
p-value	< 2.2e-16	**p-value**	< 2.2e-16	**p-value**	< 2.2e-16

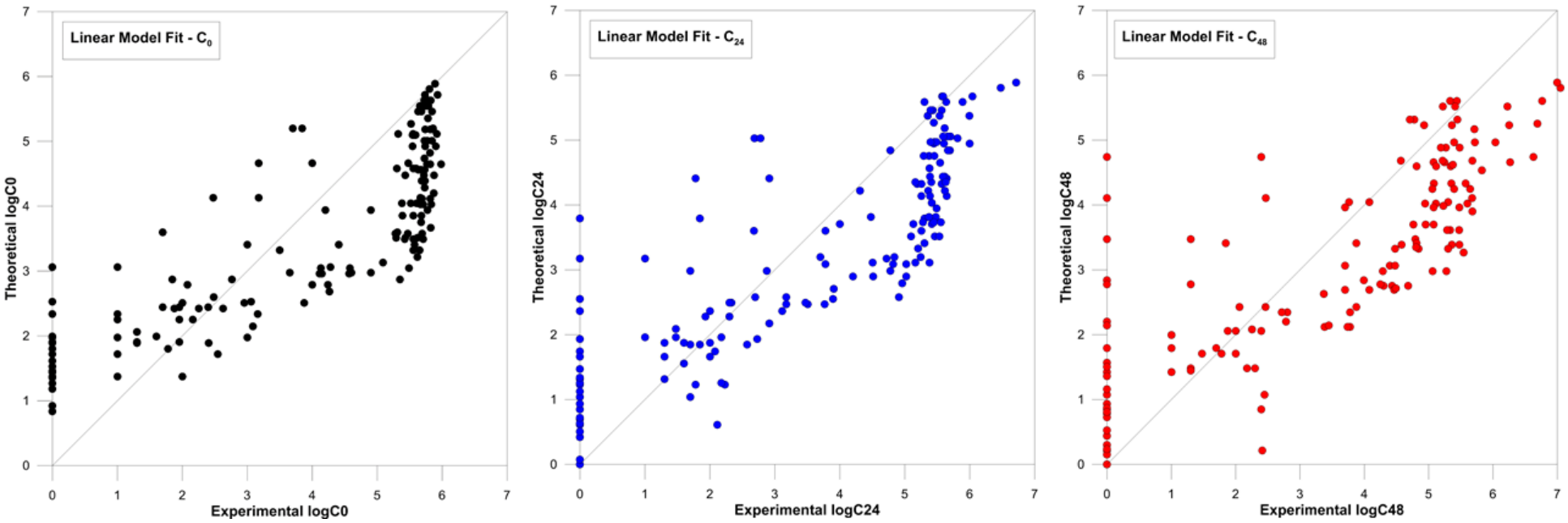

Figure 4.7.1: Goodness of fit: Experimental vs. Theoretical (Model) data. i) C_0. ii) C_{24}. iii) C_{48}.

Figure 4.7.2 presents an overview of all the experiments presented in the results section. In the vertical axis the wavelengths are presented (exception: visible light comprises a variety of wavelengths), while on the horizontal axis is the time of exposure to solar light. For each color, firstly the exposure time to PHR light is noted, followed by the 24 and 48 h of dark storage. The indicated red stages are the ones resulting in populations lower than the previous state, while green indicates higher numbers.

As far as the wavelengths are concerned, the BL blue and the actinic BL lamps never present photoreactivation (exception: 2h of exposure to actinic BL). This is due to the continuous UV action to the cells, regardless of their previous state of damage. The low PHR rate in the 2-h actinic light dose is due to the extra wavelength in the far UV region. Blue and green lamps present the most cases of PHR, especially in lightly damaged cells. In addition, blue is the only color that demonstrates (long term) PHR in heavily damaged cells (3-h exposure to solar light). This result agrees with the findings of Kumar et al. (2003) for the correlation between blue light and the UVB-induced damages. Yellow light presents long term effects of bacterial increase, regardless of the PHR dose in unharmed cells, but has no actual PHR effect; it probably causes photoactivation of the dormant cells. Finally, visible light has similar effect to the yellow light, with lower long-term risk of PHR. Nevertheless, it is very important to notice the absence of short or long term reactivation of the cells that were treated for more than 3 hours. There is no PHR observed neither during exposure at monochromatic or visible light, nor in the subsequent dark storage time. In contrast with the UVC action modes, where "total inactivation" is observed, but reversible, solar light has a detrimental effect towards photoreactivation, inhibiting the reappearance of the cells under light or dark conditions.

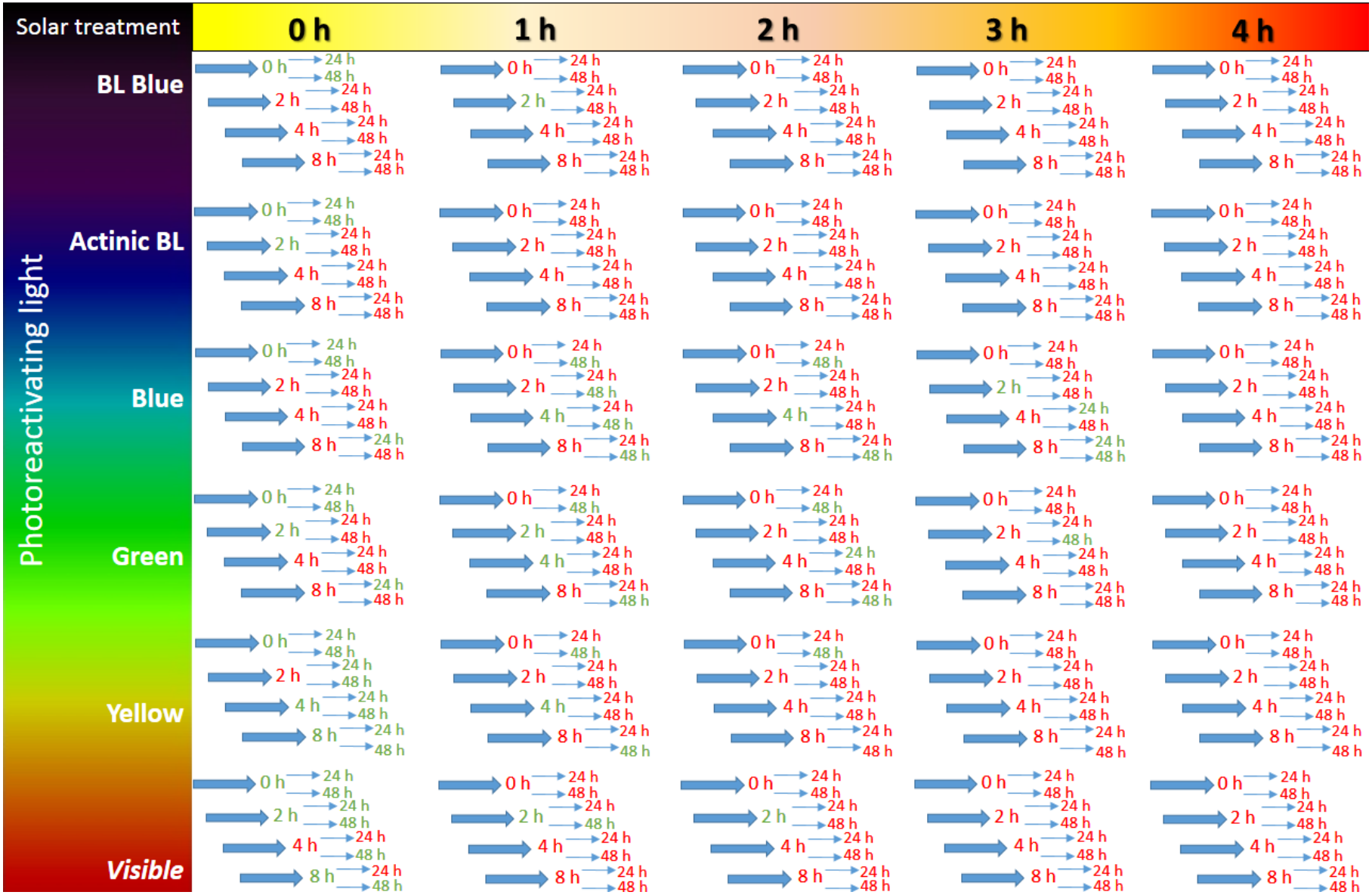

Figure 4.7.2: Overview of the PHR and DR results, grouped per solar pre-treatment dose, PHR dose and dark storage time.

4.8. Conclusions

Modification of the post-treatment matrix dilutionconditions was experimentally examined within two groups, temperature and dilution rate in different mediums. When storage temperature was modified, different responses were observed by the pre-treated bacterial samples. Keeping samples in temperatures as low as 4˚C inhibited growth, but prolonged bacterial survival. This prolongation was slightly correlated with the dose received during simulated solar treatment. Increasing temperature to 20˚C permitted growth in untreated and lightly treated samples, i.e. 30-90 min of solar illumination, and accelerated decay in the rest of the samples. Further increase of temperature to 37°C lead to excess growth for all samples except for the heavily damaged 210 and 240 min treated ones; the observed growth was attributed to the temperature effects, which are combined with the presence of nutrients, to offer bacteria optimal growth conditions.

Dilution in different matrices induced various responses according to the osmotic conditions present at the sample. When treated water was further diluted in wastewater, after a lag phase growth was observed. The delay was a function of the dose during solar pre-treatment. The exact opposite findings of this nutrient-rich medium were found when treated water was introduced in Mili-Q water. Inducing osmotic pressure combined with starvation due to the lack of food source lead to deterministic decay of the samples. Lake water, although osmotically negative, prolonged survivals due to the existence of baro-protective salts. Finally, seawater demonstrated the most hostile behavior against bacteria, which were unable to cope with the difference in osmotic pressure while injured. The survival times were the lowest among the four matrices. Regardless the matrix, a pattern was observed, where bacteria that were treated for short time presented high resistance, when were diluted in unfriendly matrices and high growth rates, when growth was permitted.

The rate of employed dilution investigated various conditions, such as low dilution (50%) up to high rates (1%). Every matrix caused different bacterial response while being diluted. Wastewater dilutions accepted positively the dilution in fresh medium, providing higher proportions of food per cell; thus more comfortable conditions were obtained and in long term lead to the same bacterial numbers, regardless the dilution rate. Dilution in Lake Leman water, in low rates, provided good survival conditions, but as dilution was increased, survival was linked to the negative effect of food deprivation and the injuries from solar treatment. Although seawater is considered a difficult environment for bacterial survival, in low dilution rates survival was prolonged, after a lag phase growth was initiated. When dilution was increased, decay was initiated for almost all samples (except 0-30 min of treatment). In 1% dilution the osmotically-induced decay prevailed, resulting in decay curves for all samples. Control experiments in Mili-Q water verified the correlation between survival and osmolarity; high dilution rate accelerated bacterial decay, even though low rates permitted growth after an initial shock/adaptation phase.

Concerning photoreactivation, the application of 6 different colors of fluorescent lamps on previously solar treated synthetic secondary effluent caused different response, according to the corresponding wavelength. In all cases, however, no regrowth or photoreactivation was observed in totally inactivated bacteria.

More specifically, lamps that emit UV-ranged wavelengths (BL blue and actinic BL), even in very low proportions initiated or accelerated bacterial inactivation, according to the previous damage state of bacteria. The effect was detrimental both in short term, during the 8-h long PHR time, and in long term (permanent effect in 24 and 48 h of dark storage). Blue and green light were the only ones to cause mild photoreactivation. Bacteria in lightly damaged phase and heavily solar wounded bacteria, respectively, demonstrated in some cases immediate recovery. In long term the effects were more visible, with elevated bacterial counts, compared to the non-photoreactivated samples. Yellow light has been found to positively affect growth in non-treated cells, causing photoactivation of the cells. The bacterial pre-exposure to solar light followed by yellow light showed continuation of the inactivation effects. The response to visible light resembled the yellow light one, with beneficial photoactivation in relatively healthy cells.

The bacterial response to photoreactivating lights was well correlated with the solar pre-treatment dose, and linear models were proposed to predict the outcome of low exposure to PHR lights ($R^2 \cong 75\%$). In overall, the risk of photoreactivation is reduced with increased exposure to solar light, regardless of the PHR wavelength and dose. Contrary to the UVC action mode, solar disinfection inflicts damage in various levels and targets, minimizing the regrowth potentials of the treated microorganisms. This regrowth risk could pose a serious threat only in bacteria able to mend the solar-inflicted lesions, even in low photoreactivating light doses.

The observations in synthetic and real matrices at laboratory level, can enable better design of solar treatment systems, since some insight has been given on the bacterial survival in a controlled environment. This work presents some aspects of the complex addressed problem, as an exploration of the boundary conditions. For instance, the sequential shift between light and dark environment can inflict further bacterial inactivation in the recipients, during solar exposure, or their regrowth during the night. There are other crucial matters affecting the survival that need to be taken into account, such as predation by natural indigenous microorganisms or the diversity of light supply during temporal weather changes. However, the simulated conditions provide a good approximation, with respect to the real application. Nevertheless, the philosophy behind the design of solar treatment methods can be implemented with such results that indicate possibilities for reduced retention times, one of the most decisive factors in these systems. Fecal contamination can be reduced and aid in more efficient downstream handling of effluents. In that way, strategies more suitable in the local context can be encouraged, such as safe discharge, controlled irrigation and use of reclaimed water.

Chapter 5. Light intermittence: The effects on disinfection and regrowth, and the complementary effect of ultrasound treatment

5.1. Methodological approach

The present part assesses the potential applications of solar treatment in water reclamation in sunny areas or areas with poor water quality. Solar disinfection of secondary treated wastewater under intermittent illumination was simulated in a lab-scale plant, using a synthetic secondary effluent and controlled laboratory conditions, namely, predefined light supply, wastewater composition, and microorganisms (*E. coli*). Also, the use of sonication was investigated as a supplementary treatment system for the dark phase of intermittent-illumination reactors, as well as different combinations of light, Fenton and ultrasound.

Regarding the light intermittence investigation, the microbial response to different light and dark phases was evaluated. Specifically, this study focuses on:

1. High-frequency intermittence (3-6 cycles per hour) by recirculating wastewater between a dark storage tank and an illuminated area. The recirculation in this setup imitates a compound parabolic collector reactor (CPC), a typical solar disinfection configuration.

2. Low-frequency intermittence, by inserting 1-h, 2-h or 3-h dark phases into 6-hour batch disinfection tests. These tests simulate the breaks in high-intensity light caused by temporal clouding in solar batch-reactor applications.

The results were evaluated through process efficiency, in terms of viable plate counts throughout the tests. Also, dark repair (DR) of the bacterial population was studied on the disinfected samples.

Also, there is a technical issue to be addressed in the intermittent nature of the CPC treatment method, and the existence of "dead" time among the experiment. Typically, a CPC photoreactor consists of the illuminated surface and the storage-recirculation tank. The recirculating flow of these reactors creates a gap in the illumination for as long as water is present in the (dark) storage tank. A proposition is to exploit this dark time by sonicating the water samples. In the same set-up as the high frequency intermittence tests, the joint ultrasound/photo-Fenton treatment for wastewater was studied. In this manner two factors that could work complementing each other can be exploited: firstly, the use of the dark intervals for sonication, along with the utilization of solar energy for the promotion of a mild photo-Fenton reaction and secondly, the

supplementary action these processes have, since, for instance, sonication can produce H_2O_2 and subsequently, could fuel the photo-Fenton process. In this part of study, synthetic secondary effluent was used, spiked with *E. coli* K12, recirculating around a sonicated dark reactor and an illuminated batch reactor, under solar simulated light. The aim is to:

i) Explore the effects of the photo-Fenton factors (light, reactants) and the ultrasonic action (US) on both short and long-term disinfection events; clarification of the effects is attempted by stepwise insertion of the participating actions.

ii) Investigate the involved operational parameters (recirculation speed, temperature, light intensity, treated volume and distribution of volumes, iron and hydrogen peroxide content, ultrasound intensity) in a small-scale set-up.

5.1.1. Recirculation reactors for high-frequency intermittence experiments

In the set-up presented in Figure 5.1.1, synthetic wastewater from a dark storage vessel (400 mL) was pumped by a peristaltic pump through three glass reactors (diameter 3.8 cm, effective irradiation surface 214.8 cm2), connected in series, of total volume 230 mL. The third reactor effluent was fully recirculated back to the dark storage vessel. The in-series reactors were irradiated by the Suntest apparatus, as explained before. Three different flow rates were essayed: 1.87, 3.44 and 4.39 L/h. The total of 700 mL wastewater in recirculation was completed by the water present in the recirculation system (70mL). The hydraulic calculations deriving from these settings are summarized and presented in Table 5.1.1, named cases I, II and III. Sampling was made through the external (dark) vessel; samples were drawn from the bottom and the recirculated wastewater returned at surface level in the vessel.

Furthermore, the illuminated volume was the 32.9% of the total volume, 10% was within the recirculation system and 57.1% remained in the dark, in every moment. In terms of light, the last two percentages constitute the total volume in the dark and the subsequent dark-to-light ratio is 2.04. This rate was constant within the three cases. Hence, the problem is reduced to the effect of the number of full cycles achieved within the 4 hours of the experiment and whether it affects the disinfection rate.

Table 5.1.1 – Summary of the hydraulic characteristics of the high-frequency intermittence experiments (cases I, II and III).

Case I: 1.87 L/h			**Case II: 3.44 L/h**			**Case III: 4.39 L/h**		
Light Exposure Time	7.38	min	Light Exposure Time	4.01	min	Light Exposure Time	3.14	min
Dark Storage Time	15.08	min	Dark Storage Time	8.2	min	Dark Storage Time	6.42	min
Full Cycle Time	22.46	min	Full Cycle Time	12.21	min	Full Cycle Time	9.57	min
In 240':								
Number of Full Cycles	11	cycles	Number of Full Cycles	20	cycles	Number of Full Cycles	25	cycles
Total Exposure Time	78.86	min	Total Exposure Time	78.86	min	Total Exposure Time	78.86	min
Total Storage Time	161.1	min	Total Storage Time	161.1	min	Total Storage Time	161.1	min
Total Time	240	min	Total Time	240	min	Total Time	240	min

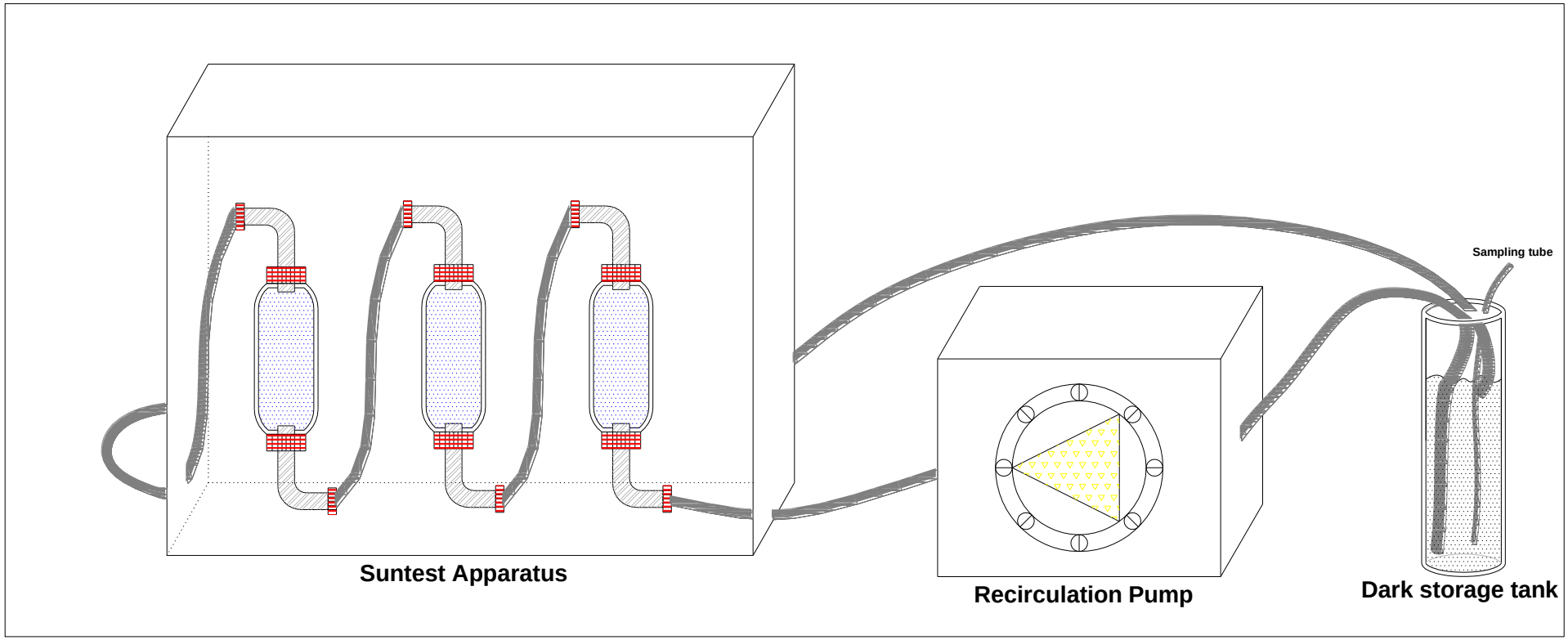

Figure 5.1.1: The 3 in-series reactors utilized in cases I, II and III of high frequency intermittence experiments. The flow is clockwise, water is introduced at surface level and sampled at the bottom of the tank.

5.1.2. Low-frequency intermittence in batch tests

The second part of the experiments, that included light intervals of 1-3 hours, was also developed in a Suntest apparatus and included the irradiation of the wastewater sample and its stoppage by removing the reactors from the light source. 50 mL batch reactors were used, made from Pyrex Glass (diameter 3.8 cm, height 9 cm with cap neck included, total volume 60 mL, effective irradiation surface 70.6 cm^2), over constant mild stirring.

Within six hours, there can be 14 different combinations of light intermission, for 1, 2 and 3-hour light stoppage. Sampling was performed hourly, regardless whether the sample was illuminated or not; reactors were removed from the Suntest and placed inside a dark box in ambient temperature. Initial bacterial population was approximately 10^6 CFU/mL in all experiments. Table 5.1.2 presents a summary of the 14 different scenarios, indicating the interval of time without light exposure. Scenarios 1-4 withhold 1 h of break, scenarios 5-10 of 2 h and scenarios 11-14 of 3 hours.

Table 5.1.2. – Light scenarios in low-frequency intermittence tests.

Scenarios	1h	2h	3h	4h	5h	6h
S 1	on	off	on	on	on	on
S 2	on	on	off	on	on	on
S 3	on	on	on	off	on	on
S 4	on	on	on	on	off	on
S 5	on	off	off	on	on	on
S 6	on	off	on	off	on	on
S 7	on	off	on	on	off	on
S 8	on	on	off	off	on	on
S 9	on	on	off	on	off	on
S 10	on	on	on	off	off	on
S 11	on	off	off	off	on	on
S 12	on	off	off	on	off	on
S 13	on	off	on	off	off	on
S 14	on	on	off	off	off	on

Dark repair of the *E. coli* present in the artificial wastewater was studied in ambient temperature (20-25°C), in absence of light, following the irradiation of the sample. The wastewater samples acquired during hourly sampling of the disinfection study of both high and low-frequency experiments, were stored in 1.5 mL sterile Eppendorf caps or the very same batch reactor previously exposed under illumination. The survival

of *E. coli* was measured 24 h after every sampling time while regrowth was measured after 24 and 48 h in the dark for the final sample, after 4 hours of illumination.

5.1.3. US/pF tests

The experimental configuration permits the sequential treatment of the synthetic wastewater; US/photo-Fenton treatment was taking place (or vice versa).The ultrasonic waves (275 kHz) were emitted from a piezoelectric 4-cm disc, fixed on a Pyrex glass plate adjusted to the bottom of the double-walled reactor. The intensities applied in all experiments were 10, 20 and 40 W. The electric power was the chosen method to calibrate the ultrasonic equipment. The in-series reactors were irradiated by the Suntest apparatus. The global irradiance values used in this part were 800, 1000 and 1200 W/m^2, while the corresponding UV values were approximately 20, 25 and 30 W/m^2.

5.1.4. Experimental design on US/pF coupling

Two sets of experiments were performed. In a first set of 8 experiments, that is referred to as step-wise construction of the joint treatment process, the elements of the US/hv/Fe/H_2O_2 joint treatment were gradually and accumulatively applied to the wastewater, in order to determine the individual role of each factor and to detect any synergy among them. Table 5.1.3 shows the conditions corresponding to each individual treatment factor when applied. Table 5.1.4 summarizes the four subsets of experiments in the step-wise design.

Table 5.1.3. – Parameters involved in the joint treatment process.

Factors	Values	Other parameters
Light	1000 W/m^2	***Temperature: 30˚C***
Ultrasound	20 W	***Recirculating Flow rate: 4.39 L/h***
Iron	1 ppm	***Treated Volume: 500 mL***
H_2O_2	10 ppm	***Initial Population: 10^6 CFU/mL***

In a second set of experiments (improvement of the process efficiency), eight different variables were individually modified at three levels, while keeping the other variables constant, in order to obtain improved working levels for each variable. Table 5.1.4 displays the three values (levels) essayed for each variable. In each experiment the remaining parameters were kept constant and set to the central value shown in the table.

Table 5.1.4. – Subsets of experiments in the step-wise construction of the joint hv/US/Fe/H_2O_2 treatment process.

Experiments	Treatment constituents
1-2	**WW and WW/Fe/H_2O_2** - Wastewater with no treatment - Wastewater + Fe/H_2O_2
3-4	**US and US/Fe/H_2O_2** - Wastewater+US - Wastewater+US+Fe/H_2O_2
5-6	**hv and hv/Fe/H_2O_2** - Light - Light+/Fe/H_2O_2 (photo-Fenton)
7-8	**hv/US and hv/US/Fe/H_2O_2** - Light+US - US+photo-Fenton

Table 5.1.5. – Overview of the investigation of the operational parameters.

Factors[1]	Level 1	Level 2	Level 3
Hydraulic			
Pump rpm	33	66	**99**
No. of Illuminated vessels	1	2	**3**
Wastewater volume (mL)	**500**	600	700
Environmental			
Temperature (˚C)	10	20	**30**
Light Intensity (W/m^2)	800	**1000**	1200
Fenton / Ultrasound			
H_2O_2 Concentration (ppm)	5	**10**	20
Fe Concentration (ppm)	0.5	**1**	2
US Acoustic Power (W)	10	**20**	40

[1]*Central values are annotated with bold.*

5.2. Effects of high frequency light intermittence

5.2.1. Disinfection of the bacterial population under different recirculation flow rates

Figure 5.2.1 shows the evolution of disinfection throughout the 4-hour light intermittence experiments. Intensity was set at 1200 W/m^2. The recirculation rate for the controls was performed in at 99 rpm. A slight increase in bacterial concentration is observed in the non-irradiated control, which is consistent with nutrient presence in the synthetic secondary effluent, and with dark conditions. The continuous irradiation control shows a consistent exponential reduction in *E. coli* of 6 $\log_{10}$ units in 3 hours (2 $\log_{10}$ per hour). Introduction of light intermittence (2.04 dark-to-light ratio) drastically impaired disinfection, yielding poorer bacterial inactivation in 3 h: 0.62, 0.33, and 0.06 $\log_{10}$, for cases I, II and III. Slightly better values, were obtained at the end of the experiment (4 h), numbering 0.87, 0.49 and 0.14 $\log_{10}$ units for cases I, II, and III, respectively (see Table 5.1.1).

All light intermittence experiments applied a total irradiation time of 78.9 min. However, experimental kinetics proved to be very sensitive to the recirculation rate, i.e., to the length of the irradiation/dark cycle. As shown in Figure 5.2.1, disregarding transient effects during the early latency period, inactivation rates were greater for greater recirculation rates. This is in accordance with a previous research by Fernandez et al. (2005). These authors speculated that their bacterial inactivation is due to mechanical stress; however, the maximum recirculation rate here was almost 70 times lower than their minimum and the subsequent stress considerably lower as well. Dark control experiment was performed in the same experimental setup and growth of the population was observed instead. Consequently, inactivation due to mechanical stress under the present experimental conditions is either negligible or lower than the bacterial growth rate.

The disinfection curves in Figure 5.2.1 also reveal that the most important observation lies within the correlation between the flow rate and the overall inactivation efficiency. It is shown that as the recirculation rate rises, and therefore the completed recirculation around the illuminated part, higher bacterial inactivation is achieved as the cumulative dose increases and, in absolute numbers, rates of 87.1, 49.3 and 14.3% were obtained in cases I, II and III, respectively. In absence of intermittence, the profound effect of intermittence is demonstrated by the total inactivation achieved in 3 hours of non-intermittent illumination.

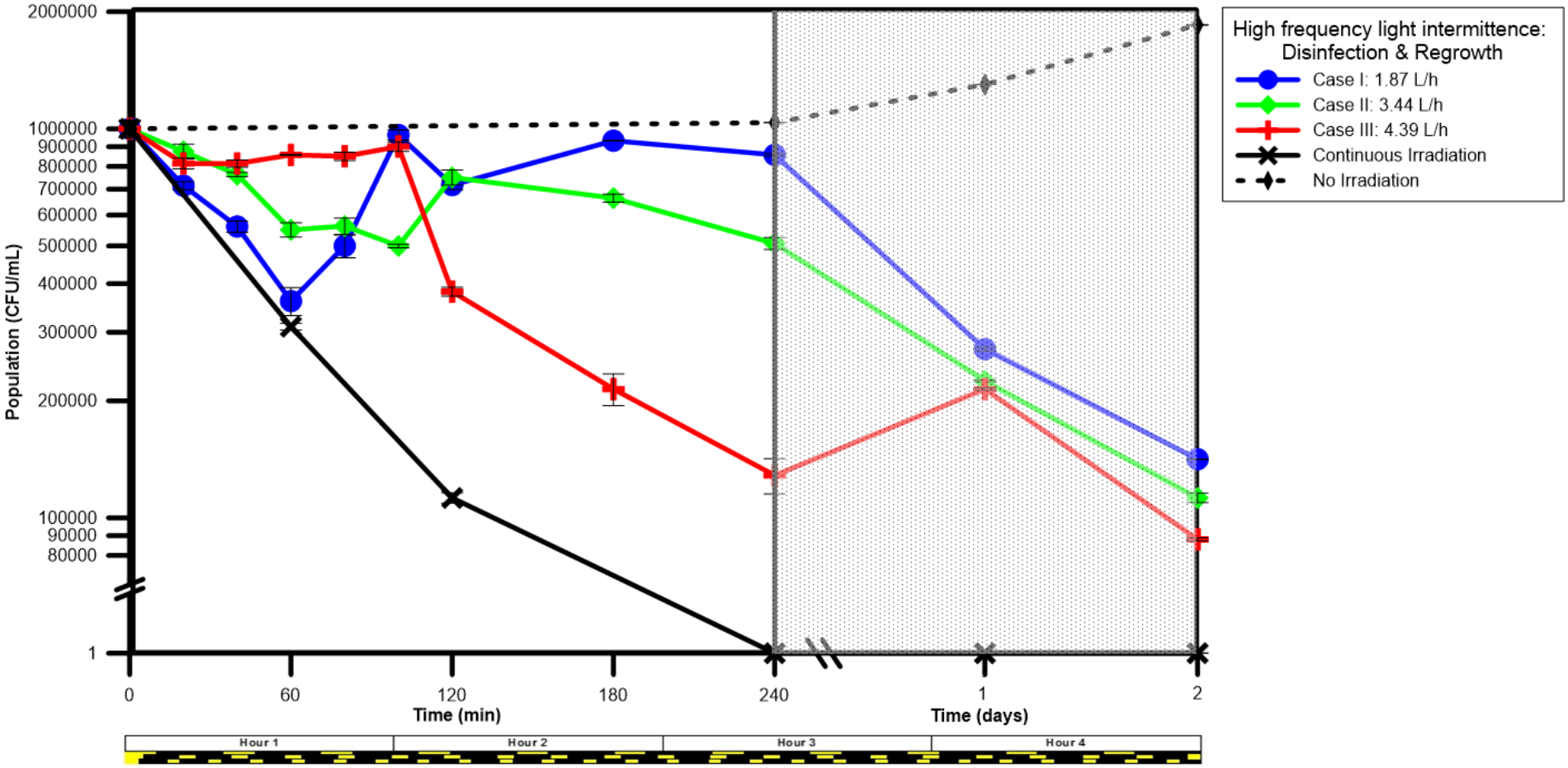

Figure 5.2.1: Disinfection curves and subsequent regrowth of remaining bacteria after the completion of the recirculation tests, within 2 days in cases I, II and III. The accompanying graph presents the distribution of light and dark during the 4-hour long experiments.

It is also shown that the sample that recirculates faster spends more intervals in the photoreactor, although shorter ones. That leads to more frequent exposure to sunlight and according to multi-hit and multi-target theory of Harm (1980), more effective illumination periods, as proved by Berney et al. (2006). This takes place because the light source is given more opportunities to hit the n number of sites needed to inactivate the bacteria. However, when the recirculation rate is lower, the longer dark storage times are strongly affecting the process, giving the necessary time to bacteria to recover from the hits taken during the exposure time. Even in slightly turbid waters, bacteria can be sheltered by aggregation and shading from particles against light attacks. Therefore, faster recirculation disaggregates the bacteria in the suspension and with the aid of the higher appearance rate under the light source, bacterial disinfection is favored.

All curves in Figure 5.2.1 reveal a fluctuation in inactivated bacteria within the first two hours. Lower recirculation rates during the first hour lead to larger initial bacterial inactivation, due to the longer light exposure; the experimentation is initiated with the three reactors into the solar simulator filled with suspended bacteria that suffered longer initial non-interrupted light exposure. Also, subsequent longer dark storage times resulted in sharper transient adaptation or recovery with local maxima. In other words, during the first 60 minutes, the lower recirculation rates, that spend longer un-interrupted periods in the light, presented lower bacterial numbers, contrary to the higher recirculation rates, that demonstrated a relatively constant population. Bacterial growth is favored in this nutrient-rich medium, and result in bacterial growth in the dark tank. On the other hand, the recirculation did not allow bacteria to spend long time in the dark, but slowly accumulate the necessary dose required, while limiting the growth in the dark. Also, notice should be taken on the positions of the sampling and recirculation tubes; the positions were chosen to avoid short-circuiting and therefore false bacterial numbers.

Moreover, it is shown that there is a variable period of adjustment of the bacterial population to the new conditions; 100 minutes for the highest recirculation rate and around 180 minutes for the lowest one. This is a common observation in almost all sun-driven experiments and is often expressed as a shoulder effect (Harm, 1980; Sinton et al., 1999; Berney et al., 2006; Ndounla et al., 2013); in continuously irradiated samples, this phenomenon is attributed to initial defense mechanisms, but here it reveals the need for a cumulative amount of dose that is required to be provided in order to efficiently decrease the populations, as described by Misstear et al. (2013).

In addition, the factor of temperature was neglected and not accounted as a possible inactivation path for bacteria. Water temperature was measured along the experiment with a thermometer in the storage tank and the measured values ranged between room temperature (21°C) and 32°C, stabilized around the upper edge. It has been reported that *E. coli* after being dispersed in water solutions are stable between these temperatures, because there is no thermal effect on bacterial viability (Fernandez et al., 2005; Sichel et al., 2007a)

According to Sichel et al. (2007a), around this temperature the metabolic activity of bacteria is higher, leading to higher risks of osmotic damage to the cells. However, the aquatic matrix that withheld the

bacterial suspension is artificially recreated wastewater, simulating the effluent of secondary treated wastewater. Thus, anions and organic matter from the wastewater provide nutrients for bacteria; their viability is maintained in higher levels than the experiments held in distilled or demineralized water matrices and the osmotic pressure is of minimum effect. The solution of wastewater already contains calcium and magnesium ions, which are the first ions detected in suspension when bacterial cells are subject to lysis in unfriendly environments (Marugan et al., 2010). Therefore, cell's demands for survival are met.

5.2.2. Bacterial regrowth (due to DR) after high-frequency intermittence irradiation

Figure 5.2.1 also shows the bacterial regrowth after 24 and 48 hours by the end of the experiment. No regrowth was observed after 48 h, while only one of the samples (corresponding to the maximum recirculation rate) presented some regrowth after 24 h. Figure 5.2.2 presents the regrowth and the bacterial survival rate as well. In most cases it is shown that the applied light dose in this particular intensity was enough to permanently damage the bacteria after one hour of cumulative exposure. As the process continues, the germicidal effect of light is more obvious, but not definite (see Figure 5.2.1, 4.39 L/h, bar: 180 min). A longer observation period could reveal for both cases whether survival is permanent or temporal.

It can be also observed that in overall, the applied irradiation time, of 78.16 minutes, is enough to reduce bacterial regrowth potential for at least 48 h of subsequent dark storage. Moreover, Figure 5.2.1 clearly shows a trend of lower survival rates after 24 and 48 h of dark storage, for samples previously submitted to rising recirculation rates. It is clear that as recirculation rate increases, the regrowth potential of bacteria is increased as well. As percentage of initial bacterial concentration, the survival rate is 14.1, 11.3 and 8.80%, for cases I to III, respectively.

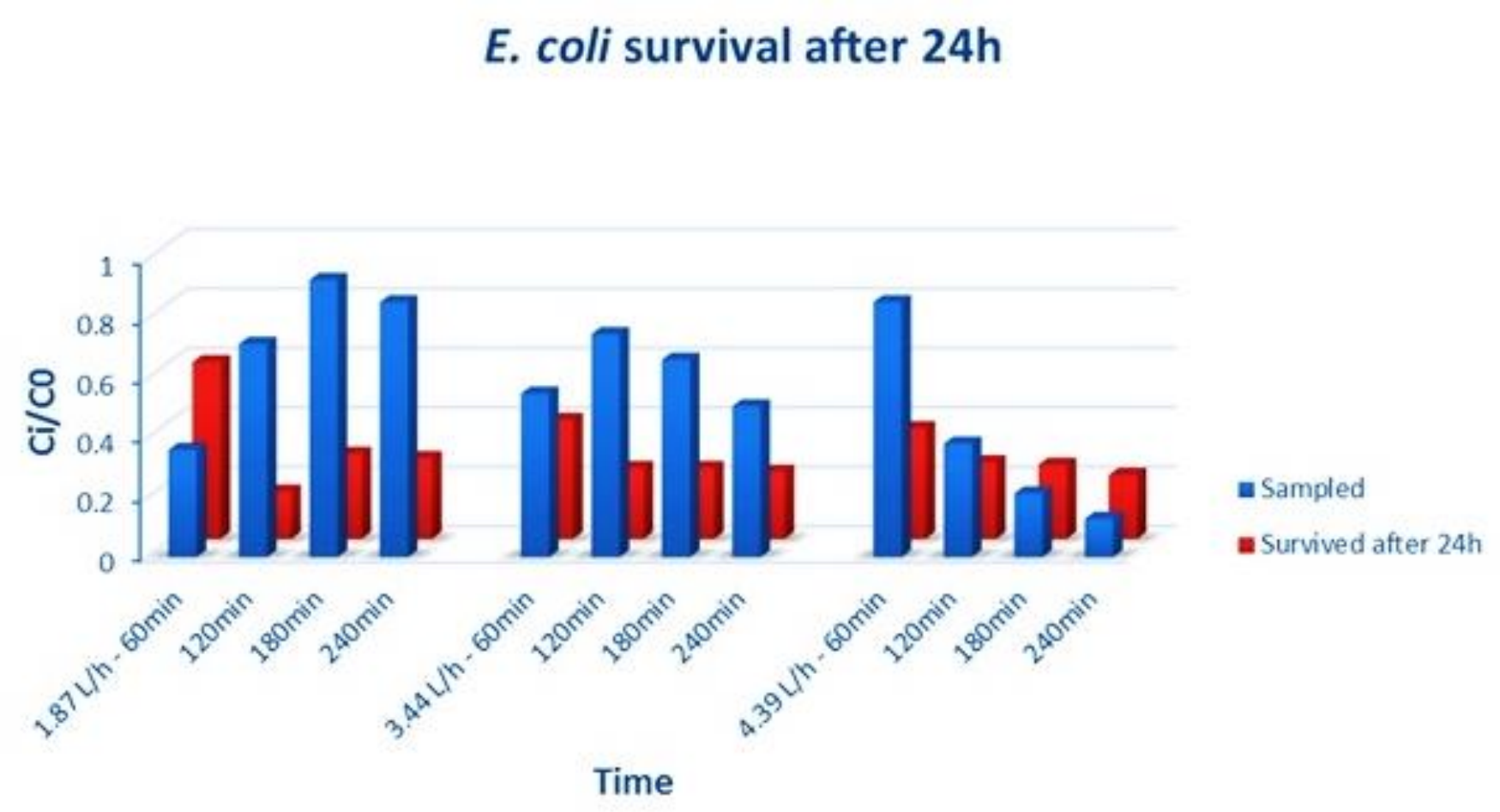

Figure 5.2.2: *E. coli* survival after 24h of dark storage in cases I, II and III with recirculation rates 1.87 L/h, 3.44 L/h and 4.39 L/h, respectively. The results present the evolution of the remaining fraction of bacteria during the experiment (sampling every 1 hour), after one day (error is less than 5-10% in all of the cases).

As described before, longer dark periods result in more time available for bacteria to repair and deploy defense mechanisms, even if bacteria have previously suffered longer illumination periods. Similar observations were made by Rincon and Pulgarin (2003), noting the importance of intermittence in survival of bacteria. Hence, intermittence has an effect in regrowth as well; the same defense mechanisms described by Misstear et al. (2013) strengthen bacteria and favor their survival. It must be reminded that bacterial growth is favored in this matrix, due to the presence of nutrients, and the long-term effect of bacterial inactivation is due to their inability to survive, and not from external or environmental factors. Therefore, the integrated light dose applied during the intermittent irradiation has been enough to induce an irreversible damage, in an extent enough to limit bacterial regrowth for the following 48 h. The importance of estimating this period was highlighted by Rincon and Pulgarin (2003) and as it seems in this case UV has rendered bacteria unable to reproduce and probably has inflicted lethal damage after the 4 hours of experiment, which ensures bacterial decay in the post-irradiation period. The neighboring bacterial counts after 1 and 2 days indicate that under the employed conditions the dose is the decisive parameter, when regrowth is under question, since similar cumulative light dose resulted to similar bacterial counts.

5.3. Low-frequency intermittence in batch tests (cloud simulation)

5.3.1. 1-hour dark intervals

Figure 5.3.1a presents Scenarios 1 to 4 (see Table 5.1.2), in terms of bacterial population over time. In these scenarios, 1-hour illumination stoppage was performed, during the 2nd, 3rd, 4th or the 5th hour of the experiment. There is a series of findings within this graph, which demonstrate the importance of continuous illumination of the bacterial sample. For instance, Scenario 4 receives un-interrupted illumination until the 5th hour and as a result, total inactivation takes place in 3 hours. Same applies for Scenarios 2 and 3, where 2 and 3 hours of continuous irradiation is provided to the samples.

By applying an irradiance of 1200 W/m^2 it is shown that this time period of 2-3 hours is enough to inflict lethal or, at least, non-repairable damage; after 3 hours, illumination was paused for an hour and bacteria, initially enumerated close to the detection limit, were no longer viable. Common characteristic in all the runs, a shoulder effect during the first hour of illumination, as discussed above and by previous researchers (Berney et al., 2006; Misstear et al., 2013). Effort was made to maintain the bacteria in stationary phase before their introduction to the synthetic wastewater so as to eliminate this concern. However, the first phases of adaptation in the new environment are usually unstable and here, along with the presence of nutrients, the favored bacterial growth is hindered by the strong and continuous illumination. Therefore, the shoulder effect is visible in all scenarios.

Finally, it is clear that bacterial inactivation is favored when the dark interval takes place in the last hours. In the case that inactivation was complete during illumination, it is shown that there is no obvious recovery of the bacterial population within the studied 6 hours. The introduction of an early dark period of 1 h resulted in an increase in the required time for total disinfection. The earlier the 1-h dark interval was introduced, the longer the increase in the time required for total disinfection: 2 additional hours when darkness was applied during the second hour, 1 additional hour if in the third hour, 1 additional hour when applied in the third hour. The required time for total disinfection significantly decreases with increasing lengths of the initial uninterrupted irradiation time: From 300 min for 1 h to 180 min for 4h of uninterrupted irradiation time.

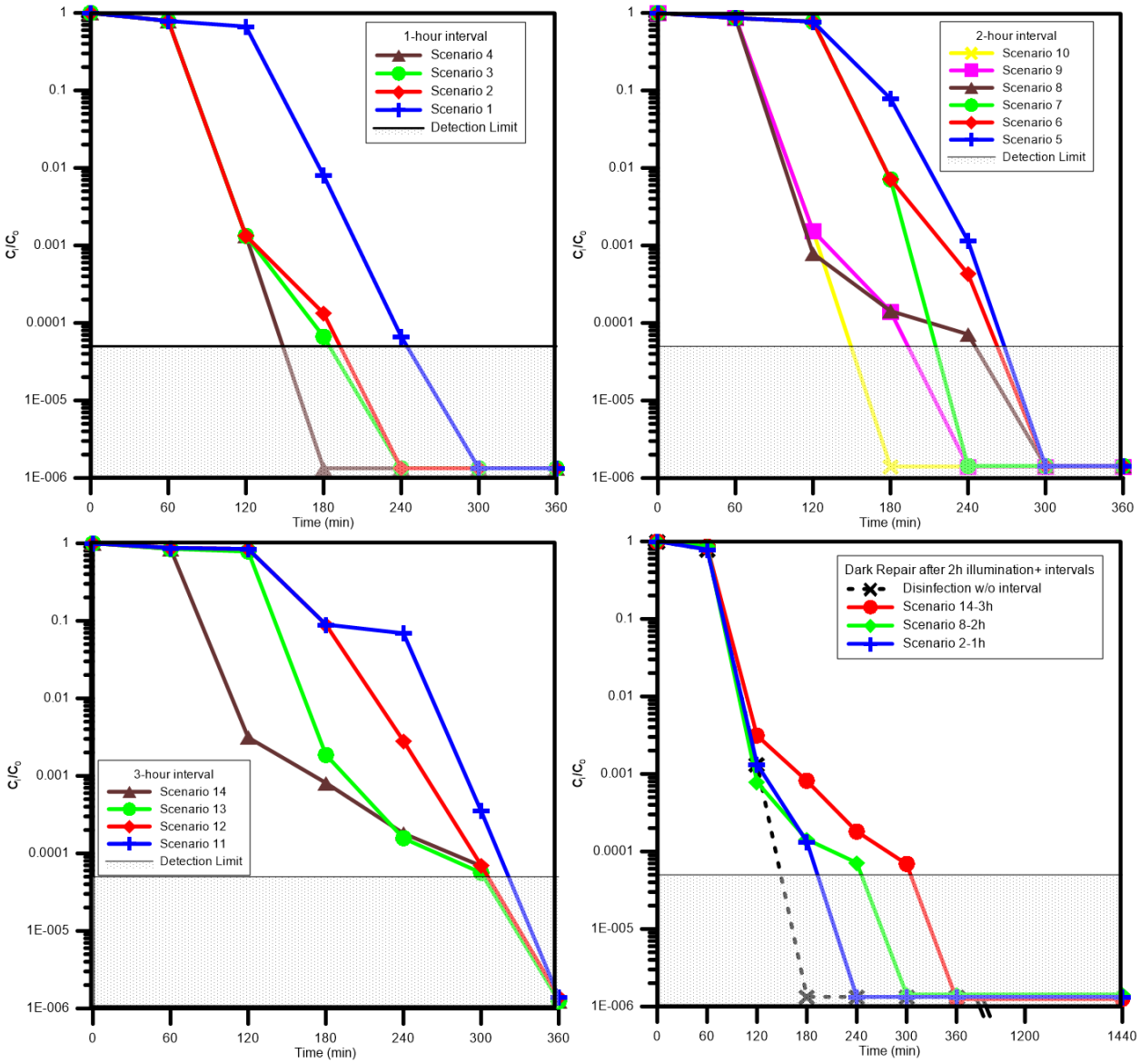

Figure 5.3.1: 1, 2 and 3-hour light interval scenarios (a, b & c), and regrowth of Scenarios 2, 8 and 11 (d). The continuous line represents the illuminated periods while the dotted line represents the dark intervals.

5.3.2. 2-hour dark intervals

In Figure 5.3.1b are presented the Scenarios 5 to 10, demonstrating the disinfection curves of the experiments including a 2-hour break within the irradiation. The normalized disinfection data presented in this Figure, suggest clearly a modification on the kinetics of the inactivation process. In the case of 1-hour intervals the disinfection curves were almost linear after the initial shoulder; in this figure the linearity is kept in the cases with three consecutive hours of illumination, before or after the dark period, especially when the 2-hour dark period is consequent. Clearly different slopes are generally observed in the segments corresponding to dark periods (dotted lines), reflecting the absence of disinfecting force.

The subsequent inactivation after the temporal stoppage of the irradiation is interesting, due to the inability of bacteria to reproduce and in parallel, the infliction of damage heavy enough to make it impossible to

recover. It has been reported that UV-irradiated *E. coli* present accelerated senescence, an irreversible state of dormancy, due to the accumulated damage in cell's components over time (Stephens, 2005; Bosshard et al., 2010b). Therefore, remaining bacteria fall into either the cultivable and active category that continue to reproduce or the dormant ones. In terms of total disinfection times, they vary from 3 to 5 hours, similarly to the 1-hour Scenarios; however, it is observed that two or three hours of non-stop irradiation is of irreversible effect. Similarly as the 1-hour intervals, the total experimental time decreases from Scenario 5 to 10.

Scenario 10 describes the only case of constant illumination during the first 3 hours and therefore demonstrates the smallest required time for total disinfection. Conversely, Scenarios 5, 6 and 8, describe the worst case; the sample of Scenario 5, after 1 hour of illumination is kept two hours in the dark, allowing the pre-mentioned repair and defense mechanisms to be developed. Hence, the overall required time is greater. Scenario 6 is also one of the worst possible scenarios, because of the same protection methods described before; every one hour irradiation is stopped for one hour and the fluctuations in intensity increase the chances of bacteria to escape the lethal effect of solar light. Also, during Scenario 8, the necessary 3 hours of irradiation are interrupted by two hours of dark storage. Similarly to Scenario 5, this effect leads to a total of 5 hours for total inactivation. Finally, Scenarios 7 and 9 represent a 2-hour non-continuous interval, where one of the 2-hours break took place after disinfection was complete.

5.3.3. 3-hour dark intervals

The last tests concern 3-hour continuous or intermittent breaks; 4 scenarios, Scenario 11 to Scenario 14 are presented in Figure 5.3.1c. The time needed for total inactivation is similar among scenarios, approximately 6 h. The kinetics of each scenario are reflected in the steepness of the curves, with the less inclined parts highlighting the dark storage periods. Scenario 14 demonstrates the fastest inactivation rate, being the only that receives light for 2 hours in a row, followed by Scenario 13, 12 and 11. Scenario 13 is more effective than Scenario 12, because of the extra hour illumination it receives, compared to the ones of Scenario 12. Scenario 11 is the worst case scenario, because it represents a situation where 60 minutes of illumination are followed by 180 minutes of dark storage. All the actions that prevent bacterial decay are present here; however, this light intensity is enough to inflict considerable damage on bacteria.

These findings verify once more that in a period of six hours, the bacterial population is eliminated. It is concluded from these scenarios that in the present conditions there is a cumulative amount of light dose to be gathered before total disinfection; a dose corresponding to the total amount of 3 hours in this irradiance is enough to disinfect bacteria in artificial wastewater. For lower light intensities, lower rates and, therefore, higher required times are expected, in accordance with the findings of other researches (Benabbou et al., 2007). However, the investigation shows a significant degree of tolerance to illumination interruption for some hours. These results are encouraging, under the scope of extrapolation to the real light situations.

5.3.4. Durability of the process – Bacterial regrowth due to dark repair mechanisms

In order to assess the regrowth risk of the disinfected samples, the glass batch reactors were kept in the dark for 48 hours and sampling was made every 24 hours of storage in the dark, in ambient temperature, as described in the previous section. The scenarios selected and presented in Figure 5.3.1.d are Scenario 2, 8 and 14. They were selected as an average case, of 2-hour constant exposure to sun rays and then submitted to 1, 2 or 3 hours of constant dark storage. Also presented, is a disinfection experiment in the exact same conditions, but without light intervals.

The importance of dark storage has been stated before; therefore, 1, 2 and 3 hours of dark storage would be expected to present increasing survival rate, accordingly to the effect of repair during the experiment. As it seems, these mechanisms were completely unable to reactivate bacteria while stored in the dark. The cumulative amount of solar irradiation has probably exceeded the threshold needed to completely inactivate life functions of bacteria. All scenarios presented no regrowth, regardless of the presence or absence of dark intervals.

Comparing these results with the effects of light intermittence in the previous experimental set-up, it seems that the most decisive parameter concerning bacterial inactivation, as well as dark repair, is the continuous, un-interrupted exposure to light. Although in both cases the irradiation rendered bacteria unable to regrow, it was due to the continuous illumination type and the bigger light residence times that the process became more efficient. In the latter case of the fourteen scenarios, since total inactivation is reached, no bacterial regrowth is observed, indicating their destruction since no reappearance is observed in any case, when in a favorable environment.

5.4. Results of the step-wise construction of the joint US/pF treatment process

As far as a potential application of mild photo-Fenton assisted by high frequency/low power ultrasound is concerned, moderate concentrations of reactants are suggested for the evolution of this work, after an initial investigation. At 1000 W/m^2 light intensity, an addition of 1 ppm iron and 10 ppm of H_2O_2 will be used, as marginal values of Fenton reagents and 20 W of US power.

5.4.1. Disinfection experiments

i) Experiments: 1-2 (WW and WW/Fe/H_2O_2).

Figure 5.4.1a presents the results of the first part of the experiments, where neither light nor US was applied. Wastewater was recirculated around the non-illuminated, non-sonicated experimental set-up and the corresponding graphs describe the changes when H_2O_2 and iron were added to the solution. An increase of the population is observed when no reactants were added, due to the existence of nutrients and salts that favor bacterial growth in this water matrix (Marugan et al., 2010). H_2O_2 is a substance with disinfecting action, while iron itself is not toxic for bacteria. The addition of both reactants causes the initiation of the Fenton reaction, which has a slow, but existing disinfecting ability and within a timeframe of 4 h, a 24.4% reduction in the initial population is noted.

ii) Experiments: 3-4 (US and US/Fe/H_2O_2).

Figure 5.4.1b demonstrates the effects sonication has on samples, alongside with the stepwise insertion of the Fenton reagents. The sample recirculates around the ultrasound vessel and the non-illuminated area, being subject to intermittent high-frequency, low intensity sonication. When ultrasound alone is applied, there is a decrease in total bacterial numbers, approaching 27.9%. The concurrent addition of both Fenton reactants (H_2O_2 and Fe^{2+}) in the sonicated sample causes an 82.1% reduction in the bacterial population, compared to 27.9 % reduction for US treatment and 24.4% for Fenton treatment alone. This indicates a synergy between sonication and the Fenton reagents; a synergy factor of 1.57 is demonstrated by the disinfecting efficiency of the reactions.

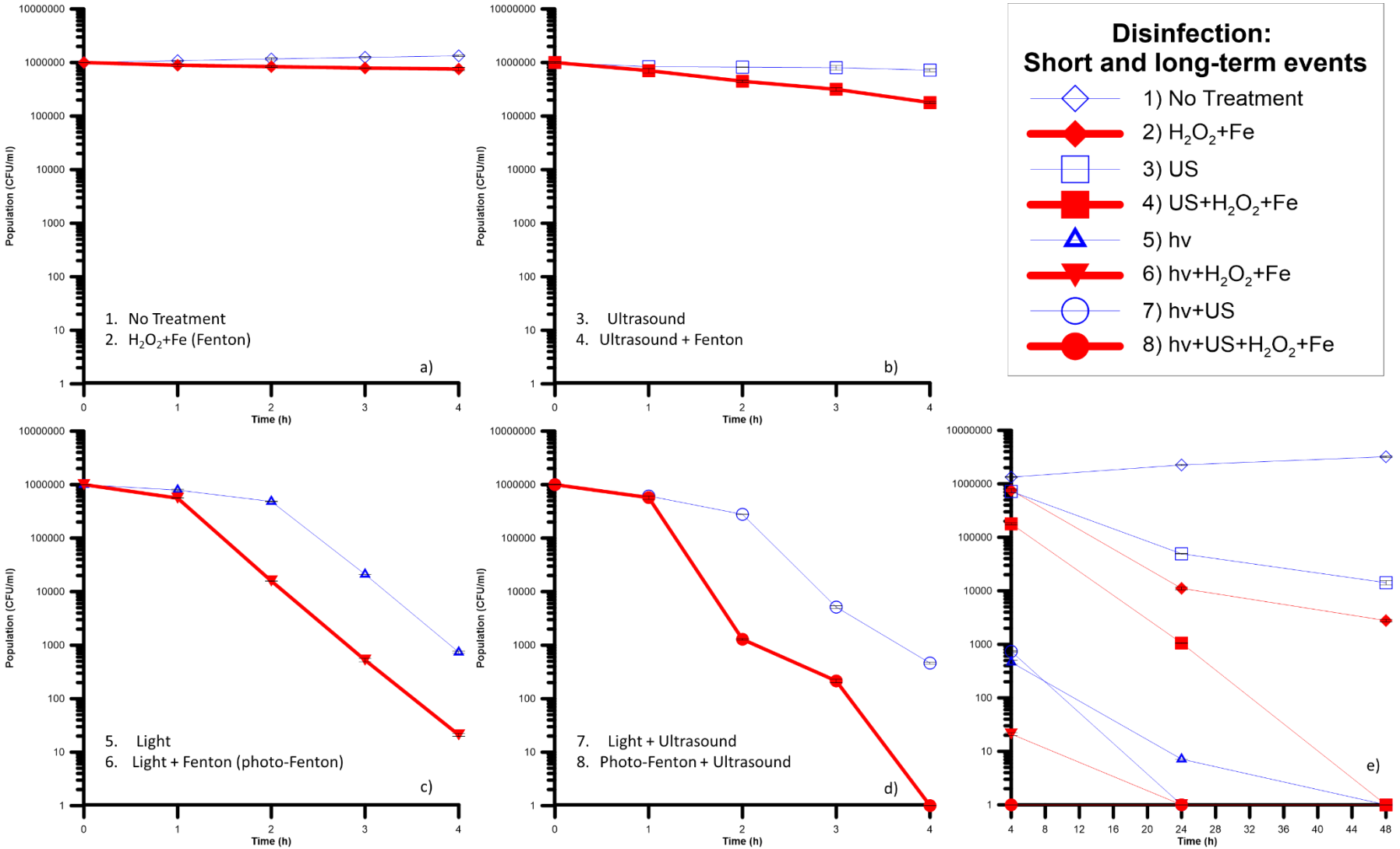

Figure 5.4.1: Experimental results from the coupling of photo-Fenton and sonication. a) Experiments 1-2 (WW and WW/Fe/H_2O_2), b) Experiments 3-4 (US and US/Fe/ H_2O_2), c) Experiments 5-6 (hv and hv/Fe/ H_2O_2) and d) Experiments 7-8 (hv/US and hv/US/Fe/ H_2O_2). e) Long-term inactivation events for 48 h (time axis initiates in the 4-h mark, after treatment).

During sonication, the breakage of the cavitation bubbles can lead to the formation of an almost point-sized heat source (Butz and Tauscher, 2002; Fellows, 2009), with local temperatures approaching 2000 K and pressures of 200 atm. These extreme conditions can cause lysis of water molecules and along with that, extra production of hydroxyl radicals (Hua and Thomson, 2000). The presence of the afore-mentioned particles in real wastewater and the bacteria (in the employed matrix) could also play another important role, since the collapse of the cavitation bubbles near a particle in the medium could cause micro-jets, depending on the size of the particle (Holm et al., 2008) and could also form "weak spots" in the body of the liquid; these are potential places to form a cavity (Leighton, 1994). It has been also reported that the presence of some salts causes a baro-protective effect on the cells (Molina-Höppner et al., 2004) and samples with higher contents of soluble solids would require higher sonication times. Apart from the physical damage, during the ultrasound treatment of the sample, there is ample generation of reactive oxygen species ($^{\bullet}OH$ radicals (Mason and Tiehm, 2001), singlet oxygen (Davidson et al., 1987; Matsumura et al., 2013), as mentioned before, which are known to stress bacteria and lead to cell death (Spuhler et al., 2010; Ndounla et al., 2013).

Finally, the addition of peptone (present in the synthetic wastewater) and in general, the presence of nitrogen compounds has been reported to delay the sonicated degradation of phenols (Zaviska et al., 2014). However, nitrogen, under the presence of ultrasound waves can form NOx (nitrate and nitrite). Its reaction with singlet oxygen (as produced before) produces peroxynitrite ($ONOO^-$) (Novo and Parola, 2008). Peroxynitrite is included in the reactive nitrogen species and can cause significant injures to various structures of the cell (free radical damage or attack against the respiratory chain) (Novo and Parola, 2008).

The synergistic action of US and Fenton processes can be attributed to the exploitation of the recombined H_2O_2 (from $^{\bullet}OH$), which is less oxidative than the hydroxyl radical itself, and with that, the re-initiation of the Fenton reaction with new reactants. Also, the ultrasound process, according to Kryszczuk (1962) increases the transient breakage of the bonds among the molecular components of the cell membrane, which increases the permeability of the cell in external substances (Dahl, 1976). Therefore, the introduction of Fe^{2+} in the cell is easier and its presence inside the cell can produce hydroxyl radicals very close to vital functions of the cell, as well as the DNA (Spuhler et al., 2010) due to the induced internal Fenton process.

iii) Experiments: 5-6 (hν and hν/Fe/H_2O_2).

The 3rd set of experiments is dedicated to the investigation of the impact of light in the sequential process. In all experiments light is provided at 1000 W/m^2, but in total, intermittent irradiation is provided to the system; there is an illuminated regime and a non-illuminated one, in the Suntest apparatus and the (inactive) sonication vessel (and tubing). In the previous sections (5.2 and 5.3), the impact light intermittence has on bacterial disinfection and survival was demonstrated, while continuous supply or very fast recirculation

around illuminated and dark regimes favors disinfection, with the same set-up. Therefore, photo-Fenton is promoted in non-intermittent regimes or, as in this case, short dark interval periods.

As it can be seen from Figure 5.4.1c, light, even in non-continuous form, is very effective and results in high inactivation rates. Its disinfecting action is dominating the removal process, until the Fenton reagents are present, and solar-assisted photo-Fenton is induced. The action of photo-Fenton is taking place within the Suntest and dark (normal) Fenton takes place during the rest of the time, in a 0.85:1 time distribution (46% photo-Fenton over 54% Fenton). After an initial delay, which is demonstrated as a shoulder in the graph, reaction is more effective by the hv/Fe/H_2O_2 than the corresponding solar treatment.

Spuhler et al. (2010) have reviewed the mechanism of bacterial inactivation by the photo-Fenton reaction in near-neutral water with organic components, and have suggested the possible sources of ROS production and cellular photooxidative damage, as well as the damage done by the ROS themselves, deriving from the photo-Fenton reaction. In the suggested treatment method, these mechanisms are completely compatible, explaining the majority of the actions and other works on near-neutral photo-Fenton mechanisms describe fully the mechanisms.

iv) Experiments: 7-8 (hv/US and hv/US/Fe/H_2O_2).

The final group of experiments are presented in Figure 5.4.1d. This graph summarizes the results of the joint treatment by light and ultrasound. It is clear, after a comparison with Figure 5.4.1c, that when light is present, its disinfecting action is dominating the process. However, it is noticed that the only case total disinfection is achieved, is by the sequential US/pF system. In this system, wastewater spends its time distributed 46% under photo-Fenton, 14% in the dark (dark-Fenton) and 40% in the sonication vessel (US/Fenton). The experimental time has less inactive periods, and it is observed that it has a significant impact in the total inactivation of the bacterial populations in less than 4h. Here, the photo-Fenton/US synergy is low in terms of bacterial counts, efficiency was improved in a relatively low percentage, but only the coupled process resulted in total disinfection in 4 h. The elevated efficiency and total inactivation for the first time, is attributed to the combination of all the previous actions (in US and/or light), as well as the following actions (a graphical summary of all the actions is presented in Figure 5.4.2):

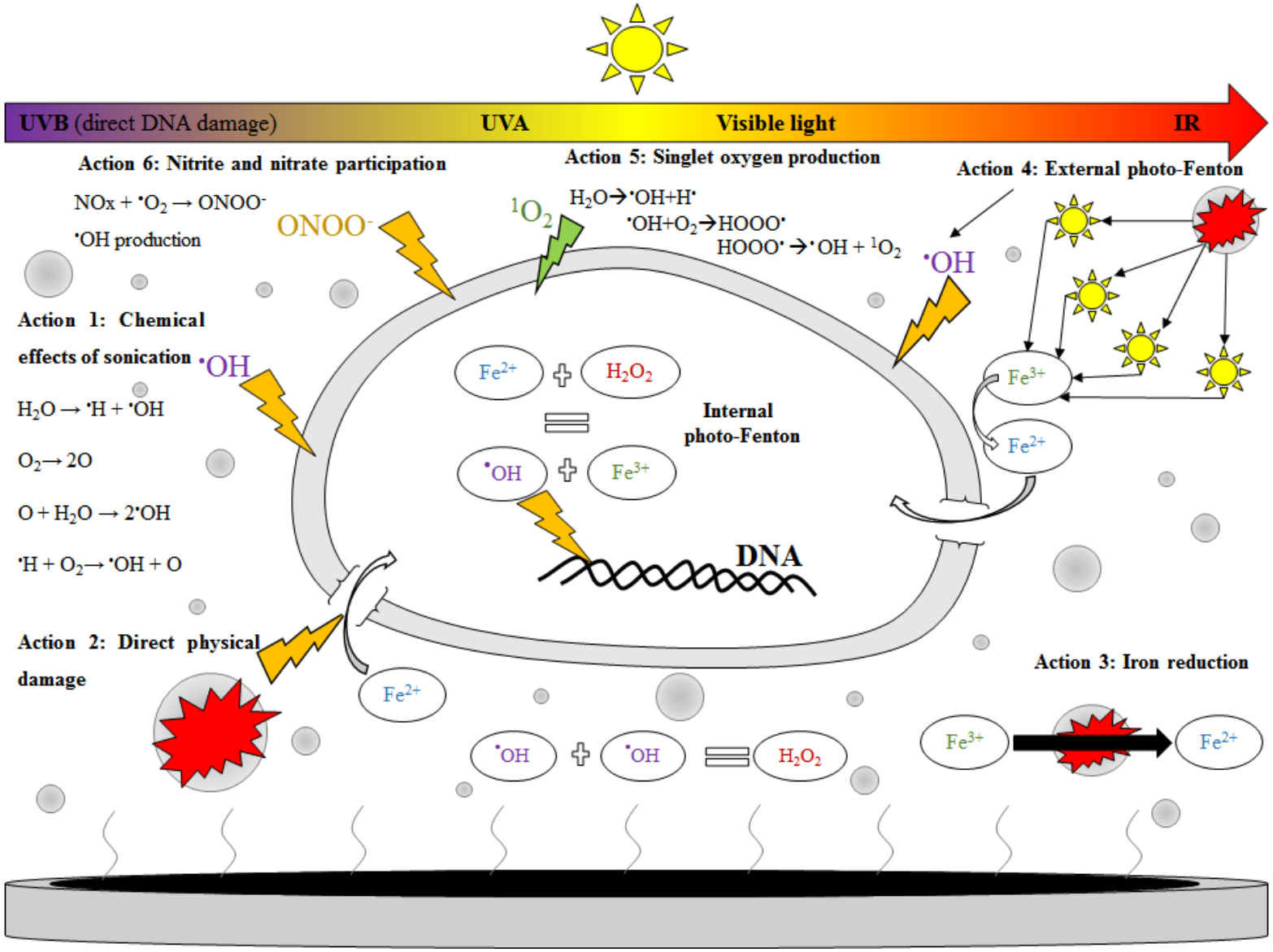

Figure 5.4.2: Suggestion of the added actions sonication has towards bacterial inactivation, when coupled with photo-Fenton. The known photo-Fenton mechanisms suggested by literature are not displayed.

i. The hydroxyl radical is a short living ROS, and it occurs not to reach the target in all cases and often recombines to create H_2O_2 (Torres et al., 2008). Therefore, the addition of ultrasound directly produces hydroxyl radicals and H_2O_2; the $^{\bullet}OH$ directly attacks the cell and H_2O_2 participates in the photo-Fenton reaction (2). Alongside with the added H_2O_2, there is additional production, fueling the Fenton reaction and thus, improving the overall efficiency of the treatment.

ii. As described before, with ultrasound waves, the loosening of transient bonds and insertion of Fe^{2+} in the cell is increased, which promotes the internal Fenton reaction. After the completion of the Fenton reaction, light reduces Fe^{3+} to Fe^{2+}, and re-initiates a radical production inside the cell (internal photo-Fenton).

iii. Low frequency ultrasound has been proven (Chauhan, 2004) to reduce Fe^{3+} in the form of ferrous ions (Fe^{2+}). The average size of the bubble however decreases when frequency is increased, as in this system (Brotchie et al., 2009); nevertheless, cavitation still takes place. Therefore, it is possible that an action like this could provide an additional source of iron available for the photo-Fenton process, and progress the regeneration of the catalyst in the (otherwise) non-illuminated part of the time. In that way, more available ferrous ions can be present in the solution.

iv. The interior part of the bubble, under implosion conditions, is known to emit light, under the phenomenon of sono-luminescence (Hua and Thompson, 2000) due to the extreme temperature and light conditions. The optical aspects of this phenomenon have been studied (Didenko and Pugach, 1994) and the emitted light wavelengths fall into the necessary ones possibly able i) to induce the regeneration of the photo-Fenton reaction catalyst, ii) inflict direct UV damage to the cell. However, the necessary energy to achieve this is still under question.

v. Apart from the radicals' production through the normal photo-Fenton cycle, the presence of light is participating in another series of reactions with nitrogen compounds. The photolysis of nitrate and nitrites (produced by the participation of the US in the process) can lead to additional hydroxyl radical production (Zaviska et al., 2014):

Photolysis of Nitrate:

$$NO_3^- + h\nu \rightarrow NO_2^- + \frac{1}{2}O_2 \quad (3)$$

$$NO_3{}^- + h\nu \rightarrow NO_2\boldsymbol{\cdot} + O^{\bullet -} \quad (4)$$

$$O^{\bullet -} + H_2O \leftrightarrow HO^{\bullet} + OH^- \quad (5)$$

Photolysis of Nitrite:

$$NO_2^- + h\nu \rightarrow \ NO^{\bullet} + O^{\bullet -} \quad (6)$$

$$O^{\bullet -} + H_2O \leftrightarrow HO^{\bullet} + OH^- \quad (7)$$

5.4.2. Post-processing events: long-term disinfecting activity of the joint process

The monitoring of the bacterial population for 48 h after the completion of the experiment has indicated some rather interesting aspects on the characteristics of the driving forces of the joint disinfection process. Figure 5.4.1e demonstrates the post-treatment bacterial counts, starting from the moment the reactions have stopped (4-h mark). There are two big groups of charts being distinguished, which present different behavior: the non-irradiated and the irradiated processes.

First of all, it is observed that if there is no light or US treatment involved, as expected, bacterial populations tend to increase their numbers. The presence of the Fenton reagents inflicts a constant, but relatively slow, elimination of the present bacteria. The bacterial population in the sonicated samples (square traces), although having survived the 4 hours of sonication, is significantly lowered in the days following treatment. This observation seems to suggest some type of permanent damage that has affected their cultivability. Even more, the US/Fenton treatment has shown that even with high remaining bacterial values, after 2 days, the damaged bacteria have almost completely succumbed, due to the combined sonication damage and the Fenton reaction that was still ongoing.

The long term effects caused by the sonication of the water sample can be summarized as follows: The employed acoustic range promotes the production of hydrogen peroxide, which is an indicator of the formation of other oxidative species (Hua and Thompson, 2000). In this frequency, the generated hydroxyl radicals are easily transferred away from the bubbles (Hua and Hoffmann, 1997; Petrier et al., 1992; 1994; 1996. The high-frequency damages include dislocation of the cell membrane, which often leads to intracellular content leakage, due to the disruption of the cell wall integrity (Koda et al., 2009; Joyce et al., 2011). As a result, bacterial viability is lost; a gradual degradation of the cell membrane takes place due to the attacks of the hydroxyl radicals in the medium and vital parts of the bacterium are attacked (Broekman et al., 2010; Koda et al., 2009), reduced potassium uptake and restricted DNA and protein synthesis have also been reported (Haas et al., 1980). Also, programmed cell death and cell apoptosis were also recently mentioned (Moody et al., 2014), which explain the delayed inactivation of cells. These processes can explain the behavior of the sonicated samples for the 48-h monitoring period. Finally, in the combined process before, the greater iron uptake by the cells due to its transformation (Kryszcuk, 1962 and Dahl, 1976) was mentioned before. This process is of high significance, supported by the post irradiation events; within 48 h there are no more cultivable bacteria, and comparing with the plain dark Fenton process, the change is attributed to the already apoptotic cells, which are easier to succumb to further oxidative damage after their sonication and finally to the increase of the internal Fenton process.

The second group of experiments, where light treatment was involved, all demonstrate zero counts within two days. Light has significantly impaired bacterial reproduction and all samples that were irradiated lead to total inactivation. Photo-Fenton treatment has proven to completely inactivate in less time (<24 h), totally eradicating the small bacterial counts left during the treatment. Total inactivation can however be reached

within 24 h under joint US/solar light treatment even in the absence of iron, due to the sequential damaging by US and solar light. No regrowth was observed in any of the experiments within a 48h period. In addition to that, the coupled US/pF process, has maintained its zero count throughout the 2-day period, with no noticeable regrowth or recovery.

5.5. Improvement of the process efficiency: Investigation of the operational parameters involved in the US/pF coupling

Having observed the total and permanent inactivation for the solar-assisted US/pF system, it is interesting to examine how other types of operational parameters could influence the process efficiency. Possibilities for improving the process and investigating its flexibility and robustness are ample. The parameters to be studied are summarized in Table 5.1.5, and divided in hydraulic, environmental and chemical (US and Fenton factors).

5.5.1. Hydraulic parameters

Figures 5.5.1a-c present the investigation that has been conducted, to study the effects of the modification of the recirculation rate, the number of in-series illuminated reactors, and the treated volume, respectively. The three recirculation rates correspond to 1.87, 3.44 and 4.39 L/h. Hulsmans et al. (2010) suggest that increasing the flow rate in a US system resulted in higher disinfection rate. However, in the system used here, changing the recirculation rate causes the faster sequential change from US to photo-Fenton, and therefore, shorter cycles of treatment. This leads to more completed rounds of sonication/Fenton, and consequently, better treatment results.

Figure 5.5.1a indicates the said effect; the explanation lies within the nature of the two actions. On the one hand, sonication assists the inactivation and the transformation of iron more times, so photo-Fenton is more efficient, and on the other hand, more completed cycles of illumination, provide higher possibilities for the emitted photons to target the bacteria (direct action) or the production of hydroxyl radicals to attack them (indirect action). Table 5.5.1 includes the hydraulic calculations concerning the timeframe of the actions.

Furthermore, in Table 5.5.1 the effect of changing the number of available reactors for the photo-Fenton treatment is presented. Reducing the number of reactors affects:

i) The available illuminated volume: The photo-Fenton action is also reduced, because less volume is under illumination (reduction of both direct and indirect damage).

ii) The volume of the sonicated water: Since the volume remains 500 mL and the reactors of ~75 mL are reduced, more water remains in the sonication chamber. Therefore, the ratio of US power/volume of water is modified and less power (but more time) is available for each mL of wastewater.

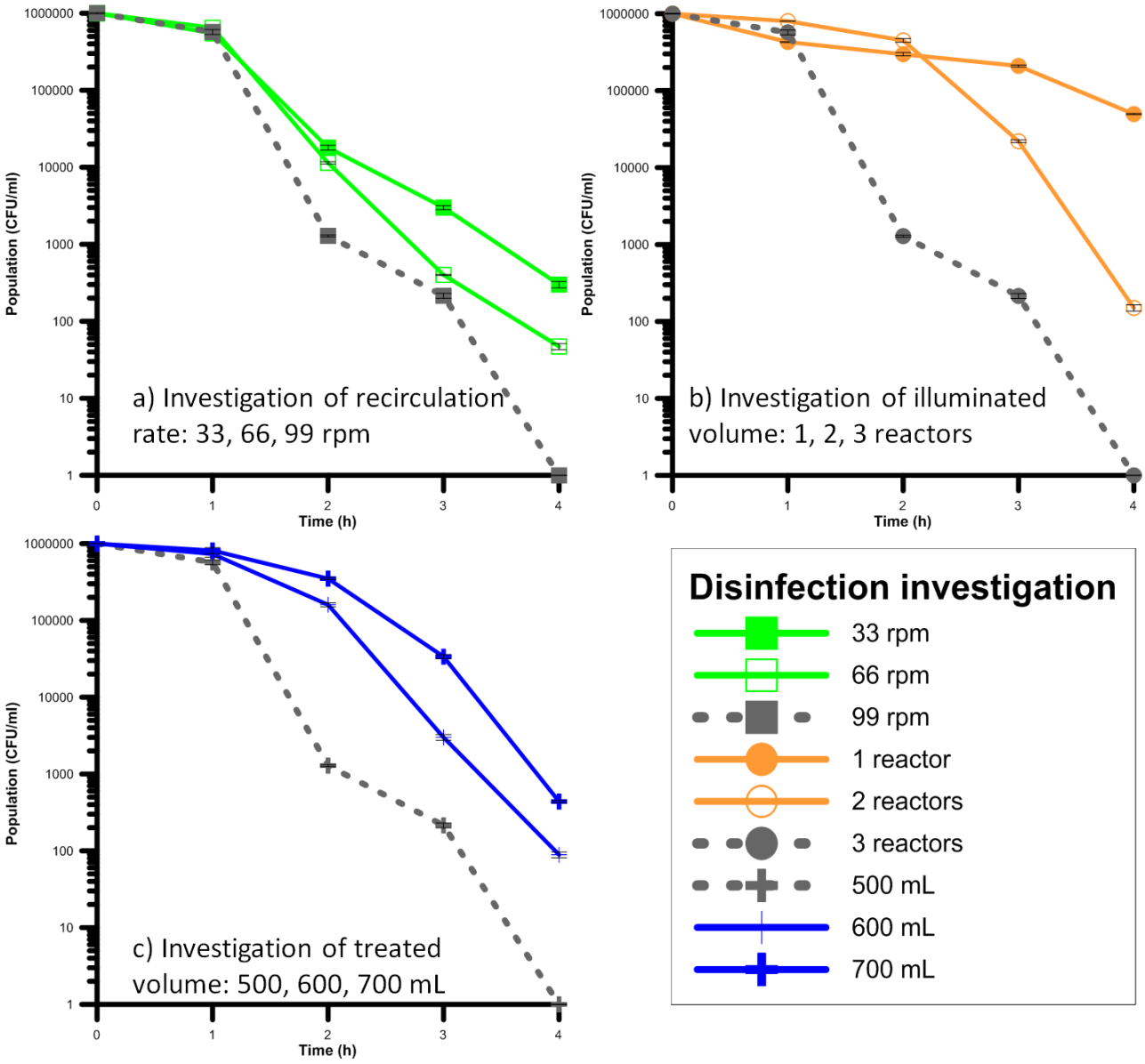

Figure 5.5.1: Influence of the hydraulic characteristics of the experimental set-up, on the efficiency of the system (1000W/m^2). a) Investigation of the recirculation rate (33, 66 and 99 rpm), b) Investigation of the illuminated volume (1, 2 and 3 reactors) and c) Investigation on the effect of the treated volume (500, 600 and 700 mL).

As a consequence, in Figure 5.5.1b, reducing the available reactors from 3 to 1 modifies the photo-Fenton to US treated volume ratio from 1.15 to 0.52 and 0.27, respectively (tubing volumes are neglected, because of the slow rate of the dark Fenton reaction). In terms of bacterial numbers, the inactivation rate is of 6, 4 and 3 $\log_{10}$U, for 3, 2 and 1 reactor available. Although this looks as a diminishing effect on the process efficiency, it also indicates that if less irradiation is available, the process is still effective, and an extension in the time would eventually lead to total inactivation. This could be an indication of the assisting/complementary character of the sonication, whenever photo-Fenton is not available.

Table 5.5.1. – Hydraulic calculations on the reactor set-up

Increasing recirculation speed from 33 to 99 rpm (1.87 to 4.39 L/h)																		
Reactors	**3**		**33**	**rpm**			**Reactors**	**3**		**66**	**rpm**			**Reactors**	**3**		**99**	**rpm**		
Volume	**500**	**mL**	**1.87**	**L/h**	**1.87**	**L/h**	**Volume**	**500**	**mL**	**3.44**	**L/h**	**3.44**	**L/h**	**Volume**	**500**	**mL**	**4.39**	**L/h**	**4.39**	**L/h**
Light	230	mL	7.38	min	46	%	**Light**	230	mL	4.01	min	46	%	**Light**	230	mL	3.14	min	46	%
Tubing	70	mL	2.25	min	14	%	**Tubing**	70	mL	1.22	min	14	%	**Tubing**	70	mL	0.96	min	14	%
US	200	mL	6.42	min	40	%	**US**	200	mL	3.49	min	40	%	**US**	200	mL	2.73	min	40	%
Total	**500**	**mL**	**16.04**	**min**	**100**	**%**	**Total**	**500**	**mL**	**8.72**	**min**	**100**	**%**	**Total**	**500**	**mL**	**6.83**	**min**	**100**	**%**
Increasing illuminated volume from 1 reactor to 3 (75 to 230 mL)																				
Reactors	**1**		**99**	**rpm**			**Reactors**	**2**		**99**	**rpm**			**Reactors**	**3**		**99**	**rpm**		
Volume	**500**	**mL**	**4.39**	**L/h**	**4.39**	**L/h**	**Volume**	**500**	**mL**	**4.39**	**L/h**	**4.39**	**L/h**	**Volume**	**500**	**mL**	**4.39**	**L/h**	**4.39**	**L/h**
Light	75	mL	1.03	min	15	%	**Light**	150	mL	2.05	min	30	%	**Light**	230	mL	3.14	min	46	%
Tubing	50	mL	0.68	min	10	%	**Tubing**	60	mL	0.82	min	12	%	**Tubing**	70	mL	0.96	min	14	%
US	375	mL	5.13	min	75	%	**US**	290	mL	3.96	min	58	%	**US**	200	mL	2.73	min	40	%
Total	**500**	**mL**	**6.83**	**min**	**100**	**%**	**Total**	**500**	**mL**	**6.83**	**min**	**100**	**%**	**Total**	**500mL**	**mL**	**6.83**	**min**	**100**	**%**
Increasing total treated volume from 500 to 700 mL																				
Reactors	**3**		**99**	**rpm**			**Reactors**	**3**		**99**	**rpm**			**Reactors**	**3**		**99**	**rpm**		
Volume	**500**	**mL**	**4.39**	**L/h**	**4.39**	**L/h**	**Volume**	**600**	**mL**	**4.39**	**L/h**	**4.39**	**L/h**	**Volume**	**700**	**mL**	**4.39**	**L/h**	**4.39**	**L/h**
Light	230	mL	3.14	min	46	%	**Light**	230	mL	3.14	min	38	%	**Light**	230	mL	3.14	min	33	%
Tubing	70	mL	0.96	min	14	%	**Tubing**	70	mL	0.96	min	12	%	**Tubing**	70	mL	0.96	min	10	%
US	200	mL	2.73	min	40	%	**US**	300	mL	4.10	min	50	%	**US**	400	mL	5.47	min	57	%
Total	**500**	**mL**	**6.83**	**min**	**100**	**%**	**Total**	**600**	**mL**	**8.20**	**min**	**100**	**%**	**Total**	**700**	**mL**	**9.57**	**min**	**100**	**%**

Finally, although literature suggests that modifying the sonication volume has not a significant effect on the efficiency of the sonication process (if the power-to volume ratio is respected) for bacterial inactivation (Hullsmans et al., 2010 and Al Bsoul et al., 2010), in Figure 5.5.1c, 2 and 3 $\log_{10}$U of differences are observed, respectively. A 20% and 40% increase of the volume lead to 33% and 50% reduction of the efficiency. This is explained by the domination of the process by the photo-Fenton reaction, rather than the sonication; it seems that it is not cost-effective to increase the total volume beyond a certain value.

5.5.2. Environmental influence

In the presented experimental set-up, an investigation of the temperature took place to assess the available operating temperatures of the coupled treatment, summarized in Figures 5.5.2a-b. The first operational limit was the temperature of 30˚C, to protect the piezoelectric disc. Recirculation of refrigerated water around the mantle of the US vessel ensured that the temperature was maintained within this limit. Reducing the operational temperature lead to decrease of the inactivation efficiency; the reaction became slower and less effective. This behavior (Figure 5.5.2a) is attributed to the reduced kinetics of the photo-Fenton reaction: it is known that temperature increases chemical reactions' kinetics, plus Ortega-Gomez et al. (2012) revealed the reduced inactivation rate in another bacterial species but also mesophilic with similar optimal growth temperature with *E. coli*, according to the Arrhenius equation.

On the contrary, altering the irradiation intensity (Figure 5.5.2b) did not significantly affect the efficiency of the process. It can be seen that ±20% difference in intensity resulted in similar required inactivation times. The initial reaction kinetics is faster at 1200 W/m^2 because of the increased direct action of the light; higher intensities lead to faster bacterial inactivation rates (Rincon and Pulgarin, 2003). The process is nevertheless effective even for lower intensities, suggesting that disinfection is possible even in days of low solar radiation.

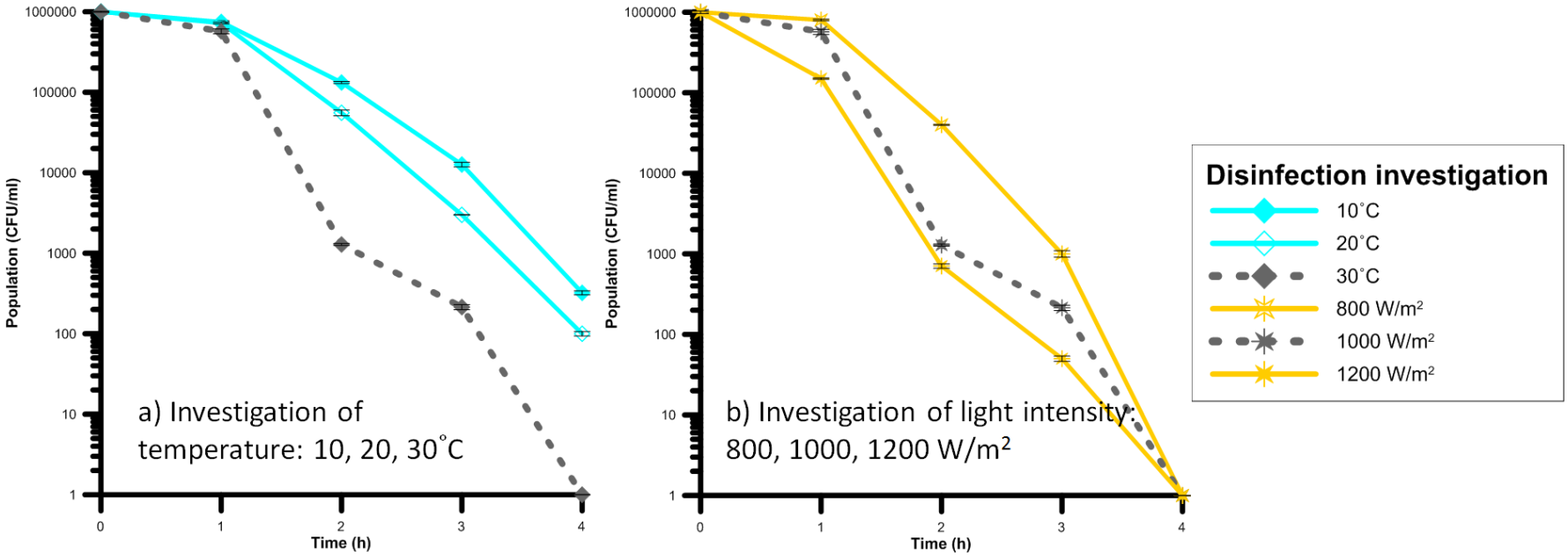

Figure 5.5.2: Influence of the environmental parameters on the efficiency of the system. a) Investigation of temperature (10, 20 and 30˚C), b) Investigation of light intensity (800, 1000 and 1200 W/m²).

5.5.3. Fenton and sonication factors

Figures 5.5.3a-c present the results of the investigation over the constituents of the Fenton reaction, as well as the only modifiable parameter of the US, the sonication power. Figures 5.5.3a and b demonstrate that there is a minimum quantity of the Fenton reagent required to be initially present, in order to maintain the integrity of the reaction throughout the treatment time. For instance, when the initial H_2O_2 concentration was reduced to 5 ppm, after the 2nd hour the reaction kinetics modified and inactivation rate was impaired. The oxidation of organic matter by the hydroxyl radicals is competing against the bacterial inactivation (Ortega-Gomez et al., 2013a). The contribution of photo-Fenton is reduced and the reaction continues with the produced H_2O_2 and the direct effects of irradiation and US. However, doubling the initial concentration of H_2O_2, provides enough $^{\cdot}OH$ radicals, to achieve the fastest inactivation time in all the experiments. Although unique, this case suggests a doubling on the supply costs of the process, but at the same time, a chance to improve otherwise impaired inactivation rates observed in previous cases.

Same effects apply for the iron content of the initial sample. When the iron concentration was halved, reaction rate and final outcome was mitigated, compared to the normal processes. Even though the US indirect action benefits iron transformation to the more useful state of ferrous ions, as a catalyst, it is obvious that it is in shortage. As soon as the initial concentration was doubled, no significant effect was observed, probably due to the saturation of the sample although presence of organic matter sustains iron in solution (Ortega-Gomez et al., 2013a). Hydroxyl radical production reached its peak and therefore no improvement was observed in bacterial inactivation.

Finally, the modification of the acoustic power was investigated, and its effects on removal efficiency are demonstrated in Figure 5.5.3c. Increasing US power results in higher particle breakage (Raman and Abbas, 2008) and more efficient removal, in the high frequencies (Hullsmans et al., 2010 and Al Bsoul et al., 2010). In the employed experimental set-up, decreasing the power from 20 to 10 W, and consequently, the power-to-volume ratio, decreased the efficiency, although in a non-linear, cost-effective manner; 50% reduction did not result to 50% decrease of the inactivation, but to 33%, although the main target is total inactivation. This suggests that the process can operate in economically low power, increasing its feasibility in real-scale application, and proves the complementary character of the two processes. Increasing the power to 40 W did not really enhance the removal efficiency, probably because 20 W was enough to induce the effects of sonication in the sample or the increase was not high enough to demonstrate measurable change, in the hourly sample scale.

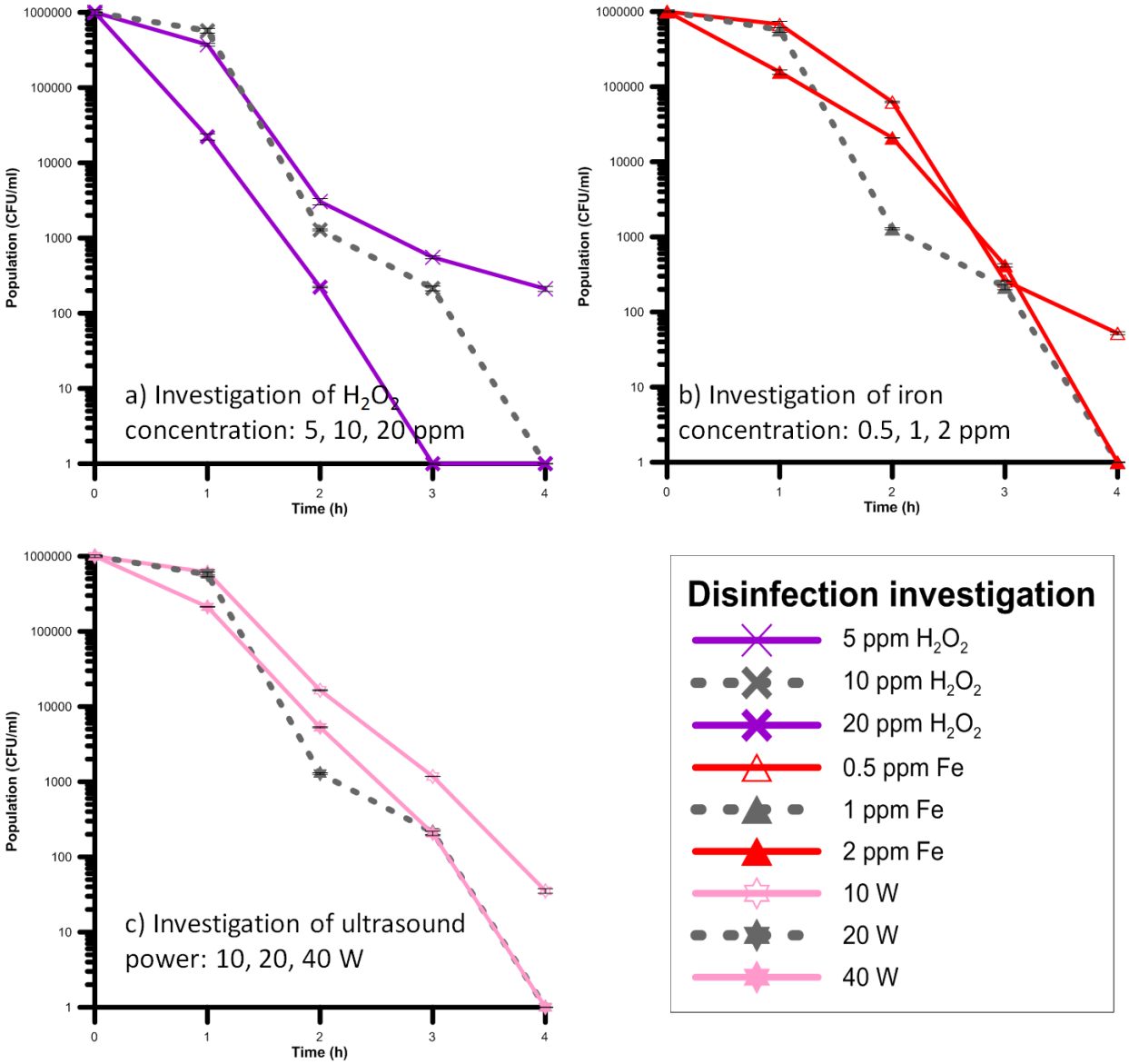

Figure 5.5.3: Influence of the Fenton reagents and the sonication intensity on the efficiency of the system. a) Investigation of the H_2O_2 concentration (5, 10 and 20 ppm), b) Investigation of the iron concentration (0.5, 1, and 2 ppm) and c) Investigation on the ultrasound power (10, 20 and 40 W).

5.6. Conclusions

The results of this study revealed that for short intermittent parts within a short period of exposure to light, recirculation speed in mechanically non-damaging rates was directly influencing bacterial inactivation. Higher speeds resulted in a less fluctuated disinfection process, due to the higher frequency of illumination, when compared to longer periods with the same total time of exposure. Slower recirculation rates enhanced bacterial defense mechanisms and promote growth, resulting in lower inactivation rates.

Also, at the intensity employed, a period of 2-3 hours of exposure to light has been proven an adequate time to effectively disinfect wastewater, by inflicting irreparable damage. Long dark intervals, when posed early in the disinfection process hindered bacterial inactivation. Concerning the kinetics of the process, the kinetics of each light interval scenario performed reflect light and dark periods by the change in curve slopes. Plus, the results of different illumination conditions during the first hour of light exposure confirmed the crucial importance of continuous, constant irradiation during this period. When these conditions prevailed, a 1-h shoulder occurred. Upon the infliction of intermittence in light supply, a shoulder up to 3-h was observed.

Moreover, it is promising that within a period of 6 hours, regardless of the existence of light intermission or not, total disinfection was achieved; the cumulative light dose necessary to disinfect wastewater was achieved within 3 hours of accumulated illumination. However, for lower light intensities higher exposure times will be expected, if the light supply is not continuous.

As far as the post-irradiation events are concerned, bacterial regrowth due to the dark repair mechanisms was not observed when total inactivation was achieved. In most cases the total exposure time and the corresponding dose was enough to render the bacteria population unable to regrow. Intermittence directly influences inactivation rate during illuminated periods but apart from the trials that achieved total inactivation, the high frequency intermittence demonstrated similar active bacterial counts, regardless of the recirculation rates. In low frequency intermittence experiments, the post-irradiation events are similar, attributed to the lethal dose achieved within the disinfection period. When total inactivation is not achieved, partial survival of bacteria in the wastewater is also observed, due to the existence of nutrients in the water matrix. If an energy threshold exists, after which the dark repair mechanism is no longer able to help bacteria recover, it seems that it has been achieved. This point has to be further examined by proper set-up, but for sure, the tests prove that effective suppression of growth has been achieved, even in a friendly environment for bacterial populations.

In the stepwise introduction of treatment factors in the US/pF joint treatment in the lab-scale, CPC-like reactor, light has been, by far, the most significant effect amongst all parameters. Light alone has proven to be much more effective than US, Fenton, or the combination of the two. Also, light combined with Fenton (photo-Fenton) and US with photo-Fenton (US-pF) have been the two most effective disinfection options.

This can be attributed to the well-known multi-level effect of light, interpreted by the direct action of the light against bacteria, the indirect ROS production and the direct role of light in Fe^{2+} reduction (photo-Fenton). High frequency-low intensity ultrasound alone has not provided significant immediate bacterial reduction, but in long term, causes either apoptotic behavior or increased susceptibility to the Fenton damage. When combined with light, US has resulted in high inactivation rates in 4 h, even 4 $\log_{10}$U when the Fenton reagents were introduced (joint US-pF process). This makes US-pF treatments an attractive alternative in permanent (bacteriologically non-recurring) treatment methods.

Regarding the contribution of the operational parameters, temperature and volume introduce important constraints: Temperature favors disinfection but must not exceed 30ºC for US source protection; increasing the sonication volume will result in higher US-to-pF ratios and lower efficiencies. However, modification of the US-to-pF volume ratio can be opted regarding the post-treatment handling of the sample; if immediate disinfecting action is required, pF can be promoted, in any other case the continuous decay US causes will result to total inactivation during sample storage. Also, addition of extra hydrogen peroxide and iron seemed to benefit bacterial inactivation. From the scope of this work, the choice of mild photo-Fenton was satisfactory, but in a real application, this choice, over normal amounts of reagents can be also altered depending on the requirements downstream.

Nevertheless, these results indicate that this US/pF process surpasses limitations that averted installations of either one of the processes on wastewater treatment, such as the dead times in the dark storage tanks, the power-to-volume ratio of the ultrasound, etc. It seems that the combination of the two actions in sequential form helps limit the disadvantages each method has separately; whenever Fenton was limited, cellular regeneration was hindered by US, thus compensating during dark periods and thus improving photo-Fenton treatment efficiency.

Such results leave an open window of opportunity of applying solar-driven disinfection of wastewater in greater extents, even in areas with interruptions during the planned experimental times. What is more important, however, is the highlighting of design strategies if the use of a CPC is intended; the tested dark-to-light ratio is one of the numerous possibilities when designing the system. The study of both high and low-frequency intermittence allows to take into account these results in other more feasible solutions in the less favored areas, such as ponds; the influence of dark periods mitigates the effects of solar disinfection and this work can contribute to the estimation of their design parameters. Even in relatively unfavorable hydraulic conditions for disinfection, the solar disinfection methods applied render the disinfected water able to be considered for secondary uses, thus saving from the drinking water supplies of the arid areas.

Chapter 6. Overall conclusions

First of all, it was found that solar disinfection was efficient when it was applied in synthetic secondary effluent. The disinfection experiments have proved that if the initial concentration of the microorganisms and the treatment conditions are known, one can determine the outcome of the treatment process, despite the fact that bacterial growth has interfered in the normal evolution of the process.

In fact, the treatment conditions influence percentage of elimination. Factors as the light intensity, the manner of delivery (continuous-intermittent) and the temperature of water during treatment are more decisive, compared with the classic time-dose approach. However, it was found that temperature influences inactivation in a dual, opposite manner. The best results of the light-temperature synergy were found in very low and very high temperatures. This classification of the results according to the applied temperature range produced a quite accurate, temperature dependent linear model, which describes well the inactivation kinetics.

When regrowth was observed it was correlated with the leftover bacteria at the end of the treatment, because the increase is noticeable in inadequately treated samples. This residual population is also linked to the temperature during solar disinfection; high temperatures were found to suppress bacterial regrowth. Storage of wastewater was efficient in highly irradiated/thermally treated bacteria and specifications on the safe combinations of light and temperature were provided, to influence the safe storage times. Hence, along with the constraints on acquiring total disinfection, predictive information on the post irradiation fate of microorganisms was obtained.

Also, the efforts on modeling the bacterial inactivation and the regrowth, only according to the intensity of light, provided with a coherent profile of the necessary dose. When temperature was accounted for, its actions resulted in discrimination between the dose effects deriving from high or low temperatures and intensities. Concerning regrowth, an efficient bacteriostatic dose was found, beyond which, bacterial survival kinetics deterministically present decay.

Furthermore, the post-treatment phase of experiments can influence the design of treatment systems and processes. It was found that according to the local context of discharge, on temperature and type of water body, the following post irradiation events vary from matrix to matrix. The two factors studied (type of matrix, rate of dilution) estimated the survival kinetics as a function of temperature; varied kinetics, from delayed to excessive growth were found according to storage temperature and nutrient availability-as shown by the ratios of dilution in the matrices. Also, the matrix itself affected the

outcome, imposing a kinetics profile, linked to the osmotic difference, as well as the presence of salts and nutrients. However, regardless the matrix, a pattern was observed, where bacteria that were treated for short times presented high resistance, when were diluted even in unfriendly matrices, and high growth rates when growth was permitted.

If different parts of the light spectrum are to be considered as a post-irradiation condition, it was observed that applying 6 different types of fluorescent lamps caused different response, according to the corresponding wavelength. In all cases, however, no regrowth or photoreactivation was observed in samples with no cultivable bacteria. Lamps that emit UV-ranged wavelengths (BL blue and actinic BL), even in very low proportions initiated or accelerated bacterial inactivation, according to the previous damage state of bacteria. The visible range on the other hand initiated mild photoreactivation (mostly blue and less green light), while the visible light (and yellow light) photoactivated the relatively healthy cells or continued the inactivating profile of the heavily damaged. In overall, the response was modeled and attributed mainly to the solar dose, but the multiple targets of the light action mode render solar-inflicted damage less probable to be mended, compared to the UVC light damage.

The applications in recirculating flow reactors revealed that for short intermittent parts within a short period of exposure to light, recirculation speed in mechanically non-damaging rates was directly influencing bacterial inactivation. Higher recirculation speeds resulted in a less fluctuated disinfection process, due to the higher frequency of illumination, when compared to longer periods of light and dark with the same total time of exposure. Slower recirculation rates enhanced bacterial defense mechanisms and promoted growth, resulting in lower inactivation rates. The kinetics of each light interval scenario performed reflected the light and dark periods by the change in curve slopes. Plus, the results of different illumination conditions during the first hour of light exposure confirmed the crucial importance of continuous, constant irradiation during this period; intermittence resulted in prolongation of the shoulder lag inactivation phase.

The enhancement with ultrasound and photo-Fenton provided a solution for the application of solar wastewater treatment systems. The applied high frequency-low intensity sonication system was moderately efficient in direct bacterial inactivation, but the long term effects represent an apoptotic behavior and/or increased vulnerability to the Fenton damage. When combined with light, sonication led to high inactivation rates, with increasing tendency when the Fenton reagents were introduced (joint US-pF process). However, in the context of developing countries this is relatively incompatible. If the construction costs are to be considered for a surface able to disinfect wastewater, the technical implementation seems rather unlikely. Therefore, application in a series of ponds is to be considered.

Regrowth is a matter that influenced the design and applications of SODIS for drinking water. Although water aimed directly for human consumption needs to be completely sterilized, wastewater does not have the same effluent standards. Hence, according to this work, bacteria should be just subjected to

treatment that will result in inactivation, even in long term. The retention times for wastewater can lead to total inactivation, and if this is achieved, there is no regrowth observed. As a result, this reappearance is a matter that should be dealt in a holistic approach; the methods applied in this Thesis have shown that re-population of the samples was mostly due to incomplete inactivation of bacteria and even more importantly, enhanced growth of the already cultivable bacteria.

References

Acra, A., Jurdi, M., Mu'allem, H., Karahagopian, Y., Raffoul, Z. (1989). Sunlight as disinfectant, Lancet, p. 280–281.

Acra, A., Jurdi, M., Mu'allem, H., Karahagopian, Y., Raffoul, Z. (1990). Water Disinfection by Solar Radiation, *International Development Research Centre, Ottawa*

Acra, A., Raffoul, Z., & Karahagopian, Y. (1984). Solar disinfection of drinking water and oral rehydration solutions: guidelines for household application in developing countries.

Al Bsoul, A., Magnin, J. P., Commenges-Bernole, N., Gondrexon, N., Willison, J., & Petrier, C. (2010). Effectiveness of ultrasound for the destruction of *Mycobacterium sp*. strain (6PY1). *Ultrason Sonochem, 17*(1), 106-110. doi: 10.1016/j.ultsonch.2009.04.005

Alrousan, D., Dunlop, P. S., McMurray, T. A., & Byrne, J. A. (2009). Photocatalytic inactivation of *E. coli* in surface water using immobilised nanoparticle TiO_2 films. *Water Res, 43*(1), 47-54.

Amsler, C. D. (2008). *Algal chemical ecology*: Springer.

Avery, L. M., Williams, A. P., Killham, K., & Jones, D. L. (2008). Survival of *Escherichia coli* O157:H7 in waters from lakes, rivers, puddles and animal-drinking troughs. *Sci Total Environ, 389*(2-3), 378-385. doi: 10.1016/j.scitotenv.2007.08.049

Barer, M. R., Gribbon, L. T., Harwood, C. R., & Nwoguh, C. E. (1993). The viable but non-culturable hypothesis and medical bacteriology. *Reviews in Medical Microbiology, 4*(4), 183-191.

Benabbou, A., Derriche, Z., Felix, C., Lejeune, P., & Guillard, C. (2007). Photocatalytic inactivation of *E. coli*: Effect of concentration of TiO2 and microorganism, nature, and intensity of UV irradiation. *Applied Catalysis B: Environmental, 76*(3), 257-263.

Berney, M., Weilenmann, H. U., Simonetti, A., & Egli, T. (2006). Efficacy of solar disinfection of *Escherichia coli, Shigella flexneri, Salmonella Typhimurium* and *Vibrio cholerae*. *J Appl Microbiol, 101*(4), 828-836. doi: 10.1111/j.1365-2672.2006.02983.x

Berney, M., Weilenmann, H.-U., & Egli, T. (2007). Adaptation to UVA radiation of *E. coli* growing in continuous culture. *Journal of Photochemistry and Photobiology B: Biology, 86*(2), 149-159.

Bichai, F., Polo-López, M. I., & Fernández Ibañez, P. (2012). Solar disinfection of wastewater to reduce contamination of lettuce crops by *Escherichia coli* in reclaimed water irrigation. *Water Res, 46*(18), 6040-6050. doi: http://dx.doi.org/10.1016/j.watres.2012.08.024

Blaustein, R. A., Pachepsky, Y., Hill, R. L., Shelton, D. R., & Whelan, G. (2013). *Escherichia coli* survival in waters: temperature dependence. *Water Res, 47*(2), 569-578. doi: 10.1016/j.watres.2012.10.027

Blesa, M. A., & Litter, M. I. (2007). Low-cost TiO_2 photocatalytic technology for water potabilization in plastic bottles for isolated regions. Photocatalyst fixation.

Block, S., Seng, V., & Goswami, D. (1997). Chemically enhanced sunlight for killing bacteria. *Transactions-American Society of Mechanical Engineers Journal of Solar Energy Engineering, 119*, 85-91.

Bohrerova, Z., & Linden, K. G. (2007). Standardizing photoreactivation: Comparison of DNA photorepair rate in *E. coli* using four different fluorescent lamps. *Water Res, 41*(12), 2832-2838.

Bosshard, F., Berney, M., Scheifele, M., Weilenmann, H. U., & Egli, T. (2009). Solar disinfection (SODIS) and subsequent dark storage of *Salmonella typhimurium* and *Shigella flexneri* monitored by flow cytometry. *Microbiology, 155*(Pt 4), 1310-1317. doi: 10.1099/mic.0.024794-0

Bosshard, F., Bucheli, M., Meur, Y., & Egli, T. (2010a). The respiratory chain is the cell's Achilles' heel during UVA inactivation in Escherichia coli. *Microbiology, 156*(7), 2006-2015.

Bosshard, F., Riedel, K., Schneider, T., Geiser, C., Bucheli, M., & Egli, T. (2010b). Protein oxidation and aggregation in UVA-irradiated *Escherichia coli* cells as signs of accelerated cellular senescence. *Environ Microbiol, 12*(11), 2931-2945. doi: 10.1111/j.1462-2920.2010.02268.x

Boyle, M., Sichel, C., Fernández-Ibáñez, P., Arias-Quiroz, G., Iriarte-Puña, M., Mercado, A., . . . McGuigan, K. (2008). Bactericidal effect of solar water disinfection under real sunlight conditions. *Applied and environmental microbiology, 74*(10), 2997-3001.

Bracho, N., Lloyd, B., & Aldana, G. (2006). Optimisation of hydraulic performance to maximise faecal coliform removal in maturation ponds. *Water Res, 40*(8), 1677-1685.

Britt, A. B. (1996). DNA damage and repair in plants. *Annual review of plant biology, 47*(1), 75-100.

Broekman, S., Pohlmann, O., Beardwood, E. S., & de Meulenaer, E. C. (2010). Ultrasonic treatment for microbiological control of water systems. *Ultrason Sonochem, 17*(6), 1041-1048. doi: 10.1016/j.ultsonch.2009.11.011

Brotchie, A., Grieser, F., & Ashokkumar, M. (2009). Effect of power and frequency on bubble-size distributions in acoustic cavitation. *Physical review letters, 102*(8), 084302.

Butz, P., & Tauscher, B. (2002). Emerging technologies: chemical aspects. *Food research international, 35*(2), 279-284.

Caballero, L., Whitehead, K., Allen, N., & Verran, J. (2009). Inactivation of *E. coli* on immobilized TiO_2 using fluorescent light. *Journal of Photochemistry and Photobiology A: Chemistry, 202*(2), 92-98.

Cappelletti, G. (2002). An experiment with a plastic solar still. *Desalination, 142*(3), 221-227.

Chan, Y., & Killick, E. (1995). The effect of salinity, light and temperature in a disposal environment on the recovery of *E. coli* following exposure to ultraviolet radiation. *Water Res, 29*(5), 1373-1377.

Chandran, A., & Mohamed Hatha, A. A. (2005). Relative survival of *Escherichia coli* and *Salmonella typhimurium* in a tropical estuary. *Water Res, 39*(7), 1397-1403. doi: 10.1016/j.watres.2005.01.010

Chauhan, M. (2004). Effect of ultrasound on the redox reactions of iron (II) and (III). *Indian journal of chemistry. Sect. A: Inorganic, physical, theoretical & analytical, 43*(10), 2098-2101.

Chiang, S. M., & Schellhorn, H. E. (2012). Regulators of oxidative stress response genes in *Escherichia coli* and their functional conservation in bacteria. *Arch Biochem Biophys, 525*(2), 161-169. doi: 10.1016/j.abb.2012.02.007

Cleaver, J. E. (2003). Photoreactivation. *DNA repair, 2*(5), 629-638.

Craggs, R., Davies-Colley, R., Tanner, C., & Sukias, J. (2003). Advanced pond system: performance with high rate ponds of different depths and areas. *Water Science & Technology, 48*(2), 259-267.

Craggs, R. J., Zwart, A., Nagels, J. W., & Davies-Colley, R. J. (2004). Modelling sunlight disinfection in a high rate pond. *Ecological Engineering, 22*(2), 113-122. doi: 10.1016/j.ecoleng.2004.03.001

Craik, S. A., Weldon, D., Finch, G. R., Bolton, J. R., & Belosevic, M. (2001). Inactivation of *Cryptosporidium parvum* oocysts using medium-and low-pressure ultraviolet radiation. *Water Res, 35*(6), 1387-1398.

Curtis, T. P., Mara, D. D., & Silva, S. A. (1992a). Influence of pH, oxygen, and humic substances on ability of sunlight to damage fecal coliforms in waste stabilization pond water. *Applied and environmental microbiology, 58*(4), 1335-1343.

Curtis, T., Mara, D. D., & Silva, S. A. (1992b). The effect of sunlight on faecal coliforms in ponds: implications for research and design. *Water Science & Technology, 26*(7-8), 1729-1738.

Dahl, E. (1976). Physicochemical aspects of disinfection of water by means of ultrasound and ozone. *Water Res, 10*(8), 677-684.

Dahlén, J., Bertilsson, S., & Pettersson, C. (1996). Effects of UV-A irradiation on dissolved organic matter in humic surface waters. *Environment International, 22*(5), 501-506.

Dalrymple, O. K., Stefanakos, E., Trotz, M. A., & Goswami, D. Y. (2010). A review of the mechanisms and modeling of photocatalytic disinfection. *Applied Catalysis B: Environmental, 98*(1), 27-38.

Darakas, E. (2001). A simple mathematical formula describing the survival kinetics of *E. coli* in natural waters. *International Journal of Environmental Studies, 58*(3), 365-372.

Darakas, E. (2002). *E. coli* kinetics-effect of temperature on the maintenance and respectively the decay phase. *Environmental monitoring and assessment, 78*(2), 101-110.

Darakas, E., Koumoulidou, T., & Lazaridou, D. (2009). Fecal indicator bacteria declines via a dilution of wastewater in seawater. *Desalination, 248*(1-3), 1008-1015. doi: 10.1016/j.desal.2008.10.017

Davidson, R. S., Safdar, A., Spencer, J. D., & Robinson, B. (1987). Applications of ultrasound to organic chemistry. *Ultrasonics, 25*(1), 35-39. doi: http://dx.doi.org/10.1016/0041-624X(87)90009-6

Davies, C. M., & Evison, L. M. (1991). Sunlight and the survival of enteric bacteria in natural waters. *J Appl Microbiol, 70*(3), 265-274.

Davies-Colley, R., Hickey, C., & Quinn, J. (1995). Organic matter, nutrients, and optical characteristics of sewage lagoon effluents. *New Zealand Journal of marine and freshwater research, 29*(2), 235-250.

Davies-Colley, R., Donnison, A., & Speed, D. (1997). Sunlight wavelengths inactivating faecal indicator microorganisms in waste stabilisation ponds. *Water Science and Technology, 35*(11), 219-225.

Davies-Colley, R. J., Donnison, A. M., Speed, D. J., Ross, C. M., & Nagels, J. W. (1999). Inactivation of faecal indicator micro-organisms in waste stabilisation ponds: interactions of environmental factors

with sunlight. *Water Res, 33*(5), 1220-1230. doi: http://dx.doi.org/10.1016/S0043-1354(98)00321-2

Dawes, I., & Sutherland, I. (1976). Microbial Physiology. Basic Microbiology: Blackwell Scientific Publications. Oxford. l85 pages.

Douki, T. (2013). The variety of UV-induced pyrimidine dimeric photoproducts in DNA as shown by chromatographic quantification methods. *Photochemical & Photobiological Sciences, 12*(8), 1286-1302.

Downes, A., & Blunt, T. P. (1877). Researches on the effect of light upon bacteria and other organisms. *Proceedings of the Royal Society of London, 26*(179-184), 488-500.

Drinan, J. E., & Spellman, F. R. (2012). *Water and wastewater treatment: A guide for the nonengineering professional*: Crc Press.

Dünkel, L. (1992). Organic Photochemistry:"A Visual Approach". *Zeitschrift für Physikalische Chemie, 177*(Part_1), 122-123.

Dunlop, P. S., Ciavola, M., Rizzo, L., & Byrne, J. A. (2011). Inactivation and injury assessment of *Escherichia coli* during solar and photocatalytic disinfection in LDPE bags. *Chemosphere, 85*(7), 1160-1166. doi: 10.1016/j.chemosphere.2011.09.006

Fabbricino, M., & d'Antonio, L. (2012). Use of solar radiation for continuous water disinfection in isolated areas. *Environmental Technology, 33*(5), 539-544. doi: 10.1080/09593330.2011.584570

FAO Corporate Document Repository, Site Selection for Aquaculture: Physical Features of Water, M.N. Kutty, 1987, http://www.fao.org/docrep/field/003/ac174e/AC174E00.htm#TOC, last accessed: 27/10/2013

Fellows, P. J. (2009). *Food processing technology: principles and practice*: Elsevier.

Fernández, P., Blanco, J., Sichel, C., & Malato, S. (2005). Water disinfection by solar photocatalysis using compound parabolic collectors. *Catalysis Today, 101*(3), 345-352.

Fernández-Ibáñez, P., Sichel, C., Polo-López, M., de Cara-García, M., & Tello, J. (2009). Photocatalytic disinfection of natural well water contaminated by Fusarium solani using TiO_2 slurry in solar CPC photo-reactors. *Catalysis Today, 144*(1), 62-68.

Flint, K. (1987). The long-term survival of Escherichia coli in river water. *J Appl Microbiol, 63*(3), 261-270.

Fotadar, U., Zaveloff, P., & Terracio, L. (2005). Growth of *Escherichia coli* at elevated temperatures. *J Basic Microbiol, 45*(5), 403-404.

Gamage, J., & Zhang, Z. (2010). Applications of photocatalytic disinfection. *International Journal of Photoenergy, 2010*.

Gameson, A. (1975). Discharge of sewage from sea outfalls, Pergammon Press, Oxford.

Geeraerd, A., Herremans, C., & Van Impe, J. (2000). Structural model requirements to describe microbial inactivation during a mild heat treatment. *International Journal of Food Microbiology, 59*(3), 185-209.

Geeraerd, A., Valdramidis, V., & Van Impe, J. (2005). GInaFiT, a freeware tool to assess non-log-linear microbial survivor curves. *International Journal of Food Microbiology, 102*(1), 95-105.

Gelover, S., Gómez, L. A., Reyes, K., & Teresa Leal, M. (2006). A practical demonstration of water disinfection using TiO_2 films and sunlight. *Water Res, 40*(17), 3274-3280.

Genthner, F. J., Upadhyay, J., Campbell, R. P., & Genthner, B. R. S. (1990). Anomalies in the enumeration of starved bacteria on culture media containing nalidic acid and tetracycline. *Microb Ecol, 20*(1), 283-288.

Giannakis, S., Merino Gamo, A. I., Darakas, E., Escalas-Cañellas, A., & Pulgarin, C. (2013). Impact of different light intermittence regimes on bacteria during simulated solar treatment of secondary effluent: Implications of the inserted dark periods. *Solar Energy, 98, Part C*(0), 572-581. doi: http://dx.doi.org/10.1016/j.solener.2013.10.022

Gill, L., & Price, C. (2010). Preliminary observations of a continuous flow solar disinfection system for a rural community in Kenya. *Energy, 35*(12), 4607-4611.

Gomes, A. I., Santos, J. C., Vilar, V. J. P., & Boaventura, R. A. R. (2009b). Inactivation of Bacteria *E. coli* and photodegradation of humic acids using natural sunlight. *Applied Catalysis B: Environmental, 88*(3-4), 283-291. doi: 10.1016/j.apcatb.2008.11.014

Gomes, A. I., Vilar, V. J. P., & Boaventura, R. A. R. (2009a). Synthetic and natural waters disinfection using natural solar radiation in a pilot plant with CPCs. *Catalysis Today, 144*(1-2), 55-61. doi: 10.1016/j.cattod.2008.12.023

Guo, M., Huang, J., Hu, H., & Liu, W. (2011). Growth and repair potential of three species of bacteria in reclaimed wastewater after UV disinfection. *Biomedical and Environmental Sciences, 24*(4), 400-407.

Haas, C. N., & Engelbrecht, R. S. (1980). Physiological alterations of vegetative microorganisms resulting from chlorination. *Journal (Water Pollution Control Federation)*, 1976-1989.

Haller, L., Amedegnato, E., Poté, J., & Wildi, W. (2009). Influence of Freshwater Sediment Characteristics on Persistence of Fecal Indicator Bacteria. *Water, Air, and Soil Pollution, 203*(1-4), 217-227. doi: 10.1007/s11270-009-0005-0

Haller, L., Poté, J., Loizeau, J.-L., & Wildi, W. (2009a). Distribution and survival of faecal indicator bacteria in the sediments of the Bay of Vidy, Lake Geneva, Switzerland. *Ecological Indicators, 9*(3), 540-547. doi: 10.1016/j.ecolind.2008.08.001

Hallmich, C., & Gehr, R. (2010). Effect of pre-and post-UV disinfection conditions on photoreactivation of fecal coliforms in wastewater effluents. *Water Res, 44*(9), 2885-2893.

Harm, W. (1980). *Biological effects of ultraviolet radiation* (Vol. 1): Cambridge University Press Cambridge.

Heaselgrave, W., & Kilvington, S. (2011). The efficacy of simulated solar disinfection (SODIS) against Ascaris, Giardia, Acanthamoeba, Naegleria, Entamoeba and Cryptosporidium. *Acta Trop, 119*(2), 138-143.

Hijnen, W., Beerendonk, E., & Medema, G. J. (2006). Inactivation credit of UV radiation for viruses, bacteria and protozoan (oo) cysts in water: a review. *Water Res, 40*(1), 3-22.

Holm, E. R., Stamper, D. M., Brizzolara, R. A., Barnes, L., Deamer, N., & Burkholder, J. M. (2008). Sonication of bacteria, phytoplankton and zooplankton: Application to treatment of ballast water. *Mar Pollut Bull, 56*(6), 1201-1208. doi: 10.1016/j.marpolbul.2008.02.007

Hua, I., & Hoffmann, M. R. (1997). Optimization of ultrasonic irradiation as an advanced oxidation technology. *Environmental Science & Technology, 31*(8), 2237-2243.

Hua, I., & Thompson, J. E. (2000). Inactivation of *E. coli* by sonication at discrete ultrasonic frequencies. *Water Res, 34*(15), 3888-3893.

Hulsmans, A., Joris, K., Lambert, N., Rediers, H., Declerck, P., Delaedt, Y., . . . Liers, S. (2010). Evaluation of process parameters of ultrasonic treatment of bacterial suspensions in a pilot scale water disinfection system. *Ultrason Sonochem, 17*(6), 1004-1009. doi: 10.1016/j.ultsonch.2009.10.013

Ingraham, J. (1999). Effect of temperature, pH, water acidity, and pressure on growth in *Escherichia coli* and *Salmonella typhimurium*. *Cellular and molecular biology. Neidhardt, C. f. Washington, DC, American Society for Microbiology, 1*, 1543-1550.

Jenkins, M. B., Endale, D. M., Fisher, D. S., Adams, M. P., Lowrance, R., Newton, G. L., & Vellidis, G. (2012). Survival dynamics of fecal bacteria in ponds in agricultural watersheds of the Piedmont and Coastal Plain of Georgia. *Water Res, 46*(1), 176-186. doi: 10.1016/j.watres.2011.10.049

Johnson, F. H., & Lewin, I. (1946). The growth rate of *E. coli* in relation to temperature, quinine and coenzyme. *Journal of Cellular and Comparative Physiology, 28*(1), 47-75.

Jonkers, H., Palin, D., Flink, P., & Thijssen, A. (2013). Microbially mediated carbonation of marine alkaline minerals: Potential for concrete crack healing.

Joyce, E., Al-Hashimi, A., & Mason, T. (2011). Assessing the effect of different ultrasonic frequencies on bacterial viability using flow cytometry. *J Appl Microbiol, 110*(4), 862-870.

Jungfer, C., Schwartz, T., & Obst, U. (2007). UV-induced dark repair mechanisms in bacteria associated with drinking water. *Water Res, 41*(1), 188-196. doi: 10.1016/j.watres.2006.09.001

Kalisvaart, B. (2004). Re-use of wastewater: preventing the recovery of pathogens by using medium-pressure UV lamp technology. *Water Science & Technology, 50*(6), 337-344.

Kashimada, K., Kamiko, N., Yamamoto, K., & Ohgaki, S. (1996). Assessment of photoreactivation following ultraviolet light disinfection. *Water Science and Technology, 33*(10), 261-269.

Kay, D., Stapleton, C. M., Wyer, M. D., McDonald, A. T., Crowther, J., Paul, N., . . . Gardner, S. (2005). Decay of intestinal enterococci concentrations in high-energy estuarine and coastal waters: towards real-time T90 values for modelling faecal indicators in recreational waters. *Water Res, 39*(4), 655-667. doi: 10.1016/j.watres.2004.11.014

Kehoe, S. C. (2001). Batch Process Solar Disinfection of Drinking Water: Process and Pathogenicity, PhD Thesis, Royal College of Surgeons in Ireland, Dublin

Kivaisi, A. K. (2001). The potential for constructed wetlands for wastewater treatment and reuse in developing countries: a review. *Ecological Engineering, 16*(4), 545-560. doi: http://dx.doi.org/10.1016/S0925-8574(00)00113-0

Koda, S., Miyamoto, M., Toma, M., Matsuoka, T., & Maebayashi, M. (2009). Inactivation of *Escherichia coli* and *Streptococcus* mutants by ultrasound at 500 kHz. *Ultrason Sonochem, 16*(5), 655-659. doi: 10.1016/j.ultsonch.2009.02.003

Kositzi, M., Poulios, I., Malato, S., Cáceres, J., & Campos, A. (2004). Solar photocatalytic treatment of synthetic municipal wastewater. *Water Res, 38*(5), 1147-1154.

Kryszczuk, M. D. (1962). *The effect of ultrasound in a chemotherapeutic study of ascites tumor cells.* Catholic University of America Press, Washington. Available from http://worldcat.org /z-wcorg/ database.

Kumar, A., Tyagi, M. B., Singh, N., Tyagi, R., Jha, P. N., Sinha, R. P., & Häder, D.-P. (2003). Role of white light in reversing UV-B-mediated effects in the N2-fixing cyanobacterium *Anabaena* BT2. *Journal of Photochemistry and Photobiology B: Biology, 71*(1–3), 35-42. doi: http://dx.doi.org/10.1016/j.jphotobiol.2003.07.002

Lage, C., Teixeira, P., & Leitao, A. (2000). Non-coherent visible and infrared radiation increase survival to UV (254 nm) in *E. coli* K12. *Journal of Photochemistry and Photobiology B: Biology, 54*(2), 155-161.

Lanao, M., Ormad, M., Mosteo, R., & Ovelleiro, J. (2012). Inactivation of *Enterococcus sp*. by photolysis and TiO_2 photocatalysis with H_2O_2 in natural water. *Solar Energy, 86*(1), 619-625.

Leighton, T. (1994). *The acoustic bubble*: Access Online via Elsevier.

Levine, N. D. (1975). Buchanan, R. E. & Gibbons, N. E., eds. 1974. Bergey's Manual of Determinative Bacteriology. 8th ed. Williams & Wilkins Co., Baltimore, Md. 21202. xxvi + 1246 pp.. *Journal of Eukaryotic Microbiology, 22*(1), 7-7. doi: 10.1111/j.1550-7408.1975.tb00935.x

Li, C., Deng, B., & Kim, C. N. (2010). A numerical prediction on the reduction of microorganisms with UV disinfection. *Journal of mechanical science and technology, 24*(7), 1465-1473.

Lindenauer, K. G., & Darby, J. L. (1994). Ultraviolet disinfection of wastewater: effect of dose on subsequent photoreactivation. *Water Res, 28*(4), 805-817.

Lonnen, J., Kilvington, S., Kehoe, S., Al-Touati, F., & McGuigan, K. (2005). Solar and photocatalytic disinfection of protozoan, fungal and bacterial microbes in drinking water. *Water Res, 39*(5), 877-883.

Mafart, P., Couvert, O., Gaillard, S., & Leguérinel, I. (2002). On calculating sterility in thermal preservation methods: application of the Weibull frequency distribution model. *International Journal of Food Microbiology, 72*(1), 107-113.

Maïga, Y., Denyigba, K., Wethe, J., & Ouattara, A. S. (2009). Sunlight inactivation of Escherichia coli in waste stabilization microcosms in a sahelian region (Ouagadougou, Burkina Faso). Journal of Photochemistry and Photobiology B: Biology, 94(2), 113-119.

Malato Rodrıguez, S., Blanco Gálvez, J., Maldonado Rubio, M., Fernández Ibáñez, P., Alarcón Padilla, D., Collares Pereira, M., . . . Correia de Oliveira, J. (2004). Engineering of solar photocatalytic collectors. *Solar Energy, 77*(5), 513-524.

Malato, S., Blanco, J., Alarcón, D. C., Maldonado, M. I., Fernández-Ibáñez, P., & Gernjak, W. (2007). Photocatalytic decontamination and disinfection of water with solar collectors. *Catalysis Today, 122*(1-2), 137-149. doi: 10.1016/j.cattod.2007.01.034

Malato, S., Fernández-Ibáñez, P., Maldonado, M. I., Blanco, J., & Gernjak, W. (2009). Decontamination and disinfection of water by solar photocatalysis: Recent overview and trends. *Catalysis Today, 147*(1), 1-59. doi: 10.1016/j.cattod.2009.06.018

Marr, A. G., & Ingraham, J. L. (1962). Effect of temperature on the composition of fatty acids in Escherichia coli. *Journal of bacteriology, 84*(6), 1260-1267.

Martin, J. W., Chin, J. W., & Nguyen, T. (2003). Reciprocity law experiments in polymeric photodegradation: a critical review. *Progress in Organic Coatings, 47*(3), 292-311.

Martín-Domínguez, A., Alarcón-Herrera, M. T., Martín-Domínguez, I. R., & González-Herrera, A. (2005). Efficiency in the disinfection of water for human consumption in rural communities using solar radiation. *Solar Energy, 78*(1), 31-40.

Marugán, J., van Grieken, R., Sordo, C., & Cruz, C. (2008). Kinetics of the photocatalytic disinfection of *Escherichia coli* suspensions. Applied Catalysis B: Environmental, 82(1–2), 27-36. doi: http://dx.doi.org/10.1016/j.apcatb.2008.01.002

Marugán, J., van Grieken, R., Pablos, C., & Sordo, C. (2010). Analogies and differences between photocatalytic oxidation of chemicals and photocatalytic inactivation of microorganisms. *Water Res, 44*(3), 789-796. doi: http://dx.doi.org/10.1016/j.watres.2009.10.022

Matallana-Surget, S., Villette, C., Intertaglia, L., Joux, F., Bourrain, M., & Lebaron, P. (2012). Response to UVB radiation and oxidative stress of marine bacteria isolated from South Pacific Ocean and Mediterranean Sea. *J Photochem Photobiol B, 117*, 254-261. doi: 10.1016/j.jphotobiol.2012.09.011

Matsumura, Y., Iwasawa, A., Kobayashi, T., Kamachi, T., Ozawa, T., & Kohno, M. (2013). Detection of High-frequency Ultrasound-induced Singlet Oxygen by the ESR Spin-trapping Method. *Chemistry Letters, 42*(10), 1291-1293.

Matsunaga, T., Tomoda, R., Nakajima, T., & Wake, H. (1985). Photoelectrochemical sterilization of microbial cells by semiconductor powders. *FEMS Microbiology letters, 29*(1), 211-214.

Matthews, R. (1991). Environment: photochemical and photocatalytic processes. Degradation of organic compounds, *Photochemical conversion and storage of solar energy* (pp. 427-449): Springer.

Mbonimpa, E. G., Vadheim, B., & Blatchley III, E. R. (2012). Continuous-flow solar UVB disinfection reactor for drinking water. *Water Res, 46*(7), 2344-2354.

McGuigan, K., Joyce, T., Conroy, R., Gillespie, J., & Elmore-Meegan, M. (1998). Solar disinfection of drinking water contained in transparent plastic bottles: characterizing the bacterial inactivation process. *J Appl Microbiol, 84*(6), 1138-1148.

McGuigan, K. G., Samaiyar, P., du Preez, M., & Conroy, R. M. (2011). High compliance randomized controlled field trial of solar disinfection of drinking water and its impact on childhood diarrhea in rural Cambodia. *Environmental Science & Technology, 45*(18), 7862-7867.

McGuigan, K. G., Conroy, R. M., Mosler, H. J., du Preez, M., Ubomba-Jaswa, E., & Fernandez-Ibanez, P. (2012). Solar water disinfection (SODIS): a review from bench-top to roof-top. *J Hazard Mater, 235-236*, 29-46. doi: 10.1016/j.jhazmat.2012.07.053

Mezrioui, N., Baleux, B., & Troussellier, M. (1995). A microcosm study of the survival of *Escherichia coli* and *Salmonella typhimurium* in brackish water. *Water Res, 29*(2), 459-465. doi: http://dx.doi.org/10.1016/0043-1354(94)00188-D

Mishra, S., & Imlay, J. (2012). Why do bacteria use so many enzymes to scavenge hydrogen peroxide? *Arch Biochem Biophys, 525*(2), 145-160. doi: 10.1016/j.abb.2012.04.014

Misstear, D. B., Murtagh, J. P., & Gill, L. W. (2013). The Effect of Dark Periods on the UV Photolytic and Photocatalytic Disinfection of Escherichia coli in a Continuous Flow Reactor. *Journal of Solar Energy Engineering, 135*(2), 021012-021012. doi: 10.1115/1.4023179

Mitchell, R. (1971). *Water pollution microbiology*: New York, Wiley-Interscience [1971-78, v. 1, c1972.

Molina-Höppner, A., Doster, W., Vogel, R. F., & Gänzle, M. G. (2004). Protective effect of sucrose and sodium chloride for Lactococcus lactis during sublethal and lethal high-pressure treatments. *Applied and environmental microbiology, 70*(4), 2013-2020.

Moncayo-Lasso, A., Sanabria, J., Pulgarin, C., & Benitez, N. (2009). Simultaneous *E. coli* inactivation and NOM degradation in river water via photo-Fenton process at natural pH in solar CPC reactor. A new way for enhancing solar disinfection of natural water. *Chemosphere, 77*(2), 296-300. doi: 10.1016/j.chemosphere.2009.07.007

Moody, A., Marx, G., Swanson, B. G., & Bermúdez-Aguirre, D. (2014). A comprehensive study on the inactivation of Escherichia coli under nonthermal technologies: High hydrostatic pressure, pulsed electric fields and ultrasound. *Food Control, 37*(0), 305-314. doi: http://dx.doi.org/10.1016/j.foodcont.2013.09.052

Munshi, H. A., Sasikumar, N., Jamaluddin, A., & Mohammed, K. (1999). *Evaluation of ultra-violet radiation disinfection on the bacterial growth in the swro pilot plant, Al-Jubail.* Paper presented at the Gulf Water Conference.

Mwabi, J., Adeyemo, F., Mahlangu, T., Mamba, B., Brouckaert, B., Swartz, C., . . . Momba, M. (2011). Household water treatment systems: a solution to the production of safe drinking water by the low-income communities of Southern Africa. *Physics and Chemistry of the Earth, Parts A/B/C, 36*(14), 1120-1128.

Nalwanga, R., Quilty, B., Muyanja, C., Fernandez-Ibañez, P., & McGuigan, K. G. (2014). Evaluation of solar disinfection of E. coli under Sub-Saharan field conditions using a 25L borosilicate glass batch reactor fitted with a compound parabolic collector. *Solar Energy, 100*(0), 195-202. doi: http://dx.doi.org/10.1016/j.solener.2013.12.011

Ndounla, J., Spuhler, D., Kenfack, S., Wéthé, J., & Pulgarin, C. (2013). Inactivation by solar photo-Fenton in pet bottles of wild enteric bacteria of natural well water: Absence of re-growth after one week of subsequent storage. *Applied Catalysis B: Environmental, 129*, 309-317.

Ndounla, J., Kenfack, S., Wéthé, J., & Pulgarin, C. (2014). Relevant impact of irradiance (vs. dose) and evolution of pH and mineral nitrogen compounds during natural water disinfection by photo-Fenton in a solar CPC reactor. *Applied Catalysis B: Environmental, 148–149*(0), 144-153. doi: http://dx.doi.org/10.1016/j.apcatb.2013.10.048

Nebot Sanz, E., Salcedo Davila, I., Andrade Balao, J. A., & Quiroga Alonso, J. M. (2007). Modelling of reactivation after UV disinfection: effect of UV-C dose on subsequent photoreactivation and dark repair. *Water Res, 41*(14), 3141-3151. doi: 10.1016/j.watres.2007.04.008

Neuman, K. C., Chadd, E. H., Liou, G. F., Bergman, K., & Block, S. M. (1999). Characterization of Photodamage to Escherichia coli in Optical Traps. *Biophysical Journal, 77*(5), 2856-2863. doi: http://dx.doi.org/10.1016/S0006-3495(99)77117-1

Noble, R. T., Lee, I. M., & Schiff, K. C. (2004). Inactivation of indicator micro-organisms from various sources of faecal contamination in seawater and freshwater. *J Appl Microbiol, 96*(3), 464-472. doi: 10.1111/j.1365-2672.2004.02155.x

Novo, E., & Parola, M. (2008). Redox mechanisms in hepatic chronic wound healing and fibrogenesis. *Fibrogenesis & tissue repair, 1*(1), 5.

Oates, P. M., Shanahan, P., & Polz, M. F. (2003). Solar disinfection (SODIS): simulation of solar radiation for global assessment and application for point-of-use water treatment in Haiti. *Water Res, 37*(1), 47-54.

OECD, (1999). Guidelines for Testing of Chemicals, Simulation Test-Aerobic Sewage Treatment 303A.

Odonkor, S. T., & Ampofo, J. K. (2013). Escherichia coli as an indicator of bacteriological quality of water: an overview. Microbiology Research, 4(1), e2.

Oguma, K., Katayama, H., & Ohgaki, S. (2002). Photoreactivation of Escherichia coli after low-or medium-pressure UV disinfection determined by an endonuclease sensitive site assay. *Applied and environmental microbiology, 68*(12), 6029-6035.

Olukanni, D. O., & Ducoste, J. J. (2011). Optimization of waste stabilization pond design for developing nations using computational fluid dynamics. *Ecological Engineering, 37*(11), 1878-1888.

Oppezzo, O. J. (2012). Contribution of UVB radiation to bacterial inactivation by natural sunlight. *Journal of Photochemistry and Photobiology B: Biology*.

Ortega-Gómez, E., Esteban García, B., Ballesteros Martín, M. M., Fernández Ibáñez, P., & Sánchez Pérez, J. A. (2013). Inactivation of *Enterococcus faecalis* in simulated wastewater treatment plant effluent by solar photo-Fenton at initial neutral pH. *Catalysis Today, 209*, 195-200. doi: 10.1016/j.cattod.2013.03.001

Ortega-Gomez, E., Fernandez-Ibanez, P., Ballesteros Martin, M. M., Polo-Lopez, M. I., Esteban Garcia, B., & Sanchez Perez, J. A. (2012). Water disinfection using photo-Fenton: Effect of temperature on *Enterococcus faecalis* survival. *Water Res, 46*(18), 6154-6162. doi: 10.1016/j.watres.2012.09.007

Ortega-Gómez, E., Martín, M. M. B., García, B. E., Pérez, J. A. S., & Ibáñez, P. F. (2013a). Solar Photo-Fenton for Water Disinfection: An Investigation of the Competitive Role of Model Organic Matter for Oxidative Species. *Applied Catalysis B: Environmental*. doi: 10.1016/j.apcatb.2013.09.051

Ouali, A., Jupsin, H., Vasel, J., & Ghrabi, A. (2013). Removal of E. coli and enterococci in maturation pond and kinetic modelling under sunlight conditions. *Desalination and Water Treatment*(ahead-of-print), 1-7.

Patwardhan, A.R. (1990). Our Water, Our Life, Council for Advancement of People's Action and Rural Technology, New Delhi

Peak, J., & Peak, M. (1982). Lethality in repair-proficient *Escherichia coli* after 365 nm ultraviolet light irradiation is dependent on fluence rate. *Photochem Photobiol, 36*(1), 103-105.

Peak, M., Peak, J., & Webb, R. (1975). Synergism between different near-ultraviolet wavelengths in the inactivation of transforming DNA. *Photochem Photobiol, 21*(2), 129-131.

Persson, J., & Wittgren, H. B. (2003). How hydrological and hydraulic conditions affect performance of ponds. *Ecological Engineering, 21*(4), 259-269.

Petin, V. G., Zhurakovskaya, G. P., & Komarova, L. N. (1997). Fluence rate as a determinant of synergistic interaction under simultaneous action of UV light and mild heat in Saccharomyces cerevisiae. *Journal of Photochemistry and Photobiology B: Biology, 38*(2), 123-128.

Petrier, C., David, B., & Laguian, S. (1996). Ultrasonic degradation at 20 kHz and 500 kHz of atrazine and pentachlorophenol in aqueous solution: Preliminary results. *Chemosphere, 32*(9), 1709-1718.

Petrier, C., in: Mason, T. J., & Tiehm, A. (2001). *Advances in Sonochemistry, Volume 6: Ultrasound in Environmental Protection* (Vol. 6): Access Online via Elsevier.

Petrier, C., Jeunet, A., Luche, J. L., & Reverdy, G. (1992). Unexpected frequency effects on the rate of oxidative processes induced by ultrasound. *Journal of the American Chemical Society, 114*(8), 3148-3150.

Petrier, C., Lamy, M.-F., Francony, A., Benahcene, A., David, B., Renaudin, V., & Gondrexon, N. (1994). Sonochemical degradation of phenol in dilute aqueous solutions: comparison of the reaction rates at 20 and 487 kHz. *The Journal of Physical Chemistry, 98*(41), 10514-10520.

Pigeot-Rémy, S., Simonet, F., Atlan, D., Lazzaroni, J., & Guillard, C. (2012). Bactericidal efficiency and mode of action: A comparative study of photochemistry and photocatalysis. *Water Res, 46*(10), 3208-3218.

Polo-López, M. I., Fernández-Ibáñez, P., Ubomba-Jaswa, E., Navntoft, C., García-Fernández, I., Dunlop, P. S. M., . . . McGuigan, K. G. (2011). Elimination of water pathogens with solar radiation using an automated sequential batch CPC reactor. *J Hazard Mater, 196*(0), 16-21. doi: http://dx.doi.org/10.1016/j.jhazmat.2011.08.052

Polo-López, M. I., García-Fernández, I., Velegraki, T., Katsoni, A., Oller, I., Mantzavinos, D., & Fernández-Ibáñez, P. (2012). Mild solar photo-Fenton: An effective tool for the removal of Fusarium from simulated municipal effluents. *Applied Catalysis B: Environmental, 111*, 545-554.

Quek, P. H., & Hu, J. (2008). Indicators for photoreactivation and dark repair studies following ultraviolet disinfection. *Journal of industrial microbiology & biotechnology, 35*(6), 533-541.

Raman, V., & Abbas, A. (2008). Experimental investigations on ultrasound mediated particle breakage. *Ultrason Sonochem, 15*(1), 55-64. doi: 10.1016/j.ultsonch.2006.11.009

Reed, R.H. (1997a). Innovations in solar water treatment. In ''Proceedings of the 23rd Water, Engineering and Development Centre Conference, Durban, South Africa,'' p. 184–185. University of Loughborough, Loughborough

Reed, R.H. (1997b). Solar inactivation of fecal bacteria in water: the critical role of oxygen. Letters in Applied Microbiology, 24 (4), p. 276-280

Reed, R. H. (2004). The inactivation of microbes by sunlight: solar disinfection as a water treatment process. *Advances in applied microbiology, 54*, 333-365.

Regensburger, J., Knak, A., Felgenträger, A., & Bäumler, W. (2011). Generation of singlet oxygen by UVB-irradiation of endogenous molecules. *Photodiagnosis and Photodynamic Therapy, 8*(2), 152. doi: 10.1016/j.pdpdt.2011.03.098

Rincón, A. G., & Pulgarin, C. (2003). Photocatalytical inactivation of *E. coli*: effect of (continuous–intermittent) light intensity and of (suspended–fixed) TiO2 concentration. *Applied Catalysis B: Environmental, 44*(3), 263-284. doi: 10.1016/s0926-3373(03)00076-6

Rincón, A.-G., & Pulgarin, C. (2004a). Field solar *E. coli* inactivation in the absence and presence of TiO2: is UV solar dose an appropriate parameter for standardization of water solar disinfection? *Solar Energy, 77*(5), 635-648. doi: 10.1016/j.solener.2004.08.002

Rincón, A.-G., & Pulgarin, C. (2004b). Effect of pH, inorganic ions, organic matter and H_2O_2 on *E. coli* K12 photocatalytic inactivation by TiO2: Implications in solar water disinfection. Applied Catalysis B: Environmental, 51(4), 283-302. doi: http://dx.doi.org/10.1016/j.apcatb.2004.03.007

Rincón, A.-G., & Pulgarin, C. (2004c). Bactericidal action of illuminated TiO_2 on pure *Escherichia coli* and natural bacterial consortia: post-irradiation events in the dark and assessment of the effective disinfection time. *Applied Catalysis B: Environmental, 49*(2), 99-112. doi: 10.1016/j.apcatb.2003.11.013

Rincón, A.-G., & Pulgarin, C. (2007a). Absence of *E. coli* regrowth after Fe^{3+} and TiO_2 solar photoassisted disinfection of water in CPC solar photoreactor. *Catalysis Today, 124*(3-4), 204-214. doi: 10.1016/j.cattod.2007.03.039

Rincón, A.-G., & Pulgarin, C. (2007b). Fe^{3+} and TiO_2 solar-light-assisted inactivation of *E. coli* at field scale: Implications in solar disinfection at low temperature of large quantities of water. *Catalysis Today, 122*(1), 128-136.

Rizzo, L., Belgiorno, V., & Napoli, R. M. A. (2004). Regrowth Evaluation of Coliform Bacteria Injured by Low Chlorine Doses Using Selective and Nonselective Media. *Journal of Environmental Science and Health, Part A, 39*(8), 2081-2092. doi: 10.1081/ESE-120039376

Rizzo, L., Sannino, D., Vaiano, V., Sacco, O., Scarpa, A., & Pietrogiacomi, D. (2014). Effect of solar simulated N-doped TiO_2 photocatalysis on the inactivation and antibiotic resistance of an *E. coli* strain in biologically treated urban wastewater. *Applied Catalysis B: Environmental*, *144*(0), 369-378. doi: http://dx.doi.org/10.1016/j.apcatb.2013.07.033

Robertson, J., J Robertson, P. K., & Lawton, L. A. (2005). A comparison of the effectiveness of TiO_2 photocatalysis and UVA photolysis for the destruction of three pathogenic micro-organisms. *Journal of Photochemistry and Photobiology A: Chemistry*, *175*(1), 51-56.

Rodríguez-Chueca, J., Mosteo, R., Ormad, M. P., & Ovelleiro, J. L. (2012). Factorial experimental design applied to *Escherichia coli* disinfection by Fenton and photo-Fenton processes. *Solar Energy*, *86*(11), 3260-3267. doi: 10.1016/j.solener.2012.08.015

Roszak, D., & Colwell, R. (1987). Survival strategies of bacteria in the natural environment. *Microbiological reviews*, *51*(3), 365.

Roth, W. G., Leckie, M. P., & Dietzler, D. N. (1988). Restoration of colony-forming activity in osmotically stressed *Escherichia coli* by betaine. *Applied and environmental microbiology*, *54*(12), 3142-3146.

Saitoh, T. S., & El-Ghetany, H. H. (2002). A pilot solar water disinfecting system: performance analysis and testing. *Solar Energy*, *72*(3), 261-269.

Salih, F. M. (2003). Formulation of a mathematical model to predict solar water disinfection. *Water Res*, *37*(16), 3921-3927.

Sat, B., Hazan, R., Fisher, T., Khaner, H., Glaser, G., & Engelberg-Kulka, H. (2001). Programmed Cell Death in *Escherichia coli*: Some Antibiotics Can Trigger mazEFLethality. *Journal of bacteriology*, *183*(6), 2041-2045.

Sciacca, F., Rengifo-Herrera, J. A., Wéthé, J., & Pulgarin, C. (2011). Solar disinfection of wild *Salmonella sp.* in natural water with a 18L CPC photoreactor: Detrimental effect of non-sterile storage of treated water. *Solar Energy*, *85*(7), 1399-1408.

Setlow, R. B. (1974). The wavelengths in sunlight effective in producing skin cancer: a theoretical analysis. *Proceedings of the National Academy of Sciences*, *71*(9), 3363-3366.

Shang, C., Cheung, L. M., Ho, C.-M., & Zeng, M. (2009). Repression of photoreactivation and dark repair of coliform bacteria by TiO_2-modified UV-C disinfection. *Applied Catalysis B: Environmental*, *89*(3), 536-542.

Sichel, C., Tello, J., de Cara, M., & Fernández-Ibáñez, P. (2007). Effect of UV solar intensity and dose on the photocatalytic disinfection of bacteria and fungi. *Catalysis Today*, *129*(1-2), 152-160. doi: 10.1016/j.cattod.2007.06.061

Sichel, C., Blanco, J., Malato, S., & Fernández-Ibáñez, P. (2007a). Effects of experimental conditions on *E. coli* survival during solar photocatalytic water disinfection. *Journal of Photochemistry and Photobiology A: Chemistry*, *189*(2-3), 239-246. doi: 10.1016/j.jphotochem.2007.02.004

Simate, I.N. (2001). Solar water distillation-Zambian perspective. In ‘‘Proceedings of the Twenty-seventh Water, Engineering and Development Centre Conference, Lusaka, Zambia,’’ p. 310–312. University of Loughborough, Loughborough

Sinha, R. P., & Häder, D.-P. (2002). UV-induced DNA damage and repair: a review. *Photochemical & Photobiological Sciences*, *1*(4), 225-236.

Sinton, L. W., Finlay, R. K., & Lynch, P. A. (1999). Sunlight inactivation of fecal bacteriophages and bacteria in sewage-polluted seawater. *Applied and environmental microbiology*, *65*(8), 3605-3613.

Sinton, L. W., Hall, C. H., Lynch, P. A., & Davies-Colley, R. J. (2002). Sunlight inactivation of fecal indicator bacteria and bacteriophages from waste stabilization pond effluent in fresh and saline waters. *Applied and environmental microbiology*, *68*(3), 1122-1131.

Sodis Fundación (1998). Notas Técnicas de la No. 1 a la 17. Cochabamba-Bolivia. Available at: www.sodis.ch

Sommer, B., Marino, A., Solarte, Y., Salas, M., Dierolf, C., Valiente, C., . . . Wirojanagud, W. (1997). SODIS- an emerging water treatment process. *AQUA (OXFORD)*, *46*(3), 127-137.

Sommer, R., Haider, T., Cabaj, A., Pribil, W., & Lhotsky, M. (1998). Time dose reciprocity in UV disinfection of water. *Water Science and Technology*, *38*(12), 145-150.

Spuhler, D., Andrés Rengifo-Herrera, J., & Pulgarin, C. (2010). The effect of Fe^{2+}, Fe^{3+}, H_2O_2 and the photo-Fenton reagent at near neutral pH on the solar disinfection (SODIS) at low temperatures of water containing *Escherichia coli* K12. *Applied Catalysis B: Environmental*, *96*(1-2), 126-141. doi: 10.1016/j.apcatb.2010.02.010

Stephens, C. (2005). Senescence: even bacteria get old. *Current Biology*, *15*(8), R308-R310.

Storz, G., & Imlay, J. A. (1999). Oxidative stress. *Current opinion in microbiology, 2*(2), 188-194.

Sunada, K., Watanabe, T., & Hashimoto, K. (2003). Studies on photokilling of bacteria on TiO_2 thin film. *Journal of Photochemistry and Photobiology A: Chemistry, 156*(1), 227-233.

Tassoula, E. A. (1997). Growth possibilities of *E. coli* in natural waters. *International Journal of Environmental Studies, 52*(1-4), 67-73. doi: 10.1080/00207239708711096

Torres, R. A., Sarantakos, G., Combet, E., Pétrier, C., & Pulgarin, C. (2008). Sequential helio-photo-Fenton and sonication processes for the treatment of bisphenol A. *Journal of Photochemistry and Photobiology A: Chemistry, 199*(2-3), 197-203. doi: 10.1016/j.jphotochem.2008.05.016

Troussellier, M., Bonnefont, J.-L., Courties, C., Derrien, A., Dupray, E., Gauthier, M., . . . Martin, Y. (1998). Responses of enteric bacteria to environmental stresses in seawater. *Oceanologica Acta, 21*(6), 965-981.

Tyrrell, R. M., & Peak, M. J. (1978). Interactions between UV radiation of different energies in the inactivation of bacteria. *Journal of bacteriology, 136*(1), 437-440.

Ubomba-Jaswa, E., Navntoft, C., Polo-Lopez, M. I., Fernandez-Ibanez, P., & McGuigan, K. G. (2009). Solar disinfection of drinking water (SODIS): an investigation of the effect of UV-A dose on inactivation efficiency. *Photochem Photobiol Sci, 8*(5), 587-595. doi: 10.1039/b816593a

Vélez-Colmenares, J. J., Acevedo, A., & Nebot, E. (2011). Effect of recirculation and initial concentration of microorganisms on the disinfection kinetics of Escherichia coli. *Desalination, 280*(1–3), 20-26. doi: http://dx.doi.org/10.1016/j.desal.2011.06.041

Vélez-Colmenares, J. J., Acevedo, A., Salcedo, I., & Nebot, E. (2012). New kinetic model for predicting the photoreactivation of bacteria with sunlight. *Journal of Photochemistry and Photobiology B: Biology, 117*(0), 278-285. doi: http://dx.doi.org/10.1016/j.jphotobiol.2012.09.005

Vicars, S. (1999). Factors affecting the survival of enteric bacteria in saline waters. PhD Thesis. Northumbria University, Newcastle upon Tyne

Villén, L., Manjón, F., García-Fresnadillo, D., & Orellana, G. (2006). Solar water disinfection by photocatalytic singlet oxygen production in heterogeneous medium. *Applied Catalysis B: Environmental, 69*(1), 1-9.

Von Sperling, M. (1999). Performance evaluation and mathematical modelling of coliform die-off in tropical and subtropical waste stabilization ponds. *Water Res, 33*(6), 1435-1448.

Von Sperling, M. (2005). Modelling of coliform removal in 186 facultative and maturation ponds around the world. *Water Res, 39*(20), 5261-5273.

Wegelin, M., & Sommer, B. (1998). Solar Water Disinfection (SODIS)—destined for worldwide use? *Waterlines, 16*(3), 30-32.

Wegelin, M., Canonica, S., Mechsner, K., Fleischmann, T., Pesaro, F., & Metzler, A. (1994). Solar water disinfection: scope of the process and analysis of radiation experiments. *Aqua, 43*(4), 154-169.

White, G. C. (2010). *White's handbook of chlorination and alternative disinfectants*: Wiley.

Xu, H.-S., Roberts, N., Singleton, F. L., Attwell, R. W., Grimes, D. J., & Colwell, R. R. (1982). Survival and Viability of Nonculturable *Escherichia coli* and *Vibrio cholerae* in the Estuarine and Marine Environment. *Microb Ecol, 8*(4), 313-323. doi: 10.2307/4250723

Xu, P., Brissaud, F., & Fazio, A. (2002). Non-steady-state modelling of faecal coliform removal in deep tertiary lagoons. *Water Res, 36*(12), 3074-3082.

Yang, L., Chang, W.-S., & Lo Huang, M.-N. (2000). Natural disinfection of wastewater in marine outfall fields. *Water Res, 34*(3), 743-750.

Yoon, C. G., Jung, K.-W., Jang, J.-H., & Kim, H.-C. (2007). Microorganism repair after UV-disinfection of secondary-level effluent for agricultural irrigation. *Paddy and Water Environment, 5*(1), 57-62.

Yukselen, M. A., Calli, B., Gokyay, O., & Saatci, A. (2003). Inactivation of coliform bacteria in Black Sea waters due to solar radiation. *Environment International, 29*(1), 45-50. doi: 10.1016/s0160-4120(02)00144-7

Zaviska, F., Drogui, P., El Hachemi, E. M., & Naffrechoux, E. (2014). Effect of nitrate ions on the efficiency of sonophotochemical phenol degradation. *Ultrason Sonochem, 21*(1), 69-75. doi: http://dx.doi.org/10.1016/j.ultsonch.2013.08.003

Zetterberg, G. (1964) Mutagenic effects of ultraviolet and visible light. In Photophysiology, ed. Giese, A.G. New York: Academic Press

Appendix A

Published articles deriving from the present Thesis, as of 10 September 2014

- Giannakis, et al., (2013),"Impact of different light intermittence regimes on bacteria during simulated solar treatment of secondary effluent: Implications of the inserted dark periods", Solar Energy, Volume 98, Part C, Pages 572-581.

- Giannakis, et al., (2014),"The antagonistic and synergistic effects of temperature during solar disinfection of synthetic secondary effluent", Journal of Photochemistry and Photobiology A: Chemistry, Volume 280, Pages 14-26.

- Giannakis, et al., (2014), "Ultrasound enhancement of near-neutral photo-Fenton for effective *E. coli* inactivation in wastewater", Ultrasonics Sonochemistry, Volume 22, Pages 515–526.

- Giannakis, et al., (2014). Monitoring the post-irradiation *E. coli* survival patterns in environmental water matrices: Implications in handling solar disinfected wastewater. Chemical Engineering Journal, Volume 253, Pages 366-376.

- Giannakis, et al., (2014), "Elucidating bacterial regrowth: Effect of disinfection conditions in dark storage of solar treated secondary effluent", Journal of Photochemistry and Photobiology A: Chemistry, Volume 290, Pages. 43-53.

Appendix B
Detailed presentation of the fit models described in Chapter 3.1.5, by GInaFit

500 W/m^2

Shoulder Model

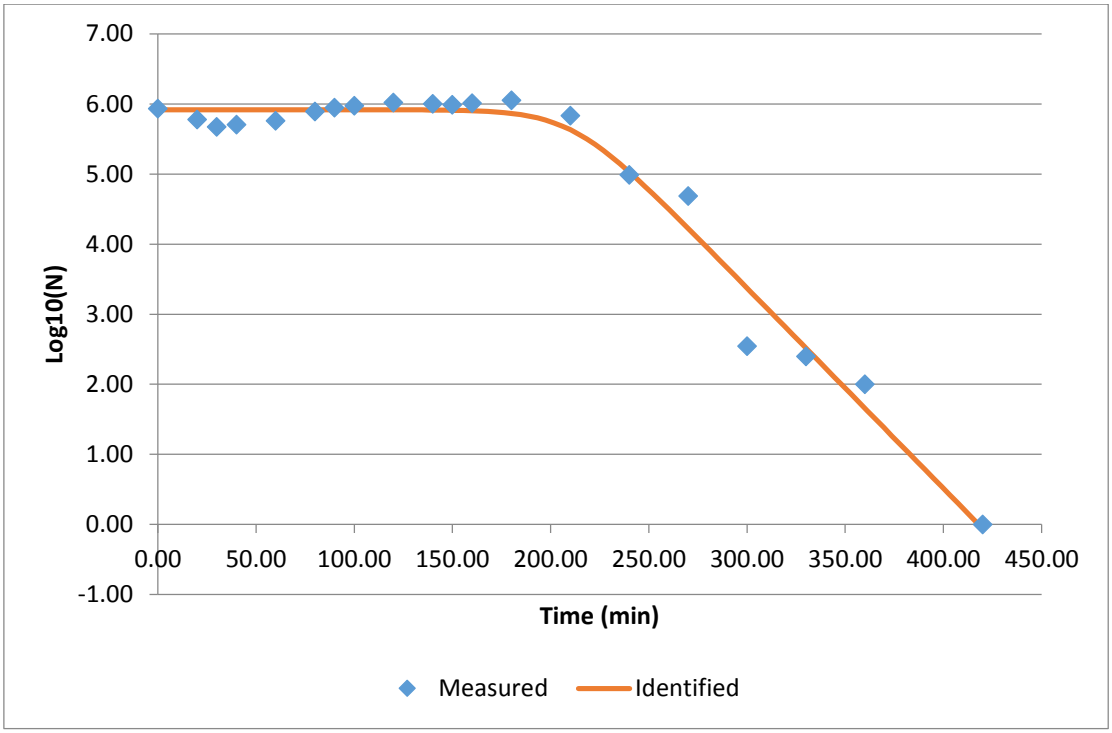

Weibull distribution model

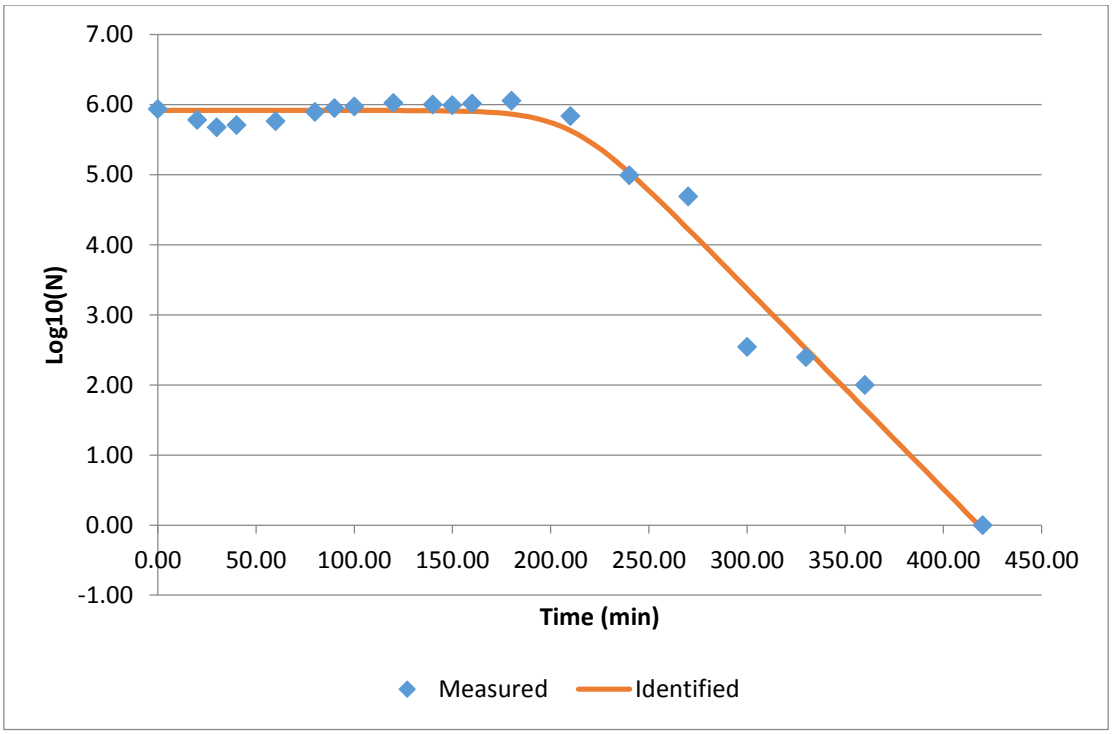

600 W/m^2

Shoulder Model

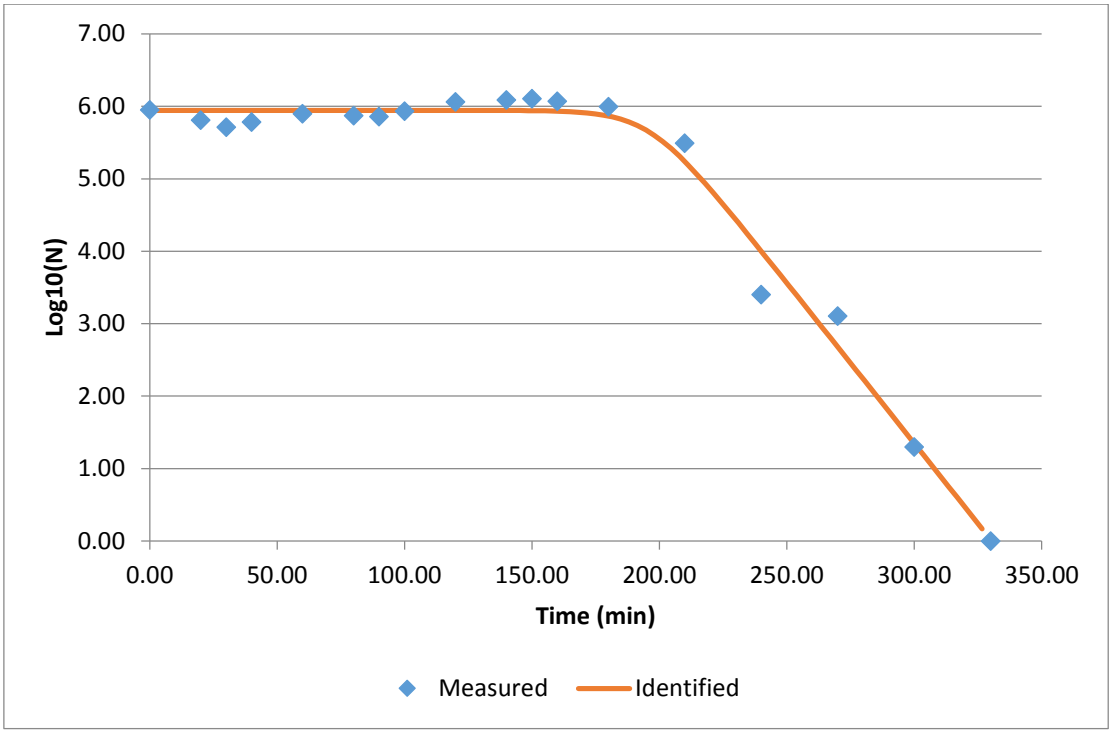

Weibull distribution model

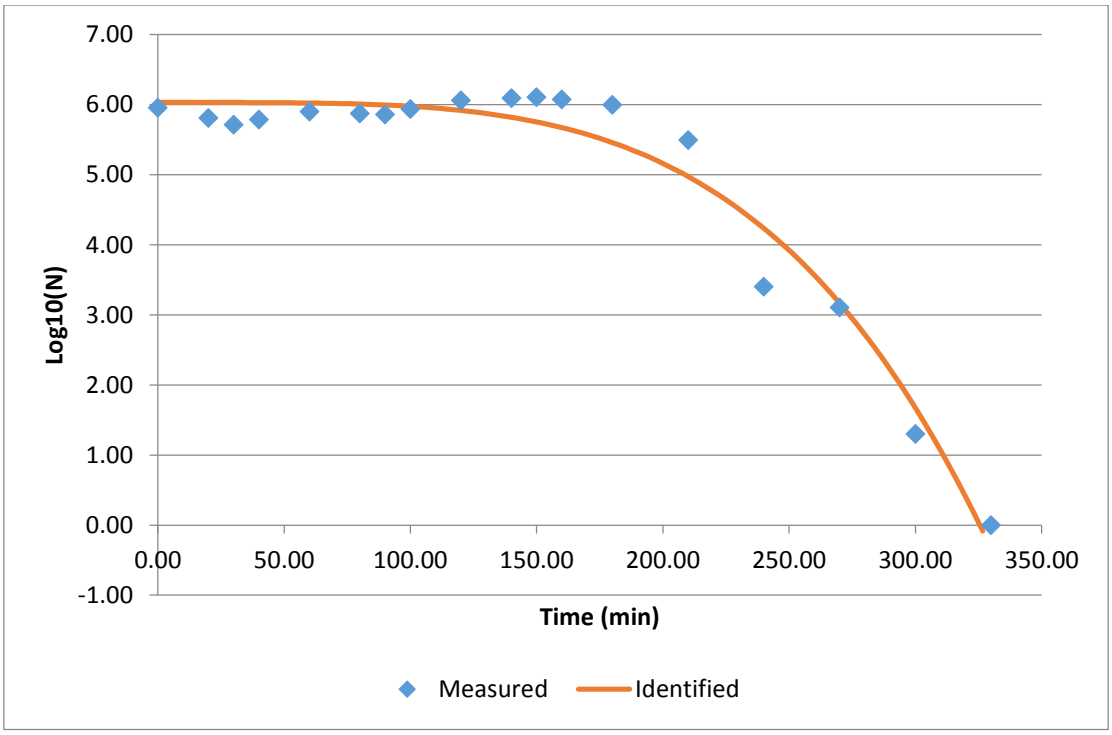

700 W/m^2

Shoulder Model

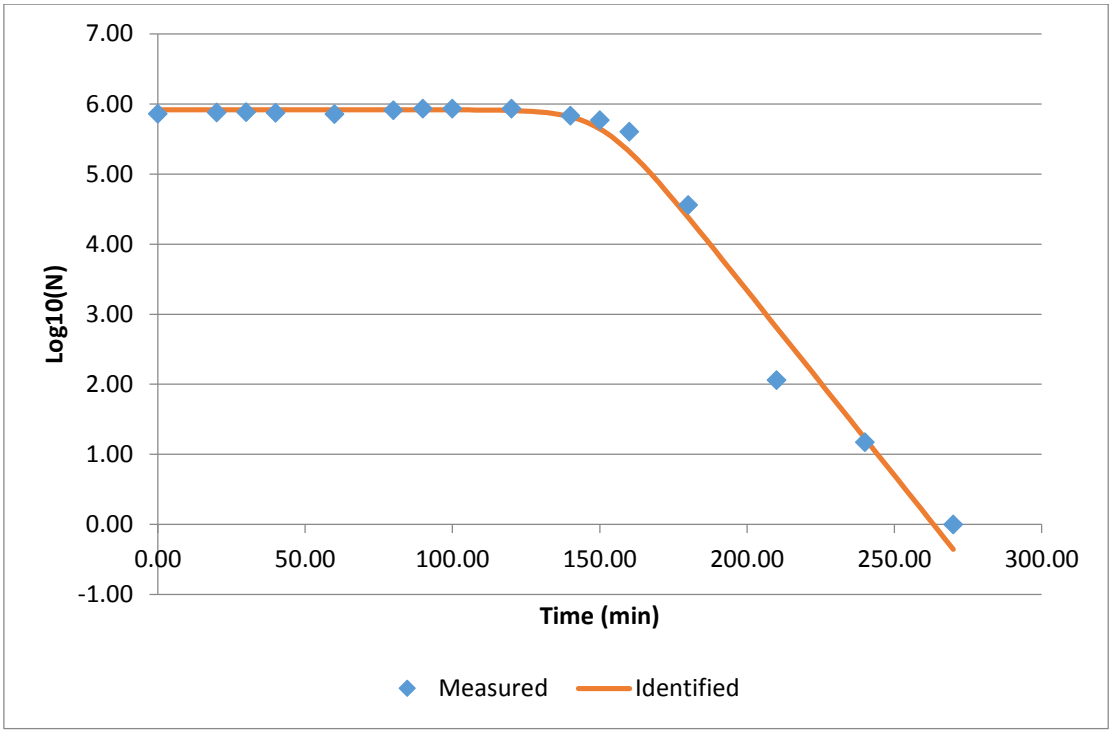

Weibull distribution model

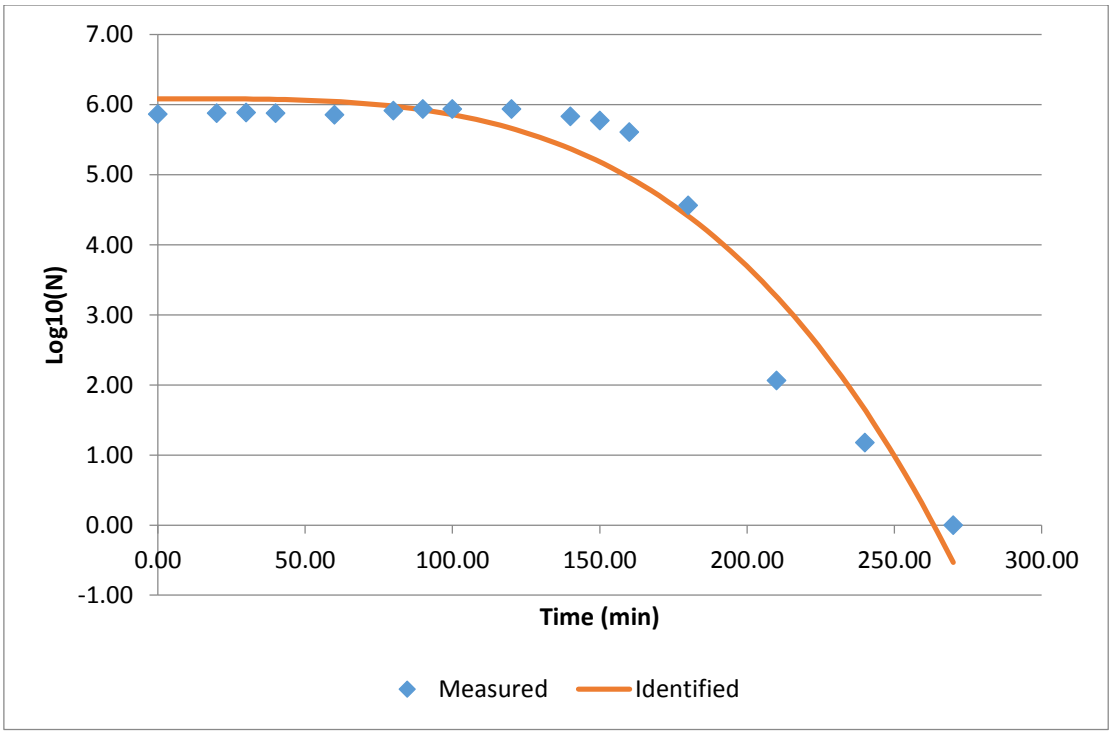

800 W/m^2

Shoulder Model

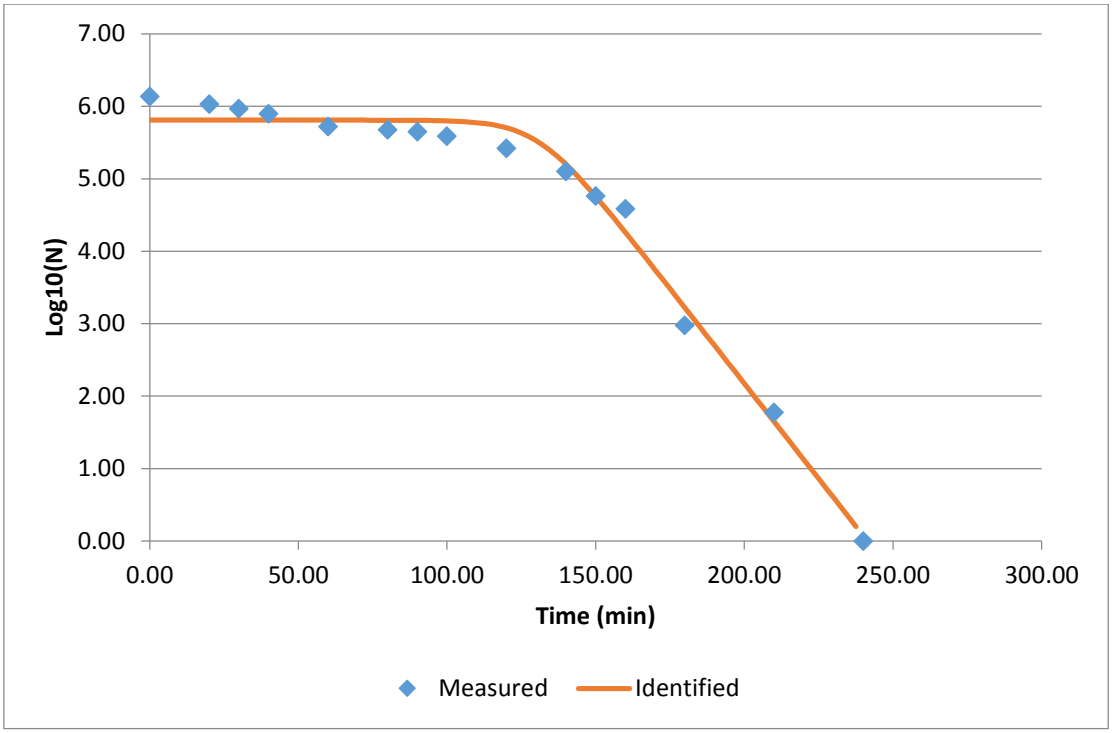

Weibull distribution model

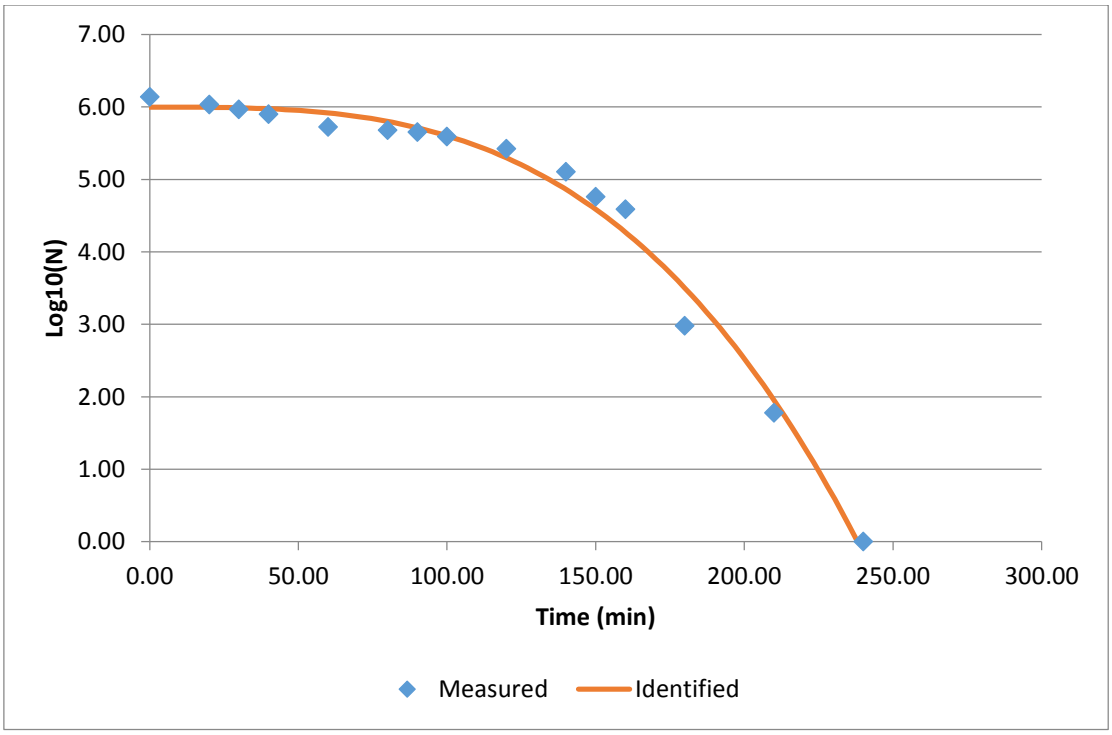

900 W/m^2

Shoulder Model

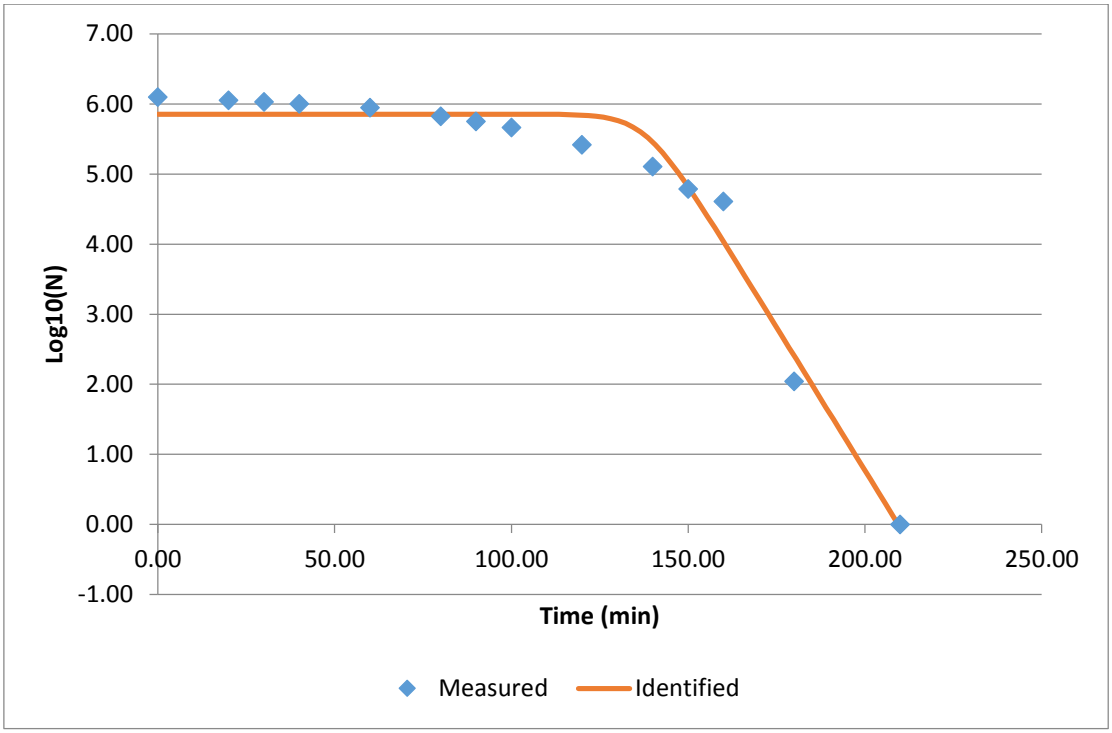

Weibull distribution model

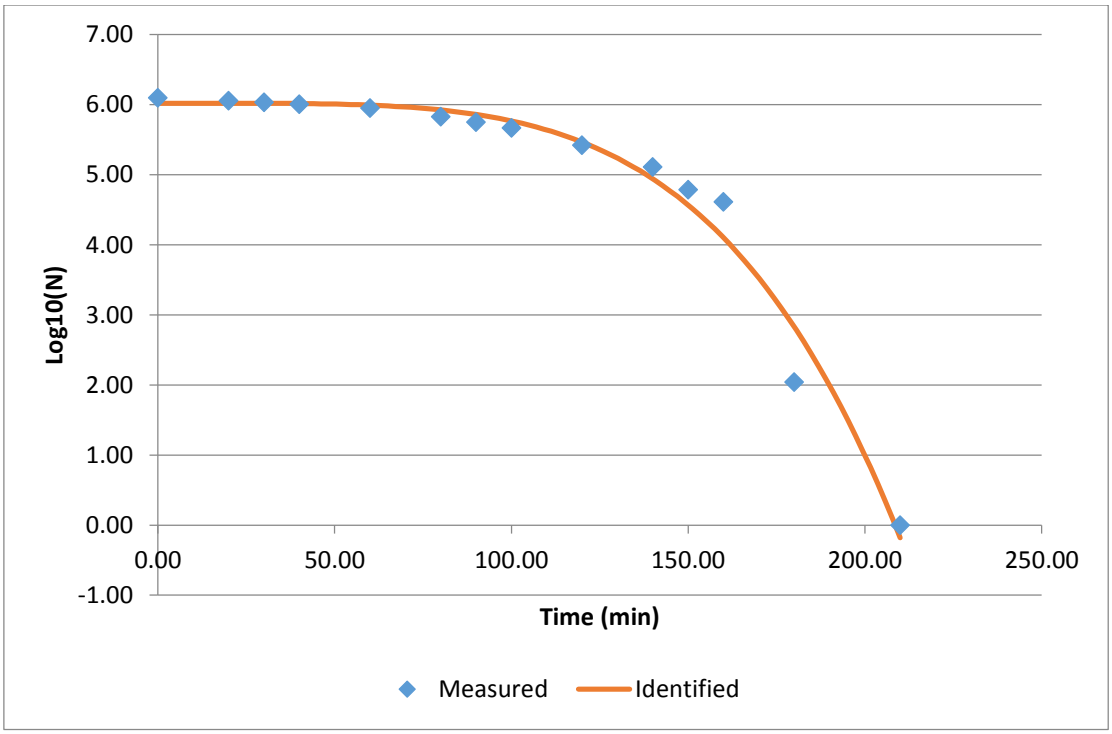

1000 W/m^2

Shoulder Model

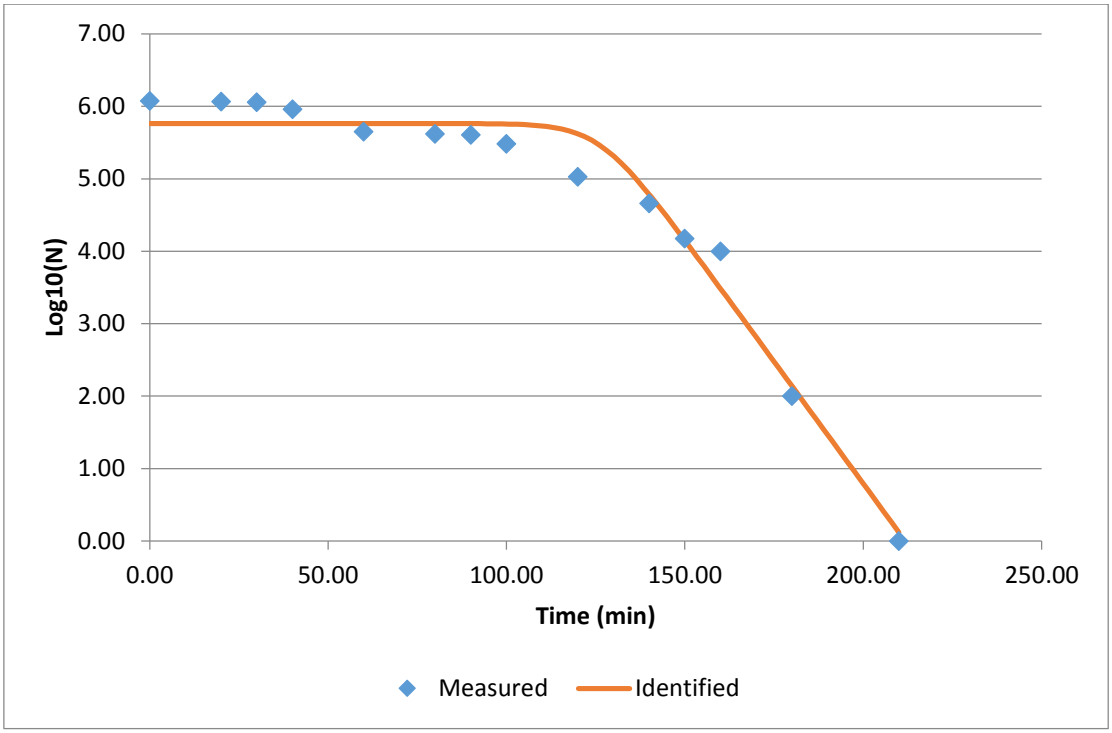

Weibull distribution model

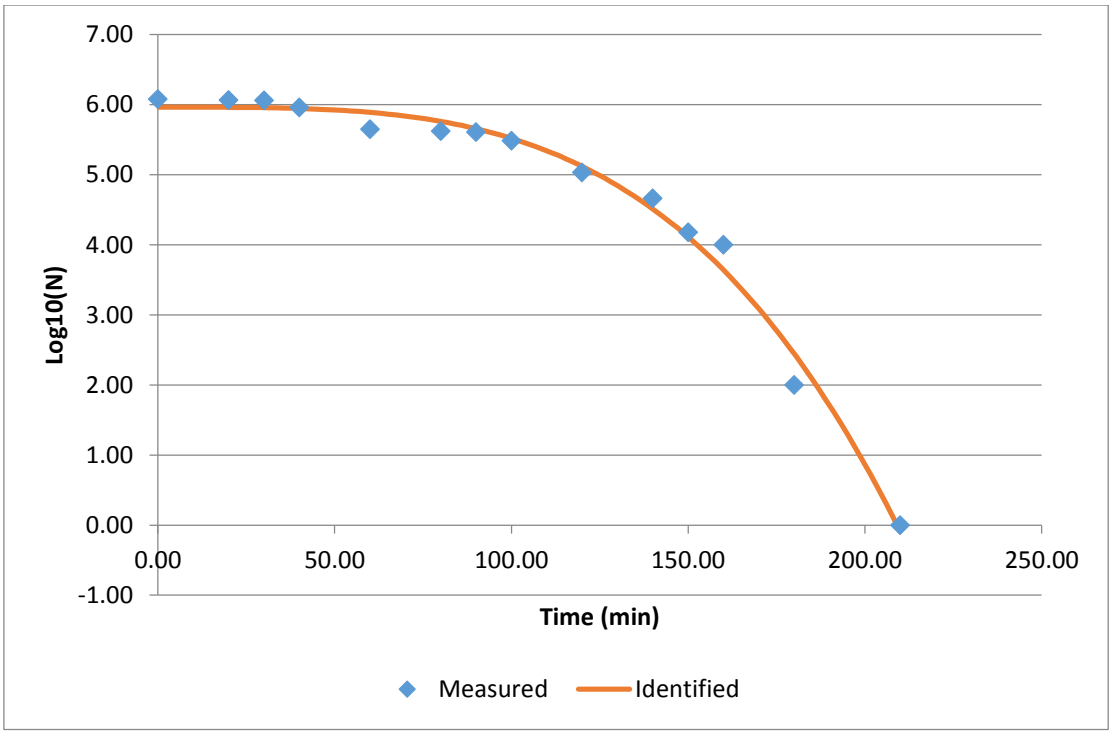

1200 W/m^2

Shoulder Model

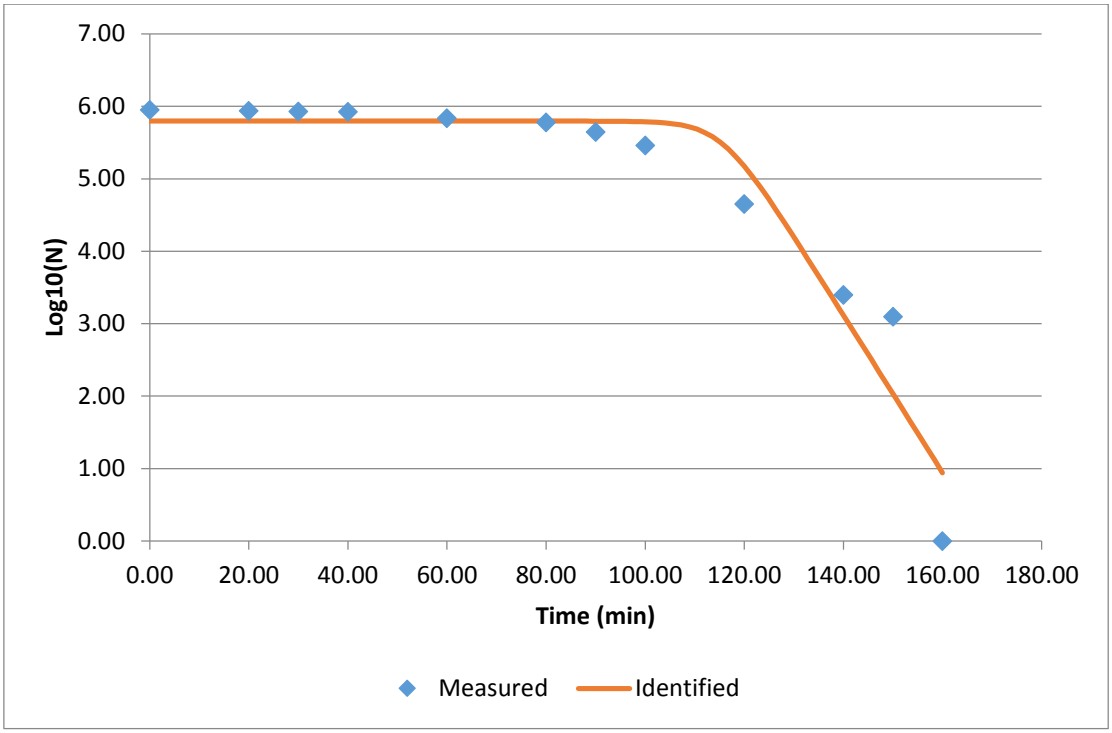

Weibull distribution model

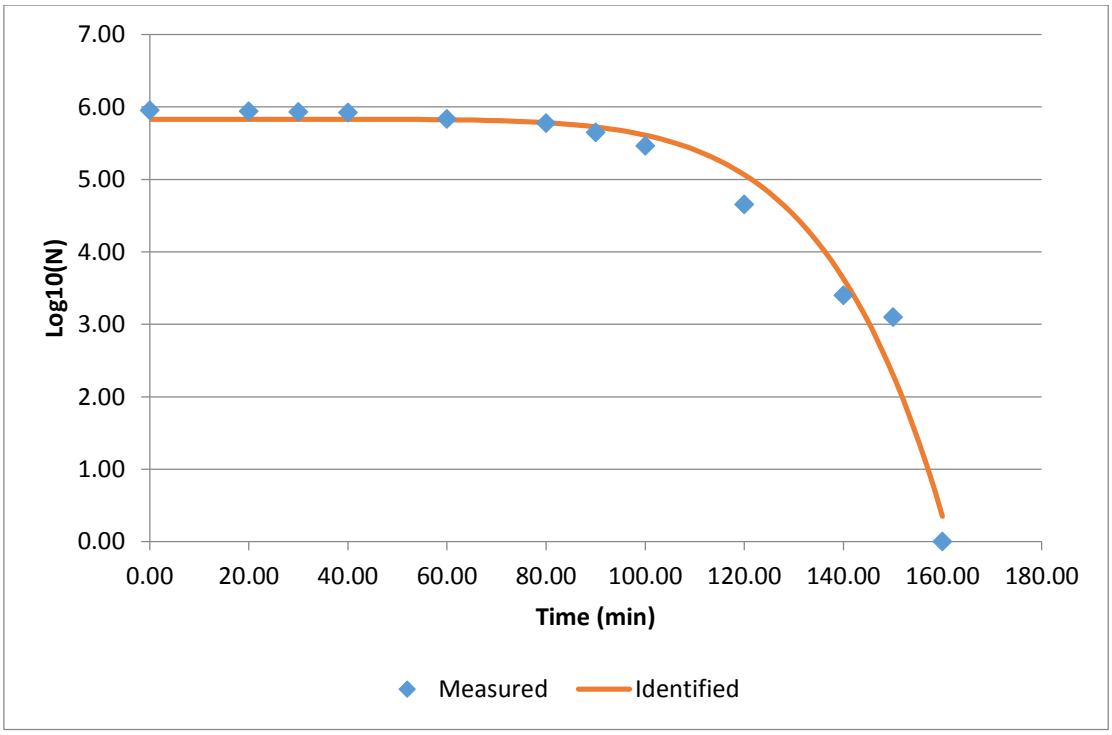

1400 W/m^2

Shoulder Model

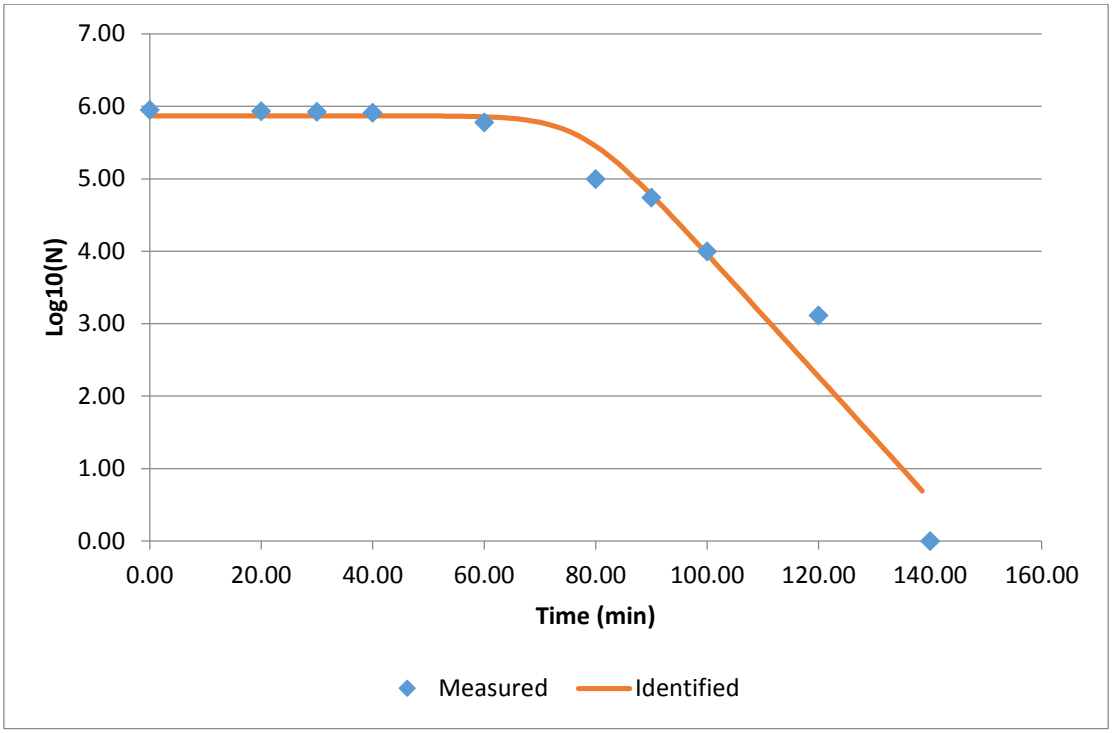

Weibull distribution model

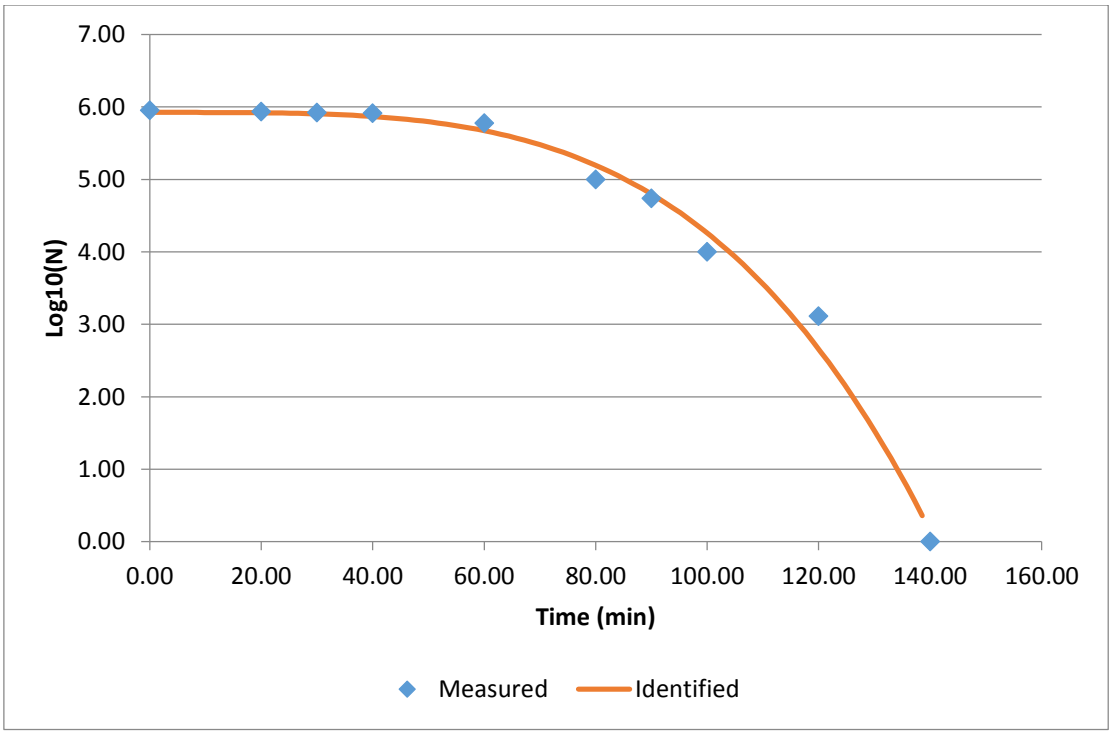

1600 W/m^2

Shoulder Model

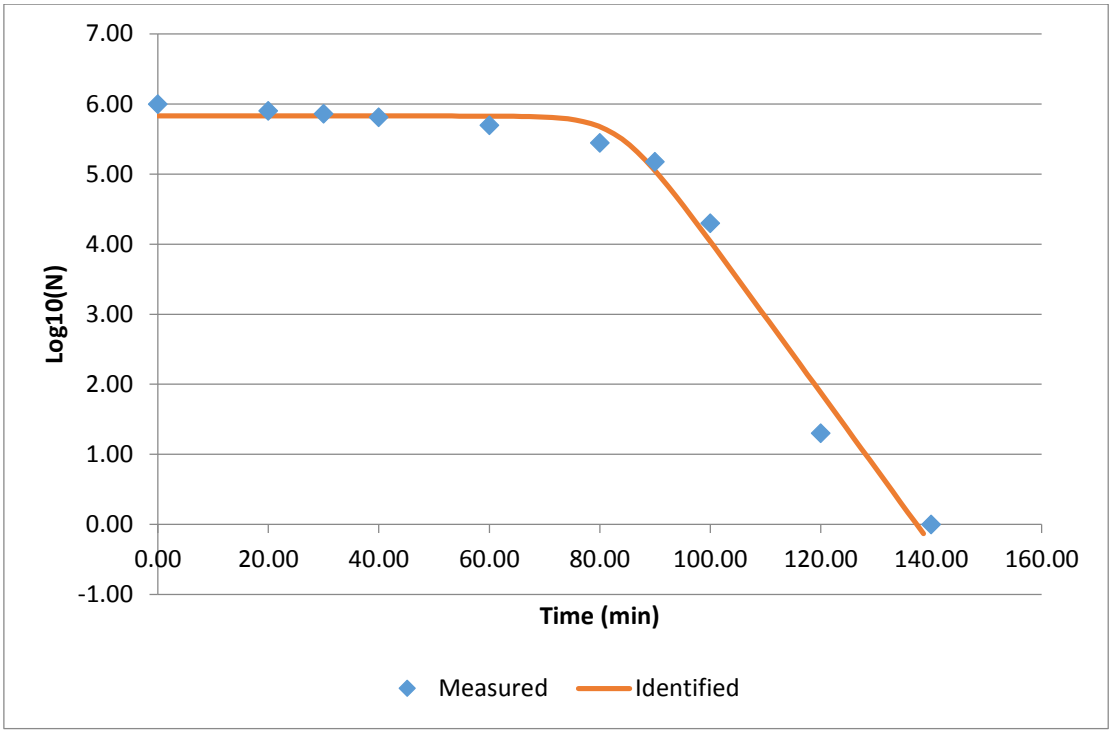

Weibull distribution model

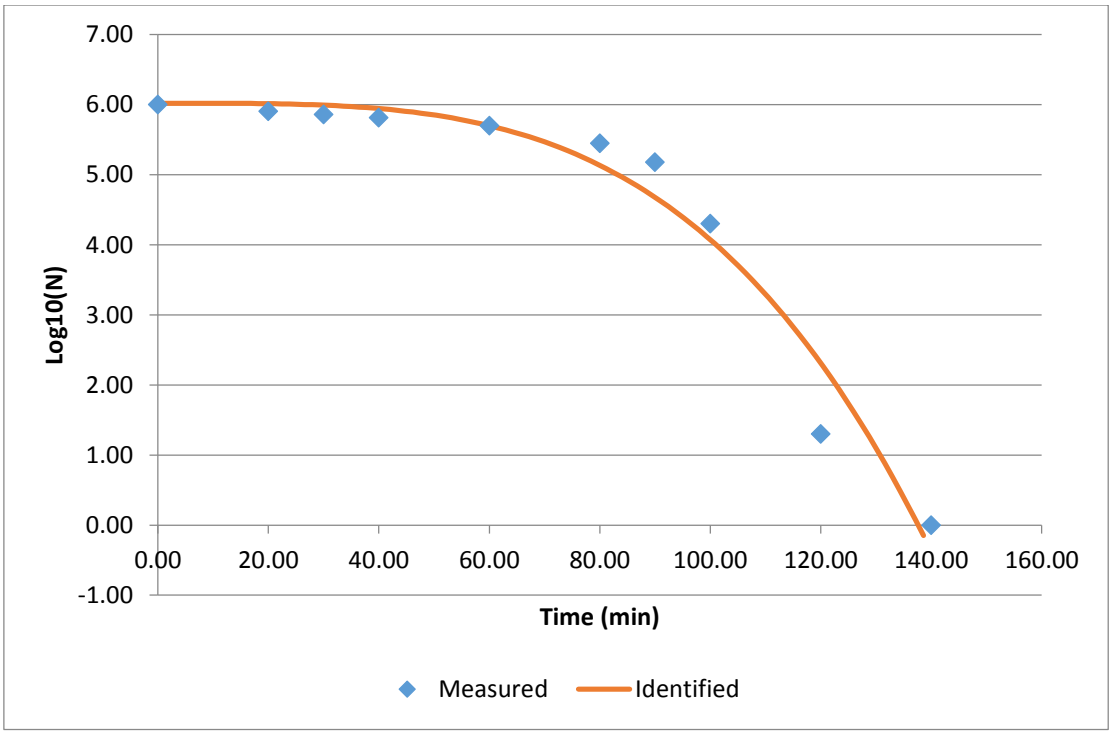

Appendix C
Executive summary in Greek

Απολύμανση δευτεροβάθμια επεξεργασμένων λυμάτων με ηλιακή ακτινοβολία και επακόλουθη βακτηριακή επανανάπτυξη: προτάσεις, περιορισμοί και περιβαλλοντικές προοπτικές

Εκτεταμένη περίληψη της Διδακτορικής Διατριβής

Οργάνωση της Διδακτορικής διατριβής

Στο εισαγωγικό πρώτο κεφάλαιο της Διατριβής γίνεται εκτενής ανασκόπηση της σχετικής βιβλιογραφίας και οριοθετούνται οι στόχοι της έρευνας. Στα επόμενα κεφάλαια παρουσιάζονται τα πειράματα που εκτελέστηκαν και ακολουθεί συζήτηση των αποτελεσμάτων. Στην αρχή κάθε κεφαλαίου αναλύονται πιο διεξοδικά οι μέθοδοι και οι πειραματικές διατάξεις που χρησιμοποιήθηκαν. Στο τέλος κάθε πειραματικής ενότητας παρουσιάζονται τα επιμέρους συμπεράσματα.

Στο δεύτερο κεφάλαιο παρουσιάζονται οι κοινές πειραματικές διατάξεις, οι μέθοδοι και τα υλικά που χρησιμοποιήθηκαν για την εκτέλεση των πειραμάτων.

Το τρίτο κεφάλαιο αναφέρεται σε πειράματα απολύμανσης δευτεροβάθμια επεξεργασμένων λυμάτων με ηλιακή ακτινοβολία. Ιδιαίτερη έμφαση δίνεται στο φαινόμενο της βακτηριακής επανανάπτυξης. Αναλύεται ο μηχανισμός της απολύμανσης του νερού με ηλιακή ακτινοβολία και των παραμέτρων που εμπλέκονται στις διεργασίες αδρανοποίησης και επανεμφάνισης των μικροοργανισμών καθώς και η επίδραση της δόσης της ακτινοβολίας με ή χωρίς θερμοκρασιακό έλεγχο.

Το τέταρτο κεφάλαιο αναλύει διεξοδικά τα φαινόμενα που λαμβάνουν χώρα μετά το πέρας της έκθεσης των μικροοργανισμών στην ηλιακή ακτινοβολία. Μελετάται η κινητική των μικροοργανισμών μετά την απολύμανση των λυμάτων με ηλιακή ακτινοβολία, και διάθεση τη διάθεσή τους στους φυσικούς αποδέκτες. Επίσης, τα φαινόμενα φωτο-επιδιόρθωσης και μεταβολής της αναμενόμενης κινητικής λόγω επανάκαμψης των μικροοργανισμών επειδή αυτοί εκτέθηκαν σε μονοχρωματική ή πολυχρωματική ακτινοβολία αναλύονται και συσχετίζονται με τις συνθήκες αποθήκευσης των λυμάτων.

Στο πέμπτο κεφάλαιο μελετάται η επίδραση της διακοπτόμενης ηλιακής ακτινοβολίας στην απολύμανση των λυμάτων με επίκεντρο το φαινόμενο της επανανάπτυξης των μικροοργανισμών οι οποίοι περιέχονται στα λύματα. Πραγματοποιείται προσομοίωση παροδικής αλλαγής των καιρικών φαινομένων με τεχνητά μέσα (φως - σκοτάδι) και διερευνώνται μέθοδοι βελτίωσης της απόδοσης των τεχνικών απολύμανσης με ηλιακή ακτινοβολία και εξάλειψη του κινδύνου επανανάπτυξης των μικροοργανισμών μέσω μεθόδων προχωρημένης οξείδωσης ως συμπληρωματική λύση.

Η Διδακτορική Διατριβή ολοκληρώνεται με τα γενικά συμπεράσματα που προκύπτουν από την έρευνα.

Διερεύνηση χρήσης της ηλιακής ακτινοβολίας για απολύμανση δευτεροβάθμια επεξεργασμένων αστικών λυμάτων εν όψει του φαινομένου της επανανάπτυξης (regrowth) των μικροοργανισμών

Σε αυτή την ενότητα της διδακτορικής διατριβής (Κεφάλαιο 3), μελετώνται οι πιο βασικές παράμετροι που επηρεάζουν την απολύμανση του νερού με υπεριώδη (ηλιακή) ακτινοβολία και δίνεται ιδιαίτερη έμφαση στις επιμέρους παραμέτρους που εμπλέκονται στη διαδικασία.

Κύριο χαρακτηριστικό της ενότητας, είναι η εφαρμογή πλήρους πειραματικού σχεδιασμού (Full Factorial Design of Experiments), μια τεχνική που επιτρέπει την σε βάθος ανάλυση των παραμέτρων και των αλληλεπιδράσεων τους, καθώς και περαιτέρω αναλύσεις και συμπεράσματα επί των αποτελεσμάτων.

Για τη γενίκευση των πειραμάτων και την παροχή προοπτικής εφαρμογής των μεθόδων σε πραγματικές συνθήκες, προσομοιώνονται πιθανές εφαρμογές και κυρίως, παρέχονται απλά, επαναλήψιμα μοντέλα πρόβλεψης της απολύμανσης και της πιθανότητας επανεμφάνισης (regrowth) των μικροοργανισμών. Το βακτήριο *E. coli,* K12, ένας κατά γενική ομολογία κοινός δείκτης κοπρανώδους μόλυνσης, χρησιμοποιείται σε όλα τα πειράματα.

Μελέτη του μηχανισμού της απολύμανσης του νερού με ηλιακή ακτινοβολία και των παραμέτρων που εμπλέκονται στην διεργασία

Για τη διερεύνηση του μηχανισμού της απολύμανσης, η διεργασία παραμετροποιήθηκε ως προς τις βασικότερες δράσεις που λαμβάνουν χώρα κατά τη διάρκεια του πειράματος. Πιο συγκεκριμένα, η ένταση και ο χρόνος έκθεσης στην τεχνητή ηλιακή ακτινοβολία, ο αρχικός μικροβιακός πληθυσμός και η θερμοκρασία τέθηκαν υπό έλεγχο. Αναλυτικά, δοκιμάσθηκαν τα παρακάτω επίπεδα:

- χρόνος έκθεσης (ακτινοβολία) 4 ωρών,
- 4 επίπεδα αρχικού μικροβιακού πληθυσμού (10^3, 10^4, 10^5 και 10^6 CFU/mL),
- 5 ελεγχόμενα επίπεδα θερμοκρασίας νερού (20, 30, 40, 50 και 60˚C), και
- 3 επίπεδα έντασης της ηλιακής ακτινοβολίας (0, 800 και 1200 W/m^2).

Τα συνθετικά λύματα υποβλήθηκαν σε ηλιακή ακτινοβολία και μελετήθηκε η κινητική των μικροοργανισμών και η μεταβολή της, ανάλογα με τις αρχικές και πειραματικές συνθήκες.

Κατά τη διάρκεια των πειραμάτων, υπό οποιεσδήποτε συνθήκες, ανά μια ώρα, ένα δείγμα καλλιεργείτο σε μη-εκλεκτικό θρεπτικό υλικό και ένα δεύτερο δείγμα παρέμενε σε συνθήκες σκότους και θερμοκρασία δωματίου για 24 και 48 ώρες, προκειμένου να μελετηθεί η ενζυματική επιδιόρθωση των ζημιών που προκλήθηκαν στους μικροοργανισμούς από τη έκθεσή τους στην ακτινοβολία.

Μελετήθηκαν και καταγράφηκαν οι συνδυασμοί όλων των παραμέτρων (240), με κριτήριο α) την απόδοση της απολύμανσης και β) τον πληθυσμό (αποικίες μικροοργανισμών) μετά από 24 και μετά από 48 ώρες. Η επεξεργασία των δεδομένων έγινε μέσω του MINITAB, που διευκολύνει την απεικόνιση πολύπλοκων σχεδιασμών και των αποτελεσμάτων τους. Τα αποτελέσματα της πειραματικής αυτής ακολουθίας, ως προς τρεις άξονες (απολύμανση, επανανάπτυξη και επίδραση της δόσης) παρουσιάζονται παρακάτω.

α) Απολύμανση

Όλα τα δείγματα εμφάνισαν διαφορετική συμπεριφορά μεταξύ 20-40°C και 40-60°C. Η ύπαρξη τροφής στα λύματα παρέχει ευνοϊκές συνθήκες ανάπτυξης των μικροοργανισμών, με αποτέλεσμα την ραγδαία αύξηση του πληθυσμού (αριθμού αποικιών) τους. Ωστόσο, μεταξύ 40 και 60°C, παρουσιάστηκε η ακριβώς αντίθετη συμπεριφορά, απόρροια της θερμόλυσης των κυττάρων.

Τα λύματα που ακτινοβολήθηκαν σε 800 W/m^2 παρουσίασαν αντικρουόμενη συμπεριφορά μεταξύ των δυο κύριων θερμοκρασιακών ομάδων. Στην περιοχή των χαμηλών θερμοκρασιών (20-40°C), η ένταση της ακτινοβολίας ήταν αρκετή ώστε να περιορίσει την ανάπτυξη των μικροοργανισμών αλλά η πλήρης απολύμανση του δείγματος ήταν αδύνατη. Επίσης, η θερμοκρασία των 40°C παρουσίασε την μικρότερη απόδοση απολύμανσης, λόγω μεγιστοποίησης του ρυθμού ανάπτυξης των μικροοργανισμών. Αντιθέτως, όταν η θερμοκρασίες ήταν υψηλές (40-60°C), παρατηρήθηκε συνέργεια ακτινοβολίας και θερμοκρασίας με αποτέλεσμα την πλήρη απολύμανση (4 ώρες, στους 50°C και 1 ώρα, στους 60°C).

Αυξάνοντας την ένταση της ακτινοβολίας στα 1200 W/m^2, επιτεύχθηκε πλήρης απολύμανση. Οι χαμηλές θερμοκρασίες επέδειξαν μεγαλύτερους απαιτούμενους χρόνους ακτινοβολίας, ενώ οι υψηλές θερμοκρασίες οδήγησαν σε πλήρη απολύμανση εντός μιας ώρας. Ο αρχικός πληθυσμός των μικροοργανισμών δεν έδειξε κάποια ιδιαίτερη επιρροή, παρά μόνο την ανάγκη για παράταση της έκθεσης στην ηλιακή ακτινοβολία, καθώς όλα τα δείγματα υπό ίδιες συνθήκες, με διαφορετικό αρχικό πληθυσμό, είχαν παρόμοια συμπεριφορά εντός του δεδομένου πειραματικού χρόνου.

Η μοντελοποίηση της απόδοσης της διεργασίας έγινε μέσω ενός γραμμικού μοντέλου (R-Sq=65.1%, S=24.42), διπλού τύπου, που περιλάμβανε όλες τις δεδομένες παραμέτρους και εξαρτάται από τη θερμοκρασία. Κάθε θερμοκρασιακή ομάδα, όπως αυτές που αναφέρθηκαν παραπάνω, διαφέρει από την άλλη, επομένως κρίθηκε σκόπιμο να διαχωριστεί ο τύπος της συνάρτησης.

β) Επανανάπτυξη των μικροοργανισμών

Για να διαπιστωθεί η επανεμφάνιση και το ποσοστό επιβίωσης των μικροοργανισμών, τα δείγματα που διατηρήθηκαν για 24 και 48 ώρες μετά την έκθεση τους σε ηλιακή ακτινοβολία επανεξετάστηκαν. Η θερμοκρασία κατά τη διάρκεια των πειραμάτων ήταν καθοριστική στην εξέλιξη της απολύμανσης, άρα

στον αριθμό των ζωντανών μικροοργανισμών στο τέλος της έκθεσης και κατ' επέκταση στο ρίσκο επανεμφάνισης μεγάλου αριθμού μικροοργανισμών. Τα δείγματα που δεν εκτέθηκαν σε ακτινοβολία παρουσίασαν φυσιολογική αύξηση του αριθμού των βακτηρίων ανάλογα με τη θερμοκρασία κατά τη διάρκεια της επεξεργασίας.

Αποδείχθηκε αρχικά ότι αν το δείγμα απολυμανθεί πλήρως, δεν υπάρχει πιθανότητα επανεμφάνισης βακτηρίων. Ο συνδυασμός UVA, UVB και ορατού φωτός προκαλεί πολύπλευρη ζημιά στα κύτταρα των βακτηρίων τα οποία τελικά αδυνατούν να επιδιορθωθούν. Επίσης, παρατηρήθηκε ότι υπάρχει κάποια ενεργειακή στάθμη πέρα από την οποία οι μικροοργανισμοί δε μπορούν να επιδιορθώσουν τις ζημιές τους. Ωστόσο, οι θερμοκρασίες γύρω στους 30°C καταδείχθηκαν ως οι ευνοϊκότερες για μακροπρόθεσμη επανανάπτυξη των μικροοργανισμών, ενώ για θερμοκρασίες μεγαλύτερες των 50°C η ζημιά που υφίστανται τα κύτταρα είναι μόνιμου χαρακτήρα.

Γενικά, η πιθανότητα επανεμφάνισης μεγάλου αριθμού βακτηρίων, εκτός από την περίπτωση μικρής/σύντομης έκθεσης στην ακτινοβολία συνδέεται με τον αριθμό των βακτηρίων που υπάρχουν στο τέλος της διαδικασίας της απολύμανσης. Τα πειράματα που εκτελέστηκαν σε χαμηλές θερμοκρασίες έδειξαν ότι ένας μεγάλος αριθμός βακτηρίων μεταφέρονται από τη μια μέρα στην επόμενη.

γ) Επιρροή της δόσης της ακτινοβολίας

Με βάση τα αποτελέσματα των πειραμάτων, μελετήθηκε η ισχύς του νόμου της αμοιβαιότητας (reciprocity law), όπου υποστηρίζεται ότι «ίδια δόση ακτινοβολίας προκαλεί το ίδιο αποτέλεσμα». Αυτό αποδείχθηκε ότι δεν ισχύει. Για υψηλότερη ένταση, η ίδια δόση ακτινοβολίας έχει καλύτερα αποτελέσματα.

Με βάση το διαχωρισμό της θερμοκρασίας σε χαμηλή (20-40°C) και υψηλή (40-60°C) περιοχή, προκύπτει η μορφή ένταξης στον νόμο της αμοιβαιότητας, για την απολύμανση του νερού και την επανανάπτυξη των μικροοργανισμών. Αποδείχθηκε πειραματικά ότι σε χαμηλές θερμοκρασίες οι χαμηλότερες εντάσεις έχουν καλύτερα αποτελέσματα, ενώ σε υψηλές θερμοκρασίες, οι υψηλότερες εντάσεις έχουν καλύτερα αποτελέσματα απολύμανσης. Η βραχυπρόθεσμη επανανάπτυξη βρέθηκε κρίσιμη για υψηλές εντάσεις και μικρούς χρόνους ακτινοβολίας, ενώ η μακροπρόθεσμη είναι κρίσιμη όταν τα δείγματα ακτινοβολούνται σε χαμηλές εντάσεις.

Μοντελοποίηση της επίδρασης της ηλιακής ακτινοβολίας στην απολύμανση και επανανάπτυξη των μικροοργανισμών στο σκοτάδι

Παράλληλα με τα πειράματα με θερμοκρασιακό έλεγχο, πραγματοποιήθηκε μια συστηματική μελέτη της έντασης της ηλιακής ακτινοβολίας, χωρίς έλεγχο της θερμοκρασίας και της επικείμενης, πιθανής επανεμφάνισης των μικροοργανισμών σε εύρος 1100 W/m^2 (500-1600 W/m^2). Διερευνήθηκε η απαιτούμενη δόση για πλήρη αδρανοποίηση των βακτηρίων και η ελάχιστη απαιτούμενη ενέργεια τερματισμού της ικανότητας επανάκαμψης των βακτηρίων (κρίσιμη ενεργειακή στάθμη).

Τα δείγματα των συνθετικών λυμάτων φωτοβολήθηκαν μέχρι να απολυμανθούν πλήρως, και ανά 30 λεπτά λαμβάνονταν ένα δείγμα το οποίο διατηρούνταν στο σκοτάδι για τη μελέτη της επανανάπτυξης των μικροοργανισμών. Ως γνωστόν, ο χρόνος είναι αντιστρόφως ανάλογος της έντασης της ακτινοβολίας. Οι μετρήσεις πραγματοποιήθηκαν ανά 30 λεπτά για εντάσεις < 1000 W/m^2 και ανά 20 λεπτά για πιο υψηλές εντάσεις. Κρίθηκε σκόπιμο να πραγματοποιηθούν πειράματα και σε πολύ υψηλές εντάσεις, οι οποίες δε μπορούν να επιτευχθούν απευθείας από τον ήλιο, αλλά με άλλα μέσα, όπως ηλιακούς συλλέκτες κ.λ.π. Οι μετρήσεις έδειξαν ότι μια δόση περίπου 3300 W/m^2 αρκεί ώστε να εξουδετερωθούν πλήρως όλα τα βακτήρια. Σημειώνεται ότι η αύξηση της έντασης της ακτινοβολίας αυξάνει πολύ την ταχύτητα της απολύμανσης.

Ωστόσο, για διαφορετικές εντάσεις, όλες οι ακτινοβολίες απαιτούν την ίδια δόση για να καλύψουν το 100% των αναγκών της απολύμανσης. Αυτό πρακτικά καταδεικνύει την ύπαρξη ενός ενεργειακού κατωφλιού, του οποίου η υπέρβαση εξασφαλίζει την απολύμανση. Διαπιστώθηκε για μια ακόμα φορά η ευμενής επίδραση των θρεπτικών συστατικών των λυμάτων στην επιβίωση των μικροοργανισμών και η ύπαρξη δυο παράλληλων αντίρροπων δυνάμεων, αυτή της ανάπτυξης και της ζημιάς που υφίστανται τα βακτήρια από την ηλιακή ακτινοβολία. Μέχρι να ξεπεραστεί το ενεργειακό κατώφλι, και μέχρι την ένταση των 800 W/m^2, παρουσιάζεται αδυναμία διατήρησης ενός προφίλ απολύμανσης.

Διαπιστώθηκε ακόμα αλλαγή της συμπεριφοράς των μικροοργανισμών ανάλογα με την ένταση ακτινοβολίας που αυτοί δέχονται. Αύξηση της έντασης της ακτινοβολίας, άρα και της δόσης, κάθε 30 λεπτά, αλλάζει την ικανότητα αυτό-ίασης των μικροοργανισμών που προκαλείται απ' αυτήν. Παρατηρήθηκε ότι για 500 W/m^2, το χρονικό σημείο όπου η επανανάπτυξη δεν είναι πλέον πιθανή, είναι τα 180 λεπτά περίπου, για 600 W/m^2 είναι τα 120-150 λεπτά, για 700 W/m^2 τα 90-120 λεπτά κ.ο.κ. Είναι πολύ σημαντικό ενεργειακό σημείο, γιατί γίνεται φανερό ότι παρόλο που δεν επιτυγχάνεται πλήρης απολύμανση, τα βακτήρια έχουν χάσει την ικανότητα επανανάπτυξης στο σκοτάδι και έχει επηρεαστεί η αναπαραγωγική τους ικανότητα. Συνεπώς μόλις τελειώσει ο κύκλος ζωής τους αδρανοποιούνται οριστικά.

Μελετήθηκε τέλος η δημιουργία ενός μοντέλου το οποίο θα προβλέπει πλήρως την απολύμανση με ηλιακή ακτινοβολία. Με την εισαγωγή της αρχικής βακτηριακής συγκέντρωσης θα γνωρίζει ο χρήστης ανά πάσα στιγμή τον πληθυσμό των μικροοργανισμών και ανάλογα με τον αριθμό των εναπομεινάντων βακτηρίων θα γνωρίζει τον απαιτούμενο χρόνο έκθεσης σε ακτινοβολία προκειμένου να εξασφαλιστεί η απολύμανση (πλήρης καταστροφή των μικροοργανισμών) σε βάθος χρόνου. Με βάση την ένταση, η δόση θα προσδιορίζει τον απαιτούμενο χρόνο έκθεσης για πλήρη απολύμανση. Η απαραίτητη δόση για οριστική καταστροφή των μικροοργανισμών χωρίς δυνατότητα επανανάπτυξης θα προκύπτει αυτόματα.

Μελέτη της βακτηριακής επανανάπτυξης ηλιακά προ-επεξεργασμένων λυμάτων - Διάθεση στο περιβάλλον

Σ' αυτή τη θεματική ενότητα (Κεφάλαιο 4), μελετώνται τα πρώτα αποτελέσματα των πειραμάτων που συνδέονται με την επανεμφάνιση των μικροοργανισμών με βάση τους δυο βασικούς μηχανισμούς επιδιόρθωσης των κυττάρων: επιδιόρθωση στο σκοτάδι (Dark repair) και φωτο-επιδιόρθωση (Photoreactivation).

Πιο συγκεκριμένα, η έκθεση στον ήλιο προηγείται μιας σειράς δοκιμών, οι οποίες σχετίζονται με το μέσο και το ποσοστό αραίωσης των λυμάτων. Δείγματα που έχουν εκτεθεί σε ηλιακή ακτινοβολία, αραιώθηκαν σε φρέσκα ανεπεξέργαστα λύματα, σε νερό λίμνης, σε θαλασσινό νερό ή σε υπερκαθαρό αποσταγμένο νερό. Το ποσοστό αραίωσης μεταβλήθηκε από 50 έως 1%.

Σε έναν άλλο πειραματικό σχεδιασμό, λύματα που έχουν εκτεθεί σε ηλιακή ακτινοβολία εκτέθηκαν σε μονοχρωματική ή ορατή ακτινοβολία μικρότερης έντασης, με σκοπό την μελέτη της φωτο-επιδιόρθωσης των ζημιών από την έκθεση. Χρησιμοποιήθηκαν πέντε διαφορετικές λάμπες μονοχρωματικής ακτινοβολίας και μια κοινή λάμπα εσωτερικού χώρου. Μετά την έκθεση, τα λύματα διατηρήθηκαν για δυο ημέρες στο σκοτάδι. Μ' αυτόν τον τρόπο διερευνήθηκε η αλλαγή της αναμενόμενης επιδιόρθωσης στο σκοτάδι.

Διάθεση αστικών λυμάτων μετά την απολύμανσή τους με ηλιακή ακτινοβολία

Μετά την ολοκλήρωση της έκθεσης σε ηλιακή ακτινοβολία, μελετήθηκε η επίδραση του μέσου αραίωσης (αποδέκτης) στην επανανάπτυξη των μικροοργανισμών στο σκοτάδι. Η αραίωση έλαβε χώρα σε φρέσκα μη-επεξεργασμένα λύματα, σε νερό λίμνης, σε αποσταγμένο και σε θαλασσινό νερό. Επίσης, εκτιμήθηκε η επίδραση του ποσοστού αραίωσης των λυμάτων του κάθε αποδέκτη στην ικανότητα επανανάπτυξης, καθώς και στο ποσοστό επανάκαμψης και επιβίωσης. Τέλος, η επίδραση της μεταβολής των θερμοκρασιακών συνθηκών και η επικείμενη μεταβολή στην επανανάπτυξη, σε ωσμωτικά ουδέτερο περιβάλλον, τέθηκε υπό διερεύνηση.

Για την επίτευξη των παραπάνω έλαβε χώρα, η ακόλουθη πειραματική ακολουθία:

Τα συνθετικά λύματα ακτινοβολήθηκαν για χρονικό διάστημα τεσσάρων ωρών. Κάθε 30 λεπτά γινόταν δειγματοληψία και μελέτη της κινητικής των μικροοργανισμών. Τα δείγματα αραιώθηκαν σε νερό των τεσσάρων αποδεκτών που προαναφέρθηκαν, σε ποσοστό 50%, 10% και 1% επί του αρχικού όγκου. Στη συνέχεια μελετήθηκε και καταγράφηκε η επιβίωση των μικροοργανισμών για χρονικό διάστημα πέντε ημερών στις συνθήκες αραίωσης. Παράλληλα, μια ακόμα οικογένεια πειραμάτων μελέτησε την επίδραση της θερμοκρασίας, για χρονικό διάστημα τριών ημερών, χωρίς αραίωση, αλλά στο ήδη επεξεργασμένο δείγμα.

Με αυτόν τον τρόπο, μελετήθηκε η επίδραση που έχει το μέσο και η αραίωση στην ικανότητα αυτο-ίασης των ζημιών που υφίστανται τα βακτήρια από το φως, καθώς και η επίδραση της θερμοκρασίας στην κινητική τους. Η ανάλυση των αποτελεσμάτων των πειραμάτων κατέδειξε ότι η θερμοκρασία είναι ο παράγοντας που προκαλεί χρονικά εκτεταμένη επιβίωση ή επιπρόσθετη αναπαραγωγή των μικροοργανισμών, στους 4 και 37 ^{o}C, αντίστοιχα. Οι διαφορετικοί αποδέκτες κατηγοριοποιήθηκαν ως προς τη δυνατότητα υποστήριξης του φυσιολογικού κύκλου ζωής των βακτηρίων, σε αυξανόμενη σειρά ως εξής: **Θαλασσινό νερό < αποσταγμένο νερό < νερό λίμνης < ανεπεξέργαστα λύματα.**

Επιβεβαιώθηκε ότι, η αραίωση δρα διπλά, ως παράγων μείωσης της διαθέσιμης τροφής αλλά και ως μοχλός φυσικοχημικής πίεσης ενάντια στην επιβίωση των εντεροβακτηρίων, στους «εχθρικούς» αποδέκτες.

Φωτο-επιδιόρθωση και μεταβολή της προβλεπόμενης κινητικής επανάκαμψης των βακτηρίων λόγω έκθεσης σε μονοχρωματική ή πολυχρωματική ακτινοβολία.

Ένας ακόμα στόχος της διατριβής, ήταν να μελετηθεί η φωτο-επιδιόρθωση των μικροοργανισμών, έπειτα από έκθεση στον ήλιο και περαιτέρω έκθεση σε μονοχρωματική ακτινοβολία. Γνωστού όντως ότι η έκθεση των βακτηρίων σε ηλιακή ακτινοβολία δημιουργεί αλλοιώσεις στο γενετικό τους υλικό, που παρόλα αυτά μπορούν να επιδιορθωθούν ενζυματικά, μελετήθηκε η έκθεση τους σε πέντε μονοχρωματικές ακτινοβολίες (300-700 nm) και ορατό φως για 2, 4 ή 8 ώρες μετά την απολύμανση των επεξεργασμένων λυμάτων με ηλιακή ακτινοβολία. Έτσι, μπορεί να πραγματοποιηθεί μια πιο αναλυτική μελέτη της μεταβολής της ικανότητας επανανάπτυξης των βακτηρίων σε σχέση με το μήκος κύματος του φωτός στο οποίο έχουν εκτεθεί και να προσδιοριστεί η απαιτούμενη δόση ηλιακού φωτός και μονοχρωματικής ακτινοβολίας για την καταστολή της ικανότητας φωτο-επιδιόρθωσης. Οι παράμετροι που εμπλέκονται στην πειραματική διαδικασία είναι:

- το μήκος κύματος της μονοχρωματικής ακτινοβολίας που ενεργοποιεί τα ένζυμα (μπλε, υπεριώδες μπλε, πράσινο, κίτρινο, ακτινικό φως) ή η πολυχρωματική ακτινοβολία (ορατό φως),
- ο ελάχιστος και ο μέγιστος χρόνος έκθεσης στο φως, για φωτο-επιδιόρθωση και
- το μέγιστο μέγεθος της ζημιάς που μπορούν να καλύψουν οι προαναφερθείσες ακτινοβολίες.

Όλα αυτά επιτυγχάνονται μέσω μελέτης της κινητικής των μικροοργανισμών ανά 30 λεπτά. Αρχικά, τα λύματα ακτινοβολούνται στα 1000 W/m^2. Ακολούθως, εκτίθενται σε χαμηλής έντασης μονοχρωματική ακτινοβολία για 2, 4 και 8 ώρες. Στα δεδομένα χρονικά διαστήματα αυτά, λαμβάνονται δείγματα και μελετάται η κινητική των μικροοργανισμών. Έπειτα δηλαδή από 2, 4 ή 8 ώρες, τα λύματα διατηρούνται στο σκοτάδι για 48 ώρες και τυχόν επανανάπτυξη των μικροοργανισμών καταγράφεται κάθε 24 ώρες. Με αυτό τον τρόπο, μελετάται η επίδραση κάθε μήκους κύματος στα βακτήρια, σε διαφορετική φυσιολογική κατάσταση (ανεπεξέργαστα, ισχυρά, εξασθενημένα κ.λ.π.) και το κατά πόσο μπορούν να ενεργοποιηθούν τα απαραίτητα φωτο-επιδιορθωτικά τους ένζυμα.

Από την ανάλυση των αποτελεσμάτων των παραπάνω πειραμάτων, προέκυψε ότι τα λύματα που περιέχουν πλήρως αδρανοποιημένα βακτήρια δεν επιδέχονται φωτο-επιδιόρθωσης, και ότι η ζημιά που προκαλείται από το ηλιακό φως είναι πολυδιάστατη και μόνιμη (μη αναστρέψιμη). Επίσης, η επιδιόρθωση των βλαβών λόγω έκθεσης στον ήλιο εξαρτάται και από το μήκος κύματος της ακτινοβολίας που ακολουθεί την έκθεση: όσο πλησιέστερα στο μπλε φως, τόσο μεγαλύτερη η ικανότητα φωτοεπιδιόρθωσης. Τέλος, η ικανότητα των ενζύμων για επιδιόρθωση των ζημιών στο σκοτάδι, μεταβάλλεται σημαντικά από την έκθεση σε μονοχρωματική ακτινοβολία. Αποδείχθηκε ότι τα βακτήρια, ανάλογα με το μήκος κύματος της ακτινοβολίας στην οποία εκτίθενται επιδέχονται αλλαγές στην φυσιολογική επιδιορθωτική ικανότητά τους στο σκοτάδι.

Επιπλοκές κατά την εφαρμογή τεχνικών λύσεων για την απολύμανση των αστικών λυμάτων με ηλιακή ακτινοβολία

Σε αυτή την ενότητα (Κεφάλαιο 5) μελετήθηκε η τεχνική εφαρμογή της απολύμανσης με ηλιακή ακτινοβολία, μέσω των γνωστών τεχνικών των αντιδραστήρων CPC, καθώς και η προσομοίωση επιπλοκών στης εφαρμογές πεδίου (ασυνεχής έκθεση στον ήλιο).

Για τη βελτίωση της απολυμαντικής ικανότητας των διεργασιών, μελετήθηκε τέλος η πιθανότητα χρήσης των αντιδραστηρίων Fenton (Fe/H_2O_2), η φωτοκαταλυτική ενίσχυση της αντίδρασης Fenton (photo-Fenton), οι υπέρηχοι και ο συνδυασμός υπερήχων και Photo-Fenton.

Επίδραση της διακοπτόμενης ηλιακής ακτινοβολίας στην απολύμανση και στην επανανάπτυξη των μικροοργανισμών οι οποίοι περιέχονται σε δευτεροβάθμια επεξεργασμένα αστικά λύματα

Αρχικά, μελετήθηκε η διακοπτόμενη έκθεση των μικροοργανισμών σε ηλιακή ακτινοβολία σε αντιδραστήρα επανακυκλοφορίας και σε αντιδραστήρα στιγμιαίας πλήρωσης με ασυνεχή έκθεση σε ακτινοβολία. Διερευνήθηκε η επίδραση της ταχύτητας επανακυκλοφορίας, με σταθερό χρονικό λόγο σκότους/ακτινοβολίας. Επίσης, στους αντιδραστήρες στιγμιαίας πλήρωσης, μελετήθηκαν 14 σενάρια διακοπής της ακτινοβολίας, με όλους τους πιθανούς συνδυασμούς φωτοβόλησης για 3 ώρες και παραμονής στο σκοτάδι για 3 ώρες. Με αυτό τον τρόπο προσομοιώθηκε η περίπτωση διακοπής της ακτινοβολίας λόγω νεφώσεων. Στο τέλος κάθε πειράματος, καταγράφηκε η επανανάπτυξη των μικροοργανισμών μετά από 24 ή 48 ώρες.

Αποδείχθηκε ότι, οι υψηλές ταχύτητες επανακυκλοφορίας βοηθούν άμεσα την απολύμανση, λόγω της συχνότερης, αν και μικρότερης διάρκειας έκθεσης στην ακτινοβολία. Παρόλα αυτά, για τον ίδιο χρόνο έκθεσης, η δόση έχει το ίδιο αποτέλεσμα στην επανανάπτυξη των μικροοργανισμών.

Μέσω των σεναρίων που μελετήθηκαν, βρέθηκε ότι αν υπάρχει κάποια ασυνέχεια στην έκθεση στο φως, όσο νωρίτερα γίνεται αυτή η διακοπή, τόσο πιο πολύ επιμηκύνεται η απαιτούμενη διάρκεια έκθεσης, για να επιτευχθεί η απολύμανση. Μετά από μια καθορισμένη δόση, δεν υπάρχει διαφορά στην απολύμανση, γιατί έχει ξεκινήσει ο προγραμματισμένος κυτταρικός θάνατος (PCD: programmed cell death), με αποτέλεσμα την κυτταρική απόπτωση και την καταστροφή κατά τη διάρκεια διακοπής της ακτινοβολίας. Τα δείγματα των προσομοιωμένων αστικών λυμάτων απολυμάνθηκαν πλήρως και δεν παρατηρήθηκε επανανάπτυξη μικροοργανισμών.

Βελτίωση των τεχνικών απολύμανσης με ηλιακή ακτινοβολία – Εξάλειψη του κινδύνου επανανάπτυξης των μικροοργανισμών.

Η απολύμανση σε αντιδραστήρες με επανακυκλοφορία έδειξε ότι απαιτεί μεγάλους χρόνους παραμονής για πλήρη απολύμανση. Οι μεγάλοι χρόνοι παραμονής απαιτούν όμως και μεγάλες κατασκευές, με βλέψεις προς την πραγματική εφαρμογή. Οπότε αναζητήθηκε μια λύση που θα μικρύνει τους χρόνους παραμονής.

Αρχικά μελετήθηκε η φωτο-κατάλυση Fenton σε αντιδραστήρες στιγμιαίας πλήρωσης, που έδειξε μεγάλη βελτίωση στους χρόνους έκθεσης (50%). Η μελέτη κάθε παράγοντα ξεχωριστά κατέδειξε τις βέλτιστες συνθήκες λειτουργίας. Έπειτα, μελετήθηκε η σύζευξη φωτοκατάλυσης και υπερήχων υψηλής συχνότητας που λειτουργούν με χαμηλή ενέργεια, για λόγους οικονομίας. Σημαντική παράμετρο αποτελεί η εκμετάλλευση του νεκρού χρόνου παραμονής των μικροοργανισμών στο σκοτάδι, όταν δηλαδή τα λύματα επανακυκλοφορούν από τον ήλιο, στη δεξαμενή αποθήκευσης.

Η στρατηγική που ακολουθήθηκε ήταν η εξής:

- Design of Experiments, με τους όρους του Fenton και των υπερήχων ($Fe+H_2O_2$, US, hv)
- Αξιολόγηση της απολύμανσης σε κάθε μια από τις (8) υποπεριπτώσεις, και παρακολούθηση της κινητικής των μικροοργανισμών για 48 ώρες στο σκοτάδι.
- Πρόταση πιθανών μηχανισμών αδρανοποίησης για την συζευγμένη μέθοδο απολύμανσης.
- Διερεύνηση των παραμέτρων λειτουργίας του συστήματος (υδραυλικές, περιβαλλοντικές και χημικές παράμετροι), για τον προσδιορισμό των ειδικών οριακών συνθηκών.

Προέκυψε ότι για να λειτουργήσει οικονομικά η διάταξη, η πιο σημαντική παράμετρος στη σύζευξη είναι το φως. Οι μικροί όγκοι, οι μεγάλες ποσότητες υπεροξειδίου του υδρογόνου και η μεγάλη ακουστική ισχύς, μπορούν να βελτιώσουν την απόδοση του συστήματος. Η συζευγμένη δράση είχε ως αποτέλεσμα την εξάλειψη του φαινομένου της επανανάπτυξης των μικροοργανισμών. Η εκμετάλλευση των χρόνων παραμονής στο σκοτάδι βελτίωσε την απόδοση της αντίδρασης στο πιο απαιτητικό τμήμα της, δηλαδή στο τελικό ποσοστό επιτυχίας.

Γενικά συμπεράσματα

Από τα πειράματα που εκτελέστηκαν για την ολοκλήρωση της Διδακτορικής Διατριβής, προέκυψε ότι η προσομοίωση της απολύμανσης δευτεροβάθμια επεξεργασμένων λυμάτων με ηλιακή ακτινοβολία αποτελεί έναν καλό δείκτη επιτυχίας της πραγματικής εφαρμογής. Η διεξοδική ανάλυση/μελέτη των εμπλεκόμενων παραμέτρων κατέδειξε σημεία «κλειδιά» για την επιτυχία της εφαρμογής. Πιο συγκεκριμένα:

Οι συνθήκες κατά τη διάρκεια της απολύμανσης καθορίζουν την επιτυχία της ή τελικά, τον αριθμό των μικροοργανισμών που έχουν απομείνει. Το ποσοστό αδρανοποίησης των εντεροβακτηρίων επηρεάζει σε μεγάλο βαθμό και την πιθανότητα επανανάπτυξης, μετά το πέρας της διαδικασίας. Η θερμοκρασία είναι ένας παράγοντας που μπορεί να δώσει ώθηση ή να αποτελέσει τροχοπέδη ενάντια στην αποτελεσματικότητα της διεργασίας. Με βάση τα πειραματικά αποτελέσματα, δημιουργήθηκαν μοντέλα πρόβλεψης της επιτυχίας της απολύμανσης αλλά και της πιθανότητας επανανάπτυξης των μικροοργανισμών μετά το πέρας της διαδικασίας.

Οι συνθήκες που επικρατούν κατά την περίοδο μετά την έκθεση στην ηλιακή ακτινοβολία επίσης διαδραματίζουν σημαντικό ρόλο στην επανεμφάνιση ενεργών μικροοργανισμών. Ανάλογα με τις ιδιαίτερες φυσικοχημικές ιδιότητες του αποδέκτη, τα βακτήρια μπορούν να παρουσιάσουν εκτεταμένη επιβίωση ή ταχεία καταστροφή. Ωστόσο, αυτές οι συνθήκες μπορούν να παίξουν σημαντικό ρόλο στον σχεδιασμό εγκαταστάσεων απολύμανσης με ηλιακή ακτινοβολία, μετριάζοντας τις ανάγκες έκθεσης στον ήλιο. Εάν βέβαια αναμένεται περαιτέρω έκθεση σε φως, οι ιδανικές συνθήκες επιβάλλουν πλήρη αδρανοποίηση των μικροοργανισμών πριν τη διάθεσή τους στο περιβάλλον, για εξάλειψη της φωτο-επιδιορθωτικής τους ικανότητας .

Τέλος, η χρήση τεχνικών μέσων για την απολύμανση δευτεροβάθμια επεξεργασμένων λυμάτων ενδείκνυται μόνο αν η έκθεση είναι συνεχής (ή σχεδόν συνεχής) και πρόκειται να απολυμανθούν μικροί όγκοι νερού. Η διακοπή στην παροχή ηλιακής ακτινοβολίας μπορεί να επιφέρει προσωρινή αύξηση στο μικροβιακό φορτίο. Όμως, η χρήση μεθόδων προχωρημένων μεθόδων οξείδωσης μπορεί να αμβλύνει τα προαναφερθέντα προβλήματα και να προκαλέσει άμεση και μόνιμη αδρανοποίηση των βακτηρίων, χωρίς κίνδυνο επανανάπτυξης.